UNIVERSITY OF UTAH
SEP 24 1956
SALT LAKE CITY

Electrochemical Society

September 1956

Cleveland Meeting Program Issue

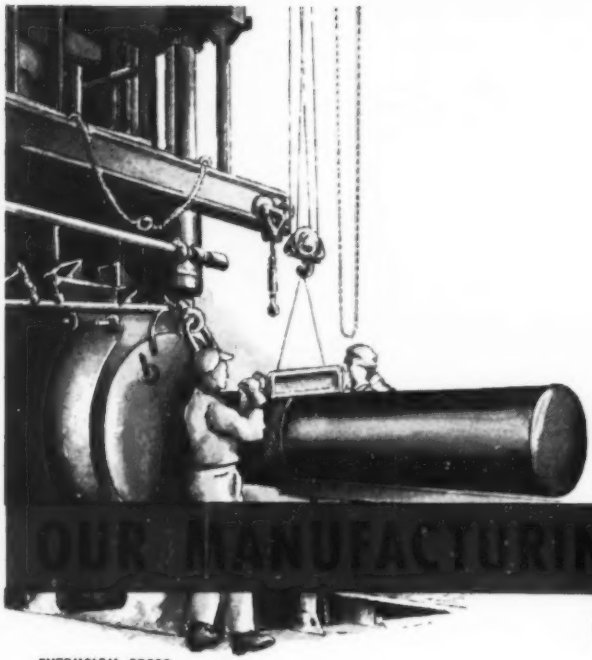

EXTRUSION PRESS
MORGANTON, N. C., PLANT

AS PARTNERS IN
YOUR PROGRESS . . .

OUR MANUFACTURING SKILL
– is a *plus* factor!

Each process stage in the manufacture of electrodes, anodes, mold stock and carbon brick must be skillfully engineered to obtain the particular end-use chemical and physical properties desired.

The advanced handling techniques and quality control safeguards developed by our engineers and technicians give customers an important *plus factor* in the reliability of GLC carbon and graphite products.

The high degree of integration between discoveries in our research laboratories, refinements in processing raw materials, and improved manufacturing methods is further assurance of excellent product performance.

ELECTRODE
GLC®
DIVISION

Great Lakes Carbon Corporation

GRAPHITE ELECTRODES, ANODES, MOLDS and SPECIALTIES

ADMINISTRATIVE OFFICE: 18 East 48th Street, New York 17, N. Y. PLANTS: Niagara Falls, N. Y., Morganton, N. C. OTHER OFFICES: Niagara Falls, N.Y., Oak Park, Ill., Pittsburgh, Pa. SALES AGENTS: J. B. Hayes Company, Birmingham, Ala., George O. O'Hara, Wilmington, Cal. SALES AGENTS IN OTHER COUNTRIES: Great Northern Carbon & Chemical Co., Ltd., Montreal, Canada; Great Eastern Carbon & Chemical Co., Inc., Chiyoda-Ku, Tokyo, Japan

EDITORIAL STAFF

R. M. BURNS, *Chairman*
CECIL V. KING, *Editor*
NORMAN HACKERMAN, *Technical Editor*
RUTH G. STERNS, *Managing Editor*
U. B. THOMAS, *News Editor*
NATALIE MICHALSKI, *Assistant Editor*
ELEANOR BLAIR, *Assistant Editor*

DIVISIONAL EDITORS

W. C. VOSBURGH, *Battery*
J. E. DRALEY, *Corrosion*
JOHN J. CHAPMAN, *Electric Insulation*
ABNER BRENNER, *Electrodeposition*
H. C. FROELICH, *Electronics*
HERBERT BANDES, *Electronics—Semiconductors*
SHERLOCK SWANN, JR., *Electro-Organic*
JOHN M. BLOCHER, JR., *Electrothermics and Metallurgy, I*
A. U. SEYBOLT, *Electrothermics and Metallurgy, II*
W. C. GARDINER, *Industrial Electrolytic*
C. W. TOBIAS, *Theoretical*

REGIONAL EDITORS

HOWARD T. FRANCIS, *Chicago*
JOSEPH SCHULEIN, *Pacific Northwest*
J. C. SCHUMACHER, *Los Angeles*
G. W. HEISE, *Cleveland*
G. H. FETTERLEY, *Niagara Falls*
OLIVER OSBORN, *Houston*
EARL A. GULBRANSEN, *Pittsburgh*
A. C. HOLM, *Canada*
J. W. CUTHBERTSON, *Great Britain*
T. L. RAMA CHAR, *India*

ADVERTISING OFFICE

JACK BAIN, *Advertising Manager*
545 Fifth Avenue, New York 17, N. Y.

ECS OFFICERS

HANS THURNAUER, *President*
Minnesota Mining & Mfg. Co., St. Paul, Minn.

NORMAN HACKERMAN, *Vice-President*
University of Texas, Austin, Texas

SHERLOCK SWANN, JR., *Vice-President*
University of Illinois, Urbana, Ill.

W. C. GARDINER, *Vice-President*
Olin Mathieson Chemical Corp., Niagara Falls, N. Y.

LYLE I. GILBERTSON, *Treasurer*
Air Reduction Co., Murray Hill, N. J.

HENRY B. LINFORD, *Secretary*
Columbia University, New York, N. Y.

Journal of the
Electrochemical Society

SEPTEMBER 1956 VOL. 103 • NO. 9

CONTENTS

Editorial

The St. Lawrence Seaway 186C

Technical Papers

Oxidation of Copper to Cu_2O and CuO. *D. W. Bridges, J. P. Baur, and G. S. Baur* 475
Effect of Prior Corrosion History on the Corrosion of Zircaloy-2 in High Temperature Water. *D. E. Thomas and S. Kass* 478
Natural and Thermally Formed Oxide Films on Aluminum. *M. S. Hunter and P. Fowle* 482
The Tin-Steel Couple in Air-Free Citric Acid Solution. *E. L. Kochler* 486
Phase Equilibria and Fluorescence in the System Zinc Oxide-Boric Oxide. *D. E. Harrison and F. A. Hummel* 491
Cathode Ray Tube Screen Charging and Conditions Leading to Positive Ion Deterioration. *A. B. Laponsky, M. J. Ozeroff, W. A. Thornton, and J. R. Young* 498
Fluorescence of Thallium-Activated Halide Phosphors. *K. H. Butler* 508
Polarographic Behavior of Organic Compounds in Methanesulfonic Acid. *S. Wawzonek, R. Berkey, and D. Thomson* 513
Preparation of High Purity Rhenium. *D. M. Rosenbaum, R. J. Runck, and I. E. Campbell* 518
Uranium Purification by Electrorefining. *L. W. Niedrach and A. C. Glamm* 521

Technical Review

Report of the Chlor-Alkali Committee of the Industrial Electrolytic Division for the Year 1955. *W. C. Gardiner, M. S. Kircher, and W. D. Sherrow* 529

Feature Section

"In Favor of Thinking Creatively." *H. H. Uhlig* 191C

Current Affairs

Complete Cleveland Meeting Program 195C
News Notes in the Electrochemical Field 213C
San Francisco Close-Ups 214C
Section News 216C
Personals 217C
Announcements from Publishers 218C
Book Reviews 218C
Literature from Industry 220C
New Products 221C
Employment Situations 222C

Published monthly by The Electrochemical Society, Inc., Mount Royal and Guilford Aves., Baltimore 2, Md., combining the JOURNAL and TRANSACTIONS OF THE ELECTROCHEMICAL SOCIETY. Editorial offices: 216 West 102nd Street, New York 25, N. Y Statements and opinions given in articles and papers in the JOURNAL OF THE ELECTROCHEMICAL SOCIETY are those of the contributors, and The Electrochemical Society assumes no responsibility for them. Nondeductible subscription to members $5.00; subscription to nonmembers $18.00. Single copies $1.25 to members, $1.75 to nonmembers. Copyright 1956 by The Electrochemical Society, Inc. Entered as second-class matter November 15, 1947, at the Post Office at Baltimore, Md., under the act of August 24, 1912.

in the development stage

.....when

call on Mallinckrodt®

For manufacturers of **transistor** and other **semi-conductor** devices,

Mallinckrodt introduced this year **TRANSISTARS***

Acetone TransistAR
Acid Acetic Glacial TransistAR
Acid Hydrofluoric 48% TransistAR
Acid Hydrochloric TransistAR
Acid Nitric TransistAR
Acid Sulfuric TransistAR
Alcohol Isopropyl TransistAR
Alcohol Methyl Absolute TransistAR
Ammonium Hydroxide TransistAR
Carbon Tetrachloride TransistAR
Ether Anhydrous TransistAR
Hydrogen Peroxide TransistAR
Hydrogen Peroxide Solution 30% Stabilized TransistAR
Sodium Carbonate Monohydrate TransistAR

*Trademark

we can contribute most to the solution of your chemical problems

Since the earliest days of the television industry, Mallinckrodt has been a supplier of chemicals necessary to the manufacture of efficient phosphors . . . precision chemicals with a minimum of impurities which poison phosphors . . . uniform chemicals where controlled physical form is of utmost importance. Mallinckrodt silicic acid, for example, is manufactured in three different forms to meet industry's demands for purity, particle size and bulk.

This experience will be of great assistance to you in solving your chemical problems.

MALLINCKRODT STANDARD LUMINESCENT (S.L.®) CHEMICALS USED FOR PHOSPHOR PRODUCTION . . .

ACID SILICIC S.L. • AMMONIUM CHLORIDE S.L. • BARIUM CARBONATE S.L. • CALCIUM CARBONATE S.L. • CALCIUM FLUORIDE S.L. CALCIUM PHOSPHATE DIBASIC S.L. • MAGNESIUM CARBONATE S.L. • MAGNESIUM OXIDE S.L. • MANGANESE CARBONATE S.L. STRONTIUM CHLORIDE ANHYDROUS S.L.

MALLINCKRODT CHEMICAL WORKS

SECOND & MALLINCKRODT STREETS, ST. LOUIS 7, MO. • 72 GOLD STREET, NEW YORK 8, N. Y.
CHICAGO • CINCINNATI • CLEVELAND • DETROIT • LOS ANGELES • PHILADELPHIA • SAN FRANCISCO
IN CANADA: **MALLINCKRODT CHEMICAL WORKS LIMITED** • MONTREAL • TORONTO

Mallinckrodt High Purity Chemicals used extensively in the electronic industry

Acids
Acetic Acid
Boric Acid
Chromic Acid
Chromium Trioxide
Hydrofluoric Acid
Nitric Acid
Sulfuric Acid

Aluminum
Aluminum Chloride
Aluminum Nitrate

Ammonium
Ammonium Bifluoride
Ammonium Carbonate
Ammonium Phosphate Dibasic

Barium
Barium Acetate
Barium Carbonate
Barium Chloride
Barium Nitrate

Cadmium
Cadmium Chloride
Cadmium Nitrate
Cadmium Sulfate

Calcium
Calcium Carbonate
Calcium Chloride
Calcium Fluoride
Calcium Nitrate
Calcium Phosphate Dibasic

Copper
Cupric Sulfate
Cuprous Chloride

Lithium
Lithium Carbonate
Lithium Chloride
Lithium Sulfate

Magnesium
Magnesium Carbonate
Magnesium Oxide

Manganese
Manganese Chloride
Manganese Carbonate
Manganese Sulfate

Mercury
Mercury Metal
Mercuric Oxide

Nickel
Nickel Nitrate

Potassium
Potassium Cyanide
Potassium Dichromate

Silicate
Silicic Acid

Silver
Silver Cyanide
Silver Nitrate
Silver Oxide

Sodium
Sodium Carbonate
Sodium Dichromate
Sodium Hydroxide

Solvents and Organics
Benzene
Carbon Tetrachloride
Chloroform
Ether
Ethyl Acetate
Isopropyl Alcohol
Methyl Alcohol
Toluene

Stearates
Calcium Stearate
Magnesium Stearate
Zinc Stearate

Strontium
Strontium Chloride
Strontium Nitrate

Zinc
Zinc Metal
Zinc Chloride
Zinc Oxide
Zinc Sulfate

Editorial

The St. Lawrence Seaway

WITHIN THE NEXT FEW YEARS, all but the very largest ocean-going cargo vessels will be able to tie up at the docks of Chicago on Lake Michigan and Duluth on Lake Superior, some 2400 miles from the mouth of the St. Lawrence and 650 ft above sea level. Construction now well under way will put the big ships past Niagara Falls into Lake Erie in 1959. Due entirely to Canadian enterprise, for many years it has been possible for lake steamers to make the run from Montreal to the upper lake ports. United States cooperation in the larger project has been long delayed, chiefly because of political wrangling in this country over Federal vs. State rights and especially over Federal vs. State vs. private power projects. The present compromise on these issues was partly forced by our need for Canadian iron ore, which can be shipped much more economically over the enlarged Seaway, and by Canadian determination to proceed with or without our participation.

The amount of excavation and construction will far exceed that involved in building the Panama Canal. A major part of the project is in a 115-mile section between Montreal and Lake Ontario: the Lachine and Soulanges areas, and the International Rapids. However, the Niagara Falls bypass requires a greater vertical lift, of more than 300 ft, and Canada will enlarge the 28-mile-long Welland Canal with its eight locks.

The main new power project is at Barnhart Island, near Massena and Ogdensburg, N. Y. The International Rapids will be flooded to a maximum depth of 90 ft, and the entire town of Iroquois, Ontario, is being moved to a new location on higher ground. The waters will be impounded by the Long Sault Dam on the American side, and by the 3200-ft Power Dam, which is bisected by the international boundary. At the Power Dam, 32 generators will be installed, each with an output capacity near 60,000 kw. The power developed will be about three times that of Boulder Dam. Later, the Canadian Government expects to construct plants at Lachine and elsewhere totaling another three-quarters of this capacity.

Impressive as such figures are, cheaper transportation of bulky cargo is the keynote of the Seaway. Most of the new power will be distributed to comparatively small users, down to individual home owners. Alcoa will get, at Massena, a large block of Barnhart Island power, but at the expense of relinquishing present facilities. In general, large-scale electrochemical industry which wishes to move into the area will most likely have to bring its own power. Industry will be attracted to the Great Lakes and River regions because both raw materials and finished products can flow to and from all parts of the world without expensive transshipment. Abundant fresh water is another attraction for chemical industry; the St. Lawrence flow is 70 times that of the Hudson. Let us hope that pollution of the river will be strictly forbidden.

Some hydroelectric development is still possible at Niagara Falls. Not considered a part of the Seaway project, a 1.9-million kw plant was recently completed on the Canadian side. A smaller plant on the American side was ruined in June by a rock slide; will most likely have its capacity incorporated in a larger new plant at a different location.

Possible new large-scale hydroelectric sites in desirable locations are extremely limited in the United States proper. Since the demand for electric power shows no sign of reaching a peak or a plateau, industry is constantly on the search for new sources.

—CVK

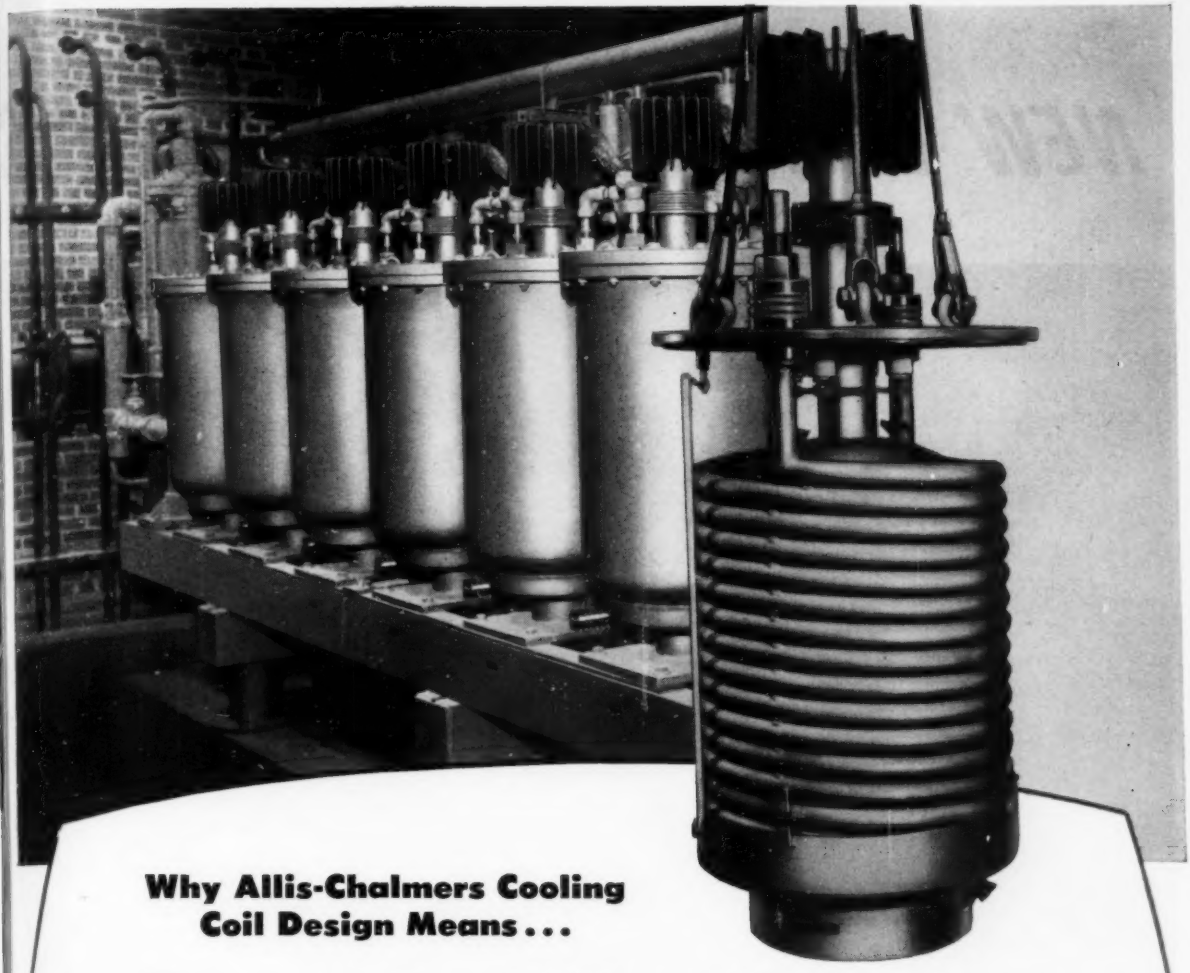

Why Allis-Chalmers Cooling Coil Design Means . . .

Better Rectifier Operation

More Efficient Heat Transfer results from internal cooling coil. The steel coil surrounds active parts, offering more cooling surface and better heat transfer than other types. Unit maintains more uniform temperature and mercury vapor pressure.

Simplified Maintenance results from Allis-Chalmers unique unit construction. All active components are attached to the anode plate for easy withdrawal, dismantling, and re-assembling — as illustrated above.

Positive Arc Barrier is formed by the cooling coil, which is insulated from the tank. The main arc is confined within the coil, preventing arc transfer to the tank.

Years of Operation in hundreds of installations have proved the reliability, ease of operation, and simplified maintenance of Allis-Chalmers mercury arc rectifiers. You can get complete information at your nearby A-C office, or write Allis-Chalmers, Industrial Equipment Division, Milwaukee 1, Wisconsin.

LIVE BETTER ELECTRICALLY

ALLIS-CHALMERS

A-C ALLIS-CHALMERS

A-5084

NEW DOW MAGNESIUM ALLOYS CR

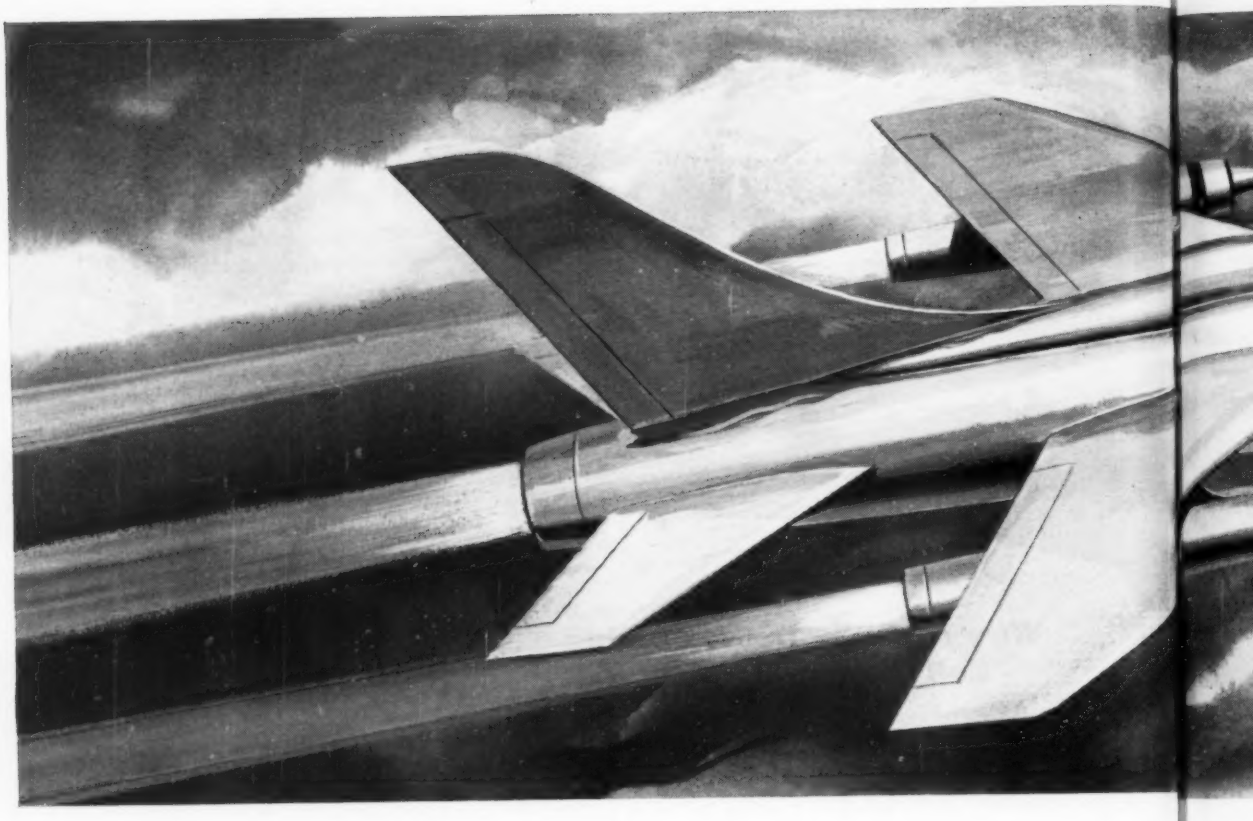

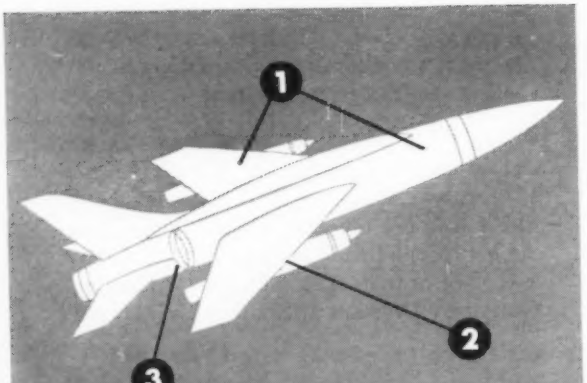

Now suggested *for a broad range of uses in missiles and aircraft, the new Dow magnesium alloys are available in the form of (1) sheet or plate, (2) extrusions, (3) castings.*

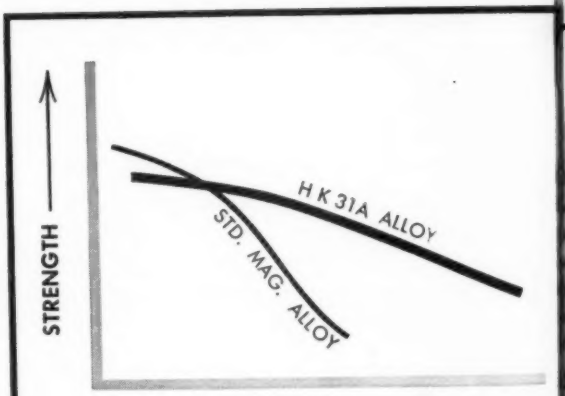

Maintenance of strength *at high temperatures is illustrated by this chart. Performance data on the new alloys at elevated temperatures can be obtained by request.*

DOW

...S CRACK HEAT BARRIER!

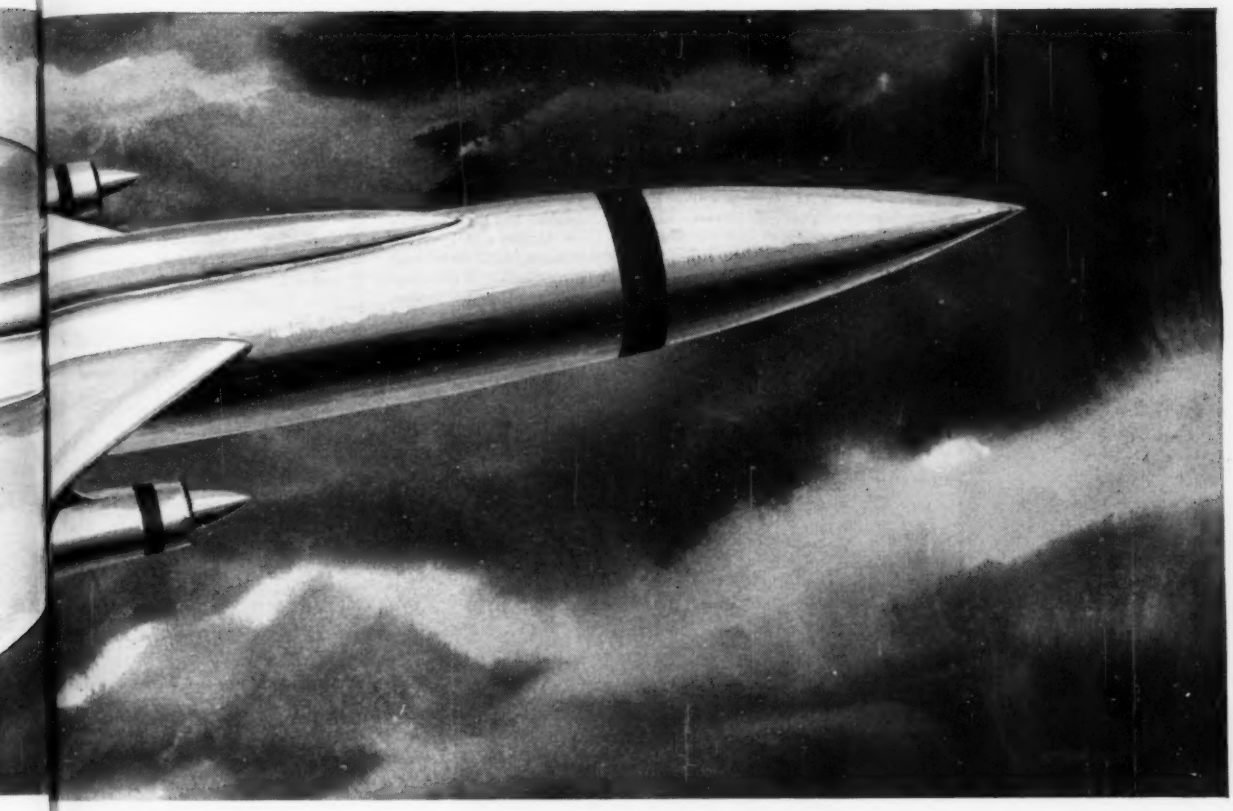

...High temperature magnesium alloys are available to lighten aircraft and missile structures

...ince again the horizons for aircraft structural design have ...en widened. Dow has developed a series of high tempera... ...re magnesium alloys which are already in pre-production ...e on aircraft, missile and engine structures. These alloys ...ow advantages at temperatures up to 700° F. Limited ...st data on properties up to 800° F. are available for some ... these alloys.

...e new alloys save precious pounds because of their good ...mbination of modulus and properties, including creep ...rength, at temperature. Shop characteristics include good ...rmability and weldability.

One of the available alloys is the magnesium-thorium composition, HK31A, which is manufactured in rolled and cast form. Under development is a similar alloy for extruded shapes and forgings. HK31A sheet and plate are available from stock and from current mill delivery schedules in standard sizes from 0.016″ to 2″.

These new magnesium alloys by Dow should be considered for your high temperature requirements. Contact your nearest Dow sales office or write THE DOW CHEMICAL COMPANY, Magnesium Sales Dept., MA 361F, Midland, Michigan.

you can depend on DOW MAGNESIUM DOW

WARREN A. MARRISON. Tompion Gold Medal, Worshipful Company of Clockmakers of the City of London, for pioneer work on development of quartz crystal oscillators as precision standards of time.

W. G. PFANN. Mathewson Gold Medal, American Institute of Mining and Metallurgical Engineers, for discovery of and pioneering research in zone melting.

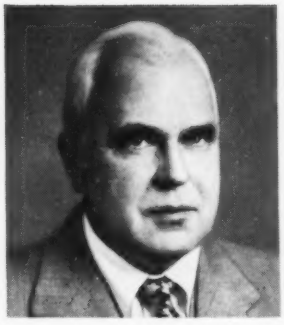

H. T. FRIIS. Medal of Honor, Institute of Radio Engineers and Valdemar Poulsen Gold Medal, Danish Academy of Technical Sciences; important work in application of short and ultra-short radio waves.

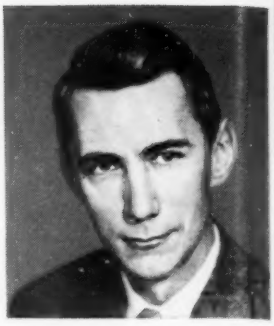

CLAUDE E. SHANNON. Stuart Ballantine Medal, Franklin Institute of the State of Pennsylvania, for contributions to a comprehensive theory of communication.

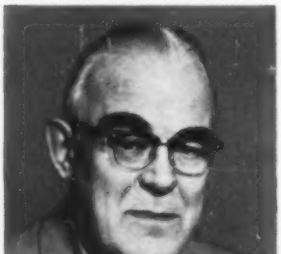

AXEL G. JENSEN. David Sarnoff Gold Medal, Society of Motion Picture and Television Engineers, for technical contributions to television; G. A. Hagemann Gold Medal for Industrial Research, Royal Technical College, Copenhagen.

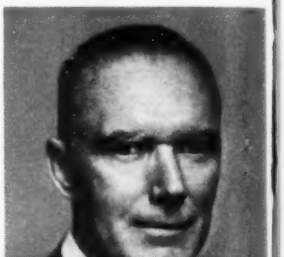

H. F. DODGE. Shewhart Medal, American Society for Quality Control, for original contributions to the art of statistical quality control.

PIONEERS OF PROGRESS

These are some of our recent medal winners at Bell Laboratories. The awards they have won symbolize recognition for outstanding achievement in the many sciences that bear on telephony. Bell Labs is extremely proud of them—and of the thousands of scientists and engineers who work with them to keep the American telephone system the greatest in the world.

Oxidation of Copper to Cu_2O and CuO

(600°–1000°C and 0.026–20.4 atm Oxygen)

Donald W. Bridges,[1] John P. Baur,[1] Gretta S. Baur, and W. Margin Fassell, Jr.[1]

Department of Metallurgy, University of Utah, Salt Lake City, Utah

ABSTRACT

Oxygen free-high conductivity copper was oxidized to CuO and Cu_2O over the temperature range 600°–1000°C in pure oxygen (0.026–20.4 atm). Correlation of weight gained, W, and time, t, was achieved through the use of the equation: $t/W = W/K_p + 1/K_1$, where K_p is the parabolic rate constant and K_1 is a constant. Pressure variation had no effect on the magnitude of K_p, if the ratio Cu_2O/CuO was constant. Quantitative x-ray diffraction analysis of the scale disclosed approximately 96% Cu_2O at high and low pressures for temperatures above 800°C. Below 750°C high pressure coatings contained 90% Cu_2O, while subatmospheric coatings continued to assay about 96% Cu_2O. Temperature correlation was obtained by means of the equation: $K_p = A \exp(-Q/RT)$, where Q = 37,000 cal and K_p is the average value for a Cu_2O/CuO ratio of approximately 96/4 (700°–1000°C).

Recent review articles (1–3) summarize much of the work on oxidation of copper. The present survey investigates the system, $Cu/Cu_2O/CuO/O_2$, at temperatures from 600° to 1000°C in pure oxygen from 0.026 to 20.4 atm. The oxygen free-high conductivity (OFHC) copper used was the same as employed in this laboratory's study of the system, $Cu/Cu_2O/O_2$ (4). Subatmospheric experimental procedure, equipment, and sample preparation methods were described in the previous paper (4). The high pressure equipment and experimental technique are as previously reported (5). All samples were oxidized for a period of 120–150 min.

Experimental Results

Kinetic measurements.—The correlation of weight gained and time was achieved through the use of the same equation employed in the oxidation of OFHC copper below the dissociation pressure of CuO (4):

$$t/W = W/K_p + 1/K_1 \qquad (I)$$

t is the observed elapsed time, W is the increase in weight, K_p is the parabolic rate constant, and K_1 is a thickness independent constant. Mathematically, this is the equation of a parabola that does not intersect the t-axis at $W = 0$. Its physical significance has been discussed by numerous workers (6–10). Table I presents the individual determinations here analyzed by means of equation (I), and at 600°C and 700°C the parabolic rate constant resulting from the application of the more conventional parabolic oxidation equation: $W^2 = K_p \cdot t$, which for low temperatures yielded an equally good representation of the data. At temperatures in excess of 700°C, W^2 vs. t plots resembled those published previously (4).

Composition of the oxide coating.—Quantitative x-ray diffraction analyses were performed on the oxide layers from 20 samples oxidized approximately 2 hr at various temperatures and pressures. The purpose was to ascertain if the composition changed with either temperature or oxygen concentration (pressure).

The oxide scale was mixed with an amount of high grade CaO such that the ratio of weight of oxide to weight of CaO was always 2/1. Peak intensities of the three lines (CuO, 35.45 degrees 2θ; Cu_2O, 36.43 degrees 2θ; and CaO, 37.37 degrees 2θ) were measured by means of a Geiger counter x-ray diffractometer and the ratios I_{CuO}/I_{CaO} and I_{Cu_2O}/I_{CaO} were calculated. The percentage composition was determined by comparison of these ratios to those of a "working curve" constructed by mixing known amounts of high grade CuO, Cu_2O, and CaO such that the ratios of the weight of CuO + Cu_2O to the weight of CaO were again 2/1.

Results of the analysis are shown on Table II. It is apparent that Cu_2O makes up more than 90% of the bulk oxide by weight at all temperatures and pressures with the exception of two samples: 600°C, 13.6 atm and 700°C, 20.4 atm. Below 750°C there seems to be an increase in the amount of CuO with an increase in oxygen pressure. Otherwise, there is no significant change of composition with change of pressure.

Above 750°C there is no indication of change in composition with temperature. Below 800°C there appears to be a slight increase in the amount of CuO (in high pressure oxidation) with decreasing temperature. Tylecote (11), reporting the results of x-ray analysis of the oxide coatings formed in 1 hr at 600°–900°C on copper oxidized in air, concluded that there was no "regular trend" in the oxide composition with temperature. Some of Tylecote's reported values are in agreement with the results of Table II obtained at the same temperature. The variation of composition with temperature reported by Valensi (12) is much greater than shown in Table II.

Considerable disagreement exists among earlier workers as to the effect of time of oxidation on the composition of the oxide scale. The ratio of Cu_2O to CuO for constant

[1] Present address: Central Research Lab., Howe Sound Co., Salt Lake City, Utah.

TABLE I. *A summary of rate constants resulting from application of equation (I) to experimental data*

Temp, °C	Pressure atm, O_2	K_p $mg^2 \cdot cm^{-4} \cdot hr^{-1}$	Average K_p	K_l $mg \cdot cm^{-2} \cdot hr^{-1}$	K_p' determined by $W^2 = K_p^1 t$
1000	0.25	355.8	302.4	42.2	
		254.2	σ = 29.1	70.2	
	0.50	338.9	p.e. = 19.6	53.6	
		270.0		56.5	
	0.75	296.5		53.6	
		291.3		65.6	
		295.0		53.5	
	1.36	327.7		60.5	
	2.04	305.3		93.0	
	3.4	322.6		47.2	
	6.8	248.3		70.6	
		324.8		59.7	
		301.4		73.6	
	10.2	287.2		58.2	
	13.6	316.5		83.1	
900	0.026	76.6	83.1	21.5	
	0.125	78.7	σ = 13.8	19.1	
		84.6	p.e. = 9.3	25.7	
	0.250	78.7		23.6	
		75.8		25.1	
	0.500	78.8		26.8	
		84.0		30.7	
	0.750	77.4		21.4	
		83.7		33.4	
	1.00	77.0		28.1	
	2.04	120.3		35.3	
	3.4	102.6		23.3	
	6.8	71.2		30.6	
		87.7		43.3	
		89.6		47.6	
		92.9		35.6	
		87.2		50.5	
	10.2	51.5		67.5	
	13.6	82.3		39.7	
		81.7		47.6	
850	0.125	40.3	43.8	14.7	
	0.250	43.1	σ = 7.8	16.5	
	0.500	44.2	p.e. = 5.2	14.7	
	0.750	43.7		14.3	
	1.00	43.7		16.2	
	2.04	59		23.5	
		63.1		17.9	
	3.4	49.1		21.4	
	6.8	47.2		33.8	
		48.7		28.4	
		44.5		34.6	
		56.9		23.9	
	10.2	46.9		13.1	
	13.6	41.4		66.0	
	20.4	38.0		41.8	
800	0.125	19.0	19.2	9.9	
		18.8	σ = 0.5	10.4	
	0.250	19.7	p.e. = 0.3	9.5	
		19.7		11.7	
		18.8		11.3	
	0.500	19.6		10.8	
		18.5		7.4	
	0.750	19.5		9.9	
	1.00	19.9	23.2	11.9	
	2.04	24.9	σ = 1.8	12.9	
	3.4	22.8	p.e. = 1.2	24.1	
	6.8	21.9		18.1	
		23.3		37.8	
		27.7		28.6	
		22.4		37.8	
		22.4		24.8	
	10.2	24.5		20.7	
	13.6	22.8		26.5	
		22.4		55.6	
	20.4	23.4		25.1	
750	0.026	8.5	8.7	7.5	
	0.125	9.0	σ = 0.3	6.1	
	0.250	8.9	p.e. = 0.2	6.2	
		8.9		6.7	
	0.500	8.3		8.9	
	0.750	8.6		8.5	
750	1.00	8.9	11.5	10.0	
	2.04	12.4	σ = 1.8	11.4	
		12.0	p.e. = 1.2	18.4	
	3.4	7.3		887.6	
		12.5		26.2	
		12.3		18.3	
	6.8	12.6		20.9	
	10.2	12.8		12.5	
	13.6	12.6		16.9	
	20.4	11.9		20.0	
700	0.125	3.3	3.04	8.0	
		2.2	σ = 0.34	5.4	
	0.250	3.2	p.e. = 0.23	5.5	
		3.3		5.3	
		3.2		7.5	
	0.500	2.9		8.6	
		3.1		9.0	
	0.750	3.1		15.7	
	1.00	4.0	6.4	6.7	
		4.4	σ = 1.9	9.1	
		5.0	p.e. = 1.3	7.2	
		7.0		6.7	
		8.2		5.7	
		8.5		4.7	
	2.04	10.8		6.6	
	3.4	5.6		12.7	
	6.8	5.5		10.8	5.8
		7.5		8.2	
	10.2	5.8		16.4	
	13.6	5.7		−190.2	5.8
	20.4	4.7		−22.0	5.4
600	0.125	1.2	1.4	7.8	0.9
	0.250	.8	σ = 0.6	1.6	0.7
		1.4	p.e. = 0.4	3.6	1.0
	0.500	.8		12.3	0.8
		1.9		7.2	1.6
	0.750	2.3		2.3	1.2
	1.00	1.6	1.84	2.4	1.6
	2.04	1.4	σ = 0.27	75.5	1.5
		1.9	p.e. = 0.19	−32.4	1.6
		2.3		−3.7	3.0
	3.4	2.1		47.3	2.1
		1.9		−3.5	
	6.8	1.4		−53.5	1.5
		2.1		−28.5	2.1
	10.2	1.8		−9.5	1.9
	13.6	2.0		7.8	1.8
	20.4	1.7		−7.5	1.8

σ = Gaussian Distribution Standard Deviation.
p.e. = Probable Error = 0.67σ.

temperature has been reported to be both dependent on oxidation time (13–15) and to be essentially constant over a reasonable time interval (11, 12). Three samples were oxidized for longer periods of time and the coatings analyzed by the same x-ray technique described above to determine if any change occurred. Results are included in Table II. It appears that at 800°C and 6.8 atm no change

TABLE II. *Composition of the oxide coating formed on OFHC copper oxidized at various temperatures and pressures*

Temp, °C	Oxygen pressure, atm	Time of oxidation	Composition	
			% Cu_2O	% CuO
900	0.5	120 min	96.3	3.7
	13.6	120 min	97.4	2.6
850	0.25	115 min	97.0	3.0
	0.50	120 min	96.5	3.5
	6.8	100 min	95.3	4.7
	10.2	120 min	96.4	3.6
800	0.125	120 min	97.5	2.5
	0.75	120 min	96.6	3.4
	6.8	120 min	93.3	6.7
	6.8	120 min	96.2	3.8
	6.8	23 hr	96.2	3.8
750	0.125	130 min	94.7	5.3
	0.25	120 min	92.0	8.0
	3.4	120 min	93.3	6.7
	10.2	120 min	92.2	7.8
700	0.25	100 min	97.6	2.4
	20.4	115 min	88.5	11.5
600	0.25	140 min	96.6	3.4
	0.50	145 min	96.2	3.8
	2.04	120 min	91.1	8.9
	13.6	155 min	88.9	11.1
	13.6	48 hr	82.6	17.4
500	6.8	48 hr	85.3	14.7

in percentage composition occurred with time. At 600°C and 13.6 atm, however, some increase was detected in agreement with the findings of Dennison and Preece (13) who reported 22% CuO after 48 hr oxidation in air at 650°C. A sample oxidized for 48 hr at 500°C and 6.8 atm showed 15% CuO, indicating that there is no great change in the CuO present at lower temperatures.

Physical appearance of the oxide scale.—The color of the oxidized samples can be summarized as follows: 900°C, gray; 850°C, dark gray; 800°C, darker gray to soot black; 750°C, soot black; 700°C, soot black; 600°C, soot black. However, the color of all the oxides reverted to brick red on grinding.

The coatings formed at 800° and 900°C adhered to the underlying metal; there was no loss of oxide during the lowering (cooling) of the sample. At lower temperatures, 600°–700°C, some spalling occurred upon cooling the samples. In all cases the oxides formed at higher oxygen pressures were easier to remove than those formed at lower pressures, probably due to the increased thickness of the former. The high pressure coatings could be removed by flexing the samples, thereby breaking the oxide free in large slabs. This operation was not possible with the low pressure oxides; and, in the most severe cases (low temperatures and low pressures), the sample could be bent nearly 180° without cracking the film. In order to remove these films scraping was required.

Discussion of Results

Fig. 1 is the plot of the logarithm of $(K_p)_{avg}$ vs. reciprocal absolute temperature, where $(K_p)_{avg}$ is the average of K_p values of Table I, which are judged by the results of Table II to contain CuO and Cu_2O in the same proportion. A "fair" straight line can be drawn through the 700°–1000°C points of Fig. 1, which are representative of K_p values resulting from samples containing 96% Cu_2O in the oxide coating. This line yields an activation energy of 37,000 cal. Valensi (12) reports 37,700 cal from a similar type plot. Tylecote (2) published a value of 38,000 cal. Castellan and Moore (16) report 37,000 cal for the activation energy involved in the diffusion of cuprous ions in Cu_2O, and from the agreement with the oxidation activation energy it could be postulated that diffusion through the Cu_2O layer is the rate-determining step.

Oxidation data below 700°C can be correlated reasonably well by the use of the standard parabolic equation, $W^2 = K_p' \cdot t$. However, the evaluation of K_p' becomes somewhat

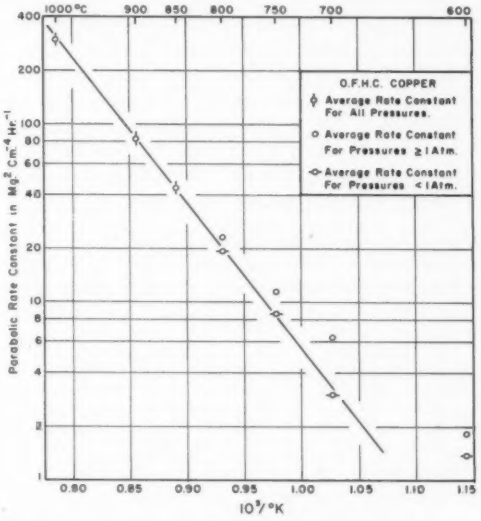

FIG. 1. Temperature dependence of average parabolic rate constants of Table I.

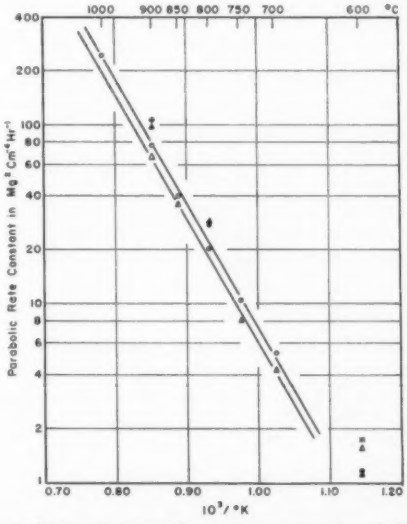

FIG. 2. Plot of logarithm of average parabolic rate constants, calculated from $W^2 = K_p't$ vs. reciprocal absolute temperature. This survey: △ = average for 1 atm; ○ = average for 6.8–20.4 atm. McKewan (3): ● = average for 1 atm; ▲ = average for 6.8–27.2 atm.

arbitrary above 700°C. For this reason equation (I) was employed. The analysis of the 600°–1000°C data above 1 atm by $W^2 = K'_p \cdot t$ is shown in Fig. 2. The average parabolic rate constants calculated from Table I (3) are also included in Fig. 2. The activation energy calculated from the slopes of Fig. 2 was 31,500 cal. In an earlier survey Tylecote (17) reported an activation energy of 31,600 cal (600°–900°C) for the oxidation in air of copper containing 0.04% phosphorus.

ACKNOWLEDGMENTS

The authors wish to thank the Office of Ordnance Research, Department of the Army, and its Watertown Arsenal Laboratory, for the funds that made this work possible. They express their thanks to Mr. Theron Odekirk who performed the bulk of the calculations involved in the preparation of Table I. Appreciation is due to Dr. John R. Lewis, Head, Dept. of Metallurgy, University of Utah, for interest shown in this project. They also acknowledge the kindness of the American Metals Co., Ltd., and its Mr. H. M. Schleicher, who graciously furnished the high purity oxygen free-high conductivity copper employed in this survey and the previous investigations (4, 18).

Manuscript received February 13, 1956.
Any discussion of this paper will appear in a Discussion Section to be published in the June 1957 JOURNAL.

REFERENCES

1. R. F. TYLECOTE, *J. Inst. Metals*, **78,** 259 (1950).
2. R. F. TYLECOTE, *ibid.*, **81,** 681 (1952).
3. W. M. MCKEWAN AND W. M. FASSELL, JR., *J. Metals*, **5,** 1127 (1953).
4. J. P. BAUR, D. W. BRIDGES, AND W. M. FASSELL, JR., *This Journal*, **103,** 266 (1956).
5. R. C. PETERSON, W. M. FASSELL, JR., AND M. E. WADSWORTH, *J. Metals*, **6,** 1038 (1954).
6. U. R. EVANS, *Trans. Am. Electrochem. Soc.*, **46,** 247 (1924).
7. U. R. EVANS, "Pittsburgh Internat. Conf. on Surface Reactions (Proc.)," p. 73, Corrosion Publishing Co., Pittsburgh (1948).
8. O. KUBASCHEWSKI AND B. E. HOPKINS, "Oxidation of Metals and Alloys," p. 43, Academic Press, Inc., New York (1953).
9. W. JOST, "Diffusion in Solids, Liquids, and Gases," p. 353, Academic Press, Inc., New York (1952).
10. C. WAGNER AND K. GRUNEWALD, *Z. physik. Chem.* (*B*), **40,** 455 (1938).
11. R. F. TYLECOTE, *J. Inst. Metals*, **78,** 301 (1950).
12. G. VALENSI, "Pittsburgh Internat. Conf. on Surface Reactions (Proc.)," p. 156, Corrosion Publishing Co., Pittsburgh (1948).
13. J. P. DENNISON AND A. PREECE, *J. Inst. Metals*, **81,** 732 (1952) (Fig. A, discussion to article on p. 229, same vol.).
14. A. DRAVNIEKS, *J. Am. Chem. Soc.*, **72,** 3761 (1950).
15. P. D. DANKOV AND D. V. IGNATOV, *Izvet. Akad. Nauk S.S.S.R.*, **1949,** (Khim.), (3), 234.
16. G. W. CASTELLAN AND W. J. MOORE, *J. Chem. Phys.*, **17,** 41 (1949).
17. R. F. TYLECOTE, *J. Inst. Metals*, **78,** 327 (1950).
18. J. P. BAUR, D. W. BRIDGES, AND W. M. FASSELL, JR., *This Journal*, **102,** 490 (1955).

Effect of Prior Corrosion History on the Corrosion of Zircaloy-2 in High Temperature Water

D. E. THOMAS AND S. KASS

Bettis Atomic Power Division, Westinghouse Electric Corporation, Pittsburgh, Pennsylvania

ABSTRACT

A method is presented which permits in a relatively short time the prediction of the corrosion behavior of Zircaloy-2 after very long exposure times in high temperature water. The technique, which is of practical value, involves changing the corrosion test temperature, and yields transient effects which are of interest from a theoretical point of view.

Zircaloy-2 is a complex alloy of sponge Zr containing 1.5% Sn, 0.12% Fe, 0.10% Cr, and 0.05% Ni (60 ppm N max) which has found extensive application. The corrosion behavior of Zircaloy-2 has been studied as a function of temperature and time, and considerable data have been reported previously (1).

The corrosion behavior of Zircaloy-2 is shown by the dotted lines in Fig. 1 and 3 in which the weight gain is plotted vs. exposure time on logarithmic scales. The curve for corrosion in 750°F (400°C) degassed steam at 1500 psi shows a change in slope at a weight gain of 40 mg/dm² in the vicinity of 40 days. It will be noted in Fig. 1 that in 680°F (360°C) degassed water, an inflection in the log weight gain-log time curve normally occurs at a weight gain of approximately 35 mg/dm² after an exposure of about 115 days. No inflection or slope changes are observed in the 600°F (315°C) or 550°F (288°C) tests, evidently because very long exposures would be required to reach the weight gain at which the change in slope occurs at the lower temperature.

The term "breakaway" has been used to describe the abrupt change in slope mentioned above in the case of

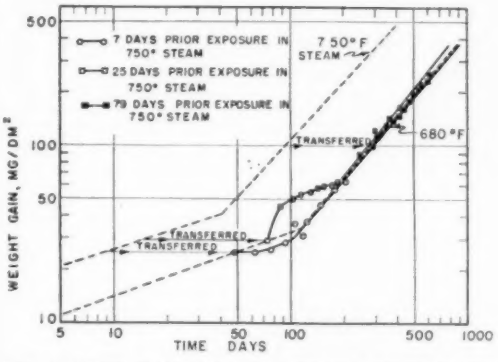

FIG. 1. Effect of transferring Zircaloy-2 corrosion specimens from higher temperatures on corrosion behavior at 680°F (360°C).

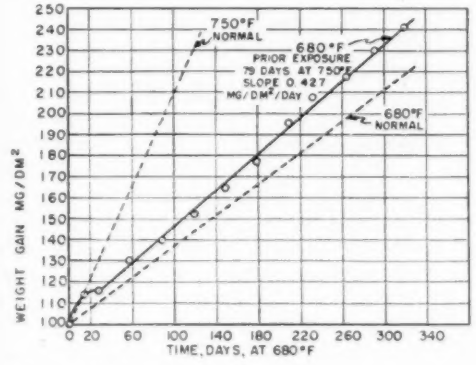

FIG. 2. Linear plot of weight gain vs. time at 680°F (360°C) subsequent to transfer from corrosion test at 400°C.

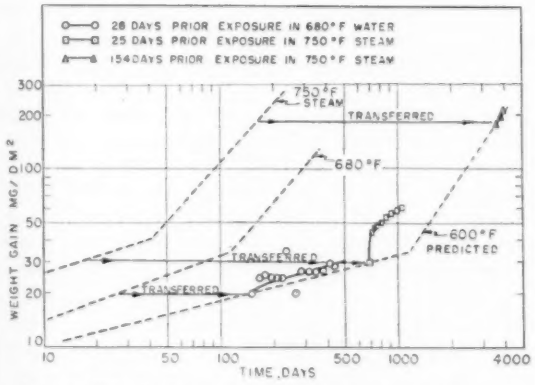

FIG. 3. Effect of transferring Zircaloy-2 corrosion specimens from higher temperatures on corrosion behavior at 600°F (315°C).

Zircaloy-2, its usage having been carried over from the behavior of unalloyed Zr. Since for unalloyed Zr "breakaway" signifies the beginning of spalling of the corrosion product, and since for Zircaloy-2 the kinetics change without spalling of the oxide, the term "transition" will be used here in connection with Zircaloy-2. The corrosion rate of Zircaloy-2 is constant after the transition and amounts to 1.1 mg/dm²/day at 750 (400°C) and 0.37 mg/dm²/day at 680°F (360°C). In view of the low value of this post-transition corrosion rate, much of the useful life of Zircaloy-2 accrues in this period. The purpose of the work described here was to determine the post-transition corrosion rate at 600°F (315°C) by a short-cut method which would avoid the long exposure times indicated in Fig. 3. It is estimated that 1150 days would be required to reach the transition at 600°F (315°C).

The short-cut method consists of exposing specimens at a high temperature for a time sufficient to pass the transition and subsequently transferring them to a lower temperature for corrosion rate measurement. The validity of such a procedure depends on the corrosion mechanism remaining unchanged in steam and water in the temperature range under consideration. The corrosion behavior of Zircaloy-2 suggests that this is the case (1).

In addition, specimens were transferred from exposures at one temperature to another before transition in the hope of obtaining transient effects which may aid in understanding the mechanism of corrosion.

Experimental Procedure

Specimens of Zircaloy-2, measuring 1 in. x 0.5 in. x 0.1 in., were vacuum annealed for 1 hr at 800°C and furnace-cooled. After having been bright etched in 38% HNO_3—5% HF—57% H_2O, ten specimens were exposed according to each of the following schedules:

Initial Exposure	Final Exposure
7 days at 750°F (400°C) (1500 psi)	680°F (360°C) (2705 psi)
25 days at 750°F (400°C) (1500 psi)	680°F (360°C) (2705 psi)
79 days at 750°F (400°C) (1500 psi)	680°F (360°C) (2705 psi)
28 days at 680°F (360°C) (2705 psi)	600°F (315°C) (1553 psi)
25 days at 750°F (400°C) (1500 psi)	600°F (315°C) (1553 psi)
154 days at 750°F (400°C) (1500 psi)	600°F (315°C) (1553 psi)
154 days at 600°F (315°C) (1500 psi)	750°F (400°C) (1500 psi)
28 days at 680°F (360°C) (2705 psi)	750°F (400°C) (1500 psi)

Weight gains were determined periodically during the initial and final exposures. The corrosion product was not removed when the specimens were transferred.

Results

In general, data pertaining to all transfers to a given temperature are represented on a single log weight gain vs. log exposure time plot. In analyzing the data the accumulated weight gain was plotted against the exposure time after transfer for each experiment, e.g., Fig. 2. The results of tests which involve transfer after the transition time are presented first since these bear directly on the main purpose of the work. The results of tests which involve transfer before the transition show interesting transient effects and are presented separately.

Transfers after Transition

The group of specimens which was first exposed to 750°F (400°C) steam for 79 days then transferred to 680°F (360°C) water corrode at the latter temperature essentially as would be expected for samples having the same weight gain attained by exposure at the lower temperature (*see* Fig. 1 and 2). The post-transition corrosion rate calculated for the transferred specimens is 0.42 mg/dm²/day as compared to 0.37 mg/dm²/day for those specimens exposed only to 680°F (360°C) water. If the

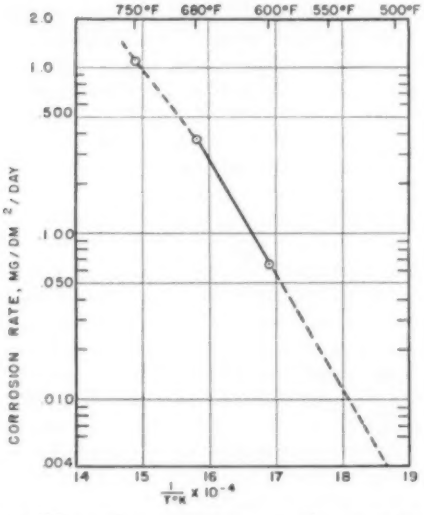

FIG. 4. Effect of temperature on the post-transition corrosion rate of Zircaloy-2 in water and steam.

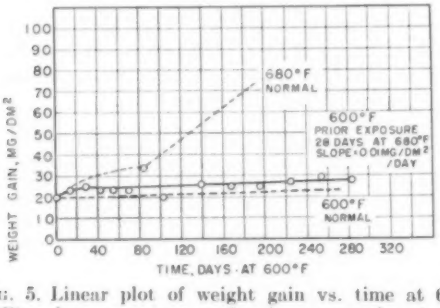

FIG. 5. Linear plot of weight gain vs. time at 600°F (315°C) subsequent to transfer from corrosion test at 680°F (360°C).

transient effect is disregarded for the moment, it is seen that the specimens initially exposed in 750°F (400°C) steam for 25 days eventually corrode at a post-transition rate of 0.46 mg/dm²/day when transferred to 680°F (360°C) water. Thus it is seen that the post-transition corrosion rate determined by the transfer method is in essential agreement with that obtained by continuous exposure.

A similar procedure was used to determine the post-transition corrosion rate at 600°F (315°C). Data for a group of specimens exposed for 154 days in 750°F (400°C) steam prior to exposure in 600°F (315°C) water are presented in Fig. 3. The linear portion of the corrosion curve so obtained has a slope of 0.065 mg/dm²/day. Using this post-transition corrosion rate it is possible to complete the corrosion curve for 600°F (315°C). In order to do this it is necessary to assume a value for the weight gain at the transition point. The corresponding weight gain values at higher temperature are 100 mg/dm² in 850°F (455°C) (1500 psi) steam, 51 mg/dm² in 750°F (400°C) (1500 psi) steam, and 34 mg/dm² in 680°F (360°C) water. Thus the weight gain at transition decreases with decreasing temperature, and the data suggest that with decreasing temperature the transition weight gain approaches a limiting value. It does not appear possible to make an accurate extrapolation to lower temperatures on the basis of existing data. A similar situation arises when an extrapolation of time to transition is attempted. It was therefore assumed that the transition weight gain is the same at 600°F (315°) and 680°F (360°C). Thus a transition point on the 600°F (315°C) curve in Fig. 3 was selected at 34 mg/dm² which corresponds to an exposure time of 1150 days. Beginning at this point a line was drawn corresponding to the experimentally determined post-transition corrosion rate of 0.065 mg/dm²/day.

The temperature dependence of the post-transition corrosion rate is illustrated in Fig. 4. Considering only the two points corresponding to corrosion in the liquid phase, an activation energy in the neighborhood of 32,000 cal/mole is suggested. This is about three times the activation energy for the rate constants applicable to corrosion prior to transition.

Transfer before Transition

Those specimens which were first exposed for a time insufficient to reach the transition and subsequently exposed at a lower temperature show a peculiar tendency for the corrosion rate characteristic of the high temperature to persist for considerable times after transfer to a lower temperature. An example of such memory behavior is seen in Fig. 3 for specimens transferred to 600°F (315°C). In Fig. 5 the actual data points may be compared with the curve which would have been followed had the exposure continued at 680°F (360°C) and the curve which would have been followed had the specimens been continuously exposed at 600°F (315°C). Data points tend to follow the former curve for a time and then to become parallel to the latter curve. Similar behavior is illustrated in Fig. 1 and 3. In Fig. 1 the memory phenomenon is seen to persist for about 100 days after transfer, and the transition weight gain appears to be shifted to a higher value for specimens transferred after 25 days at 750°F (400°C).

On the other hand, specimens transferred to 680°F (360°C) after 7 days in 750°F (400°C) steam do not show the memory phenomenon. The data points do not differ significantly from the expected curve for 680°F (360°C) exposure.

It should be noted that specimens transferred from a higher temperature to a lower temperature after transition

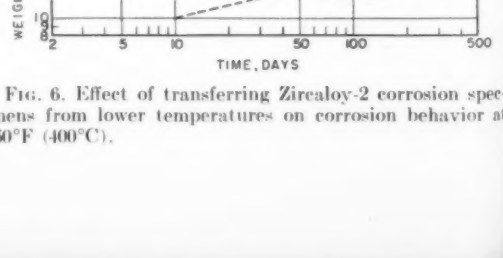

FIG. 6. Effect of transferring Zircaloy-2 corrosion specimens from lower temperatures on corrosion behavior at 750°F (400°C).

also exhibit a memory behavior as may be seen in Fig. 1 and 3.

Two experiments were performed in which the specimens were exposed first at a low temperature then at a higher temperature. Results are shown in Fig. 6. There is a slight indication that the corrosion rate after transfer is initially less than would be normally expected at the higher temperature.

Discussion

Determination of post-transition corrosion rates by the transfer technique appears to be reasonably reliable and accurate. It is believed that this technique can be applied to other alloys of the Zircaloy type, that is, alloys containing 0–2.5% tin with up to 0.5% total Fe, Ni, and Cr, since it is known that such alloys exhibit similar behavior in steam and in water.

The curious memory phenomenon should be explicable in terms of the corrosion mechanism. For the purpose of this discussion it is convenient to consider two aspects of the corrosion of Zircaloy-2, the first being the initial diffusion-controlled period, and the second the termination of the diffusion-controlled period.

The oxide film formed during the pretransition period is believed to grow by the diffusion of oxygen ions via oxygen ion vacancies from the water/oxide interface to the metal/oxide interface. It would be expected that an oxide film of a given thickness grown at a high temperature would have a greater oxygen ion vacancy gradient than that grown at a lower temperature. It is not surprising then that transfer to a lower temperature would result in an initially higher corrosion rate which persists until the excess anion vacancy gradient is removed. Referring to a particularly well defined case of the memory phenomenon shown in Fig. 5, it is seen that the increment of weight gain resulting from the memory phenomenon is about 4 mg/dm² for samples transferred when the weight gain was 20 mg/dm². At first glance it may appear that the number of vacancies which were filled is the difference between the total anion vacancy content of the film grown at the higher temperature and that of a film of the same thickness grown at the lower temperature, and to fill this number of vacancies apparently required 4 mg/dm² of oxygen. This implies that in excess of 20% of the oxygen ion sites in the ZrO_2 lattice are vacant, and is far greater than is to be expected. However, the more rapid corrosion rate associated with the presence of the excess vacancy gradient immediately after transfer must also result in a correspondingly continued rapid rate of generation of vacancies at the advancing metal/oxide interface. Thus, the passage of many more vacancies than suggested above would be required before the corrosion rate decays to normal.

It will be noted in Fig. 1 that no memory was observed for those samples transferred to 680°F (360°C) after having been exposed for 7 days at 750°F (400°C). This appears to be inexplicable on the basis of diffusion of excess vacancies. Since these specimens have a thinner oxide than any of the other specimens at the point of transfer, a smaller transient would be expected. However, a marked transient was observed for specimens transferred after 25 days and having only a slightly greater oxide thickness at transfer as may be seen in Fig. 5.

Alternatively, the memory phenomenon may be thought of as a premature and temporary termination of the diffusion-controlled period as a result of disturbances accompanying the temperature change. It has been suggested that the transition normally results when the pickup of hydrogen during corrosion causes hydride to form at the metal oxide interface. Since the solubility of hydrogen decreases with decreasing temperature, it is suggested that the memory phenomenon may result when the exposure at the higher temperature causes the hydrogen content at the metal/oxide interface to exceed the solubility limit characteristic of the lower temperature so that transition sets in upon transfer to the lower temperature. Upon continued exposure at the lower temperature the hydride may dissolve and the hydrogen diffuse away from the metal/oxide interface and cause the corrosion behavior to revert to normal as in Fig. 5, or, alternatively, normal transition characteristic of the lower temperature may begin as in Fig. 1 (25 day samples) before the hydride can diffuse into the bulk of the sample. The lack of the memory phenomenon shown in Fig. 1 (7 day samples) may be explained on the basis that at the higher temperature the hydrogen content at the metal/oxide interface did not exceed the solubility characteristic of the lower temperature, since the samples were held for only 7 days at 750°F (400°C) before transfer as compared to 25 days for the samples which exhibited a transient effect. Such an explanation is open to question, however, since current work indicates that the transition occurs in pure dry oxygen at the same time and weight gain as it does in steam, suggesting that hydrogen is not a factor.

The termination of the diffusion-controlled corrosion process evidently occurs when a critical oxide thickness characteristic of the exposure temperature is reached. When the critical oxide thickness is exceeded, structural faults such as cracks due to stresses developed in the film may occur. Since the critical oxide thickness increases with temperature, it seems reasonable to assume that stress in a film of a given thickness at a higher temperature is less than that in a film of the same thickness at a lower temperature. Thus, upon transfer from a high temperature to a low temperature, stress in the oxide film would be less than would be normal at the lower temperature, and it should be possible for the oxide to grow to a greater than normal thickness before transition occurs. Such a situation appears to exist in Fig. 1 (25 day samples) and Fig. 3 (25 day samples) which show corrosion rates at 80 and 420 days, respectively, which are less than post-transition rates, while the oxide thickness (weight gain) exceeds considerably the critical oxide thickness characteristic of continuous exposure of the lower temperature.

The memory phenomenon thus appears to be explicable, except in one anomolous case, on the basis of the anion diffusion process, on questionable ground with regard to the formation of hydride at the metal/oxide interface, and only partially explicable on the basis of stress in the oxide film.

In the practical sense the memory phenomenon suggests that on varying the temperature cyclically the effective

corrosion temperature is very close to the maximum temperature of the cycle.

Conclusions

The linear corrosion rate of Zircaloy-2 which occurs at very long exposure times at low temperatures can be determined in a relatively short time by measurement of the corrosion rate at the low temperature in question after sufficient previous exposure at a higher temperature to reach the linear portion of the weight gain-time curve. This technique should be applicable to other alloys of the Zircaloy type.

The transient effects which persist for a time after a change of temperature has been effected are discussed in terms of several aspects of corrosion mechanism. No completely satisfactory explanation of this behavior is offered.

Acknowledgment

This work was performed under AEC Contract AT-11-1-GEN-14.

Manuscript received October 13, 1955.
Any discussion of this paper will appear in a Discussion Section to be published in the June 1957 Journal.

REFERENCE

1. "Metallurgy of Zirconium," edited by B. Lustman and F. Kerze, Vol. 4, Div. VII, NNES, Chap 11, McGraw-Hill Book Co., New York (1955).

Natural and Thermally Formed Oxide Films on Aluminum

M. S. Hunter and P. Fowle

Aluminum Research Laboratories, Aluminum Company of America, New Kensington, Pennsylvania

ABSTRACT

Structure and rate of formation of natural and thermally formed oxide films on Al are discussed. It is shown that these films consist of a layer of barrier-type oxide, the thickness of which is primarily a function of temperature, and a porous layer, the thickness of which is determined by time and natural forces associated with the environment. Effects of temperature and environment on the formation rate and ultimate thickness of these layers are described.

One of the outstanding merits of Al is its remarkable resistance to atmospheric corrosion. This is somewhat surprising in view of its high position in the activity series. The reason for such high resistance to attack is the oxide film provided Al by nature. Although this film is extremely thin and thus easily damaged, it has such remarkable self-healing properties that, if damaged, it immediately starts to reform. The manner in which the natural oxide film forms on Al, its structure, and some of the factors affecting its rate of growth and ultimate thickness are discussed in the present paper.

Published information has revealed many interesting and valuable facts regarding the nature of natural films on Al. It has been shown that in dry oxygen at room temperature the natural film reaches an ultimate thickness of about 10Å in a matter of minutes (1). Various investigators, however, have demonstrated that the film formed in ordinary air is much thicker and takes weeks, months, and even years to reach its ultimate thickness (2–4). It has been suggested that films formed in the former case are impermeable barrier-type films; in the latter case, although the film still has a compact barrier type of film adjacent to the metal, it also has an outer layer of porous or more permeable oxide (5).

Method

The principal method of measurement used in this investigation, described in detail in a previous publication (6), is a simple electrical procedure capable of measuring the thickness of compact barrier-type oxide films with high accuracy. This method is based on the mechanism of film formation on an Al anode in an electrolyte that does not dissolve the oxide. Under these conditions, 1 v of applied potential forms oxide to a maximum thickness of 14Å on the metal surface, after which only leakage current flows. When voltage is applied gradually to a sample having a barrier oxide layer, the voltage required to produce current flow just equal to normal leakage is a measure of the thickness of the oxide barrier layer; multiplying this voltage by 14 gives the thickness in Ångstrom units. It has been found that this method measures only oxide films of the compact barrier type and that it is capable of measuring the thickness of such films with an accuracy of about 3Å.

The measuring procedure consists, briefly, of making the specimen the anode in a 3% solution of $C_4H_6O_6$ adjusted to a *p*H of 5.5 with NH_4OH. Potential is applied gradually and thickness is determined from the voltage required to produce normal leakage current.

Natural Films on Al

In the preliminary stage of the present work, the barrier measurement method was applied to a number of samples of Al and Al alloy sheet that had been stored in the laboratory at room temperature for periods of from one week to several years. It was found that on every specimen a

definite barrier could be measured, and that it was the same, approximately 10Å, on each, regardless of the storage period.

This thickness is the same as that which was observed to form on Al in dry oxygen. Thus, this value apparently represents the greatest thickness of barrier-type oxide which can be formed at room temperature, regardless of time and environment. As such, it probably represents the distance through which Al can move under the forces of thermal agitation associated with temperature, or under the influence of the potential field within the coating suggested by Mott (7). This situation is analogous to that observed in anodically formed barrier-type oxide films where the operative force is the applied potential. On this basis, it would appear that the forces controlling the formation of natural and anodically formed films on aluminum are basically the same.

As has been mentioned, a number of investigators have demonstrated that the film formed on Al at room temperature is much thicker than 10Å, the actual thickness depending on the time and the atmospheric conditions under which the film is formed. It is evident, therefore, that the natural film formed in a normal atmosphere must consist of two layers. Adjacent to the metal is a compact layer of barrier-type oxide. Covering the barrier layer is an outer layer that does not respond to the barrier measurement; therefore, it must be of a more permeable type of oxide. Since it has been shown that a film formed in a moist atmosphere contains an appreciable amount of water (8), this outer layer is probably formed from the barrier oxide by hydration.

The natural film on Al can be visualized as the net result of the competition between opposing forces—those tending to build up a compact oxide barrier layer, and those tending to break it down. The ultimate structure of the oxide depends on the relative rates of these competing forces. If the destructive forces are absent, the natural film will be of the barrier type and will form rapidly to a limiting thickness. If the destructive forces are predominant, oxide may be broken down almost as fast as it is formed, and little barrier will remain. In the intermediate range, in which the constructive and destructive forces can reach a reasonable balance, relatively thick natural films are formed.

Natural Barrier Formation in Moist Air

In the formation of natural barrier-type films in moist air, both destructive and constructive forces are at work. At any temperature, as shown in Fig. 1, barrier thickness rises gradually to a limiting thickness under the conditions of the experiment. The rate of oxide formation is probably the same as in the absence of moisture, but the destructive effect of the environment is relatively great, with the result that the net thickness of barrier oxide increases slowly. Ultimate barrier thickness increases with temperature, which gives support to the theory that thermal agitation controls barrier thickness. When the ultimate thickness has been reached, horizontal portions of Fig. 1, the barrier no longer thickens, but barrier oxide formation may still be taking place. In this case, a balance has been established between the forces of formation and breakdown, and although barrier thickness remains constant, the total thickness of the film may still be increasing.

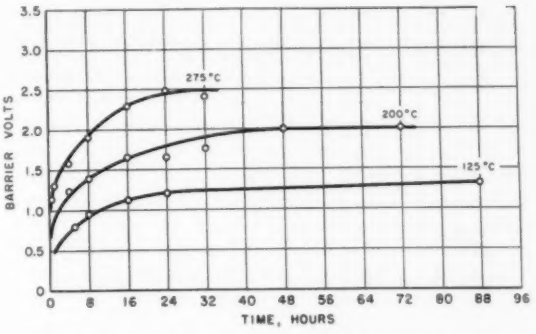

Fig. 1. Growth of oxide films on high purity aluminum in moist air.

A more direct indication of the destructive action of atmospheric moisture on the natural film was observed from the change in the barrier layer thickness of films formed at one temperature and then held at a lower temperature in humid atmospheres. A sample heated at 200°C for a sufficient time to build the barrier portion of the film to its ultimate thickness of 28Å was stored at room temperature in air saturated with water vapor. At the end of 48 hr the barrier thickness had dropped 9Å, a loss of about 30%.

Additional evidence of the destructive effect of the environment is the fact that the assorted samples stored at room temperature, which were discussed earlier, all had the same barrier thickness. Several of these specimens undoubtedly had initially high barrier layer thicknesses because they had been exposed to temperatures as high as 538°C (1000°F), but by the time they were measured the barrier layer had decreased to the thickness corresponding to that of a film formed at room temperature. From this it is apparent that, in the presence of destructive environmental forces, the thickness of the barrier portion of a natural oxide film, regardless of the temperature at which it was originally formed, tends toward a steady-state value determined by the temperature of its environment.

Natural Barrier Films Formed in Dry Air and Dry Oxygen

In the formation of natural films in the absence of moisture, only the constructive forces are at work. Under such conditions, the times required to complete barrier formation are much shorter, as shown by Fig. 2. Even at low temperatures, such as those shown in Fig. 1, the ultimate thickness of barrier is reached in an hour or less in contrast to the 12–36 hr periods required in the presence of moisture. As with moist air, an ultimate barrier thickness is reached for any given temperature and, of even greater importance, the ultimate thicknesses are the same in both environments. In the present case, however, film growth has probably ceased when the ultimate barrier thickness is attained.

As the temperature of film formation is increased, unusual behavior in the time-barrier voltage curve is encountered beginning at about 475°C. At this temperature,

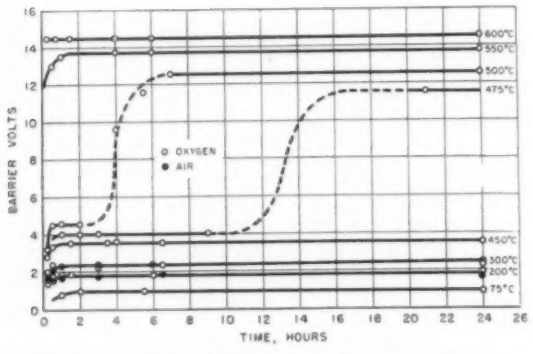

FIG. 2. Growth of oxide films on high purity aluminum in dry atmospheres.

a constant barrier thickness is reached rapidly, but, if formation time is prolonged, barrier values begin to increase for a second time. At higher temperatures, such as 500°C, two plateaus are again observed, but the time required to reach the first plateau and the time before the second rise are shorter than at the lower temperature. At still higher temperatures, the first plateau is lost and barrier values rise rapidly to high steady levels. Thus, at intermediate temperatures two different barrier thicknesses are measured; at low and at very high temperature only one barrier thickness is measured. In all cases, however, there is a constant increase in ultimate barrier thickness with increasing temperature at both the low and high levels.

From these curves, it is evident that at any given temperature the ultimate barrier thickness is the same in dry air and slightly moist air as it is in dry oxygen. It is apparent, therefore, that the maximum possible barrier thickness is a function only of temperature.

Structure of Natural Oxide Films

Electron microscopy and electron diffraction revealed that the unusual behavior of the curves shown in Fig. 2 was associated with the structure of the oxide. The barrier films represented by the first plateau are amorphous in nature; those represented by the upper plateau are a crystalline form of Al_2O_3, namely η-alumina. In the intermediate temperature range, the two-step curve indicates, first, the formation of an ultimate thickness of amorphous barrier and, later, the formation of an ultimate thickness of crystalline barrier. It is apparent that at intermediate temperatures the rate of amorphous barrier formation is much more rapid than the crystallization of this material to form the crystalline barrier. At higher temperatures, the rate of crystallization rises rapidly, occurring about as rapidly as oxide is formed, and the only ultimate barrier thickness observed is that of the crystalline barrier.

By following the progress of crystallization by electron microscopy and electron diffraction, the actual crystallization of amorphous oxide to crystalline oxide was observed, as shown by Fig. 3. At low temperatures, or at intermediate temperatures for short times, only amorphous oxide was found by both methods (Fig. 3A). After longer times at intermediate temperatures or very short times at high

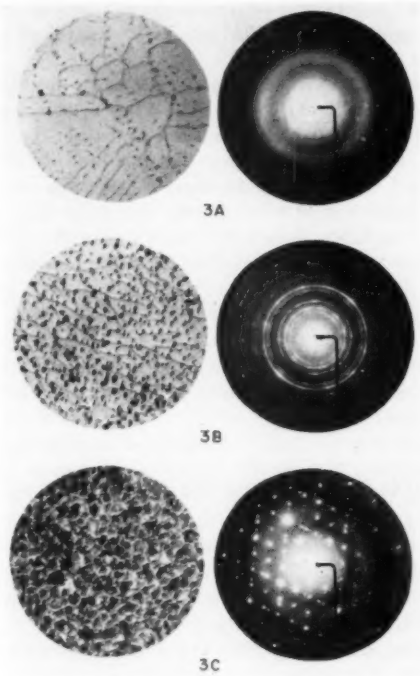

FIG. 3. Progress in crystallization of thermally formed films on aluminum as shown by electron micrographs (left) at 15,000× (before reduction for publication), and electron diffraction patterns (right).

temperatures, crystals of η-alumina were observed by the electron microscope and partial crystallinity was indicated by electron diffraction (Fig. 3B). After long periods at intermediate and high temperatures, complete crystallinity was apparent in the microstructure and diffraction patterns (Fig. 3C).

Ultimate Thickness of Natural Barrier Films

If the ultimate thickness of natural barrier films is considered in relation to the temperature of formation, it is found that barrier thickness is a linear function of temperature as shown by Fig. 4. In this plot, which shows a two-part curve, the lower portion represents the ultimate thickness of amorphous barrier which can be formed; the

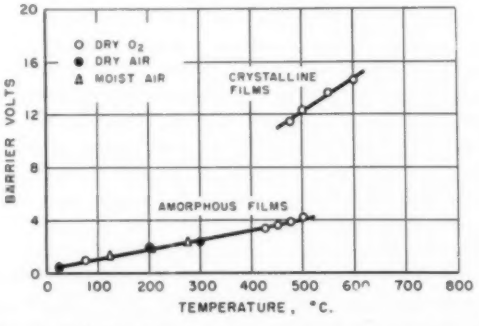

FIG. 4. Relationship between temperature and barrier thickness of natural oxide films on aluminum.

upper part represents the ultimate thickness of crystalline barrier which can be formed. Measurements made in extremely short times would probably extend the amorphous barrier curve to higher temperatures. Also, if samples were held at temperature for sufficient time, it should be possible to extend the curve representing crystalline barriers into the temperature range of 250°–450°C, which is the range in which η-alumina first forms.

From the values shown for ultimate amorphous barrier thickness, it is apparent that this ultimate thickness is a function of temperature rather than environment, since the ultimate thicknesses for moist air, dry air, and dry oxygen all fall on the same line. This would hold true in the case of moist air only if the rate of hydration was not too great. In the case of other environments which could supply sufficient oxygen to form the film but which were highly destructive to the oxide, the ultimate barrier thickness might never be reached.

In view of the linear relationship between barrier thickness and temperature, it is possible to derive a factor for natural barrier films which is analogous to the unit barrier thickness of anodically formed barrier type films. On the basis of the data presented in Fig. 4, it is apparent that about 10Å of amorphous barrier oxide is formed for each 100°C increase in temperature, whereas crystalline films appear to be formed at a rate of about 28Å for each 100°C rise in temperature.

Summary and Conclusions

Naturally and thermally formed films on Al must consist basically of two layers, a layer of compact barrier-type oxide in contact with the metal and an outer layer of more permeable oxide. The barrier layer is formed by the simple combination of Al and oxygen and exhibits rectifying characteristics similar to those of anodically formed barrier films. The maximum possible thickness of this natural barrier is controlled by temperature alone, in the same manner that the thickness of an anodic barrier film is controlled by the applied voltage. In the case of natural barrier oxide, this thickness is probably a function of thermal agitation on the atomic scale which, in turn, is a function of temperature. These natural barrier films may be either amorphous or crystalline, depending on whether they are formed below or above the temperature required to form η-alumina.

The outer portion of natural and thermally formed films is created from the barrier layer by reaction of the compact oxide with components of the environment, principally moisture. It is different from the barrier oxide in that it passes current freely in either direction, in this respect being similar to the porous portion of anodically formed oxide films. The thickness of the outer portion of natural oxide films is a function of time and the destructive effects of the environment, since the creative forces attempt to form the barrier layer to its maximum possible thickness and thus continue to furnish material for the formation of the outer layer.

Although this work has been confined solely to aluminum, it is likely that similar situations exist with films on zirconium, titanium, tantalum, and any other metal which characteristically develops a natural film of the compact barrier type.

Acknowledgment

The authors wish to express their appreciation to F. Keller under whose direction this work was conducted.

Manuscript received October 13, 1955. This paper was prepared for delivery before the Pittsburgh Meeting, October 9 to 13, 1955.

Any discussion of this paper will appear in a Discussion Section to be published in the June 1957 Journal.

REFERENCES

1. F. Keller and J. D. Edwards, *Metal Progr.*, **54**, 37 (1948).
2. G. Hass, *Optik*, **1**, 134 (1946).
3. A. Steinheil, *Ann. Physik*, **19**, 465 (1934).
4. N. Cabrera and J. Hamon, *Compt. rend.*, **225**, 59 (1947).
5. F. Keller and J. D. Edwards, *Metal Progr.*, **54**, 200 (1948).
6. M. S. Hunter and P. Fowle, *This Journal*, **101**, 481 (1954).
7. N. F. Mott, *Trans. Faraday Soc.*, **43**, 429 (1947).
8. F. Keller and J. D. Edwards, *Metal Progr.*, **54**, 196 (1948).

The Tin-Steel Couple in Air-Free Citric Acid Solution

E. L. Koehler

Armour Research Foundation of Illinois Institute of Technology, Chicago, Illinois

ABSTRACT

In air-free citric acid solution, specimens of uncoupled black plate were found to evolve hydrogen at rates equivalent to the dissolution rates of the steel. Additions of up to 0.3 g $SnCl_2 \cdot 2H_2O$/liter progressively decreased corrosion rates. Tin is anodic to and protects steel sacrificially in solutions containing dissolved tin. Hydrogen evolution is decreased by coupling steel to tin, not solely by inhibition but also by an apparent shift in the anodic polarization curve of the steel. All observed effects on the corrosion rates in this medium, whether traceable to the steel, dissolved tin inhibitor, or coupling to tin, appear to be the results of variations in anodic properties.

Solutions of citric acid have been used a number of times to study the corrosion of tin-steel couples with the idea that such studies are representative of corrosion in fruit-containing cans (1–3). While it is not considered here that this medium may be used directly to evaluate factors contributing to the shelf life of cans, it appears evident that the corrosion mechanisms involved will be similar in many respects to those in canned fruit. The advantage in using citric acid solution rather than food for fundamental studies are easy preparation, greater reproducibility and, presumably, a simpler corrosion mechanism. The purpose of this work is to elucidate the corrosion mechanisms of the tin-steel couple in air-free citric acid solution.

Experimental

The steels used in this work were in the form of full-hard, cold-rolled sheets of typical tin-plate compositions, and were electrocleaned in hot sodium orthosilicate solution. They were all annealed at 650°C. The protective atmosphere used was either dry hydrogen or wet hydrogen. It is known that wet-hydrogen annealing produces a "pickle-lag" in the steel, a condition traceable to oxidation of the grain boundaries in a surface layer of metal (4). It has been found[1] that this condition causes poor internal corrosion resistance. It was thus possible to include one factor in this work which is known to influence the shelf life of cans.

After annealing, the steel pieces were wrapped in paper and stored in a desiccator until used. The storage time in the desiccator apparently had no significant effects on test results. Steel surfaces were bright and clean. Care was taken not to touch them with the fingers, or otherwise alter them after electrocleaning. Specimens were tested with the surfaces in this condition, without abrading or any other type of preparation.

Steel specimens cut from the sheet were 6 cm x 4 cm (48 cm^2 area). For purposes of coupling these to tin, two parallel cuts, 2 mm apart, were made from the center of a 4 cm edge to the center of the specimen. The 3 cm long ribbon thus formed was bent up at right angles to the specimen.

The tin used was rolled to about 0.145 in. thickness and cut into 3.5 cm squares (24.5 cm^2). A hole, approximately 6 mm in diameter, was punched in the center. The ribbon projecting from the steel specimen was passed through this hole, and a tapered glass pin was forced through it, pressing the steel ribbon into the softer tin and giving intimate contact. The tin used was commercial Grade A Longhorn tin; the same lot was used throughout the test work. Prior to use, tin specimens were electrocleaned and treated for 5 min in cold, concentrated HCl solution.

Testing was done in Pyrex glass cells, of the type shown in Fig. 1. The test couple or steel specimen rested on the bottom of the cell, held in an almost vertical position by contact of the glass pin against the side of the cell.

The citric acid solution was 0.2M (*p*H 1.9). Solutions were prepared from redistilled water and reagent grade chemicals. Air was expelled from the solution by heating to boiling, followed by flushing with nitrogen while cooling to the filling temperature. This was done in a special flask designed for filling the cells without introducing any air. Cells were flushed with nitrogen gas prior to filling. They were filled by suction, and the height of citric acid solution in the attached buret was adjusted to zero. Cells were then put in a constant temperature water bath. Silicone stopcock grease was used in all stopcocks and in the ground glass joints. Tygon flexible tubing was used in filling the cells. A point was made of never permitting the solution to contact rubber.

The level in the water bath was about 1 in. above the top of the cells. Testing temperature was usually 60° ± 0.05°C, although some work was done at 55° and 37.78°C. During the test, hydrogen gas was evolved and collected in the top of the cell, where it was held at the temperature of the water bath. This displaced citric acid solution through the hooked tube and up the buret, where it was measured. The top of the buret was closed off by means of a rubber bulb, and the displaced nitrogen from the buret went into this bulb. Data were taken for tin and steel weight losses and for the volume of hydrogen gas evolved.

The volume of hydrogen evolved is reported in several ways. Where it was desired merely to make a comparison of relative evolution rates, it is reported as "indicated" hydrogen, which indicates a direct buret reading, or "uncorrected" hydrogen, which is corrected only for the pres-

[1] By prune pack tests at the American Can Co.

sure corresponding to the height of the liquid in the buret. Where it was desired to compare the amount of hydrogen evolved with the equivalent of the metals taken into solution, corrections are made to STP. In calculating the hydrogen equivalent of the metals taken into solution it is assumed that iron is oxidized to the ferrous state and tin is oxidized to the stannous state.

Potential Cells

For making potential measurements, another type of corrosion cell was used (Fig. 2). The potential cell was positioned in the constant temperature bath, the bridge cell and reference electrode being outside the bath. Hydrogen gas was again measured by means of a buret to correlate potential measurements with hydrogen evolution rates. Lead wires were not exposed to the solution, since the two vertical tubes shown were filled with nitrogen. Steel specimens were the same as volume cell specimens. The 2 mm ribbon was spot welded to an iron lead wire.

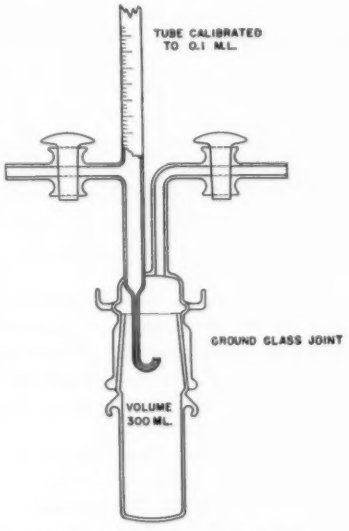

FIG. 1. Gas measuring cell

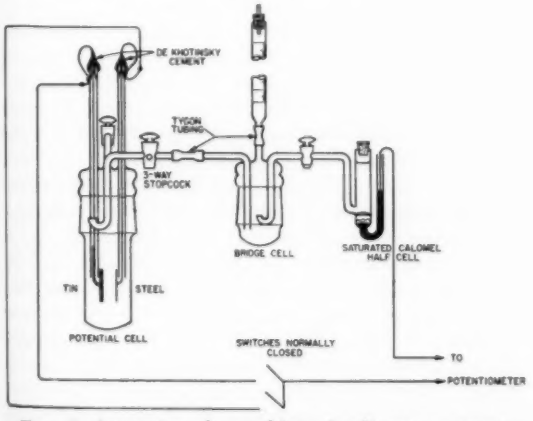

FIG. 2. Apparatus for making simultaneous measurements of hydrogen evolved, uncoupled tin potential, uncoupled steel potential, and potential of the couple.

The tin anodes used were cast disks of the same surface area as the square rolled anodes used in the volume cells. The disk was cast with a projection, bonded to an iron lead wire as indicated. The tops of the lead-in tubes were sealed with "De Khotinsky" hard cement.

The corroding potential of the couple against the reference electrode was followed throughout the period of the test. This potential was effectively at the position of a point midway between the tin and the steel. Uncoupled potentials for tin and the steel were also measured throughout the corrosion period. Such potentials naturally shift after uncoupling. Measurements indicated were made one minute after uncoupling for reasons to be given later. An indication of the magnitude of protective current was determined by the potential drop across a 10 ohm resistance or by using a zero-resistance ammeter.

TESTS ON UNCOUPLED STEEL

No difficulties were encountered in making tests on uncoupled steel in 0.2M citric acid solution at 60°C. Reproducibility of results was excellent. Typical results for a dry hydrogen annealed steel are given in Fig. 3 for seven volume-type cells. All seven tests were started at the same time; they were discontinued after varying time intervals up to five hours. After an initial period, hydrogen was evolved at the theoretical rate. The difference between the two curves represents hydrogen which goes into solution in the steel or in the citric acid solution, or possibly hy-

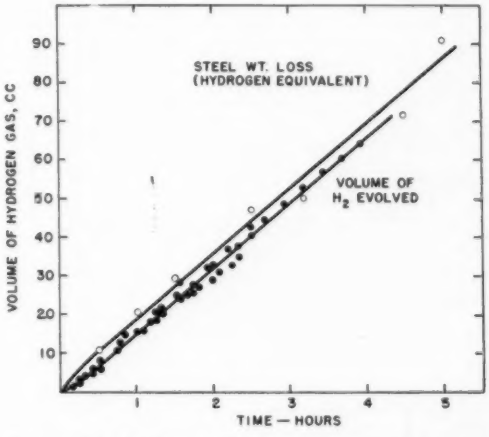

FIG. 3. Weight loss and hydrogen evolved for an uncoupled dry hydrogen annealed steel (steel J). ● = hydrogen volumes corrected to 0°C and 760 mm Hg for the seven tests; ○ = hydrogen equivalents of the steel weight losses.

TABLE I. *Results of tests on uncoupled steels*

Steel	Rate of hydrogen evolution—cc/hr	
	Dry H_2 annealed	Wet H_2 annealed
J	26.6	51.2
G	27.0	60.4
W	39.3	51.3
X	24.4	28.2
Y	27.0	30.0
Z	37.1	68.2

TABLE II. *Chemical analyses of test steels*

Steel	C	Mn	P	S	Si	Cu	Al	Ni	Mo	Cr
J	0.056	0.37	0.011	0.041	<0.002	<0.04	<0.006	<0.02	<0.01	<0.02
G	0.065	0.38	0.010	0.043	<0.002	<0.04	<0.006	<0.02	<0.01	<0.02
W	0.073	0.40	0.009	0.032	<0.002	<0.04	<0.006	<0.02	<0.01	<0.02
X	0.070	0.30	0.013	0.042	<0.002	<0.04	<0.006	<0.02	<0.01	<0.02
Y	0.056	0.35	0.013	0.047	<0.002	<0.04	<0.006	<0.02	<0.01	<0.02
Z	0.074	0.38	0.010	0.033	<0.002	<0.04	<0.006	<0.02	<0.01	<0.02

drogen which was not evolved because of equivalent reduction of some depolarizer present.

Table I shows the average rates of hydrogen evolution for six steels studied, in both the dry and wet hydrogen annealed conditions. In all cases the wet hydrogen annealed steel was attacked more rapidly than the dry hydrogen annealed steel. The steels had different corrosion rates and differed also in their response to a wet hydrogen anneal. No readily apparent correlation could be seen on comparing this behavior with the chemical analyses of the steels, which are given in Table II. Increased corrosion rates for the wet hydrogen annealed steels were found to

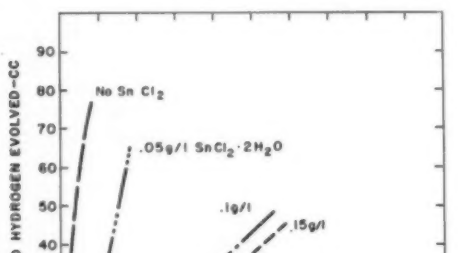

FIG. 4. Effect of stannous chloride on corrosion of a dry hydrogen annealed steel (steel Z).

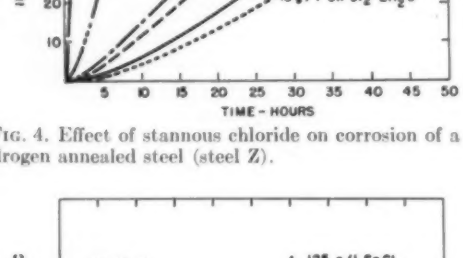

FIG. 5. Effect of stannous chloride on corrosion of a wet hydrogen annealed steel (steel Y).

persist well beyond the "pickle lag" layer, which contains the grain boundary oxides.

Dissolved Tin

Numerous tests were made on specimens of uncoupled steel with stannous chloride added as an inhibitor. As little as 0.025 g/l $SnCl_2 \cdot 2\,H_2O$ provided definite inhibition. Greater amounts produced larger effects. Results for a dry hydrogen annealed steel and a wet hydrogen annealed steel are shown in Fig. 4 and 5, respectively. Dissolved tin exhibited a greater effect on the corrosion rate of the wet hydrogen annealed steel than that of the dry hydrogen annealed steel, at least in the initial period.

Dissolved tin is known to act as an anodic inhibitor. In agreement with this, increasing amounts of dissolved tin were found to shift the corroding potential in the positive direction. The potential of wet hydrogen annealed steel "W", for example, was found to shift from −0.610 to −0.485 v on going from 0 to 0.3 g/l $SnCl_2 \cdot 2\,H_2O$.

Coupled Tests

Hydrogen evolution results of coupled tests in air-free citric acid solution are prone to be very erratic. Quite frequently corrosion rates of duplicate coupled specimens were found to vary as much as several hundred per cent. A large portion of this variation is due to the relative potentials of the steel and tin.

Tin by itself in 0.2M citric acid solution at 60°C assumed a potential of approximately −0.584 v relative to a saturated calomel electrode at 25°C. It tended to remain quite close to this value throughout the period of the tests. Specimens of uncoupled tin exposed for a week evolved no measurable hydrogen, and the amount of weight loss in this period was insignificant. This is attributable to the high hydrogen overvoltage of tin. Accordingly, any weight loss of tin in a coupled test is equivalent to the galvanic current flowing between the steel and the tin. Considerable attention has been given the fact that tin sacrificially protects steel in air-free solutions of food acids, in spite of the fact that the standard electrode potential of steel is considerably more negative (less noble) than that of tin (1, 5). This has been attributed (*a*) to the high hydrogen overvoltage of the tin, and (*b*) to the fact that tin forms stable complex ions with food anions, such as citrate, and therefore it assumes a more negative corroding potential. Both factors are probably involved; uncoupled corroding potentials of the steels studied, however, were in the range of −0.589 to −0.612 v. Accordingly, some other factor or factors are also involved in making the tin negative to the steel. As shown in Fig. 6, potential data indicate that, when tin and steel

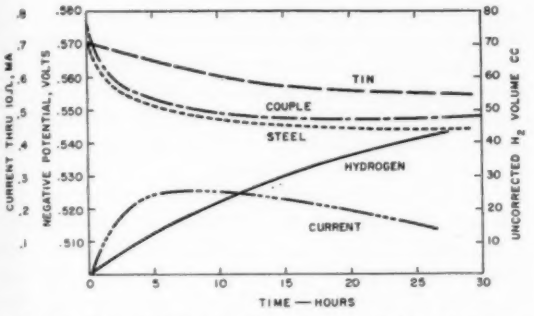

FIG. 6. Potential relationships for a coupled dry hydrogen annealed steel (steel Z).

are coupled, the potentials of both shift in the positive direction. The steel potential shifts more than the tin, and thereby becomes positive to the tin. It is interesting to note that for the particular steel illustrated in Fig. 6 the initial potential of the couple does not lie between that of the tin and that of the steel.

The potential shift of the steel in the positive direction may be attributed at least partially to the inhibiting effect of dissolved tin. With no tin initially in solution, the steel is anodic to the tin and is unprotected. At this time tin goes into solution very slowly. Until sufficient tin goes into solution to inhibit the reaction, steel corrodes rapidly. The duration of this period is dependent on minor variations in the character of the tin and steel surfaces. Accordingly, there is great variation in the results secured on coupled tests in air-free citric acid solution. This situation is overcome by adding a small amount of stannous chloride to the solution used in making the tests, enough to make the tin initially anodic to the steel. An addition of 0.025 g/l $SnCl_2 \cdot 2\ H_2O$ is sufficient for dry hydrogen annealed steels, but the wet hydrogen annealed steels require a larger amount.

This work is concerned only with tests made in the absence of air. Tests conducted in the presence of air have oxygen available as a depolarizer, by virtue of which tin dissolves at a fairly rapid rate regardless of its potential relative to steel. It is to be expected that in this case the above irregularities will not be encountered.

As in the case of uncoupled steel, hydrogen is evolved from a tin-steel couple at the theoretical rate, except during the initial period of the test. This is illustrated for a dry hydrogen annealed steel coupled to tin in Fig. 7. The major portion of the hydrogen results from oxidation of iron. On comparing only the relative corrosion rates of the tin and of the iron it would appear from customary concepts that the tin is not providing much galvanic protection for the steel even though the tin is anodic to the iron. It is evident that more is involved than simple cathodic protection. When coupled to tin, the rate of corrosion of steel is greatly reduced; in fact, the final rate of hydrogen evolution, which is equivalent to the combined solution rates of iron and tin, is only about 3% as great as for a piece of uncoupled black plate. Normally, cathodic protection involves a shift in potential in the negative direction, accompanied by an increase in the rate of the reduction processes. In the present case, there is actually a decrease in the total corrosion rate accompanied by a potential shift in the positive direction. This may be accomplished by a shift in the anodic polarization curve in the positive direction. Such an effect has been attributed to inhibition by dissolved tin. Unquestionably this is a major effect; however, another cause for such a shift appears to exist. This seems to originate in the coupling of the steel to tin.

As has been indicated in Fig. 4, the major amount of inhibition attainable with stannous chloride addition is obtained by virtue of the first 0.1 g/l added. At 0.3 g/l, the corrosion rate is less sensitive to dissolved tin. Comparative corrosion tests have been run with the addition of 0.3 g/l $SnCl_2 \cdot 2\ H_2O$ to the citric acid solution, using specimens of the same steel in both the coupled and uncoupled conditions. In such cases there is still a very great decrease in hydrogen evolution rate for the coupled specimens. This is illustrated in Fig. 8.

Perhaps even more convincing are the results shown in Fig. 9. These comparative tests on a wet hydrogen an-

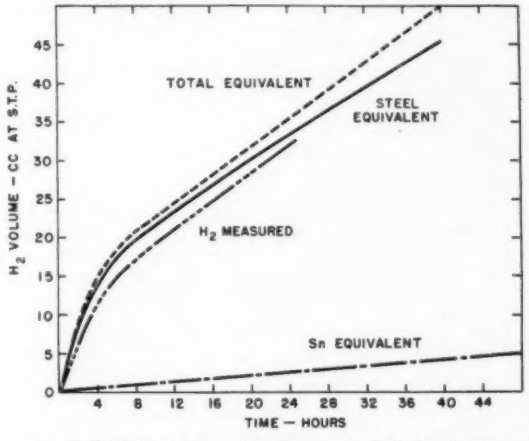

FIG. 7. Weight loss results for a coupled dry hydrogen annealed steel in citric acid solution containing 0.025 g/l $SnCl_2 \cdot 2H_2O$.

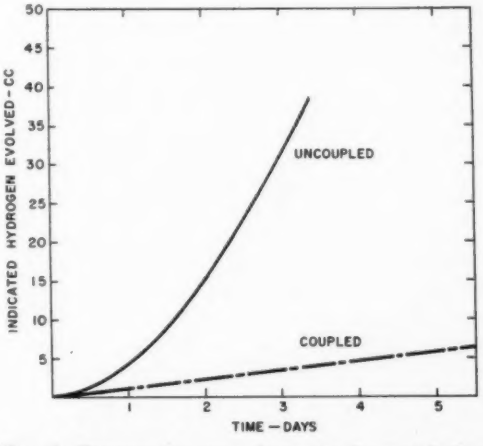

FIG. 8. Comparative corrosion rates for wet hydrogen annealed steel Y, coupled and uncoupled, with 0.3 g/l $SnCl_2 \cdot 2H_2O$.

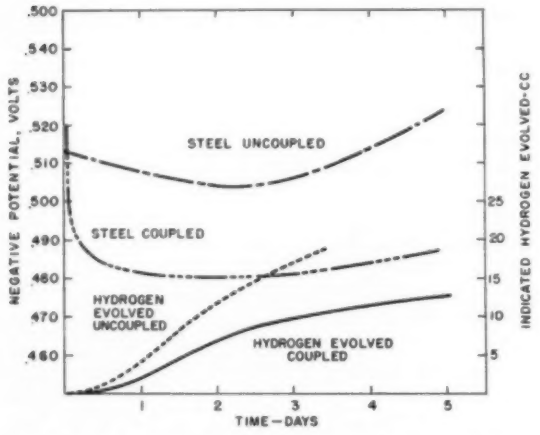

FIG. 9. Comparative relationships for uncoupled steel with 0.3 g/l $SnCl_2 \cdot 2H_2O$ and couple with 0.2 g/l $SnCl_2 \cdot 2H_2O$ (wet hydrogen annealed steel Y).

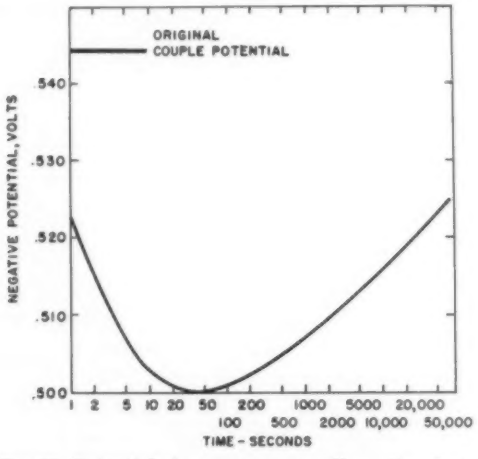

FIG. 10. Potential changes on uncoupling after first day of test—steel against saturated calomel half-cell.

nealed steel were run in potential-type cells. The uncoupled specimen was run in a solution containing 0.3 g/l $SnCl_2 \cdot 2\ H_2O$, and the coupled in a solution containing 0.2 g/l. Of course, in the coupled test, the amount of tin in solution increased by virtue of the corrosion of tin. The amount of tin in solution at any one time, however, could be calculated from the amount initially in solution and the galvanic current flowing between the steel and tin. By such a method it was found to take more than $2\frac{1}{2}$ days for the dissolved tin concentration in the coupled cell to reach the equivalent of 0.3 g/l $SnCl_2 \cdot 2\ H_2O$. Decreased hydrogen evolution rate and potential shifts in the positive direction are established well before this time, indicating that inhibition by dissolved tin cannot explain completely the decreased rate of hydrogen evolution for a tin-steel couple.

Further confirmation for the existence of such an anodic coupling shift has been found in certain food products where dissolved tin is not an effective inhibitor, yet coupling to tin produces a marked decrease in the rate of hydrogen evolution. Such data are not considered here.

An indication of anodic coupling shift is obtained by continuously recording potentials after uncoupling. A number of such tests have been run. Fig. 10 shows potentials of a steel specimen measured against a saturated calomel half-cell after uncoupling. The test was allowed to run for one day before the tin and steel were uncoupled. The corroding medium was 0.2M citric acid solution with 0.1 g/l $SnCl_2 \cdot 2\ H_2O$. On uncoupling, it would be expected that the potential of the tin would shift in the negative direction, and that of the steel in the positive direction. Potentials of tin (not shown) do shift in the negative direction about 5–10 mv. In the figure it is shown that the potential of the steel shifts in the positive direction for about 40 sec, after which it slowly shifts in the negative direction. This is direct evidence that coupling to tin somehow causes a long time shift of the anodic polarization curve for the steel in the positive direction. No completely acceptable explanation for this "anodic coupling shift" is at present known.

Data shown in Fig. 10 raise the question as to what point on this curve such "steel" potentials as indicated in Fig. 6 and 9 represent. Such potentials were measured approximately one minute after uncoupling and should correspond to the minimum in the curve.

Corrosion Rate and Potential

In tests in citric acid with air present, Hoar (3) has shown that if, for various steel specimens, the corroding potential is plotted against the corrosion rate, the points all fall along a single cathodic polarization curve. It follows that differences in corrosion rates for the steels and the inhibiting effect of dissolved tin are all reflections of anodic differences. The same has been found to hold for these tests in air-free citric acid solution at 60°C. In Fig. 11 are plotted the potential of the steel against the logarithm of the rate of hydrogen evolution. Potentials correspond to the flat portion of the steel curve in Fig. 6. Corrosion rates, likewise, are the final rates as measured in comparable volume-type cells. All results are seen to lie along a straight line, indicating that all differences in corrosion rate are

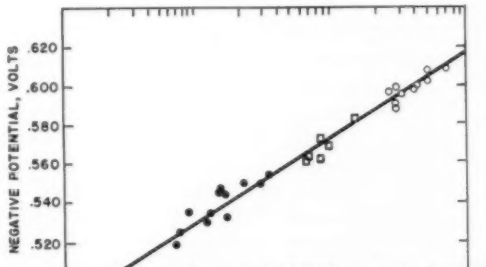

FIG. 11. Relationship between corrosion rate and corroding potential. ○ = results for uncoupled steel in citric acid solution; □ = results obtained with the addition of 0.025 g/l $SnCl_2 \cdot 2H_2O$; ● = steel potentials for tin-steel couples.

anodic effects. The corroding potential thus serves to give a direct indication of the corrosion rate. Unfortunately, it must be cautioned that this relationship cannot be generally extended to corrosion relationships in fruits or fruit juices.

ACKNOWLEDGMENT

Results presented in this paper were obtained in connection with a project on the corrosion of tin plate sponsored by the Inland Steel Co. The author wishes to thank this organization, and in particular Dr. E. D. Martin, for their support and for permitting publication of these results. He further wishes to acknowledge the help of Dr. H. T. Francis and Miss C. Jennings of the Armour Research Foundation.

Manuscript received March 21, 1955.
Any discussion of this paper will appear in a Discussion Section to be published in the June 1957 JOURNAL.

REFERENCES

1. T. P. HOAR, *Tech. Pub. Intern. Tin Research Develop. Council*, No. 5, Series A.
2. T. P. HOAR, *ibid.*, No. 30, Series A.
3. T. P. HOAR AND D. HAVENHAND, *ibid.*, No. 36, Series A.
4. E. L. KOEHLER, *Trans. Am. Soc. Metals*, **44**, 1076 (1952).
5. E. F. KOHMAN AND N. H. SANDBORN, *Ind. Eng. Chem.*, **20**, 76 (1928).

Phase Equilibria and Fluorescence in the System Zinc Oxide-Boric Oxide

D. E. HARRISON[1] AND F. A. HUMMEL

Department of Ceramic Technology, The Pennsylvania State University, University Park, Pennsylvania

ABSTRACT

Phase relationships in the system zinc oxide-boric oxide have been re-examined in detail. Two compounds exist, $5ZnO \cdot 2B_2O_3$ and $ZnO \cdot B_2O_3$, both of which exhibit low and high temperature polymorphic forms. Low temperature (α)$ZnO \cdot B_2O_3$ inverts sluggishly to the cubic high temperature (β)$ZnO \cdot B_2O_3$ at 600°C and very rapidly at 900°C. The melting point is 982° ± 3°C. Low temperature (α)$5ZnO \cdot 2B_2O_3$ is biaxial negative and inverts rapidly and reversibly to the high temperature (β) form at 964° ± 4°C. It melts incongruently at 1045°. General agreement with previous investigators has been obtained on the liquidus curve and the extent of liquid immiscibility in the system. The thermal expansion and fluorescent properties of the compounds are described. The low temperature α-$5ZnO \cdot 2B_2O_3$ phase with 0.03 moles MnO fluoresces orange, and the high temperature cubic β-$ZnO \cdot B_2O_3$ phase with 0.006 moles MnO fluoresces green, under both 2537Å and cathode ray excitation.

Six anhydrous zinc borate compounds have been reported and there has been much conjecture on the origin of the yellow and green luminescence which was characteristic of various preparations of previous investigators.

Mallard (1) reported the compound $3ZnO \cdot 2B_2O_3$ obtained by fusion of B_2O_3 and ZnO. Le Chatelier (2) isolated the same borate in the form of dodecahedrons by dissolving the matrix glass in acid. The $3ZnO \cdot 2B_2O_3$ compound was described as the only zinc borate, glassy or crystalline, insoluble in acid.

Ouvrard (3) obtained the orthoborate $3ZnO \cdot B_2O_3$ by fusing an equimolecular composition of B_2O_3 and $KF \cdot HF$ with one mole of ZnO. The orthoborate appeared as flat prisms showing high birefringence and straight extinction. It was decomposed by warm water and easily soluble in dilute acid.

Guertler (4) found that two liquids formed when zinc oxide was dissolved in fused boric acid. At greater than 53.39% ZnO a single liquid resulted. As the composition approached the $3ZnO \cdot 2B_2O_3$ molecular ratio, crystals were obtained. These were assumed to be the compound reported by Le Chatelier.

The compositions between 55 and 75% ZnO were examined by de Carli (5) by means of heating curves. Two maxima at about 900°C were observed at the $ZnO \cdot B_2O_3$ and $2ZnO \cdot B_2O_3$ compositions. Tournay (6) heated together equimolecular proportions of ZnO and B_2O_3 at temperatures up to 1000°C. After dissolving the soluble material in acid, the residue was determined to be nearly the $3ZnO \cdot 2B_2O_3$ composition.

Ingerson, Morey, and Tuttle (7) investigated the system using a quench technique (Fig. 1). Two compounds were reported: $ZnO \cdot B_2O_3$ which melted congruently at 1000°C and $5ZnO \cdot 2B_2O_3$ which melted incongruently at 1080°C. Although these authors intended to present only a brief survey of the system incidental to the study of the behavior of willemite in the ternary system ZnO-B_2O_3-SiO_2, essentially all of the principal features of the binary system

[1] Present address: Ceramics Division, Fuel Department, Leeds University, Leeds, England.

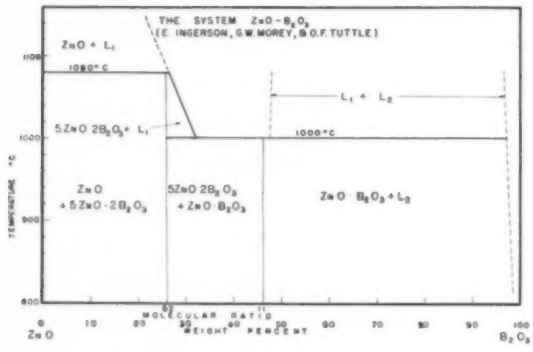

FIG. 1. The system ZnO-B_2O_3 (Ingerson, Morey, and Tuttle). (Figure courtesy of *The American Journal of Science*.)

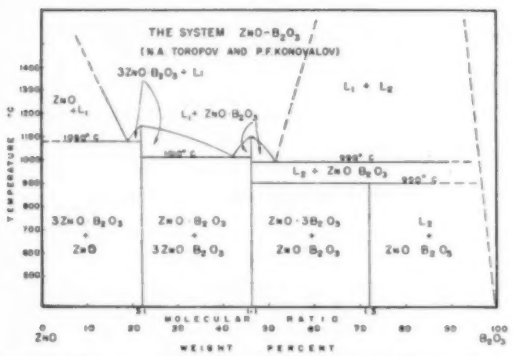

FIG. 2. The system ZnO-B_2O_3 (Toropov and Konovalov)

were determined at this time, except for the inversions of the two compounds and the composition and temperature of the eutectic. Toropov and Konovalov (8) investigated the system by means of heating curves (Fig. 2). Three compounds were reported: $3ZnO \cdot B_2O_3$ which melted congruently at 1125°C; $ZnO \cdot B_2O_3$ which melted congruently at 1050°C; and $ZnO \cdot 3B_2O_3$ which dissociated at 900°C into $ZnO \cdot B_2O_3$ and a liquid containing 2% $ZnO \cdot B_2O_3$. Terol Alonso and Gandara (9) re-examined the $ZnO \cdot B_2O_3$, $3ZnO \cdot 2B_2O_3$, $2ZnO \cdot B_2O_3$, and $3ZnO \cdot B_2O_3$ compositions. They concluded that $3ZnO \cdot 2B_2O_3$ and $2ZnO \cdot B_2O_3$ were compounds.

Phase relationships in this system were reinvestigated for the purpose of isolating the compounds which existed, studying their polymorphic forms and determining which forms were responsible for the observed fluorescence.

Experimental Procedure

Reagent grade Mallinckrodt boric acid and New Jersey Zinc Co. zinc oxide were used in preparing the various compositions. The finely divided zinc oxide was of purity sufficient for phosphor production and therefore satisfactory for phase equilibrium studies. It held 1.5% of adsorbed moisture as indicated in Table I. Repeated determinations of the B_2O_3 content of the boric acid gave 56.00% as compared to a theoretical 56.30%.

Preparation of compositions and heat treatments.—The required amounts of ZnO and H_3BO_3 were mixed in an agate mortar with reagent grade acetone until it evaporated and a dry powder resulted. Calcines were prepared in platinum crucibles at temperatures ranging from 500° to 950°C with firing times of from 10 hr to 6 weeks. For survey work in a temperature gradient, a platinum-wound furnace was used. For heat treatments at constant temperature, silicon carbide element furnaces were used.

Dry pressing was used to form bars measuring 1 cm square by 10 cm long. Calcination at 500° to 600°C for 3–5 days yielded specimens suitable for thermal expansion measurements.

TABLE I. *Composition of* $ZnO \cdot B_2O_3$ *mixtures*

No.	Molecular ratio $ZnO : B_2O_3$	Wt % composition $ZnO : B_2O_3$		ZnO (g) (98.50% ZnO)	H_3BO_3 (56.00% B_2O_3)
1	1:4	22.61	77.39	2.30	13.82
2	1:3	28.03	71.97	2.85	12.86
3	1:2	36.88	63.12	3.75	11.28
4	1:1	53.89	46.11	5.47	8.24
5		60.00	40.00	6.10	7.15
6		62.00	38.00	6.30	6.79
7	3:2	63.67	36.33	6.47	6.49
8		64.00	36.00	6.50	6.43
9		65.00	35.00	6.60	6.25
10		66.00	34.00	6.71	6.07
11		68.00	32.00	6.91	5.72
12		70.00	30.00	7.11	5.36
13	2:1	70.03	29.97	7.10	5.35
14	5:2	74.50	25.50	7.57	4.55
15	3:1	77.81	22.19	7.90	3.96
16	4:1	82.37	17.63	8.37	3.15

TABLE II. *Zinc borate compositions containing manganese*

Molecular ratio ZnO	B_2O_3	MnO	Wt % composition ZnO	B_2O_3	MnO	ZnO (g) (98.50% ZnO)	H_3BO_3 (56.00% B_2O_3)	$MnSO_4$ (57.20% MnO)
1.000	1.000	.006	53.73	45.98	0.28	27.29	41.07	0.25
5.000	2.000	.030	74.21	25.40	0.39	37.69	22.69	0.34

Apparatus and techniques.—

(*A*) X-ray Patterns: X-ray data were obtained from Norelco and General Electric recording spectrometers using $Cu_{K\alpha}$ radiation (λ = 1.537Å), filtered with nickel.

(*B*) Quench Technique: Liquidus and solidus temperatures were determined by procedures similar to those described by Shepherd, Rankin, and Wright (10), using calcines or glasses as starting material. Thermocouples were calibrated using lithium metasilicate (mp, 1201°C) and gold (mp, 1063°C).

(*C*) Refractive Index Determinations: The immersion technique was used to determine the refractive indexes of glasses and crystals to an accuracy of ±0.002, using white light and index oils which were calibrated with an Abbe refractometer.

(*D*) Differential Thermal Analysis (D.T.A.): Differential thermal analysis data were obtained with automatically recording apparatus described by Gruver (11).

(E) Thermal Expansion: Thermal expansion measurements were obtained with a calibrated fused silica dilatometer. At least two measurements were made on each sample.

(F) Fluorescent Measurements: Emission curves were obtained with an automatically recording General Electric spectroradiometer. Visual examination was made with 2537Å and cathode ray excitation.

Experimental Results and Discussion

Phase Relationships

General subsolidus study.—A detailed examination of the phase relationships below the solidus was undertaken in order to prove or disprove the existence of the compounds which have been claimed. The selection of compositions included all previously claimed compounds plus certain other possible molecular ratios (*see* Table I). All 16 compositions were heated at 800°C for 10 hr. Zinc oxide persisted in x-ray patterns of compositions containing more than 74.5% ZnO (5:2 molecular ratio) indicating that 5:2 was probably a compound and that no other compound existed between the 5:2 ratio and ZnO. Compositions richer in B_2O_3 than the 1:1 ratio gave only the cubic form of ZnO:B_2O_3 previously reported by Ingerson, Morey, and Tuttle (7), according to both microscopic and x-ray examination.

All lines in the x-ray patterns of compositions intermediate between a 5:2 and 1:1 ratio could be accounted for by the lines given by these two "end-member" compositions. The presence of cubic $ZnO \cdot B_2O_3$ in the mixtures was easily confirmed by microscopic examination.

Heat treatment at 850°C for 24 hr gave essentially the same results as described above.

Additional heat treatment at lower temperatures such as 650° and 750°C (10 hr) brought out the fact that the x-ray pattern of the 1:1 compound had become a much more complex one, containing many more lines than patterns obtained from the 800° and 850°C treatments.

Under the microscope, crystals of $ZnO \cdot B_2O_3$ prepared at 650°C were birefringent. At 750°C, both cubic and birefringent forms of the 1:1 compound co-existed, according to both x-ray and optical examination. Such mixtures were observed in not only the 1:1 composition, but also in compositions lying on either side of this ratio, for example in the 3:2, 1:2, and 1:3 compositions.

D.T.A. data were obtained for the 3:2, 1:1, and 1:2 compositions which had been previously heated to 800°C for 10 hr. A sharp, irreversible endothermic peak was observed at 900°C, possibly due to conversion of a low temperature form of $ZnO \cdot B_2O_3$ to the cubic high temperature form. The product in the 1:1 and 1:2 compositions after D.T.A. was shown by x-ray data to be cubic $ZnO \cdot B_2O_3$. The x-ray pattern of the 3:2 composition contained some moderately intense peaks characteristic of the 5:2 compound as well as the distinctive peaks of cubic $ZnO \cdot B_2O_3$.

These preliminary data strengthened the evidence that only the two compounds previously identified by Ingerson, Morey, and Tuttle existed, since now both optical and x-ray data supported the conclusion. The D.T.A. data also pointed toward an inversion in the $ZnO \cdot B_2O_3$ compound which had not been mentioned by previous investigators.

However, the more detailed work on the two compounds and the quench work described in the next sections provided the data on which the final conclusions were based.

Data on $ZnO \cdot B_2O_3$.—Further differential thermal analyses on the zinc metaborate composition previously heated at various temperatures in the range 600°–800°C repeatedly gave an endothermic peak at 900°C and a second peak at 980°C, the fusion temperature. The sluggish nature of the inversion complicated determination of its equilibrium temperature, and the following detailed study was necessary to understand the kinetics of the inversion process.

Seven 10-ml capacity porcelain crucibles each containing 1 g of $ZnO \cdot B_2O_3$ which had been calcined at 600°C for 5 days were placed in a fused silica container which measured 1 x 3 x 5 in. X-ray examination showed that the starting material contained no high temperature $\beta ZnO \cdot B_2O_3$. The container was placed on a refractory setter pin so as to surround it with 2 in. of air space and bring it directly under the control couple in the hottest zone of an automatically controlled Hoskins electric muffle furnace. A chromel-alumel thermocouple, accurate to ±4°C, was used to measure the temperature inside the silica container. Samples were removed periodically and air quenched. The concentration of the high temperature form of zinc metaborate in the quenched samples was determined by measuring the intensity of its most intense x-ray reflection

TABLE III. *Rate of* α-$ZnO \cdot B_2O_3 \rightarrow \beta$-$ZnO \cdot B_2O_3$ *inversion at various temperatures*

% Concentration of β-$ZnO \cdot B_2O_3$	Time (hr)	% Concentration of β-$ZnO \cdot B_2O_3$	Time (hr)
713°C		740°C	
3.4	7	11.4	2
9.3	24	16.0	4
16.1	50.5	20.7	7.4
21.2	76.2	27.0	16.7
25.5	96.2	35.7	31.8
28.3	144	43.3	63.8
34.4	207		
760°C		786°C	
16.5	2	29.8	1
23.1	4	37.8	2
26.5	8	48.9	4
34.7	17	55.2	7
42.1	32	58.4	11
48.4	67	61.9	16
51.9	144	67.5	25.2

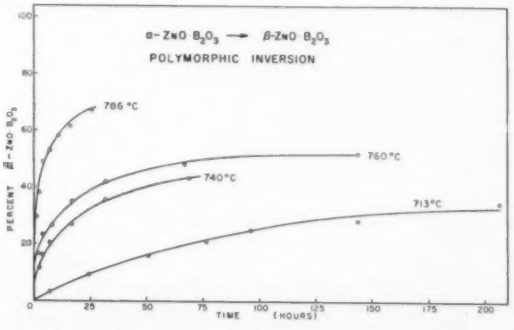

FIG. 3. Rate of inversion of α to β $ZnO \cdot B_2O_3$

TABLE IV. *X-ray patterns for zinc borate compounds*

β-ZnO·B₂O₃						α-ZnO·B₂O₃		α-5ZnO·2B₂O₃		β-5ZnO·2B₂O₃	
Swanson (1951)			Present work								
d	hkl	I/I₀	d	hkl	I/I₀	d	I/I₀	d	I/I₀	d	I/I₀
5.29	110	6	5.31	110	45	6.92	10	5.95	5	5.91	15
3.74	200	3	3.75	200	25	6.28	10	5.83	10	3.93	10
3.048	211	100	3.07	211	100	5.47	40	4.23	35	3.23	10
2.364	310	23	2.37	310	90	5.28	80	4.15	30	3.00	40
2.158	222	1	2.16	222	15	4.25	40	4.10	10	2.93	70
1.997	321	20	2.00	321	90	4.15	85	3.88	10	2.58	10
1.869	400	13	1.873	400	85	4.10	50	3.60	30	2.36	10
1.761	411	38	1.765	411	95	3.90	20	3.38	70	2.26	50
1.672	420	2	1.675	420	30	3.75	20	3.20	100	2.22	10
1.594	332	3	1.595	332	15	3.69	50	3.08	15	2.16	5
1.0788	444	1	1.081	444	5	3.60	35	3.05	15	2.11	5
1.0568	710	1	1.059	710	20	3.56	25	3.00	25	2.04	10
1.0365	640	1	1.038	640	10	3.51	25	2.91	55	2.00	25
1.0169	721	3	1.018	721	35	3.45	20	2.87	10	1.957	100
0.9991	642	1				3.38	55	2.80	65	1.895	10
0.9812	730	2				3.21	75	2.79	65	1.817	10
0.9490	732	1				3.15	65	2.67	15	1.778	10
0.9198	811	3				3.08	25	2.55	75	1.716	10
0.9062	820	1				3.06	20	2.49	45	1.698	10
0.8932	653	1				3.00	30	2.44	55	1.678	45
						2.94	50	2.40	30	1.626	20
						2.88	75	2.34	70	1.570	10
						2.84	40	2.30	20	1.549	10
						2.79	25	2.25	20	1.532	10
						2.69	20	2.20	30	1.508	15
						2.67	21	2.15	25	1.488	20
						2.54	100	2.11	10	1.465	20
						2.50	60	2.10	10	1.437	30
						2.44	30	1.99	55	1.414	25
						2.40	20	1.98	40	1.398	50
						2.34	40	1.937	90	1.397	35
						2.30	20	1.884	10	1.339	25
						2.26	20	1.852	10	1.301	10
						2.24	40	1.794	15	1.233	15
						2.21	20	1.771	20	1.188	40
						2.17	25	1.734	60	1.176	25
						2.12	15	1.684	25	1.160	10
						2.10	10	1.664	10	1.137	10
						2.07	10	1.647	35	1.125	10
						2.03	10	1.623	20	1.114	10
						2.00	30	1.621	20	1.094	20
						1.99	20	1.610	30	1.090	60
						1.945	60	1.590	10	1.084	20
						1.906	10	1.583	10	1.066	20
						1.831	15	1.570	20	1.052	25
						1.791	15	1.540	15	1.041	30
						1.768	15	1.519	5	1.029	15
						1.752	15	1.503	15	1.016	15
						1.734	10	1.482	10		
						1.710	20	1.467	15		
						1.684	10	1.455	15		
						1.645	30	1.439	25		
						1.623	15	1.412	10		
						1.610	10	1.389	20		
						1.590	15	1.363	10		
						1.556	10	1.321	15		
						1.544	15	1.307	10		
						1.503	15				
						1.482	15				
						1.467	10				
						1.455	15				
						1.441	15				
						1.412	10				
						1.389	20				
						1.361	15				
						1.342	10				
						1.313	10				
						1.301	10				
						1.284	10				

a. 7.4726

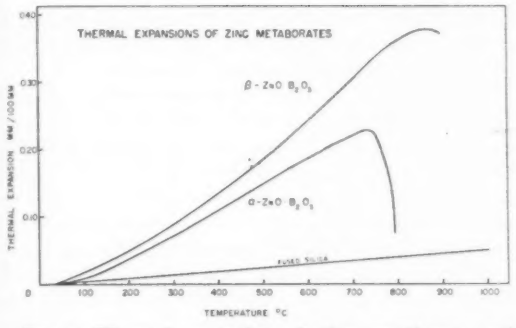

FIG. 4. Thermal expansion of zinc metaborate polymorphs.

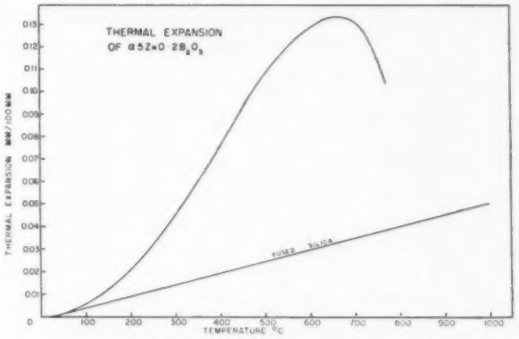

FIG. 5. Thermal expansion of α-$5ZnO \cdot 2B_2O_3$

(d = 3.07) and comparing it with the intensity observed in a sample which had completely inverted to the high temperature cubic form. Intensities were determined by a counting method using a Geiger counter spectrometer. Excellent sensitivity and accuracy could be achieved using any of the very intense peaks (d = 3.07, 2.37, 2.00, 1.765) of cubic $ZnO \cdot B_2O_3$, but the 3.07 line was most satisfactory.

Four sets of samples were treated at 713°, 740°, 760°, and 786°C. Concentrations of β-$ZnO \cdot B_2O_3$ with time are listed in Table III and they are shown graphically in Fig. 3. Calculations based on these data and long term heat treatments (6 weeks) in the neighborhood of 600°C showed this to be the equilibrium inversion temperature in air.

The high temperature form, β-$ZnO \cdot B_2O_3$, was isotropic, having a refractive index of 1.740. An x-ray pattern is given in Table IV. It is compared with the A.S.T.M. pattern of Swanson (12).

The low temperature form, α-$ZnO \cdot B_2O_3$, was birefringent, having maximum and minimum indices of 1.682 and 1.638. An x-ray pattern is given in Table IV.

The linear thermal expansions of the high and low forms are shown in Fig. 4. α-$ZnO \cdot B_2O_3$ which had been prepared by calcining a bar at 600°C for 5 days exhibited an average coefficient of thermal expansion of 35.0×10^{-7} cm/cm/°C between 50° and 600°C. Between 700° and 800°C, the sample began to contract, indicating inversion to the high temperature form. X-ray examination after the expansion run showed that most of the sample had inverted to the (β) form. β-$ZnO \cdot B_2O_3$ had an average coefficient of thermal expansion of 49.5×10^{-7} cm/cm/°C in the range 50–700°C.

Data on $5ZnO \cdot 2B_2O_3$.—Differential thermal analysis of the $5ZnO \cdot 2B_2O_3$ compound revealed a rapid reversible endothermic peak near 980°C as well as an irreversible peak at 1045°C. High temperature x-ray patterns were taken in the region from 700° to 980°C to substantiate the reversibility of the inversion indicated by D.T.A. By detailed study of many patterns, the rapid reversible inversion was found to occur at 964 ± 4°C. It was discovered that the high temperature (β) form of $5ZnO \cdot 2B_2O_3$ could be retained at room temperature due to the mechanical restraint of the sample holder. X-ray patterns taken at 980°C and on a sample quickly cooled to room temperature were identical, except for a systematic shift in the 980° pattern due to thermal expansion of the crystal. Specimens which were quickly cooled to room temperature in the sample holder gave patterns for β-$5ZnO \cdot 2B_2O_3$ as long as they remained in place, but as soon as they were removed and ground in a mortar, they inverted to well crystallized low temperature α-$5ZnO \cdot 2B_2O_3$. X-ray patterns of the α and β modifications (taken at room temperature) are given in Table IV.

Low temperature $5ZnO \cdot 2B_2O_3$ was biaxial, negative, with n_α 1.672, n_β 1.741, and n_γ ca. 1.75.

Thermal expansion was determined on a bar fired at 600°C for 3 days (Fig. 5). Low temperature $5ZnO \cdot 2B_2O_3$ had a relatively low linear coefficient of thermal expansion of 24.4×10^{-7} cm/cm/°C between 50° and 600°C. Above that temperature contraction of the bar occurred due to sintering. The effect of the polymorphic inversion on the thermal expansion was not examined.

Liquidus and solidus determinations.—It was felt that the investigation of the system might be complicated by compositional changes during the original melting of the glasses or later during the quench work. To assess this possibility, the 1:1 composition which had been prepared as a calcine and by fusion was analyzed by chemical and ignition loss methods. The 5:2 composition was analyzed by ignition loss only. Results are assembled in Table V.

Compositional changes less than 0.7 wt % were considered satisfactory for the accuracy to which the phase relationships were determined.

Compositions between 53.89% and 70.0% ZnO fused readily at 1100°C to liquids capable of being retained as transparent glasses by quenching the platinum crucible in water. The refractive indexes are shown in Fig. 6 and listed in Table VI. At greater than 70.0% ZnO, it was impossible to retain glass no matter how rapidly the sample was quenched. Between these limits, liquidus and solidus temperatures were determined by a quench technique. For most determinations the starting material was glass. Occasionally checks were made using batch material which

TABLE V. *Analyses of zinc borate compositions*

Sample	Chemical Analysis				Ignition Loss	
	Calculated		Observed		Calculated wt. % loss	Observed wt. % loss
	ZnO	B_2O_3	ZnO	B_2O_3		
$ZnO \cdot B_2O_3$						
750°/72 hr	53.89	46.11			27.07	27.54
1100°/30 min	53.89	46.11	54.54	45.46	27.07	27.64
$5ZnO \cdot 2B_2O_3$						
800°/6 hr	74.50	25.50			17.51	17.82
1100°/30 min	74.50	25.50			17.51	17.84

TABLE VI. *Liquidus and solidus determinations in the system* ZnO-B_2O_3

No.	Composition wt % ZnO	Composition wt % B_2O_3	Refractive index of glass	Temperature	Phases present
4	53.89	46.11	1.640	988	Glass
				984	Glass
				980	β-$ZnO \cdot B_2O_3$
				976	β-$ZnO \cdot B_2O_3$
5	60.00	40.00	1.652	987	Glass
				985	Glass
				979	Glass + β-$ZnO \cdot B_2O_3$
				970	Glass + β-$ZnO \cdot B_2O_3$
				965	Glass + β-$ZnO \cdot B_2O_3$
6	62.00	38.00	1.660	987	Glass
				982	Tr. β-$ZnO \cdot B_2O_3$ + Glass
8	64.00	36.00	1.665	985	Glass
				981	Tr. β-$ZnO \cdot B_2O_3$ + Glass
				966	β-$ZnO \cdot B_2O_3$ + Glass
				957	β-$ZnO \cdot B_2O_3$ + α-$5ZnO \cdot 2B_2O_3$
9	65.00	35.00	1.670	983	Glass
				980	Tr. β-$ZnO \cdot B_2O_3$ + Glass
				976	β-$ZnO \cdot B_2O_3$ + Glass
				970	β-$ZnO \cdot B_2O_3$ + Glass
				962	Tr. Glass + β-$ZnO \cdot B_2O_3$
				960	α-$5ZnO \cdot 2B_2O_3$ + β-$ZnO \cdot B_2O_3$
10	66.00	34.00	1.674	980	Glass
				979	Glass
				976	Glass
				974	β-$5ZnO \cdot 2B_2O_3$ + Glass
				969	β-$5ZnO \cdot 2B_2O_3$ + Glass
				966	β-$5ZnO \cdot 2B_2O_3$ + Glass
				962	α-$5ZnO \cdot 2B_2O_3$ + Glass
				960	β-$ZnO \cdot B_2O_3$ + α-$5ZnO \cdot 2B_2O_3$
11	68.00	32.00	1.678	1005	Glass
				999	Tr. β-$5ZnO \cdot 2B_2O_3$ + Glass

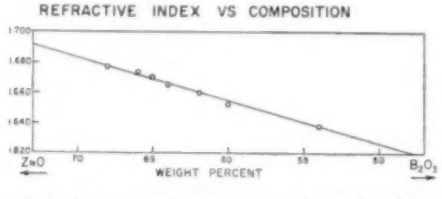

FIG. 6. Refractive index vs. composition for zinc oxide-boric oxide glasses.

had been calcined in the range 700°–900°C. The results are given in Table VI.

Zinc metaborate, $ZnO \cdot B_2O_3$, was found to melt congruently at 982° ± 3°C to a glass having an index of about 1.640. If the glass was devitrified between 650° and 850°C, a mixture of isotropic ($\beta ZnO \cdot B_2O_3$) and birefringent ($\alpha ZnO \cdot B_2O_3$) crystals resulted. At 900°C or above, the glass would yield mainly β 1:1 and at 600°C, mainly α 1:1. It should be noted that these results are similar to those obtained by subsolidus reaction of batch materials.

Glass of the metaborate composition exhibited unusual behavior during devitrification. Fragments of glass which had been heated at 650°C for 4 days acquired a very slight opalescence but they remained essentially transparent. Upon grinding the glass in a mortar, complete devitrification to α-$ZnO \cdot B_2O_3$ occurred. Large transparent fragments of glass which had been broken exhibited highly birefringent crystals along the planes of fracture.

With increasing zinc oxide content the liquidus remained flat to a concentration of 64.0% ZnO. It then dropped abruptly to a eutectic at 961° ± 3°C located at 65.5% ZnO and it rose again to 1005°C at 68.0% ZnO. Above this point the liquidus was not determined.

β-$ZnO \cdot B_2O_3$, as beautifully developed dodecahedrons, crystallized from glasses whose compositions were between 1:1 and the eutectic. β-$5ZnO \cdot 2B_2O_3$ crystallized from glass on the zinc oxide side of the eutectic, but it was never observed optically because it inverted to the low form on grinding. Below the solidus β-$ZnO \cdot B_2O_3$ and α-$5ZnO \cdot 2B_2O_3$ crystallized from glasses lying between these two composition points.

The $5ZnO \cdot 2B_2O_3$ compound was determined to melt incongruently at 1045°C by observing that the D.T.A. peak in 5:2, 3:1, and 4:1 mixtures occurred at this temperature. These data supported the previous observation of Ingerson, Morey, and Tuttle (7) that ZnO separated from the 5:2 melt at high temperatures.

The immiscible liquid region.—Five to ten gram platinum crucible melts gave a relatively clean separation of the two liquids for compositions 1, 2, and 3 at temperatures of 1000°–1100°C. Starting with batch material which had been heated at 400°–500°C, quench trials on compositions 1, 2, and 3 provided accurate measurement of the temperature of the two liquid separation.

The zinc oxide-rich liquid in equilibrium with the B_2O_3-rich liquid contained 53.5% ZnO, which is in remarkably good agreement with the 53.39% ZnO reported by Guertler (4) in 1904, and with the recent work of Ingerson, Morey, and Tuttle. The heavy liquid had a refractive index of 1.640.

Two features of the liquidus curve shown in Fig. 7 and 8 are worthy of some discussion. First, it should be recognized that the diagram is not strictly correct in a very small region to the right of the melting point of $ZnO \cdot B_2O_3$. To comply with the requirements of the Phase Rule, a slight decrease in the liquidus temperature should be experienced as B_2O_3 is added to the 1:1 composition resulting in an invariant point where two liquids and crystalline β-$ZnO \cdot B_2O_3$ are in equilibrium at a temperature slightly below the congruent melting point of the 1:1 compound.

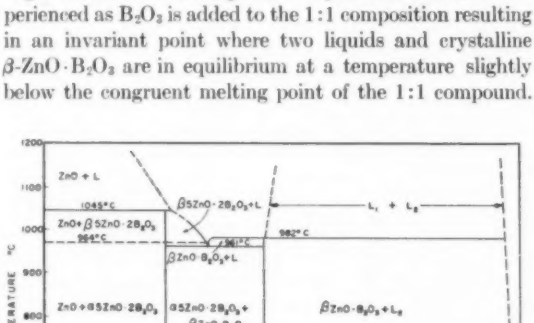

FIG. 7. The system ZnO-B_2O_3

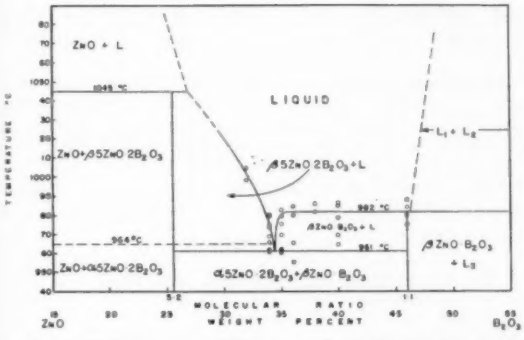

FIG. 8. Enlargement of the eutectic region in the system ZnO-B_2O_3.

Experimental difficulties attending the determination of the exact composition and temperature of this point lead to its elimination in the present diagrams.

The second point which should be discussed is the flatness of the liquidus curve in the range between the $ZnO \cdot B_2O_3$ composition and the eutectic. This curve resembles that shown by Morey (13) for a region of the system $Na_2O \cdot 4B_2O_3$-SiO_2 and by Greig (14) for the high silica portion of the system BaO-SiO_2.

In the case of the ZnO-B_2O_3 system, the flatness suggests the possible existence of a second pair of immiscible liquids or perhaps an extension of the two-liquid region which has been shown on the diagrams.

During the course of this work some evidence indicated that one of these possibilities may occur. Glass fragments of composition 9, containing 65% ZnO, were held at 1050°C for 12 hr in a platinum crucible. Tiny cigar shaped lenses developed at the edges of the fragments, which grew in size if the temperature was increased. Attempts to explore this behavior in quench envelopes at temperatures of 1000°–1125° and times of 5–60 min were unsuccessful for glass compositions containing 62 and 65% ZnO, since part or all of the liquids frequently ran out of the envelopes and no positive separations were developed. However, a number of trials using relatively large fragments of glass in platinum crucibles repeatedly yielded the lenses mentioned above and it is possible that a two-liquid field exists above 982°C for compositions between the 1:1 and 5:2 ratio.

It was evident from the preliminary trials that it would be very difficult and time-consuming to establish composition and temperature limits of such a region, if it existed, and no further work was done.

If such a region exists, it could account for the flatness of the liquidus. If it does not exist, then the curve must slope downward very slightly from the congruent melting point of the 1:1 compound toward the eutectic, as indicated in the diagram and discussion of Ingerson, Morey, and Tuttle (7).

Fluorescent Studies

Cohn (15) observed the fluorescence and thermoluminescence of zinc borate glasses containing manganese and made quantitative determinations of intensity vs. concentration of manganese for each case. From his data on the optimum concentration of manganese required for maximum fluorescence and thermoluminescence, he drew conclusions regarding the structure of the host glass and the nature of the emitting center.

Kabakjian (16) investigated the fluorescence of zinc borate compositions with and without manganese. He worked with a composition containing 57% ZnO and 43% B_2O_3 which he claimed was at the limit of glass formation and called this mixture "zinc borate compound for want of a better term". (When crystallized from a fusion this mixture should yield both compounds in the ratio 7 parts $ZnO \cdot B_2O_3$ to 1 part $5ZnO \cdot 2B_2O_3$.) He found a greater than 30 fold increase in brightness in the phosphors during the change from the "vitreous to the granular state" and speculated on the structure and mechanism of the fluorescence in the "pure" and activated "zinc borate compound".

Leverenz (17) has presented emission curves for zinc borate mole ratios of 3:1, 2:1, 3:2, and 1:1 (ZnO:B_2O_3). He found that the 1:1 peaked near 5420Å and the 3:1 and 2:1 near 5950Å. The 3:2 spectrum had characteristics intermediate between those of the 1:1 and 2:1 mixtures.

In this study $ZnO \cdot B_2O_3$:006MnO was prepared as a glass and in both crystalline modifications. Examination under 2537Å ultraviolet radiation showed that the glass fluoresced orange, β-$ZnO \cdot B_2O_3$ a bright green, and α-$ZnO \cdot B_2O_3$ only very faintly. The behavior under cathode ray excitation was similar, except that the α-form fluoresced with greater intensity. Under 2537Å radiation glass which had been devitrified in a gradient furnace operating between 300°–950° showed a color change at about 650°C from orange to bright green. An increase in the intensity of the green fluorescence between 650° and 900°C indicated the increase in amount of crystallization of β-

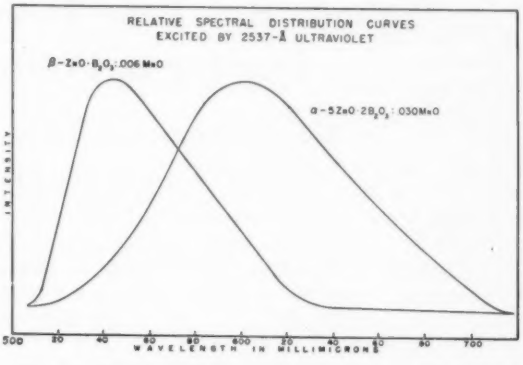

FIG. 9. Spectroradiometer curves for α-$5ZnO \cdot 2B_2O_3$ and β-$ZnO \cdot B_2O_3$.

TABLE VII. *Fluorescent color of zinc borate phosphors under 2537Å or cathode excitation*

Phosphor	2537Å	C. R.
α-$ZnO \cdot B_2O_3$:0.006MnO	Faint	Weak yellowish-green
β-$ZnO \cdot B_2O_3$:0.006MnO	Green	Green
α-$5ZnO \cdot 2B_2O_3$:0.030MnO	Orange	Orange
β-$5ZnO \cdot 2B_2O_3$:0.030MnO	Unknown	Unknown

$ZnO \cdot B_2O_3$ from the glass with rising temperature, confirming the previous observations shown in Fig. 3.

Samples of α-$5ZnO \cdot 2B_2O_3$:.030MnO were prepared at various temperatures. The compound fluoresced orange under 2537Å and cathode ray excitation. Fig. 9 shows spectroradiographs for β-$ZnO \cdot B_2O_3$:.006MnO fired at 850°C for 12 hr and α-$5ZnO \cdot 2B_2O_3$:.030MnO fired at 900°C for 12 hr. The relative intensities shown in Fig. 9 have been adjusted to 100%. Actually, β-$ZnO \cdot B_2O_3$ is considerably brighter than α-$5ZnO \cdot 2B_2O_3$ under both 2537Å and cathode ray excitation. The fluorescence data are summarized in Table VII.

Summary

1. The ZnO-B_2O_3 phase diagram of Ingerson, Morey, and Tuttle has been refined at the liquidus and new data on the polymorphic inversions of the $5ZnO \cdot 2B_2O_3$ and $ZnO \cdot B_2O_3$ compounds have been presented.

2. With manganese activation, the low temperature α-$5ZnO \cdot 2B_2O_3$ fluoresces orange and the high temperature cubic β-$ZnO \cdot B_2O_3$ fluoresces green under both 2537Å and cathode ray excitation.

Zinc borate glasses and the low temperature (α) modification of $ZnO \cdot B_2O_3$ are but weakly fluorescent.

Acknowledgment

The authors are grateful to the Chemical Products Plant of the General Electric Company for financial and technical assistance during the course of the work and to Mr. R. S. Mackie for permission to publish this paper.

Manuscript received December 12, 1955. Contribution No. 55-16 from the College of Mineral Industries, The Pennsylvania State University and abstracted from a thesis submitted by D. E. Harrison in partial fulfillment of the requirements for the Ph.D. degree.

Any discussion of this paper will appear in a Discussion Section to be published in the June 1957 JOURNAL.

REFERENCES

1. ER. MALLARD, *Compt. rend.*, **105,** 1260 (1887).
2. H. LECHATELIER, *ibid.*, **113,** 1034 (1891).
3. L. OUVRARD, *ibid.*, **130,** 335 (1900).
4. W. GUERTLER, *Z. anorg. Chem.*, **40,** 225 (1904).
5. F. DECARLI, *Atti accad. Lincei*, (6)**5,** 41 (1927).
6. R. TOURNAY, *Compt. rend.*, **203,** 558 (1936).
7. E. INGERSON, G. W. MOREY, AND O. F. TUTTLE, *Am. J. Sci.*, **246,** 31 (1948).
8. N. A. TOROPOV AND P. F. KONOVALOV, *Doklady Akad. Nauk S.S.S.R.*, **66,** 1105 (1949).
9. S. T. ALONSO AND M. J. OTERO DE LA GANDARA, *Anales real soc. espan. fis. y quim. (Madrid)*, **B48,** 750 (1952).
10. E. S. SHEPHERD, G. A. RANKIN, AND F. E. WRIGHT, *Am. J. Sci.*, 4th Ser., **28,** 293 (1909).
11. R. M. GRUVER, *J. Am. Ceram. Soc.*, **31,** 323 (1948).
12. H. E. SWANSON AND E. TATGE, *J. Research Nat. Bur. Standards*, **46,** 321 (1951).
13. G. W. MOREY, *J. Soc. Glass Technol.*, **35,** 270 (1951).
14. J. W. GREIG, *Am. J. Sci.*, **13,** 27 (1927).
15. B. E. COHN, *J. Am. Chem. Soc.*, **55,** 953 (1933).
16. D. H. KABAKJIAN, *Phys. Rev.*, **51,** 365 (1937).
17. H. W. LEVERENZ, "An Introduction to Luminescence of Solids," p. 234, John Wiley & Sons, Inc., New York (1950).

Cathode Ray Tube Screen Charging and Conditions Leading to Positive Ion Deterioration

A. B. LAPONSKY, M. J. OZEROFF,[1] W. A. THORNTON, AND J. R. YOUNG

Research Laboratory, General Electric Company, Schenectady, New York

ABSTRACT

Screen charging in standard cathode ray tubes is related to the effective yield of secondary electrons. This yield depends strongly on the nature and geometry of the screen surface. If the surface is smooth, a sticking potential can be defined, above which the screen potential does not rise; if the surface is rough, as with a standard powder layer, field dependence of effective secondary electron yield causes more complex charging effects. Dependence of screen charging on phosphor thickness, coverage, particle size and shape, and on gas pressure in the tube is considered.

Ion-focussing field configurations, associated with negative screen charging in tubes of different shapes, are correlated with observed patterns of phosphor deterioration by positive ions; production of these ions is considered. Effects of raster geometry, anode materials, and the magnitude of the focussing field are mentioned. Observations relevant to x-burn in commercial television tubes are summarized.

Insulating properties of phosphor screens in standard cathode ray tubes lead to dependence on secondary emission in establishing screen potential. Under certain conditions, equilibrium screen potential differs greatly from the potential of the tube anode. Effects arising from this screen-anode potential difference and from the internal electrostatic fields associated with it have long been of interest and importance. One of these effects, of potential

[1] Present address: Microwave Lab., General Electric Co., Palo Alto, Calif.

concern in commercial applications of the cathode ray tube, is a decrease in electron-induced luminescence of the phosphor screen due to bombardment of the phosphor by accelerated and focussed positive ions. An understanding of this effect involves study of (*a*) screen charging, (*b*) ion-focussing fields, (*c*) ion production, and (*d*) phosphor deterioration in the cathode ray tube.

Some of the early literature (1–7) is concerned with screen charging and first attempts to measure the potential of the insulating phosphor screen. Other papers (8–12) mention the role of ions and internal fields in producing the phosphor deterioration or "ion burn." Recently (13) screen-charging dependence on secondary emission has been considered in some detail. Some of the ideas advanced in the above references are unsupported by direct experimental evidence. It is the purpose of the present paper to present an integrated discussion of the conditions leading to positive ion deterioration of cathode ray tube phosphor screens. This discussion is based on experiments performed as well as on the existing literature. Details heretofore unpublished include: (*a*) data in the high anode voltage region by electronic measurement of screen potential; (*b*) data on dependence of screen charging on surface geometry, screen thickness and coverage, particle size and shape, and residual gas pressure; (*c*) dependence of ion-focussing field configuration on tube and raster geometry; (*d*) ion production dependence on anode material; (*e*) dependence of observed phosphor deterioration by positive ions on the strength of the internal electric field.

In the idealized case, the screen potential follows the anode potential between the first and second crossovers (the unity values of the secondary yield curve). As the anode rises above the potential corresponding to the second crossover, the screen remains at this point (the sticking potential) and a screen-anode potential difference ΔV appears. Associated with ΔV is a field throughout the tube volume which serves to accelerate secondary electrons toward the anode for collection.

Operation and associated effects in a practical tube are considerably more complex than the idealized case discussed above. A number of additional considerations, the studies of which form the body of this report, are the following. (*A*) Residual gas is present in practical tubes. Ions are formed by primary and secondary electrons and by other ions, and under certain conditions are also accelerated to the screen. (*B*) Ion production by secondary electrons striking the anode coating may also be an important effect. (*C*) The phosphor layer is rough and, as will be discussed in detail later, its secondary emission characteristics depend on the electric field at the screen, that is, on the magnitude of ΔV.

Screen Charging

The secondary electron emission process, while fundamental in the operation of unaluminized cathode ray tubes, is sufficiently complex that evaluation of actual tube performance is difficult. Studies of the effect of variation in the secondary yield on the screen potential have furthered the understanding of cathode ray tube operation and are reviewed in the following sections.

Indications of adverse charging effects.—One of the most prominent indications of adverse charging of the cathode ray tube screen has occurred in present-day television picture tubes. This is the so-called x-burn, a typical example of which is shown in Fig. 1. It occurs most prominently in rectangular tubes, although under certain conditions described later, it can occur in circular tubes also. It occurs mainly in tubes operating at second anode voltages greater than about 15 kv and is most easily observed at low voltages. In general, it appears only after many hours of tube operation, but in some cases it has been observed after only 10–15 min of operating time. A second indication of adverse screen charging has to do with reduced light output of screens at the higher voltages. If one increases the accelerating voltage of a standard unaluminized cathode ray tube, taking care to avoid current saturation, one finds that beyond a certain voltage range the light output does not continue to increase linearly, as would be expected.

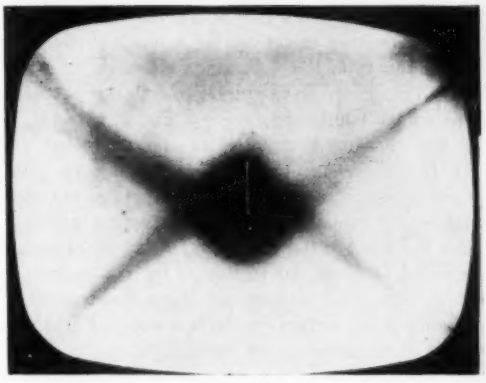

Fig. 1. Typical x-burn in rectangular tube

Surface effects.—Perhaps the simplest target surface is that of a smooth conductor. Such a surface closely approximates the condition under which the bombarding energy and angle of incidence alone control the electron yield (for a given target). The relation between the potential of a smooth conducting floating target and the anode potential of a tube may be described by plots such as curve A, Fig. 2, for a smooth silver target in which the tangent of α is unity, indicating sticking (4, 6). The importance of the surface condition to the charging process

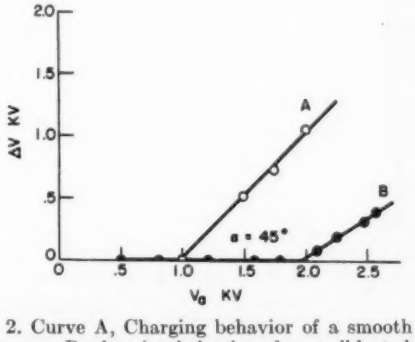

Fig. 2. Curve A, Charging behavior of a smooth silver target; curve B, charging behavior of a sandblasted nickel target.

becomes evident when a plot of ΔV vs. V_a is made for a floating conducting target having a rough surface. For a surface of this type, the secondary yield might be expected to depend markedly on the target-to-collector potential as well as on the bombarding energy. Fig. 2, curve B, indicates the charging occurring for a sandblasted nickel target. It is evident from the figure that a slope of unity does not necessarily occur when the target ceases to follow the anode. For insulating and semiconducting targets such as glass and some of the phosphors, target charging might be expected to be similar to that of the conductors; here the deviations from sticking are quite pronounced. The importance of the surface condition is seen in Fig. 3, where the effect of roughness on the charging process is observed; similar observations have been reported (4). Sticking was observed to occur for only one insulator, Fig. 4, for a smooth glass television tube face-plate target.

Evidence indicates that the charging process must be quite sensitive to conditions occurring at the target surface. Absence of sticking of the rough conductor and the rough insulator would seem to demand an explanation for the charging process in terms of electric fields external to the bombarded surface. As discussed below, occurrence of larger slopes in the ΔV vs. V_a curves for relatively smooth surfaces compared to rough surfaces suggests that effective secondary yields are controlled in part by trapping or by formation of space charges in the crevices of the rough surfaces; also, an increase in the effective secondary electron collection with increasing ΔV could then be responsible for the second crossover rising slightly as the anode-to-target potential increases.

A striking feature of this study of screen-charging phenomena in cathode ray tubes is the prevalence of a typical curve, Fig. 5, which may be represented in the region above V_o roughly by the relation

$$\Delta V = \tan \alpha (V_a - V_o)$$

where $\tan \alpha$ is often near 0.7.

The screen potential V_s continues to rise as V_a is increased above V_o, although at a slower rate. Sticking of rough screens has been observed in no case. Since the effective secondary emission yield δ_{eff} must always equal unity in the steady state, V_s must always correspond to the effective second crossover value of electron bombarding energy. Therefore, the only interpretation of Fig. 5 is that above V_o the effective second crossover moves to higher energies with the increase in ΔV that accompanies an increase in V_a. That is, the information of Fig. 5 may be presented alternatively as in Fig. 6; however, the information concerns only the second crossover points of the family of δ vs. ϵ, curves (secondary emission yield δ vs. primary electron energy ϵ).

Fig. 7, obtained by d-c measurements on a conducting

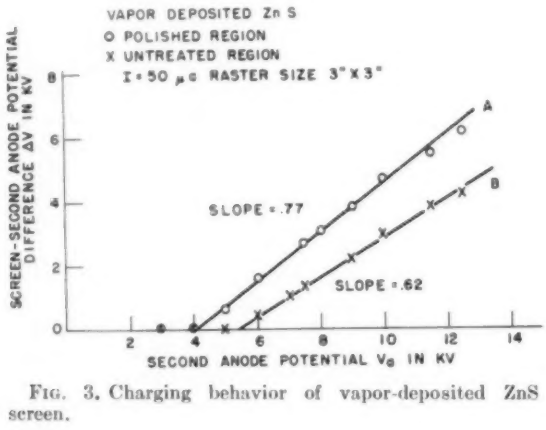
VAPOR DEPOSITED Zn S
O POLISHED REGION
X UNTREATED REGION
I = 50 μa RASTER SIZE 3" X 3"
SCREEN-SECOND ANODE POTENTIAL DIFFERENCE ΔV IN KV
SECOND ANODE POTENTIAL V_a IN KV
SLOPE = .77
SLOPE = .62
A
B

FIG. 3. Charging behavior of vapor-deposited ZnS screen.

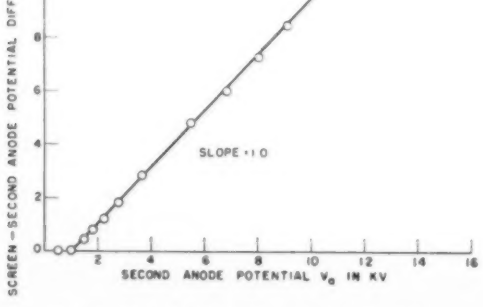
LEAD GLASS SCREEN
I = 100 μa RASTER SIZE = 8" X 8"
SCREEN-SECOND ANODE POTENTIAL DIFFERENCE ΔV IN KV
SECOND ANODE POTENTIAL V_a IN KV
SLOPE = 1.0

FIG. 4. Charging behavior of smooth glass

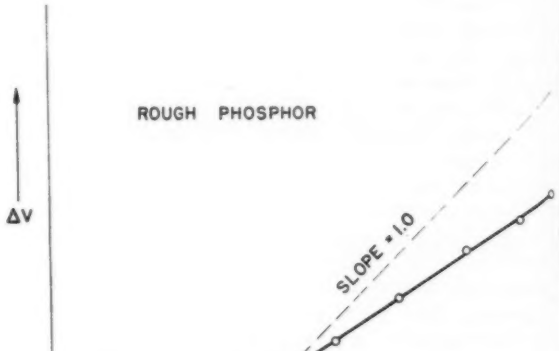

FIG. 5. Screen-charging in a typical cathode ray tube

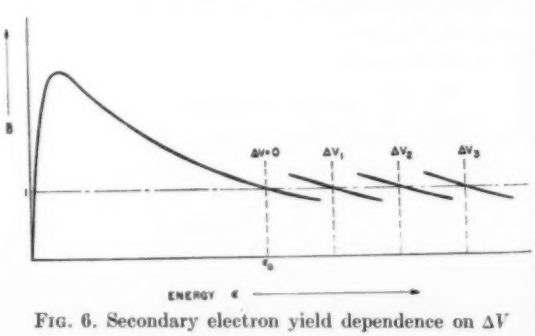

FIG. 6. Secondary electron yield dependence on ΔV

face plate tube, indicates that secondary emission ratio increases, with increase in collecting field, throughout the energy range; this is consistent with the moving of the effective crossover to higher energy with increase in field.

To arrive at an idea of how the observed field dependence of screen potential may come about, consider an ordinary cathode ray tube with a rough screen, and V_a being raised from zero. The anode at all times acts as collector; the screen at all times adjusts its potential with respect to the anode so that the latter collects one secondary electron per incident primary. At bombarding energies less than V_o, more than one secondary is produced at the screen surface per incident primary. In order that only one of these secondaries be collected in the steady state, the screen potential would be expected to rise above that of the anode by an amount that depends on the secondary electron energy distribution. One condition that may occur at the surface of the screen is suggested by considering a simple model. Assume that the screen surface is a tightly packed field of hemispheres. A constant flux of primaries produces secondaries, in this case because of increasing angle of incidence, more copiously the deeper down the primary strikes. The secondaries may escape in one free path, collide with and stick to the phosphor surface, or be degraded in energy by one or more collisions with the phosphor or other electrons until some approach thermal energies. A steady-state space charge is set up. Space charge gradient, density, and current density out of the interstice depend on the potential difference between the phosphor surface and some neighboring equipotential surface; this in turn depends on ΔV and thus on the potential V_s assumed by the screen.

One hypothesis to account for the screen-charging behavior is the following: whatever the "intrinsic" secondary emission characteristic of a phosphor may be (the δ vs. ϵ curve for a smooth sample showing no collecting field dependence) it is altered when the sample possesses a typical rough surface. The true second crossover becomes very high (above 25 kv) under the normally unrealizable condition that every secondary electron produced is collected. This high second crossover may be attributed to the increase in secondary emission with mean angle of incidence of the primaries. A moderate increase in δ should result in a large upward shift of the second crossover because here the negative slope of the δ vs. ϵ curve is small. The high true second crossover implies that at all normal operating voltages more than one secondary per primary is produced.

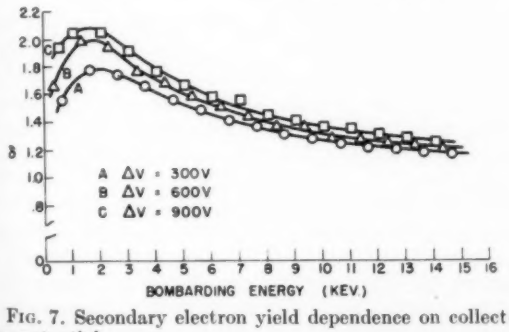

FIG. 7. Secondary electron yield dependence on collecting potential.

Since the effective secondary emission yield is always unity in the steady state, the screen potential continually adjusts itself, as the anode potential is changed, so that (*a*) field leakage into the interstice and (*b*) the electron density and energy distribution found there are such that current out is equal to current in.

Put in another way, the only externally controlled variable considered here is the anode potential. A change in this is accompanied by a change in screen potential, which may always be considered to be an equilibrium value. Once V_a is established, V_s controls two quantities: (*a*) the collecting field E at the phosphor surface, related to ΔV, and (*b*) the energy ϵ of the primary electron as it strikes the phosphor. The value of ϵ controls δ which in turn is related to electron density ρ; the effective ratio δ_{eff} remains equal to unity. Thus V_s moves to a value where E and ρ lead to $\delta_{eff} = 1$. The discussion above involves only the field collection of secondary electrons. Other processes may be important such as field enhanced secondary emission (9).

Dependence of screen charging on phosphor coating thickness and coverage.—Some early observations indicated that x-burn occurs more rapidly in television tubes whose screens are thinner than normal (14). It has also been reported that very thick screens are not as good as those of intermediate thickness with regard to maintaining anode potential (15). Therefore, it seemed worth while to investigate further the dependence of screen-anode potential difference on various screen thicknesses of a standard white sulfide phosphor.

A common coating weight employed in unaluminized television tubes is 5.5 mg/cm². Therefore, tubes were made using 2.75 mg/cm², 5.5 mg/cm² and 11 mg/cm² of standard white ZnS phosphor. Two tubes of each coating weight were made in standard 17-in. rectangular television tube bulbs. Tubes of each coating weight were placed on life test in a standard television chassis, using an auxiliary high voltage anode supply. Anode voltage was maintained at 25 kv and beam current at 150 μa. The raster size was approximately 10 x 12 in. Screen potential was measured periodically during the life testing, using the Kelvin method (16).[2] Using the electron gun as an ionization gauge, pressure was determined periodically during the life of the tubes and was found to remain almost constant, below 10^{-5} mm Hg, in all of the tubes throughout this set of experiments.

Fig. 8*a* shows a typical plot of ΔV vs. V_a at different intervals during the life of a tube with a screen coating of 2.75 mg/cm²; Fig. 8(*b*) shows typical results obtained from a tube with a screen coating of 5.5 mg/cm². Differences noticed between the light-screen tubes and the standard tubes are: (*A*) the screen follows the anode in potential up to 25 kv, the limit of measurement, in standard-screen

[2] The television tube screen potential measurements in this paper were obtained using the Kelvin method. This utilizes the screen as one plate of a condenser and another vibrating plate in front of the tube face as the other condenser plate. Alternating current to the vibrating plate reduces to zero (or a minimum) when this plate is at the potential of the screen. Hence, measurement of the d-c potential of this plate when the alternating current to it is a minimum gives the value of the screen potential.

tubes before life testing, but does not for light-screen tubes; (*B*) the breakover point remains nearly constant with life in standard-screen tubes, but moves to lower anode voltages in the light-screen tubes; (*C*) the breakover point occurs at higher anode voltages for the standard-screen tubes than for the light-screen tubes; (*D*) the breakover point is sharp in the standard-screen tubes while in the light-screen tubes there is a more gradual variation. Fig. 8(*c*) shows results obtained from one of the tubes with a screen coating of 11 mg/cm². These results are similar to those obtained from tubes with the standard screen coating.

The increase in slope of the curves above the break point with life indicates that a larger collecting field is necessary to collect one secondary per primary. The reason for this is not certain but may involve a change in the geometry of the phosphor layer or a decrease (3) in the efficiency of secondary emission.

In an effort to determine other properties of the different screens, the tubes were cracked open and the screens observed under a microscope. Many regions of bare glass were present in the light screen, while almost complete coverage occurs in the medium and heavy screens. Since the secondary emission properties of glass are low compared with the phosphor at higher accelerating voltages, this bare glass would be expected to increase the screen-anode potential difference at high anode voltages. This is observed for the light screen-coating tubes. Therefore, it appears that screen charging does depend on the screen-coating weight or phosphor coverage of the glass, but sticking does not occur for the screen-coating

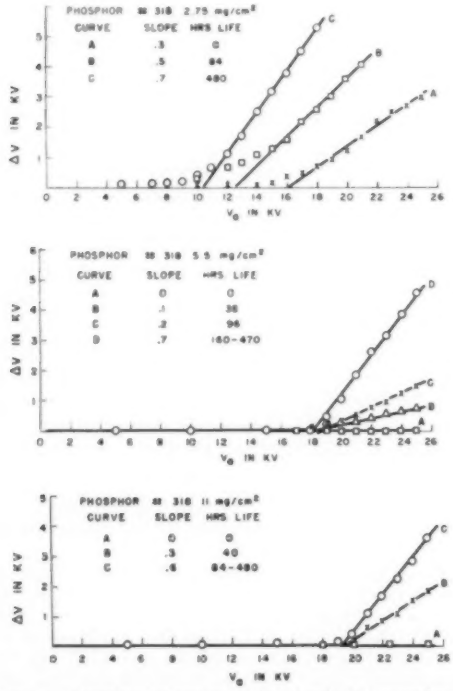

FIG. 8. Charging behavior of (a) (*top*) thin powder phosphor screen; (b) (*center*) standard powder phosphor screen; (c) (*bottom*) thick powder phosphor screen.

weights employed here. These results are different than those quoted by Zworykin and Morton (15) although those authors do not specify the screen material or coating weights used.

Dependence of screen charging on particle size and shape.—The concept of "roughness" as applied to cathode ray tube particle-layer screens needs definition. A useful one relates roughness to the mean angle of incidence of electrons in the primary beam, when the beam is traveling normal to the plane of the screen. This differs from the usual meaning of roughness, which involves size and shape of surface elements.

The mean angle of incidence of primaries approaching from a given direction depends only on the shape and not on the dimensions of the elements. In the presence of a collecting field at the phosphor layer, with its leakage between the grains, the size of the elements may well have little effect. Assuming a constant primary electron current density, the average angle of incidence of primaries on the field of hemispheres is 45°. This value of mean angle of incidence is probably about right in some practical cases, since photomicrographs of some typical phosphors show rounded spheroidal grains. Even in the case of jagged crystals, if orientation of crystal surfaces to the primary flux is integrated over the incidence angle, the mean angle again is thought to be 45°. Such reasoning leads one to expect little or no dependence of the number of secondaries emitted on either size or shape of phosphor particles making up the screen.

Experiments designed to detect a trend in screen-charging behavior with differences in particle size and shape have been made. Twelve 17-in. rectangular cathode ray tubes have been tested, two of each of six combinations, as follows:

Phosphor component	Mean particle size (μ)
Blue	<5
Blue	~10
Blue	~20
Yellow	<5
Yellow	~10
Yellow	~20

Photomicrographs of the two components show that blue-emitting phosphor crystals are relatively rough and jagged compared with the yellow particles, which are smooth and spheroidal. Differences in screen charging and ion deterioration of the phosphors were small, and no significant trend was evident, based on the limited statistics of these experiments.

Effect of gas pressure on screen charging.—A possible correlation between gassy television picture tubes and absence of x-burn was mentioned (17) some time ago. A number of tubes, peculiar in that x-burn did not occur during high voltage testing, was found to have pressure higher by a factor of 1000 than typical production tubes. Furthermore, the screens of these tubes were found to follow the anode in potential, within 200 v, up to 25 kv; that is, no screen-anode potential difference existed during test and hence no ion focusing or x-burn occurred. Subsequently, studies were begun to determine directly dependence of screen charging on ambient pressure. The first of these showed that the screen-anode potential dif-

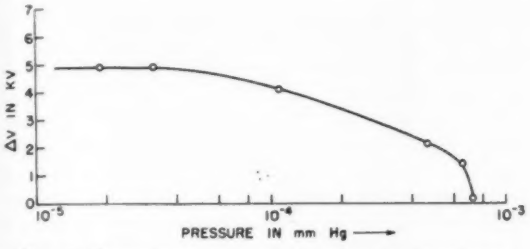

FIG. 9. Dependence of target-charging on gas pressure

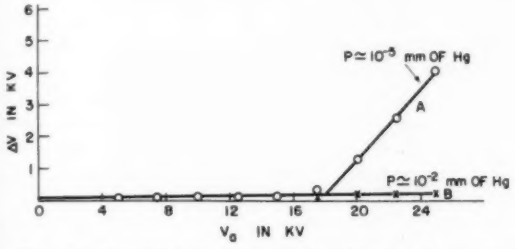

FIG. 10. Dependence of screen-charging on gas pressure in a standard tube.

ference ΔV decreased sharply toward zero at a pressure near 10^{-3} mm Hg (Fig. 9). These data were obtained by measuring the potential of a small phosphor-covered conducting slide in a demountable system, by means of an electrostatic voltmeter. A study was made of a standard television tube which had shown both ion burn and a large ΔV at higher voltages. This tube was placed on a continuously pumped system, and ΔV vs. pressure obtained by the Kelvin method. Resulting curves for nitrogen, hydrogen, and air were identical in form to that of Fig. 9. Finally, in Fig. 10 appears a routine ΔV vs. V_a curve for a standard tube (curve A). After further operation, the screen was observed to follow the anode within 300 v (curve B), and at that time the residual gas pressure was found to have risen to near 10^{-2} mm Hg. The mechanism that causes the screen to charge toward the anode potential at these higher pressures has not been established. At higher pressures, many more positive ions will be produced by the interaction of the primary and secondary electrons with the gas molecules. Therefore, one possible mechanism is that large numbers of positive ions strike the screen and thereby raise the screen potential; the same ions, striking the screen, produce "secondary" electron emission. Values of this secondary emission ratio γ up to 10 electrons per ion for 100–1000 ev light ions on metals have been reported (18).

Ion Focusing Fields; Ion Production and Deterioration Effects

Introduction

Internal electrostatic fields, produced in cathode ray tubes operated under conditions such that a screen-anode potential difference exists, are of interest in regard to the acceleration and focusing of ions present in the tube volume (8, 19). As has been seen, an insulating phosphor screen will, under bombardment by electrons of high enough energy, assume a potential considerably more negative than that of the anode or collector. Although this potential is not uniform across the screen, the effect of this nonuniformity seems to be negligible in comparison with effects due to the mean screen-anode potential difference ΔV.

The tube volume contains an electron flux consisting of high-energy (monochromatic) primaries whose distribution depends upon the method of scanning, and of lower energy secondaries whose energy depends upon their position in the field. Predominantly, positive ions are formed within the volume and at the two surfaces. The ion yield from a given volume or surface element of a material is a function of electron energy and current density. Positive ions are accelerated toward the screen; starting with near zero energy, they will follow paths roughly paralleling the field lines and will strike with energies ranging from zero to $e\Delta V$, depending on the point of origin of each. If the screen is sensitive to positive ions, it will show the effects of an integrated ion current at each point. In the absence of a gradient of field intensity, no focusing will occur.

In the practical case of the large production cathode ray tube, in which the anode is shaped somewhat like a right circular cone, some rough generalizations may be made. The primary beam is swept through most of the tube volume. The average beam current per unit volume varies as $1/r^2$; the radius r is the distance from the center of beam deflection which is near the neck-funnel intersection of the tube, measured toward the face plate. Aside from other effects, ion production per unit volume, by primary electrons interacting with the residual gas, therefore will fall off sharply with distance from the rear of the volume. If secondary electron production per unit area of screen is assumed constant, and the secondaries are liberated with only a few electron volts of energy on the average, then secondary current density in the volume will depend on focusing effects of electrostatic fields. Where a ΔV is present, the equipotential configuration appears somewhat as in Fig. 11; thus, more secondaries bombard a unit area of anode surface near the tube skirt than at the rear of the tube. While ion production by secondaries per unit volume may be somewhat greater toward the edges of the tube, that due to primaries increases by factors of 10–100 times toward the rear of the tube.

Round tube.—Fig. 11 illustrates the equipotential surfaces and field lines found in a round tube of typical geometry. Also shown is a suggested plot of positive-ion current density across the screen in the steady state. A strong maximum in positive-ion current density is expected in the center of the round tube for two reasons: (*a*) ion production is greatest at the rear of the tube, and the paths of these ions tend to remain near the axis of the tube; (*b*) focusing of ions at the center of the face plate, by the field, is present; this by itself contributes to ion-density maximum at the center. Observations on round tubes show that an intense central spot does occur, but that it has more sharply defined edges than the foregoing description might lead one to expect.

Rectangular and triangular tube.—The rectangular cathode ray tube in common use has a somewhat pyramidal shape. The four corners are blunt, as are the edges

of the pyramid. These edges become less and less well defined toward the neck region of the tube until, about two-thirds of the way to the neck, the anode loses all four-cornered symmetry and becomes nearly spherical. The four-cornered geometry of such a tube alters the electric field as compared with that in a round tube so as to cause positive-ion focusing into a definite and unique pattern. Ions traveling along field lines originating in the rear of the tube, where four-corner effects are absent, will be focused into a diffuse center spot similar to that characteristic of the round tube of Fig. 11. Ions originating in regions where corner effects are present in the equipotential configuration are concentrated at the screen into a rather sharp pattern resembling an X. This focusing action can be understood qualitatively. Coaxial cylindrical equipotentials, for instance, result in focusing at the axis of any charged particle originating with zero energy in such a field (*see* Fig. 12*a*). The family of equipotential surfaces in a rectangular tube in which a screen-anode potential difference exists will appear in cross section similar to that of Fig. 11. However, a section determined by a plane perpendicular to the tube axis and near the face plate will appear as in Fig. 12*b*. There the fine lines represent intersections with the face plate of four planes of symmetry through the corners (edges of pyramid). The sketch shown in Fig. 12*c* of equipotential surfaces in the corner region indicates the focusing action.

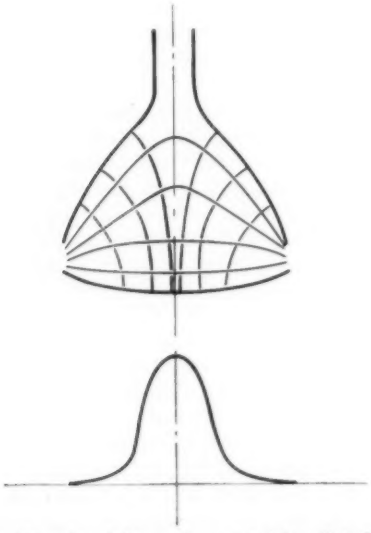

FIG. 11. Focusing fields and expected ion distribution in a round tube.

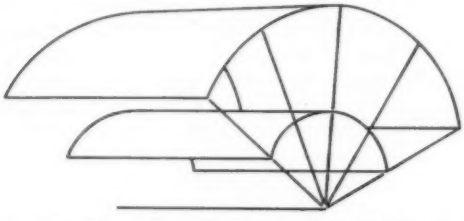

FIG. 12*a*. Focusing action of coaxial cylindrical equipotentials.

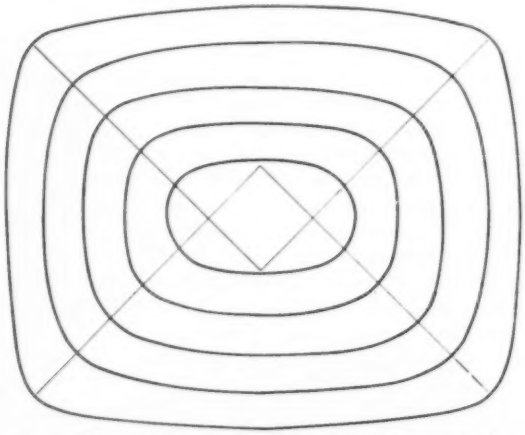

FIG. 12*b*. Axial cross section of equipotentials in a rectangular tube.

In Fig. 13 appear three photographs of positive-ion patterns on screens of different geometry. The round tube shows the ion spot of Fig. 11. The rectangular tube shows a similar diffuse area and superposed upon it the relatively sharp X of Fig. 12*b*. The tube whose screen is pictured in Fig. 13*c* is a regular tetrahedron, one face of which forms the screen. The corners and edges of this tube are sharply defined in order to maximize focusing effects. The expected Y-pattern is clearly shown. Since corner effects exert an influence throughout the tube, the diffuse center spot is less marked.

With regard to the round and rectangular tubes, x-burn should occur only in the rectangular tubes where four-corner symmetry is present, so long as the entire screen (round or rectangular) is scanned or overscanned and thus is approximately an equipotential surface.

Effect of raster geometry.—Where a rectangular raster is scanned in a round tube, an x-burn can occur, as shown in Fig. 14. While the scanned area remained at a potential far below that of the anode, adjacent unbombarded areas of the screen charged to high potentials, approaching the anode potential. When this occurs, four-corner geometry

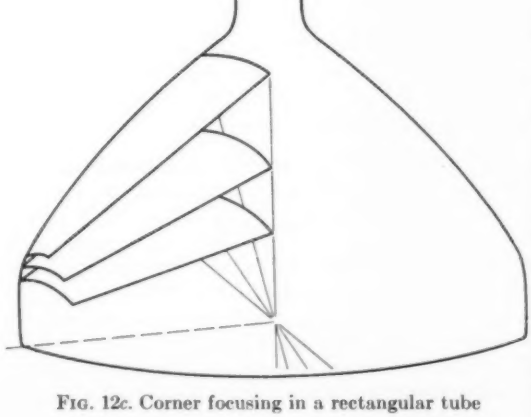

FIG. 12*c*. Corner focusing in a rectangular tube

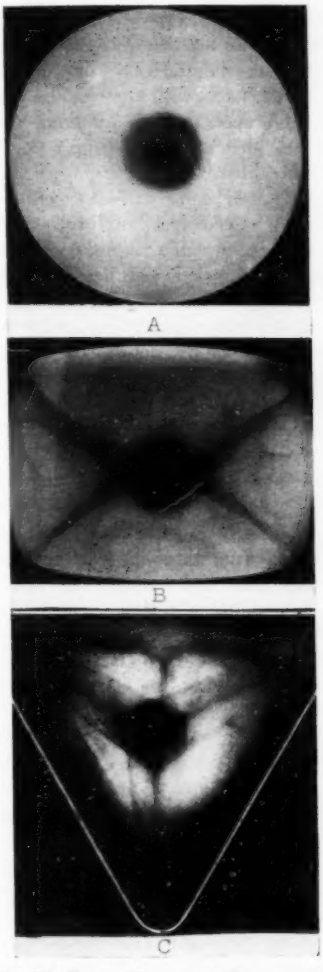

FIG. 13. Ion pattern vs. tube geometry

of the ion-focusing fields is again present, although somewhat dissimilar to that found in a rectangular tube.

Tube geometry vs. raster geometry.—In order to determine the effect of the raster on x-burn, a rectangular tube was life-tested with a small rectangular raster rotated about 30° from the horizontal. After 100 hr of life testing, a normal x-burn was found. Variation of the screen-anode potential difference over the face of this tube was measured and found to be present but small. Here it is apparent that a variation in screen-anode potential difference is present between regions inside the raster area and those outside. However, in this tube this variation was not sufficient to affect the normal orientation of the x-burn. In another tube (Fig. 15) the unbombarded areas remained near anode potential while the rotated raster area was several kilovolts below the anode in potential. In this case the x-burn was rotated with the raster, as if the focusing fields now depended on raster orientation alone. Therefore, either tube geometry or raster geometry can predominate in the orientation of x-burn, depending on how the bombarded and unbombarded portions of the screen charge.

Positive-ion production and phosphor deterioration.—Positive ions may be produced in a cathode ray tube by: (*a*) the interaction of high-energy primary electrons with the residual gas in the tubes, (*b*) the interaction of lower energy secondary electrons with the residual gas, and (*c*) the interaction of secondary electrons with the anode material of the tube. Other sources of positive ions may be present, but only the above are considered in this discussion.

Suppose a television tube operates with a residual gas pressure of 10^{-6} mm Hg and with a beam current of 100 μa. Consider the production of positive ions only in the region between the final gun anode aperture and the tube screen. Here the electron energy is usually 10 to 20 kev and the ionization probability for air is about 10^{-6} ion per electron per centimeter path at 10^{-6} mm Hg (20, 21). The ionization path length for the electron in a standard television tube is approximately 20 cm. Therefore, a positive-ion current of about 2×10^{-9} amp would be produced in the region between the final anode aperture and the screen. These positive ions will be accelerated toward the screen if it is negative with respect to the anode.

The effective secondary emission ratio of the screen is always unity under equilibrium conditions, so the number of secondary electrons leaving the screen is the same as the number of primaries arriving. If the screen is sufficiently negative with respect to the anode, secondary electrons will attain energies sufficient to produce ionization on their way to the anode. Since the screen-anode

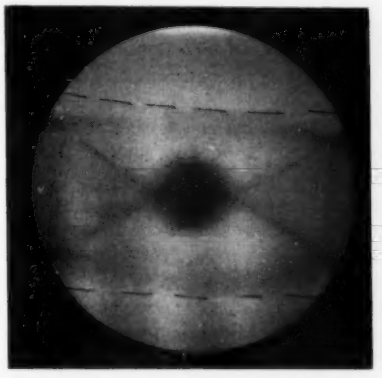

FIG. 14. X-burn in a round tube

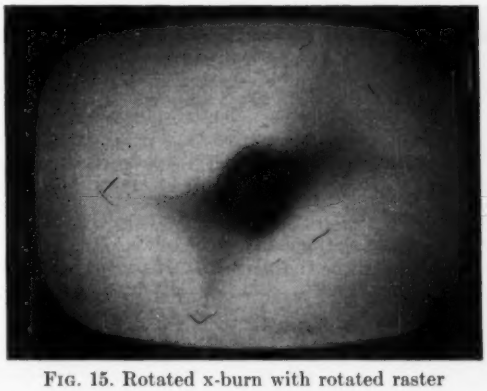

FIG. 15. Rotated x-burn with rotated raster

potential difference may be a kilovolt or more, the ionization probability for these electrons would be greater than for the higher energy primary beam. The mean ionizing path length would be somewhat less, however, and one might expect the production of positive ions by secondary electrons to be roughly equal to that by primaries.

Positive-ion production at the anode coating has been considered (22) as the cause of x-burn. Information is not available on the probability of producing positive ions by electron bombardment of the anode material. However, from indirect evidence, this process as a major source of ions seems rather unlikely.

Observations have been made (23) of the quantity of positive ions necessary to produce a detectable reduction in the luminescent efficiency of a sulfide phosphor. It was found that for H_1^+ and H_2^+ ions accelerated to energies of 2.5 kev or greater, a current of about 10^{-9} amp/mm^2 bombarding for 1 sec produces detectable deterioration, when viewed under 5-kev electron bombardment. The area of a 17-in. television screen is approximately 10^5 mm^2. If the estimate of the number of positive ions produced by the interaction of primary and secondary electrons with the residual gases in the bulb is correct, the screen will be bombarded with an ion current of about 10^{-9} amp. In order to produce detectable positive-ion deterioration over the entire screen, assuming the ions have energies as given above, it would take 10^{+5} sec or about 30 hr. Now, if the ions were focused into an X with an area one-tenth of the total screen area, deterioration could be detected in approximately 3 hr. This would indicate that x-burn could occur in a very short time by this mechanism alone, if the screen potential is suitably low.

Effect of anode coating material on x-burn.—It has been proposed (22) that the positive ions producing x-burn originate at the aquadag anode when it is bombarded by secondary electrons from the screen. Different anode materials might be expected to provide different quantities of positive ions per bombarding electron. It was therefore thought worth while to investigate the effect of different anode materials on x-burn. Tubes were made having anode coatings of platinum, silver, and aluminum. The tubes were life-tested, at an anode voltage of 25 kv, with the raster confined to the phosphor area, so that the high-energy electrons would not strike the anode material. The growth of x-burn was observed and the screen-anode potential difference measured at various intervals during the testing. The existence of a screen-anode potential difference of several kilovolts was noted in most of these tubes within the first 50 hr of life-testing, and results obtained resembled the curves shown in Fig. 8*b*. In every case when a screen-anode potential difference of 1 kv or more was observed, x-burn could also be detected. Intensity of the x-burn was greater for the tubes that had a larger screen-anode potential difference. There was little difference between the rate of occurrence of x-burn in these tubes and the aquadag anode tubes.

Several metal-cone rectangular television tubes were also life-tested, and x-burn occurred in every case in which a screen-anode potential of 1 kv or more was present. These metal-cone tubes did not have an inner aquadag coating on the cone; only the neck region was coated.

These results make it appear a little more likely that the positive ions that are believed to produce the x-burn originate in the tube volume by the interaction of primary and secondary electrons with the residual gas molecules. It is possible, however, that the materials used as anode coatings all provided a copious supply of positive ions under electron bombardment.

Dependence of x-burn on screen potential.—Early observations led to the correlation of the occurrence of x-burn with the existence of a potential difference between tube anode and screen (19). This has been amply verified during the present work. Nothing was known of the magnitude of this potential difference ΔV necessary to produce x-burn, nor of the dependence, if any, of burn intensity on ΔV; therefore, the following experiments were performed. In order to maintain the screen at any desired potential with respect to the aquadag anode, the face plates of rectangular 17-in. glass tubes were made conducting by depositing a film of tin oxide on the inner surfaces.[3] An electrical connection was made to this transparent conductive film through the skirt of the tube. A standard ZnS powder phosphor was then settled on the conductive film. Standard cathode ray tube processing techniques were employed on these tubes. Two tubes were placed on life test with the conductive screen coating connected electrically to the second anode. Anode voltage was maintained at 25 kv and beam current at 150 μa throughout the life test. The beam was scanned over the screen, providing a raster dimension of about 10–12 in. Periodically, the second-anode voltage was reduced to 2.5 kv in order to observe the growth of x-burn. No x-burn appeared in either of the tubes during the 450 hr of life-testing. These results indicate that x-burning will not occur if the screen remains at the same potential as the anode.

Next, the electrical connection to one tube screen was disconnected from the anode and the screen allowed to float at a potential that was determined by its secondary emission properties. Life-testing was then continued for 20 hr. On reduction of the anode voltage to 2.5 kv, a pronounced x-burn was noticed. This x-burn could be detected with anode voltages up to 10 kv. It was later found that the floating potential of the screen was 2.8 kv below the anode during this final 20 hr of life-testing. Thus, x-burn will occur in a short time if the screen drops appreciably below the anode. It was of interest to determine the effect of smaller screen-anode potential differences on the growth of x-burn. Therefore, the other tube was further life-tested with the screen 1 kv below the anode. After 4 hr an x-burn was observed under 2.5 kv electrons.

It is not necessary for a variation in potential to exist across the screen in order for x-burn to occur, as shown by its occurrence in the presence of the conducting face plates.

It was observed that the intensity of the normal x-burn is greater for a larger screen-anode potential difference. This may be due to any one or more of the following processes: (*a*) higher energy positive ions striking the screen may produce a greater deterioration per ion; (*b*) the greater probable penetration depth of the ions may mean that the deterioration is more easily observed at a

[3] Obtained through the courtesy of J. L. Sheldon, Corning Glass Co.

given electron-bombarding energy; (*c*) more gas may be liberated from the anode material by the higher energy secondaries, thus enabling more positive ions to be produced; (*d*) if the positive ions originate at the anode surface, the probability of production of these ions may be increased at higher bombarding energies. Adequate information is not available at present to determine which of the above is most important or if still another mechanism is responsible for the increase in x-burn intensity with increasing screen-anode potential difference.

Summary

Screen charging behavior depends strongly on the nature of the bombarded surface. Both conducting and insulating screens, if very smooth, follow the anode up to a "sticking potential" and charge no higher regardless of anode voltage. On the other hand, a roughened surface (sand-blasted metal, vapor-deposited phosphor, settled powder-phosphor screens) continues to rise in potential above the discontinuity although at a slower rate; the slope in this region varies as the roughness of the bombarded surface. The fact that screen potential for a rough phosphor layer neither follows the anode to high potentials nor "sticks" at some intermediate value is related to the collecting action of the electric field near the phosphor grains on a steady-state secondary electron space charge in the interstices. Phosphor layer weights also govern screen charging. A standard weight of about 5 mg/cm² shows secondary emission sufficient initially to follow anode potentials at least as high as 25 kv; with bombardment, screen-anode potential difference ΔV appears at high voltages and increases with time, at a given anode voltage, approaching a limit. Thicker screens behave similarly. As screen weight is decreased below 5 mg/cm² and a larger fractional area of bare glass is exposed to the primary electrons, the screen ceases to follow initially and, for a given bombardment time, shows a larger ΔV. No dependence of screen-charging behavior on phosphor particle size and shape is observed; this is consistent with the probability that the mean angle of incidence of primary electrons on a powder phosphor layer is also independent of particle size and shape. A correlation is observed between high residual gas pressure (10^{-2} – 10^{-3} mm Hg) and the absence of potential difference ΔV.

Ion-focussing fields, due to a screen-anode potential difference, are described by the geometrical configuration of equipotential surfaces in tubes of several shapes. These configurations are shown to lead to observed patterns of ion-induced phosphor deterioration in round, rectangular, and triangular tubes. In the case of underscanning, four-cornered symmetry of focussing fields may again exist and the x-like burn pattern occur regardless of tube geometry.

Positive-ion production by bombardment of residual gas by primary and secondary electrons appears to be the major process; correlation is shown between the number of ions necessary to produce visible reduction in phosphor light output and the number of positive ions probably produced by electron bombardment of the gas. Furthermore, ion-induced screen deterioration appears to be independent of anode material.

Positive ion burn in commercial cathode ray tubes is evidently best controlled by elimination of the ion-focussing fields in the tube. In the absence of the aluminizing process or its equivalent, maintenance of secondary emission of phosphor screens appears to be the major problem, since typical screens show secondary emission properties sufficiently good initially to maintain the tube field-free. There was no observed instance when a considerable field was present in a tube that positive ion burn did not take place rapidly. This deterioration of the phosphor requires a sufficiently high screen-anode potential difference, near 1–2 kv, to be visible in the region of normal tube operating voltages. "Sticking" of the screen potential was observed in this work only with smooth surfaces, and does not occur with standard powder screens because of field dependence of the effective secondary emission ratio. The common x-pattern is not restricted to rectangular tubes, but can occur wherever four-cornered geometry of ion-focussing fields exists.

Acknowledgments

The authors are indebted to many members of the General Electric Research Laboratory, and other Departments of the General Electric Company, for their cooperative assistance during this investigation.

Manuscript received August 19, 1955. This paper was prepared for delivery before the Cincinnati Meeting, May 1 to 5, 1955.

Any discussion of this paper will appear in a Discussion Section to be published in the June 1957 Journal.

References

1. J. B. Brown, *J. Opt. Soc. Amer.*, **27,** 186 (1937).
2. W. B. Nottingham, *J. Appl. Phys.*, **8,** 762 (1937).
3. H. Nelson, *ibid.*, **9,** 592 (1938).
4. C. Hagen, *Physik. Z.*, **40,** 621 (1939).
5. E. R. Piore and G. A. Morton, *J. Appl. Phys.*, **11,** 153 (1940).
6. H. von Salow, *Z. tech. Phys.*, **21,** 8 (1940).
7. V. K. Zworykin and G. A. Morton, "Television," John Wiley & Sons, Inc., New York (1940).
8. C. H. Bachman and C. W. Carnahan, *Proc. Inst. Radio Engrs.*, **26,** 529 (1938).
9. K. G. McKay, "Advances in Electronics," Vol. I, p. 66, Academic Press New York (1948).
10. G. F. J. Garlick, "Advances in Electronics," Vol. II, p. 151, Academic Press, New York (1950).
11. H. Leverenz, "Luminescence of Solids," p. 388, John Wiley & Sons, Inc., New York (1950).
12. R. Granacki, Paper presented at Electrochemical Society Meeting, Philadelphia, May 1952.
13. J. de Gier, A. C. Kleisma, and J. Peper, *Philips Tech. Rev.*, **16,** 26 (1954).
14. C. Dichter and A. I. Friedman, Private communication.
15. V. K. Zworykin and G. A. Morton, "Television," 2nd ed., p. 90, John Wiley and Sons, New York (1954).
16. J. R. Young, *Rev. Sci. Inst.*, **26,** 647 (1955).
17. C. Dichter, Private communication.
18. H. S. W. Massey and E. H. S. Burhop, "Electronic and Ionic Impact Phenomena," pp. 542 ff, Oxford Press, London (1952).
19. V. C. Campbell, Unpublished material.
20. S. Dushman, "Vacuum Technique," p. 351, John Wiley & Sons, Inc., New York (1949).
21. J. B. Hoag and S. A. Korff, "Electron and Nuclear Physics," p. 488, D. van Nostrand and Co., New York (1948).
22. L. R. Koller, Unpublished material.
23. J. R. Young, *J. Appl. Phys.*, **26,** No. 11, 1302 (1955).

Fluorescence of Thallium-Activated Halide Phosphors

KEITH H. BUTLER

Sylvania Electric Products Inc., Salem, Massachusetts

ABSTRACT

Measurements of the emission spectra with several exciting wave lengths and of the excitation spectra with several analyzing wave lengths have been made on KCl:Tl and NH_4Br:Tl with a range of Tl concentrations. Experimental data are analyzed and discussed with relation to the energy levels of the Tl ion involved in the excitation and emission.

The absorption spectra of Tl-activated alkali halide phosphors (1, 2) have been studied extensively and their excitation and emission spectra (3, 4) have received some attention.[1] In addition an attempt has been made to calculate from first principles the absorption and emission spectrum of Tl-activated KCl (5) and to correlate this with experimental data, including data on thermoluminescence.

There appeared, however, to be some possible ambiguities in the assignment of specific excitation and emission bands to transitions between states of the thallous ion, and this prompted a study of the spectra of the alkali halides in an effort to clarify these uncertainties.

This paper reports on measurements of the spectra of NH_4Br, which is crystallographically similar to the halides of Cs, and for which no published data could be found on either absorption or fluorescence, and on measurements of the spectra of KCl, amplifying previous data (3, 4).

Experimental Procedure

A trial of various methods of preparation showed that powder samples of the phosphors could be made by the method of Hutten and Pringsheim (6) and this was adopted. Reagent grade NH_4Br was mortar ground with C. P. thallous chloride to form a phosphor containing 10^{-2} mole fraction of Tl. This concentrated solid solution was successively diluted with additional NH_4Br to give phosphors in which the mole fractions of Tl were 10^{-3}, 10^{-4}, and 10^{-5}. Visual inspection under a u.v. source showed uniform fluorescence was obtained after a few minutes grinding. The purity of the reagent grade NH_4Br was checked by use of the excitation radiometer at a high level of sensitivity and no fluorescence could be detected at any wave length of excitation.

C. P. KCl was found to contain trace amounts of an impurity giving an excitation band at 272 mμ,[2] which resulted in very faint emission bands peaking at 335 and 485 mμ in the uncorrected emission spectra. Purification by fractional crystallization removed this impurity to the point where no fluorescence could be detected. Samples with 3.2×10^{-2}, 1.6×10^{-2}, and 8×10^{-3} mole fraction Tl were prepared by grinding the KCl with C. P. thallous chloride. Other samples were made by successive dilution of these with the pure KCl. Results were confirmed by using phosphors prepared from melts.

The excitation radiometer[3] used for the measurements will be described elsewhere. Basically, it uses radiation from a high pressure xenon arc in a quartz envelope, monochromatized by a Beckman model DU monochromator. A selected wave length from the exit beam of the excitation monochromator is focused on a phosphor coating on a small plaque. The emitted fluorescent light is focused on the entrance slit of a second Beckman monochromator (the analysis monochromator) and the intensity of a selected wave length is measured by a 1P28 photomultiplier. The magnitude of the exciting energy, with which the magnitude of the emission is compared, is measured by a second 1P28 photomultiplier tube receiving a fraction of the exciting radiation via a quartz beamsplitter. The ratio of two photomultiplier signals, after amplification and automatic attenuation of each signal, is directly plotted by a recorder at intervals of 25Å. Either the excitation spectrum or the emission spectrum can be scanned automatically.

The attenuation circuit of the excitation monitor is adjusted to correct for the relative output of the xenon arc, the slit width of the first Beckman, and the sensitivity of the monitor photocell so that the recorded output at a fixed analysis wave length is a measure of the relative quantum efficiency of fluorescence. This adjustment of the automatic attenuator was made by using $NaC_7H_5O_3$ as a reference material of constant quantum efficiency (7). The attenuator corrections for the analysis circuit were determined by using phosphors of known emission characteristics[4] to extrapolate data into the ultraviolet.

To obtain maximum response from the analysis photomultiplier much of the data was determined with use of a constant attenuation in the analysis circuit and slit widths of 2.0 mm. In these data the emission curves obtained are not corrected for slit width or photomultiplier sensitivity. Other data giving the true emission curves were obtained with selected samples.

In the case of KCl:Tl it was necessary at times to narrow the slits on the excitation monochromator somewhat to obtain satisfactory resolution of the spectra. Slit widths

[1] Excellent bibliographies will be found in references (1), (4), and (6).

[2] This is probably due to Pb^{++} [Cf. Hilsch, *Z. Physik.*, **44**, 860 (1927)] as pointed out by one reviewer of this paper.

[3] Built by Bayside Physics Lab. of Sylvania.

[4] Phosphors emitting between 280 and 320 mμ were kindly furnished by R. Nagy.

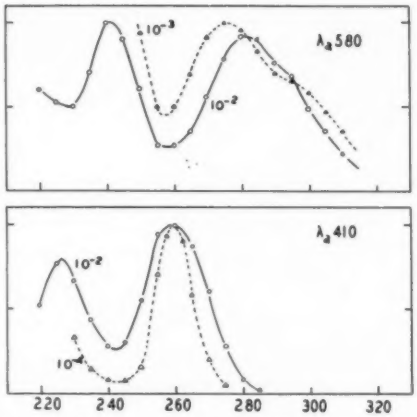

FIG. 1. Excitation spectra of NH_4Br:Tl measured at different emission wave lengths.

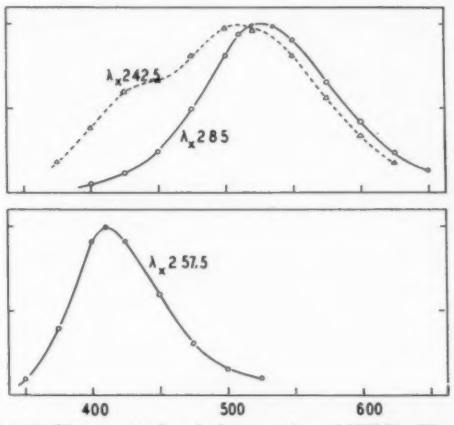

FIG. 2. Uncorrected emission spectra of NH_4Br:Tl measured with different exciting wave lengths.

of 0.50, 1.00, or 2.00 mm were used, while for the analysis monochromator a slit width of 2.00 mm was suitable.

RESULTS WITH NH_4Br

The general character of the spectra of NH_4Br:Tl can be readily described. The excitation spectrum has four bands peaking at 227, 242, 258, and 280 mμ, while the emission spectrum has two bands with maxima[5] at 400 and 535 mμ. The emission band at 400 mμ is excited only by the excitation bands at 227 and 258 mμ, while the band at 535 mμ is excited by the bands at 242 and 280 mμ. The intensity of emission at 535 mμ is much lower than that of the 400 mμ band even with optimum wave length of excitation.

To determine the characteristic excitation spectrum for the short wave emission band, it was found desirable to use an analysis wave length of 410 mμ or lower, while in the case of the long wave emission an analysis wave length of 590 mμ gave the best resolution of the excitation bands. Similarly the best resolution of the emission spectrum was obtained by using wave lengths of 257.5 and 285 mμ for excitation.

Fig. 1 shows the excitation spectra of the phosphor with two different analysis wave lengths for two Tl concentrations in each case. It should be noted that increasing Tl concentration broadens the excitation spectrum for 400 mμ emission, but apparently narrows the band for 535 mμ emission. The band centered at 280 mμ has a definite hump on the long wave length side and the amount of asymmetry is variable with concentration.

Fig. 2 shows the uncorrected emission spectra of the phosphor for three different exciting wave lengths with a Tl concentration of 10^{-3} mole fraction. The important characteristic to be noted here is that excitation at 240 mμ gives substantially the same emission peak as excitation at 285 mμ. The deviation at shorter wave length will be discussed later. The effect of Tl concentration is shown in Fig. 3 using data from uncorrected spectra. The emission band at 415 mμ is appreciably less dependent on concentration than the band at 540 mμ. Over the range of concentrations shown the intensities in the uncorrected spectra can be expressed by the following equations:

$$\Delta (\log I_{415}) = 0.20\,\Delta (\log C)$$
$$\Delta (\log I_{540}) = 0.35\,\Delta (\log C)$$

There seems to be no indication of concentration quenching even at 10^{-2}Tl.

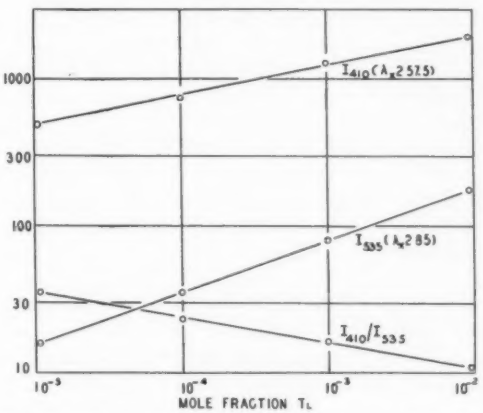

FIG. 3. Effect of Tl concentration on the peak intensity of the two emission bands of NH_4Br:Tl.

RESULTS WITH KCl

The general character of the emission spectrum of KCl:Tl found in the present work is essentially that described by Hutten and Pringsheim (6) and by Johnson and Williams (4). There is a strong emission band at 302 mμ, a weaker band at 492 mμ, and a possible band at about 380 mμ. The main excitation band, which extends from 240 to 275 mμ, is found, however, to be a complex[6] formed from two closely spaced components.

Fig. 4 shows the effect of Tl concentration on the peak intensity of the 302 mμ emission band with an exciting wave length of 245 mμ and on the peak intensity of both

[5] For the uncorrected spectra the maxima are found at 415 and 540 mμ.

[6] The complex nature of the excitation band was observed by Johnson and Williams (4) but apparently they did not recognize the existence of two components.

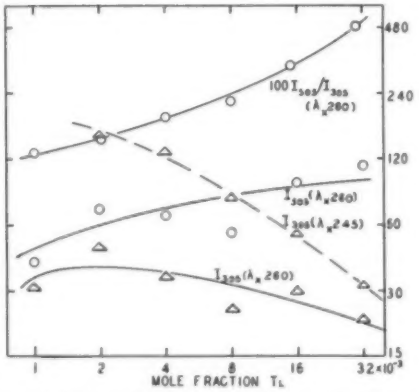

FIG. 4. Effect of Tl concentration and exciting wave length on the peak intensity of the two emission bands of KCl:Tl.

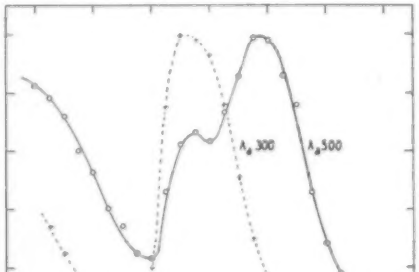

FIG. 5. Excitation spectra of KCl:Tl measured at different emission wave lengths.

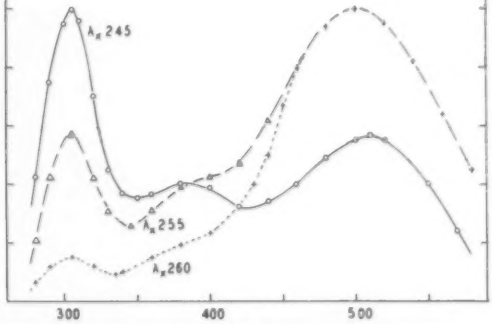

FIG. 6. Uncorrected emission spectra of KCl:Tl measured with different exciting wave lengths.

the main emission bands, when the exciting wave length is 260 mμ. In both cases data from uncorrected spectra were used, and unrelated arbitrary intensity values were used with each value of λ_x. The ratio of the visible to the ultraviolet is also shown for excitation with 260 mμ. The variation in this ratio is a sensitive indication of Tl concentration and is more reliable than measurement of intensity of emission. Fig. 5 shows the change in shape of the excitation curve as the analysis wave length is changed from 300 to

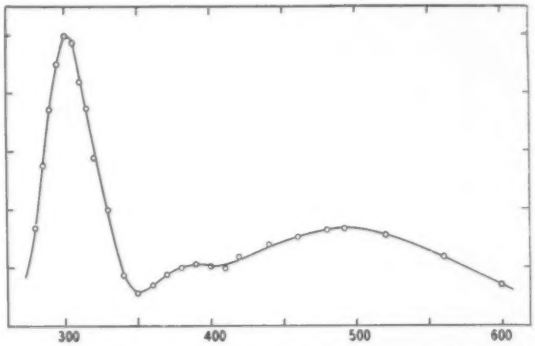

FIG. 7. Emission spectrum of KCl:Tl excited by λ 260 and corrected for photocell response.

500 mμ,[7] while Fig. 6 shows the changes in the uncorrected emission spectrum with exciting wave lengths of 245, 255, and 260 mμ. Fig. 7 shows the corrected emission curve for 260 mμ excitation. While these curves were obtained using a phosphor containing 4×10^{-3}Tl, similar variations are found with all concentrations from 1×10^{-3} up to 3×10^{-2}.

DISCUSSION

NH_4Br has a crystal structure of the CsCl type. In this structure each ion is surrounded by eight ions of the opposite charge. The packing is less close than that found in the KCl type of lattice where each ion is surrounded by only six ions of the opposite charge. The radius of the ammonium ion is about 1.43Å; this is very close to the radius of Tl of 1.44 so that substitution should occur very readily. The fact that mortar grinding gives reproducible phosphors with uniform fluorescence shows that Tl migrates into the lattices very easily, while the lack of concentration quenching and the failure to develop new emission bands at high concentration suggests that Tl ions form isolated centers.

It is probable that the Tl^+ ion in solid solution in ionic crystals has the same electron configuration and ground state as the free ion. This is $6s^2$, $^1S_0$. The first excited states, with a $6s6p$ configuration, are $^3P_0^\circ$, $^3P_1^\circ$, $^3P_2^\circ$ and $^1P_1^\circ$ in order of increasing energy. It is believed that the dipole radiation selection rules for angular orbital momentum $\Delta L = \pm 1$ and for total angular momentum $\Delta J = 0, \pm 1$ ($J = 0$ to $J = 0$ is forbidden) and for parity are applicable to activator ions in the crystal as well as to the free ion. While the multiplicity selection rule for LS coupling requires that $\Delta S = 0$, experimental evidence shows violation of this. However, the transition $^1S_0$ $(6s^2) \rightarrow {}^1P_1^\circ$ $(6s6p)$ would be expected to be the more probable. Therefore, the strong excitation band of NH_4Br:Tl, centered at 258 mμ, is attributed to this transition. The weaker band at 280 mμ can then be assigned to the other allowed transition $^1S_0$ $(6s^2) \rightarrow {}^3P_1^\circ$ $(6s6p)$. The corresponding emission bands, resulting from the return transitions to the ground state, are centered at 400 and 535 mμ, respectively. A summary of the experimental spectra for the two transitions is shown in Fig. 8. In this figure the corrected and normalized emission spectra are given along

[7] The curves have been normalized, thus obscuring the fact that the excitation efficiency is much higher for 300 mμ emission than for 500 mμ.

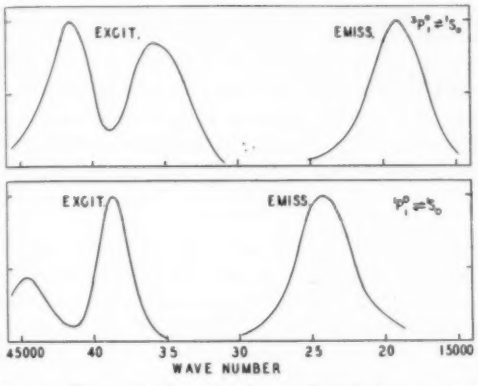

FIG. 8. Normalized excitation and emission spectra of the two excited states of Tl in NH_4Br:Tl.

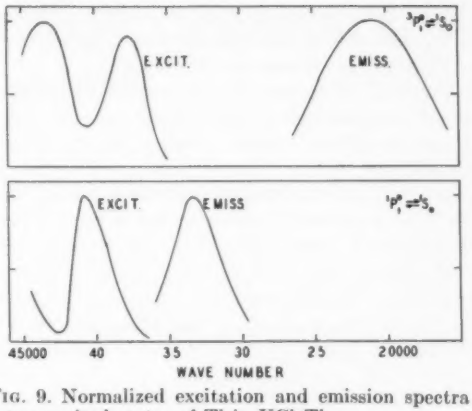

FIG. 9. Normalized excitation and emission spectra of the two excited states of Tl in KCl:Tl.

with the normalized excitation spectra on a wave number basis.

It is somewhat difficult to explain the asymmetry of the 280 mμ excitation band since the experimental evidence, showing that the asymmetry is concentration dependent, seems to point toward a separate state which does not, however, give a separate emission band. One tentative hypothesis is that this asymmetry is due to excitation to the $^3P_0^\circ$ state, normally a forbidden transition, followed by a thermal promotion to the $^3P_1^\circ$ state, possible because of crossing of the potential energy curves, at separations below the equilibrium value, with a small energy barrier. At present there is no experimental evidence either for or against this hypothesis. Another explanation is that the asymmetry is due to formation of pairs of Tl ions.

It is interesting to note that there is no experimental indication of energy transfer between the excited states $^1P_1^\circ$ and $^3P_1^\circ$ of the 6s6p configuration at room temperature for NH_4Br:Tl.

For KCl:Tl it is apparent from Fig. 5 that the main excitation band has at least two components located at about 245 and 260 mμ. The data reported in Fig. 6 show that excitation by 245 mμ gives predominantly 302 mμ emission while excitation by 260 mμ gives predominantly 492 mμ emission. It should be emphasized that the 302 mμ band is much stronger than the 492 mμ band, a fact obscured by the use of uncorrected photocell response curves in these figures, but readily seen by comparing Fig. 6 and 7.

If it is assumed[8] that the 245 mμ excitation band and the intense 302 mμ emission band are due to the more probable of the allowed transitions, namely $^1S_0 \rightarrow {}^1P_1^\circ$, then the 260 mμ excitation band, giving 492 mμ emission, can be assigned to the other allowed transition $^1S_0 \rightarrow {}^3P^\circ_1$. Fig. 9[9] shows normalized excitation and emission spectra on a wave number basis for the two transitions.

[8] This differs from the assumption made by Williams and co-workers, that 245 mμ excitation and 302 mμ emission result from excitation to $^3P_1^\circ$, while 200 mμ excitation and 492 mμ emission result from excitation to $^1P_1^\circ$.

[9] The $^3P_1^\circ$ curve is based on measurements at 530 mμ while the curve in Fig. 5 was taken at 500 mμ. At 530 mμ there are clearly defined maxima in the excitation curves at 37,700 and 43,500 cm^{-1} which are distorted when the slightly shorter measuring wave length of 500 mμ is used.

In the case of NH_4Br:Tl, excitation in either the 242 or the 280 mμ emission band gives identical strong emission at 530 mμ, with a weak added band at 400 for excitation at 242. With excitation at either 225 or 260 mμ the emission is almost entirely at 400 mμ. Similarly excitation of KCl:Tl by either 230 or 260 mμ gives relatively strong emission at the 492 mμ band, with the same band shape.

This virtual identity of emission indicates that the emitting transitions are the same regardless of which of two exciting transitions take place.

There are several possible explanations for the excitation bands at shorter wave lengths.

1. They may be due to splitting of the energy levels.
2. They may be due to absorption by the matrix in disturbed regions near the luminescent centers.[10]
3. They may be due to excitation to states of the 6s7p configuration.
4. In the case of KCl, if Williams' assignment of levels is correct, they could be $^1P_1^\circ$ states of 6s6p.

All of these hypotheses involve difficulties and a clear-cut selection is not possible without additional experimental data. In the case of KCl, Williams' choice of levels makes it difficult to explain the marked experimental difference in emission with a slight shift in exciting wave length from 245 to 260 mμ. Splitting of energy levels would require a crossing of potential energy curves. Absorption by the matrix in the tail of the fundamental absorption band does not seem to be adequate to explain the 242 mμ excitation band in NH_4Br since the matrix absorption appears to be at a wave length below 200 mμ.

The major difficulty[11] with the hypothesis that the 6s7p levels are excited lies in the very marked lattice interaction perturbations involved and a very difficult quantitative calculation is needed to determine if such perturbations are possible. However, this hypothesis allows an explanation of certain experimental data more simply than the other mechanisms mentioned above.

[10] Suggested by F. Seitz in his review of the paper.

[11] While oscillator strength for the $6s \rightarrow 7p$ transition is low in the gaseous ion, placing it in a crystal matrix may greatly change transition probabilities, much as the presence of argon in a gas discharge affects the relative intensity of the 185 and 254 mμ lines of Hg.

If the 242 mμ band for NH_4Br:Tl is due to excitation to the $^3P_1^\circ$ state of 6s7*p* and if the electron drops first to 6s7*s* and then to 6s7*p*, without the selection rule $\Delta S = 0$ holding rigorously, then both the $^3P_1^\circ$ and $^1P_1^\circ$ states of 6s6*p* would be excited and emission should occur in both the 400 and the 535 mμ emission bands as was found experimentally.

The effect of temperature on the emission of KCl:Tl with 254 mμ excitation can be explained by temperature broadening or by temperature shift, if the band is actually an overlapping complex of $^3P_1^\circ$ and $^1P_1^\circ$ states of 6s6*p*. The assumption of thermal transfer from $^3P_1^\circ$ to $^1P_1^\circ$ would not then be required in KCl:Tl, thus increasing the resemblance of this phosphor to NH_4Br:Tl.

Preliminary Data on Other Halides

The assignment of energy levels proposed both for NH_4Br:Tl and for KCl:Tl differs considerably from that suggested by Williams (5) for KCl:Tl. The mechanism also differs in that the existence of thermal transfer between $^1P_1^\circ$ and $^3P_1^\circ$ may not be required. While it might be suggested that the difference in behavior of the two phosphors is due to difference in crystal structure, this is ruled out by data on other alkali halides for which the crystal structure difference is not found. Preliminary results on NH_4Cl, KBr, and KI, with a single Tl concentration, show that these phosphors have spectra similar to NH_4Br with well resolved emission and excitation bands. The location of the peaks in the uncorrected photocell response curves is given in Table I.

Initial results on NaCl, NaBr, and NaI also have been obtained at a single Tl concentration. These phosphors resemble KCl:Tl in having two well resolved emission bands with one main excitation band above 220 mμ, this being a complex of two components. In all of these phosphors the shape of the excitation band depends strongly on which of the emission bands is used in the measurement. Also excitation on the short wave-length side of the main band leads to predominance of the short wave emission; while excitation on the long wave-length side leads to predominance of the long wave-length emission.

TABLE I

Matrix	Emission bands in mμ	Excitation bands in mμ
NH_4Cl	385, 510	210, 222, 240, 260
KBr	360, 480	222, 230, 261, 274
KI	425, 490	242, 262, 287, 305

TABLE II

Matrix	Emission bands in mμ	Excitation band in mμ
NaCl	295, 395	255
NaBr	310, 530	270
NaI	430, 490	287

The location of the peaks in the uncorrected photocell response curves are given in Table II.

The wave-length changes in both the emission and excitation spectra show that three major factors affect the energy levels of the activator ions. These are anion size, cation size, and crystal structure. More complete data on these phosphors will be reported in later papers.

Summary

Two types of emission and excitation spectra are found in the Tl-activated alkali halides. In one type, represented by NH_4Br:Tl, both the excitation and the emission bands are well separated. In the other type, represented by KCl:Tl, the emission bands are well separated but the excitation bands overlap.

In NH_4Br:Tl the emission band at 400 mμ can be excited by bands at 227 or 258 mμ, while the emission band at 535 mμ can be excited by bands at 242 or 280 mμ. The following tentative energy level assignments are proposed for these spectra.

Wave lengths in mμ	Excited state
258 and 400	$^1P_1^\circ$ (6s6*p*)
280 and 535	$^3P_1^\circ$ (6s6*p*)
227	$^1P_1^\circ$ (6s7*p*)
242	$^3P_1^\circ$ (6s7*p*)

If there is excitation to 6s7*p* it is suggested that the electron returns via 6s7*s* to 6s7*p*.

In KCl:Tl the excitation band at 240 to 270 mμ appears to be composed of two components centered at 245 and 260 mμ. Excitation at 245 gives strong emission at 302, while excitation at 260 gives strong emission at 492 mμ. An analogous assignment of energy levels is tentatively proposed for these spectra.

Wave lengths in mμ	Excited state
245 and 302	$^1P_1^\circ$ (6s6*p*)
260 and 492	$^3P_1^\circ$ (6s6*p*)
below 200	$^1P_1^\circ$ and $^3P_1^\circ$ (6s7*p*)

Manuscript received October 12, 1955. This paper was prepared for delivery before the Cincinnati Meeting, May 1 to 5, 1955.

Any discussion of this paper will appear in a Discussion Section to be published in the June 1957 Journal.

REFERENCES

1. P. H. Yuster and C. J. Delbecq, *J. Chem. Phys.*, **21**, 892 (1953).
2. M. Forro, *Z. Physik*, **58**, 613 (1930).
3. W. V. Mayern, *ibid.*, **61**, 321 (1930).
4. P. D. Johnson and F. E. Williams, *J. Chem. Phys.*, **20**, 124 (1952).
5. F. E. Williams, *J. Phys. Chem.*, **57**, 780 (1953) and earlier papers.
6. E. H. Hutten and P. Pringsheim, *J. Chem. Phys.*, **16**, 241 (1948).
7. F. S. Johnson, K. Wantanabe, and R. Tousey, *J. Opt. Soc. Amer.*, **41**, 702 (1951).

Polarographic Behavior of Organic Compounds in Methanesulfonic Acid

S. Wawzonek, R. Berkey, and D. Thomson

Department of Chemistry, State University of Iowa, Iowa City, Iowa

ABSTRACT

Aromatic nitro compounds and triarylcarbinols gave normal polarographic waves in methanesulfonic acid. Aromatic ketones and aldehydes gave waves which were complicated by maxima. Nitro compounds were reduced to the phenylhydroxylamines which were rearranged by the acid to the *p*-aminophenols. The triarylcarbinols were reduced to the triphenylmethanes under anhydrous conditions and to the free radicals in the presence of water. Ketones and aldehydes were reduced to the pinacols which, under the influence of the strong acid, underwent the pinacol rearrangement.

Most of the work on the behavior of organic compounds in strong acids has been dependent upon cryoscopic studies. The only polarographic study of organic compounds in strong acids reported to date has been in 98.65% sulfuric acid and has dealt mainly with aromatic nitro compounds (1). Carbonyl compounds which form conjugate acids and triarylcarbinols which form carbonium salts with strong acids have not been studied.

In the present work the suitability of methanesulfonic acid as a solvent for the polarographic study of organic compounds has been investigated and the behavior of aromatic nitro compounds, ketones and aldehydes, and triarylcarbinols studied.

Experimental

Polarographic data were obtained with a Sargent Model XII polarograph using an electrolytic cell similar to that described previously (2). The capillary used had a drop time of 4.19 sec and a $m^{2/3}t^{1/6}$ of 1.59 $mg^{2/3}sec^{-1/2}$ at a mercury height of 60 cm on an open circuit.

Methanesulfonic acid.—This acid was purified by filtering the technical acid obtained from Eastman Kodak Co., and then distilling at reduced pressure (1 mm) four times. The boiling point of the product used was 120°/1mm; the freezing point was 19.5°–20.1°.

The pure acid had a decomposition potential of −0.835 v. Addition of water and organic compounds shifted this value to more negative potentials.

The resistance of the pure acid in the polarographic cell was 1890 ohms. Addition of water and organic compounds lowered this resistance. Results are shown in Table I.

The resistance of the solutions in the polarographic cell was determined with a Wheatstone Bridge using a battery-powered 1000 cycle audio-oscillator as a current source and earphones to determine the null point.

Electrolyses.—Large scale electrolyses were carried out in a cell similar to that described earlier (3).

Electrolysis of benzaldehyde.—Methanesulfonic acid (350 ml) was placed in the electrolytic cell, fitted with a platinum gauze anode and a stirred mercury pool cathode, and degassed by bubbling nitrogen through it for 1 hr. Freshly distilled benzaldehyde (10 ml) was added and a current from an 85 v generator passed through for 8 hr. The initial current of 0.5 amp dropped to a value of 0.18 amp in this time. The electrolysis cell was cooled with an ice bath during this whole period. The resulting acid solution was filtered from the mercurous methanesulfonate (15 g) formed and poured into water. Extraction with ether gave an oil from which benzaldehyde (4.8 g) was recovered by distillation under reduced pressure, 90°/40 mm. The solid residue when recrystallized from ethanol gave desoxybenzoin (1.6 g) melting at 58°–9° and a tarry polymer (2.6 g).

Electrolysis of nitrobenzene.—Nitrobenzene (10 ml) was treated in methanesulfonic acid (350 ml) in a manner similar to that used for benzaldehyde. The resulting acid solution was filtered from the mercurous methanesulfonate (4.8 g) and neutralized with sodium hydroxide. Extraction with ether gave a product which was acidified with 5% HCl and steam distilled. The steam distillate gave nitrobenzene (4.3 g). The residue when made basic and steam distilled gave no aniline. Extraction with ether after neutralization followed by drying of the ether solution and then saturating with dry hydrogen chloride gas gave *p*-aminophenol hydrochloride (3.5 g) m.p. 201°–3° (4).

Electrolysis of benzophenone.—Benzophenone (5 g) was electrolyzed in methanesulfonic acid (400 ml) using a mercury anode and a mercury cathode. The resulting solution was filtered from the mercurous methanesulfonate (25 g) and poured into water. The resulting precipitate upon fractionation from ethanol gave two products. The first of these was benzophenone (2.2 g) and the second (2.5 g) benzopinacolone, m.p. 181°–182°.

Electrolysis of triphenylcarbinol.—Electrolysis of triphenylcarbinol (5 g) in methanesulfonic acid (400 ml) using a platinum anode and a mercury cathode for 8 hr was followed by filtration of the solution from the mercurous methanesulfonate (35 g) and pouring the filtrate into water. The resulting solid was separated by fractional crystallization from ethanol into triphenylcarbinol (2.5 g) and triphenylmethane (1.5 g), m.p. 90°.

Mercurous methanesulfonate.—This salt which was formed in the electrolyses was synthesized by treating mercurous oxide with methanesulfonic acid. Methanesul-

TABLE I. *Effect of various substances upon the resistance of methanesulfonic acid*

Compound	Resistance (ohms)
1% Water	358
2.91% Water	336
4.76% Water	275
9.09% Water	256
0.1*M* NH_4Cl	582
0.00526*M* $(C_6H_5)_3COH$	1170
0.00997*M* $(C_6H_5)_3COH$	880
0.00997*M* $(C_6H_5)_3COH$ + 4.76% H_2O	360
0.00997*M* $(C_6H_5)_3COH$ + 9.09% H_2O	260

fonic acid (32 g) was dissolved in water (70 ml) and neutralized with mercurous oxide. The resulting solution was decolorized twice with Nuchar (2 g), filtered, and concentrated until crystals formed. Cooling to 0° gave crystals which melted at 320°–322°.

Anal. calcd. for Hg SO_3CH_3: C, 4.10; H, 1.02. Found: C, 4.28; H, 1.06.

The compounds investigated were either obtained from stock or prepared according to directions in the literature.

Results

The present investigation indicates that methanesulfonic acid is a suitable solvent for the polarographic reduction of organic compounds in a range up to −0.9–1.0 v measured against the mercury pool. The self-ionization of the acid is large enough so that no inert electrolyte is needed. The resistance of 1900 ohms is low enough for polarographic studies. Addition of water and certain organic compounds shifted the decomposition potential to more negative values and made a slightly larger range of potentials available for study. The addition of 0.1*M* ammonium chloride, which liberated hydrogen chloride and formed ammonium methanesulfonate, did not affect the decomposition potential but lowered the resistance to 582 ohms. Addition of water and of organic compounds likewise lowered the resistance as shown in the experimental section. The amount of lowering was such that correction for *IR* drop was not necessary.

The polarographic waves obtained were well defined in most cases. Exceptions are mentioned in the discussion of the individual classes. Varying concentrations of each compound were used and are reported, since the waves close to the discharge potential of the electrolyte were only well defined at the higher concentrations of the substances being reduced.

Results for nitrobenzene and *p*-nitrotoluene are given in Table II. Reduction products of nitrobenzene such as aniline, phenylhydroxylamine, and *p*-aminophenol gave no reduction waves in methanesulfonic acid.

The first wave in each case was well defined and diffusion-controlled. At concentrations higher than 0.5 mM a round maximum appeared which did not decrease to the diffusion current at the higher concentrations. This maximum was suppressed by the addition of water.

The second wave was only well defined at the higher concentrations of nitro compounds and was kinetic in nature. This wave occurred at concentrations of nitro compound larger than 0.403 mM even though it is not listed for several concentrations in the table. Since the maximum for the first wave did not return to the diffusion current of the latter, the diffusion current constant (I_d) of the second wave decreases as that for the first wave increases. The second wave was not visible in the presence of water.

TABLE II. *Polarographic behavior of aromatic nitro compounds in methanesulfonic acid*

Conc. millimoles/liter	1st wave $E_{\frac{1}{4}}$ (v) vs. Hg pool	I_d[a]	2nd wave $E_{\frac{1}{4}}$ (v) vs. Hg pool	I_d[a]
Nitrobenzene				
0.110	−0.26	3.30		
0.220	−0.27	3.06		
0.403	−0.30	3.12[b]	−0.97	53.3
0.462[c]	−0.25[c]	3.36[c]		
0.715	−0.27[d]	2.95		
0.824	−[d]	4.71	−0.97	40.7
1.52	−[d]	10.0	−0.95	29.1
2.18	−[d]	26.4	−1.07	20.5
3.46	−[d]	15.57		
3.26[e]	0.34	3.63	No wave visible	
***p*-Nitrotoluene**				
0.118	−0.29	3.59		
0.293	−0.31	3.11		
0.466	−0.30	2.87		
0.646	−0.29[d]	3.08		
0.820	−[d]	3.10	−0.99	40.7
3.54	−[d]	4.26	−0.98	11.7
3.32[e]	−0.34	2.54	No wave visible	

[a] $I_d = \dfrac{i_d}{Cm^{2/3}t^{1/6}}$

[b] Diffusion controlled. The diffusion current at 60 cm Hg was 2.00 amp and at 40 cm Hg was 1.66 amp.

[c] Temperature 35°.

[d] Maximum.

[e] The acid contained 6.10% water by volume.

Polarographic results obtained for the various triarylcarbinols in anhydrous methanesulfonic acid and methanesulfonic acid containing water are given in Table III. The behavior of triphenylmethyl chloride which dissolves in methanesulfonic acid with the liberation of hydrogen chloride is also reported in this table for comparison. The study of these compounds in the presence of water was carried out in order to obtain more information about the mechanism.

The aromatic ketones studied gave waves only at high concentrations which were similar in nature to the curves with the rounded maxima for nitrobenzene but much smaller in size. In Table IV both the height of the maximum and the height of the leveling off point are given. The latter was found to vary with the mercury height in a manner similar to that found for diffusion currents. The height of the maximum behaved differently with changes in mercury height and seems to be affected by the concentrations of the compounds used. Water, when added to the solution, eliminated the maximum only at higher concentrations, (23.07%). The diffusion current constant (I_d) under the last conditions is small and may have been lowered by the precipitation of some of the ketone.

The behavior for the aromatic aldehydes was not consistent. Benzaldehyde gave no definite wave at high

TABLE III. *Polarographic behavior of triarylcarbinols in methanesulfonic acid with varying amounts of water*

% H_2O[a] by volume	Conc. of carbinol in millimoles/liter	1st wave		2nd wave	
		$E_{\frac{1}{2}}$ (v) vs. Hg pool	I_d[b]	$E_{\frac{1}{2}}$ (v) vs. Hg pool	I_d[b]
Triphenylcarbinol					
0	0.508	−0.63	1.05(0.85)[c]	—	—
0	0.508	−0.61	(0.66)[c, d]	—	—
1.0	0.503	−0.61	0.92	—	—
2.91	0.493	−0.60	0.95	—	—
4.76	0.484	−0.56	0.84	—	—
9.09	0.461	−0.55	0.54	−0.67	0.33
0	0.918	−0.67	1.15	—	—
4.76	0.874	−0.59	0.63	−0.76	0.40
9.09	0.835	−0.52	0.49	−0.75	0.32
16.66	0.765	−0.48	0.30	−0.76	0.38
		−0.55[e]	0.19		
0	2.30	−0.70	1.02	—	—
4.76	2.19	−0.56	0.53	—	—
9.09	2.09	−0.52	0.31	—	—
		−0.60[e]	0.19		
16.66	1.92	−0.45	0.14	—	—
		−0.52[e]	0.36		
23.08	1.77	−0.42	0.12	−0.88	0.40
		−0.48[e]	0.33		
0	4.10	−0.67	0.68	—	—
4.76	3.91	−0.59	0.49	—	—
9.09	3.73	−0.54	0.23	—	—
		−0.61[e]	0.23		
16.66	3.42	−0.47	0.12	—	—
		−0.61[e]	0.30		
23.08	3.16	−0.44	0.15	−0.91	0.40
		−0.49[e]	0.24		
		−0.62[f]	0.06		
0	6.01	−0.71	0.60	—	—
4.76	5.72	−0.58	0.49	—	—
9.09	5.46	−0.53	0.22	—	—
		−0.60[e]	0.24		
		−0.72[f]	0.08		
16.67	5.01	−0.46	0.15	—	—
		−0.52[e]	0.22		
		−0.66[f]	0.05		
23.08	4.62	−0.43	0.176	−0.97	0.55
		−0.48[e]	0.175		
		−0.63[f]	(small)		
Triphenylmethyl chloride					
0	0.917	−0.67	1.22	—	—
4.76	0.874	−0.59	0.62	−0.77	0.39
9.09	0.834	−0.54	0.46	−0.77	0.34
16.66	0.765	−0.48	0.30	−0.77	0.31
		−0.56[e]	0.20		
0	0.893	−0.76	(14.1)[g]		
Tri-*p*-anisylcarbinol					
0	1.01	No wave until 16.66% H_2O added			
16.66	0.842	−0.81	0.87	—	—
23.08	0.777	−0.78	0.80	—	—
33.33	0.635	−0.72	0.88	—	—
0	5.75	No wave until 16.66% H_2O added			
16.66	4.79	−0.86	0.84	—	—
23.08	4.42	−0.86	0.81	—	—
33.33	3.83	−0.74	0.29	−1.16	0.14
		−0.94[e]	0.40		
41.18	3.38	−0.63	0.19	—	—
		−0.85[e]	0.43	—	—

TABLE III—*Continued*

% H_2O[a] by volume	Conc. of carbinol in millimoles/liter	1st wave		2nd wave	
		$E_{\frac{1}{2}}$ (v) vs. Hg pool	I_d[b]	$E_{\frac{1}{2}}$ (v) vs. Hg pool	I_d[b]
Diphenyl-α-naphthylcarbinol					
0	1.12	−0.65	0.71	—	—
9.09	1.02	−0.56	0.32	—	—
16.66	0.924	−0.52	0.13	—	—
23.08	0.861	Precipitation occurred			
Diphenyl-*o*-tolylcarbinol					
0	0.972	−0.64	0.83	—	—
4.76	0.926	−0.58	0.63	−0.78	0.22
9.09	0.884	−0.53	0.64	−0.78	0.31
16.66	0.810	−0.48	0.58	−0.78	0.30
Tri-*p*-biphenylcarbinol					
0	1.16	−0.64	1.60	—	—
4.76	1.10	−0.60	1.23	−0.72	0.12
9.09	1.055	−0.57	0.86	−0.69	0.20
16.66	0.956	−0.50	0.56	−0.68	0.16
33.3	0.774	−0.33	0.30	−0.67	0.09
		−0.53[e]	0.17		

[a] Percentages represent the addition of 0.1, 0.3, 0.5, 1.0, 2.0, and 3.0 ml of water to 10 ml of acid.

[b] $I_d = \dfrac{i_d}{Cm^{2/3}t^{1/6}}$

[c] Diffusion current in microamperes.

[d] Mercury reservoir height = 40 cm.

[e] Second part of split wave.

[f] Third part of split wave.

[g] Current in microamperes. Some of the HCl gas escaped during the dissolving of the compound so that a quantitative measurement of the current was not possible.

concentrations of the compound or in the presence of water. *p*-Chlorobenzaldehyde gave signs of a wave only at high concentrations and in the presence of at least 23.00% water. *p*-Tolualdehyde gave a wave in anhydrous methanesulfonic acid. The span of the limiting current was not large enough to determine whether this curve was a maximum or not. The addition of water caused the curve to vanish. An increase in temperature had little effect on the height.

Discussion of Results

Results in Table II indicate that aromatic nitro compounds behave normally in anhydrous methanesulfonic acid. By analogy to the behavior in aqueous acid solutions the wave must correspond to a 4 electron reduction. The product, however, is *p*-aminophenol and is formed by the rearrangement of the intermediate phenylhydroxylamine. The isolation of *p*-aminophenol exclusively in a large-scale electrolytic reduction of nitrobenzene and the absence of a wave for phenylhydroxylamine in this solvent is in agreement with this mechanism. The results of the macroscale experiment closely resemble those obtained with nitrobenzene in glacial acetic acid-sulfuric acid (4).

$$C_6H_5NO_2 + 4e + 6CH_3SO_3H \rightarrow$$

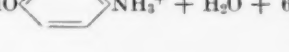

TABLE IV. *Polarographic behavior of aromatic aldehydes and ketones in methanesulfonic acid with varying amounts of water*

% H_2O[a] by volume	Conc. in millimoles/liter	$E_{\frac{1}{2}}$ vs. Hg pool	I_d[b] max	I_d[b] min	i_d max	i_d min
Benzophenone						
0	1.41–2.71	No wave				
0	5.64	−1.03	5.61	[c]	50.3	—
0	5.64[d]	−1.02[d]	—	—	47.1[d]	—
0	11.09	−0.99	2.50	1.80	44.0	31.3
0	11.09[d]	−1.00[d]	—	—	36.4[d]	25.3[d]
4.76	10.55	−0.98	1.96	1.14	32.9	20.1
4.76[d]	10.55[d]	−0.97[d]	—	—	26.9[d]	15.64
9.09	10.08	−0.96	0.95	—	16.8	12.0
9.09[d]	10.08[d]	−0.96[d]	—	—	13.5[d]	9.6[d]
23.07	9.53	−0.95		0.28		
0	1.20[e]	No wave				
f	1.00	−0.98		1.39	—	2.31
f[d]	1.00[d]	−0.98[d]			—	1.92[d]
***p*-Chlorobenzophenone**						
0	1.06–2.65	No wave				
0	5.25	−0.96	4.21	3.22	35.2	26.9
0[d]	5.25[d]	−0.96[d]	—	—	31.1[d]	22.0[d]
0	6.64	−0.97	3.18	2.24		
0	8.04	−0.97	2.39	1.46		
***p*-Phenylbenzophenone**						
0	0.942–3.95	No wave				
0	5.29	−1.02	2.08	1.79	15.9	13.7
0	5.29[d]	−1.00[d]	—		14.8[d]	11.0
4.76	5.04	−1.01	1.06	[c]	8.47	[c]
4.76[d]	5.04	−1.02			6.93[d]	
***p*-Tolualdehyde**						
0	2.97	No wave				
0	5.52	−1.00	4.14	[c]		
0	7.44	−1.02	2.79	[c]		33.0
0	7.44[d]	−0.98[d]	—	[c]		22.4[d]
0	8.71	−0.98	2.20			
9.09	7.91	No wave				
0	9.18	−1.03	2.06	[c]		
0	9.18[g]	−0.98[g]	2.06[g]	[c]		
0	11.9	−1.02	1.25	[c]		
0	11.9[g]	−1.01[g]	1.25[g]	[c]		

[a] Percentages represent the addition of 0.5, 1.0, and 3.0 ml of water to 10 ml of acid.

[b] $I_d = \dfrac{i_d}{Cm^{2/3}t^{1/6}}$

[c] The limiting current span is small and combines with the discharge of the methanesulfonic acid.

[d] Mercury reservoir at 40 cm.

[e] In the presence of 0.1*M* $NH_4O_2SCH_3$.

[f] In 0.1*N* HCl—50% ethanol.

[g] Temperature 35°.

The second wave, which is very much larger, is practically completely kinetic in nature and must be a catalytic hydrogen wave brought on by the *p*-aminophenol formed in the reduction.

The half-wave potentials for nitrobenzene and *p*-nitrotoluene differ very little from each other. This similarity was also found by James (1) in 98.65% sulfuric acid. The data obtained in methanesulfonic acid for these compounds are surprisingly similar to those obtained by James (1).

Examination of the results in Table III indicates that the various triphenylcarbinols form triphenylcarbonium ions which are reducible polarographically at the dropping mercury electrode in methanesulfonic acid. The diffusion current constant (I_d) when compared with that obtained for nitrobenzene at concentrations below 0.5 mM (Table II), which takes up four electrons, points to a two-electron change or a reduction to the triphenylmethane. The waves were diffusion controlled and had a slope of approximately 0.059. These data suggest the following steps for the electrode reactions:

$$(C_6H_5)_3C^+ + e \rightarrow (C_6H_5)_3C\cdot$$

$$(C_6H_5)_3C\cdot + e + CH_3SO_3H \rightarrow (C_6H_5)_3CH + CH_3SO_3^-$$

The free radical is reduced rapidly and directly to the triphenylmethane. The possibility also exists that the lability of the free radical in this solvent is caused by the following reaction:

$$2(C_6H_5)_3C\cdot + CH_3SO_3H \rightarrow (C_6H_5)_3CH + (C_6H_5)_3C^+ + CH_3SO_3^-$$

This reaction would be similar to that reported for the triphenylmethyl radical in glacial acetic acid (5).

An electrolytic reduction of triphenylcarbinol on a large scale gave triphenylmethane and is in agreement with the over-all mechanism. The attempt to verify this mechanism further by studying the reduction of the intermediate compound, triphenylmethyl or hexaphenylethane, was prevented by the insolubility of the latter in methanesulfonic acid.

In such electrolyses in this solvent copious amounts of the insoluble mercurous methanesulfonate are formed. The formation of this salt in electrolyses using a platinum anode probably resulted from the mercury transported from the cathode compartment into the anode portion by entrainment during the electro-osmosis of the solvent. Stirring the mercury cathode forms mercury droplets fine enough to pass through the sintered glass diaphragm and to allow amalgamation of the platinum anode.

Further evidence for the reduction of the triphenylcarbonium ion is the identical polarographic behavior of triphenylmethyl chloride. This compound dissolves in methanesulfonic acid with the liberation of hydrogen chloride and the formation of triphenylmethyl methanesulfonate. The hydrogen chloride is removed by degassing with nitrogen since it gives a wave at −0.76 v.

The ease of reduction was approximately the same for all the carbonium ions with the exception of the tri-*p*-anisylcarbonium ion. The similar behavior for triphenylcarbonium ion and α-naphthyldiphenylcarbonium ion is in agreement with the observation made by Conant (6) using the classical method, that these two compounds have single electrode potentials differing only by 20–40 mv.

The greater stability of the tri-*p*-anisylcarbonium ion toward reduction is in agreement with its stability toward hydrolysis.

The diffusion current for the triphenylcarbonium ion is proportional to concentration in the region 0.508–2.30 mM. Beyond this region the diffusion current constant becomes smaller.

Addition of water to the methanesulfonic acid solutions of the triarylcarbinols in limited amounts caused the formation of two polarographic waves. The sum of these two waves was approximately equal to the wave observed under anhydrous conditions. Since the second wave occurs at more negative potentials and close to the decomposition potential of the acid, it was not observed for all the examples or concentrations studied. Both waves are diffusion controlled and had slopes of approximately 0.058 for the examples analyzed.

The first wave under these conditions corresponds to the reduction of the carbonium ion to the free radical which, because of the change in solvent brought about by the addition of water, becomes more stable and therefore can dimerize to the hexaphenylethane,

$$(C_6H_5)_3C^+ + e \rightarrow (C_6H_5)_3C\cdot$$
$$2(C_6H_5)_3C\cdot \rightarrow (C_6H_5)_3C{-}C(C_6H_5)_3$$

which is not reducible at this potential and must dissociate very slowly to triphenylmethyl, since no kinetic current is observed for the first wave. That solvents have an effect on the stability of triarylmethyl free radicals is shown by the large variation in the equilibrium constant for the dissociation of hexaphenylethane in various solvents (7, 8) and by the different behavior of such free radicals in concentrated hydrochloric acid from that in glacial acetic acid (5). In the former the free radical forms a dimer known as the Chichibabin compound.

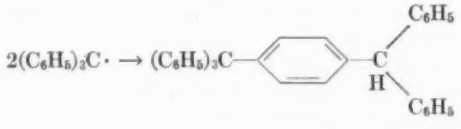

The second wave in the presence of water would represent a reduction of the carbonium ion directly to the triarylmethane.

$$(C_6H_5)_3C^+ + 2e + H^+ \rightarrow (C_6H_5)_3CH$$

The smaller wave height obtained may be caused simply by a loss of some of the free radical during the reduction through the dimerization to the Chichibabin compound.

The half-wave potential of the first wave shifted to more positive potentials with the addition of water. This shift may be caused simply by a change in the anode potential with the addition of water. The second wave shows the opposite behavior and shifts to more negative potentials. This behavior would be in agreement with the decrease in acidity brought about by the dilution since hydrogen ions are involved in the second reduction process.

The first wave at higher concentrations of water was found to split into two and three waves. The second wave, when apparent, was not affected by these conditions. The second part of the split wave increased with an increase in the amount of water at the expense of the first part and probably represents the reduction of the hydrated carbonium ion to the free radical. In the presence of large concentrations of water the carbonium ion would form the hydrated ion or the conjugate acid of the carbinol,

$$(C_6H_5)_3C^+ + H_2O \rightleftarrows (C_6H_5)_3COH_2^+$$

The shift of this equilibrium is very slow since the waves were diffusion controlled. The half-wave potential for the hydrated carbonium ion is more negative than that for the carbonium ion. This behavior is in agreement with the results obtained by Conant and Chow (9) by the classical method in glacial acetic acid solutions.

The second part of the split wave was not observed for diphenyl-α-naphthylcarbinol even though the first part decreased with the addition of water. This carbinol was the least soluble of the examples studied and may precipitate partially in these solutions even though this phenomenon was not observed visually.

The third part of the split wave which occasionally occurred was very small and may be simply a desorption wave.

The interpretation of the polarographic behavior of the aromatic ketones and aldehydes is made difficult by the proximity of the curve to the discharge of methanesulfonic acid. The high diffusion current constant (I_d) max obtained for benzophenone and the high concentrations necessary to bring out the curve indicate that maxima are involved in these waves. The leveling off current for benzophenone and *p*-chlorobenzophenone was diffusion controlled, however, and implied that the formation of the conjugate acid, which is being reduced, in the following equilibrium is rapid:

$$(C_6H_5)_2C{=}O + CH_3SO_3H \rightleftarrows (C_6H_5)_2C{=}OH^+ + CH_3SO_3^-$$

A similar diffusion-controlled current was found for benzophenone in a 0.1*N* hydrochloric acid-50% ethanol solution.

The electrode reaction is the following and is substantiated by the formation of benzopinacolone in the large-scale electrolytic reduction of benzophenone. These results closely resemble the macroscale reduction of benzophenone in glacial acetic acid-sulfuric acid mixtures (10).

$$2(C_6H_5)_2C{=}OH^+ + 2e \rightarrow \begin{matrix}(C_6H_5)_2C{-}OH\\ |\\ (C_6H_5)_2C{-}OH\end{matrix}$$

$$\begin{matrix}(C_6H_5)_2C{-}OH\\ |\\ (C_6H_5)_2C{-}OH\end{matrix} \xrightarrow{H^+} (C_6H_5)_3C{-}COC_6H_5$$

Benzaldehyde which did not give a visible polarographic wave gave desoxybenzoin in a large-scale reduction. This behavior implies that the reduction of benzaldehyde occurs simultaneously with that for the supporting electrolyte.

Manuscript received February 2, 1956. Part of this paper was prepared for delivery before the New York Meeting, April 12 to 16, 1953, and was abstracted from the Ph.D. Thesis of R. Berkey (1955) and the M.S. Thesis of D. Thomson (1953), State University of Iowa, Iowa City, Iowa. The greater part of the research was supported by the A.E.C. under Contract AT (11-1)-72 Project #6.

Any discussion of this paper will appear in a Discussion Section to be published in the June 1957 JOURNAL.

REFERENCES

1. J. C. JAMES, *Trans. Faraday Soc.*, **47**, 1240 (1951).
2. S. WAWZONEK AND M. E. RUNNER, *This Journal*, **99**, 457 (1952).
3. S. WAWZONEK, E. W. BLAHA, R. BERKEY, AND M. E. RUNNER, *ibid.*, **102**, 235 (1955).
4. K. ELBS, *Z. Elektrochem.*, **2**, 472 (1896).
5. J. B. CONANT AND N. M. BIGELOW, *J. Am. Chem. Soc.*, **53**, 676 (1931).
6. J. B. CONANT, L. F. SMALL, AND B. S. TAYLOR, *ibid.*, **47**, 1959 (1925).
7. J. E. LEFFLER AND R. A. HUBBARD, *J. Org. Chem.*, **19**, 1089 (1954).
8. K. ZIEGLER AND L. EWALD, *Ann.*, **473**, 163 (1929).
9. J. B. CONANT AND B. F. CHOW, *J. Am. Chem. Soc.*, **55**, 3752 (1933).
10. S. SWANN, JR., *Trans. Electrochem. Soc.*, **64**, 313 (1933).

Preparation of High Purity Rhenium

D. M. ROSENBAUM, R. J. RUNCK, AND I. E. CAMPBELL

Battelle Memorial Institute, Columbus, Ohio

ABSTRACT

Rhenium powder containing a maximum of 0.05% impurities has been prepared by hydrolysis of rhenium pentachloride and subsequent hydrogen reduction of the resultant hydrated rhenium dioxide. Particle size of the rhenium powder is such as to lead to easy densification by methods standard to powder metallurgy. Advantages of this method of preparation over previously employed methods are given.

Despite the fact that rhenium is quite rare, being only one-tenth as abundant as iridium, its potential usefulness in specialized applications has prompted an extensive investigation of its properties.

Rhenium was discovered in 1925 and concentrated and separated shortly afterward. Because of the importance of the discovery in further confirmation of the periodic theory of the elements and the controversial nature of the claims surrounding its discovery, rhenium received considerable attention for a few years. However, the limited availability of ores and the potentially high cost of the metal soon relegated it to the role of a laboratory curiosity. As additional deposits of rhenium have been discovered, it has found limited commercial use, and the recent prospect of a continuing commercial source in modest quantities has stimulated interest in this potentially useful metal.

In 1952, Battelle Memorial Institute undertook an investigation of the properties of rhenium for the Aeronautical Research Laboratory of the Wright Air Development Center.

Of particular interest were potential high temperature applications of the metal itself. Of the metals, only tungsten, which rhenium resembles in many of its properties, has a higher melting point.

At the outset of the investigation, little was known about fabrication of the metal. However, it was concluded that the techniques used in the fabrication of tungsten should be followed in fabricating rhenium. Although there was no specific information on the effect of impurities in the metal on its fabrication and properties, experience with other metals had led to the conclusion that certain nonmetallic impurities might have a decidedly adverse effect on the properties of the metal. In any event it was desirable to prepare high purity powder to provide uniform metal of high quality for fundamental studies of its properties. Therefore, preparation of high purity rhenium powder was undertaken.

EXPERIMENTAL WORK

Three methods of preparation were investigated, all using potassium perrhenate, the anticipated principal commercial source of rhenium, as the starting material. These methods have been referred to as the potassium perrhenate method, the ammonium perrhenate method, and the halide method. In the first, potassium perrhenate is reduced with hydrogen, potassium hydroxide is removed by leaching, and the crude rhenium powder reduced again to give fairly pure rhenium powder. In the second, potassium perrhenate is converted to ammonium perrhenate which is then reduced to metal with hydrogen. The chief advantage of the ammonium perrhenate method is the production of metal of lower potassium and oxygen content. In the halide method, rhenium pentachloride is prepared from crude rhenium powder, and converted by hydrolysis to rhenium oxide, which is then reduced with hydrogen to give a high purity rhenium powder. The halide method has given consistently purer metal than the first two and has the added advantage of involving substantially fewer operations than the ammonium perrhenate method.

POTASSIUM PERRHENATE METHOD

The potassium perrhenate method which involves steps common to all three of the preparative schemes is discussed first.

Commercial potassium perrhenate was converted to crude rhenium metal by reaction with hydrogen at 500°C in a vertical stainless steel reactor 4 in. in diameter by 24 in. high. The reactor, charged with 3 lb of potassium perrhenate, was first heated to 200°C and held at that tempera-

ture for 1 hr. It was then heated to 500°C and the reduction was carried out by passing purified dried hydrogen through the reactor at 18 cc/sec (STP). About ½ lb of potassium perrhenate was reduced per hour under these conditions. Reduction was considered complete when condensation of moisture from the exit gas could no longer be detected.

On completion of the reduction reaction, the charge was cooled to room temperature in an inert or reducing atmosphere. The reaction products, consisting of rhenium metal and small amounts of rhenium dioxide, potassium perrhenate, and potassium hydroxide, were then washed with hot distilled water until essentially free of alkali.

The leached rhenium-rhenium dioxide mixture was placed in a molybdenum boat and further reduced in hydrogen for 2 hr at 1000°C. The metal product was leached with dilute HCl to remove residual KOH, and then washed by decantation with hot distilled water until neutral. The powder was then again treated with hydrogen at 1000°C. Approximately 93% of the rhenium was recovered as rhenium powder. An additional 5% of the available rhenium was recovered from the wash water as unreacted potassium perrhenate, finely divided rhenium dioxide, and rhenium metal.

A typical analysis of the powder, given in Table I, indicates that traces of potassium remained in the powder. Additional leachings failed to reduce the amount of potassium in the powder.

In consolidating rhenium metal powder (1), it was necessary to reduce the particle size to less than 325 mesh in order to obtain pressed bars of sufficient green strength to permit handling. The sintered bars of rhenium metal powder made by direct reduction of potassium perrhenate had a density only 60% of the theoretical density and could not be fabricated. Many of these bars melted at temperatures far below the known melting point of rhenium.

TABLE I. *Table of analysis*

Element	Weight Per Cent		
	Rhenium metal prepared from potassium perrhenate	Rhenium metal prepared from ammonium perrhenate	Rhenium metal prepared by the halide method
Aluminum	0.009	0.094	0.008
Calcium	0.008	0.017	0.002
Chromium	0.004	N.F.*	N.F.
Copper	0.0012	0.0021	0.0002
Iron	0.05	0.024	0.012
Lead	N.F.	N.F.	N.F.
Magnesium	0.002	0.038	0.005
Manganese	0.007	0.002	0.007
Molybdenum	0.15	N.F.	N.F.
Nickel	0.003	N.F.	N.F.
Potassium	0.41	N.F.†	N.F.
Rhenium	Major	Major	Major
Silicon	0.005	0.028	0.015
Sodium	0.15	N.F.	N.F.
Tungsten	N.F.	N.F.‡	N.F.
Total	0.799	0.205	0.049

* N.F. = Not found.

† Not found in the first batches of rhenium prepared by this method, but found in increasingly greater amounts, up to 0.40%, in later batches.

‡ When tungsten carbide rods were used in the ball milling operation, the amount of tungsten present was 0.25.

Elements checked for but not found: Sb, As, Ba, Be, Bi, B, Cd, Co, Cb, Ga, Ge, Au, Pt, Ag, Sr, Te, Sn, Ti, V, Zn, Zr.

In consolidating and fabricating rhenium, procedures similar to those employed in the fabrication of tungsten were followed. Rhenium powder was pressed into bars at pressures up to 30 tons/in.^{2}. The bars were presintered at 1200°C in hydrogen for 2 hr in an externally heated furnace and then heated resistively in hydrogen at temperatures of approximately 2700°C for 1 hr.

Powder prepared by the ammonium perrhenate or chloride methods could be converted into bars which could be worked into sheet or wire, but the bars obtained from powders prepared by the potassium perrhenate method were of low density and could not be fabricated. The poor densification and low melting points of bars obtained from powder prepared directly from potassium perrhenate may be attributed to the effect of residual potassium oxide.

Ammonium Perrhenate Method

Of the 0.8% impurities present in the powder obtained from potassium perrhenate, over one-half was potassium. Since further treatment of the powder did not reduce the potassium content, it was decided that potassium perrhenate should be converted to ammonium perrhenate which could then be reduced to produce a metal low in potassium.

In the preparation of ammonium perrhenate, potassium perrhenate was first reduced to a rhenium-rhenium dioxide mixture by the method previously described. This mixture was then converted to rhenium heptoxide by reaction with oxygen at 800°C in a Vycor tube furnace, the volatilized heptoxide condensing in the cooler portions of the tube (*see* Fig. 1).

The rhenium heptoxide was leached from the Vycor tube with as small a quantity of distilled water as possible, giving a perrhenic acid solution which was filtered to remove any acid insoluble materials. The filtrate was then neutralized with concentrated ammonium hydroxide to precipitate ammonium perrhenate. The ammonium perrhenate was filtered off and the filtrate was concentrated by evaporation to recover the small amount of ammonium perrhenate which remained in solution. The precipitated ammonium perrhenate contained some ferric hydroxide, which probably was obtained as a result of contamination of the powder with iron from the initial reactor. The ferric hydroxide was removed in a Soxhlet extractor using dilute ammonium hydroxide as a solvent for the ammonium perrhenate.

Approximately 85% of the rhenium present in the potassium perrhenate is recovered as ammonium perrhenate. Rhenium values in leach waters and filtrates were, however, recovered by further processing.

The ammonium perrhenate was obtained principally in the form of large crystals, about ¼ in. in diameter. In order to obtain the rhenium powder in as finely divided form as possible, the crystalline ammonium perrhenate was comminuted in a Canadian rubber-lined ball mill using Burundum balls. The initial impurity pickup in ball

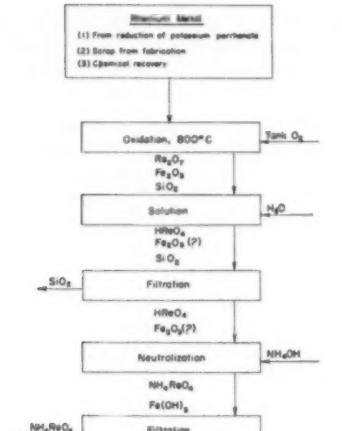

FIG. 1. Flow sheet for preparation of rhenium by the ammonium perrhenate method.

milling amounted to about 0.15% but as the balls became slightly worn, the impurity level went up rapidly to a point where the mill could no longer be used. Therefore, tungsten carbide rods were substituted for Burundum balls. The carbide rods gave a tungsten pickup of about 0.25% but this had neglegible effect on the fabrication, because tungsten is soluble in rhenium without noticeable solution hardening.

After reduction to minus-325 mesh the ammonium perrhenate was placed in a molybdenum boat in a ¼-in. layer and reduced with hydrogen. It was first reduced at 300°C for 1 hr and then at 800°C for 1 hr, following which it was cooled to room temperature in a hydrogen atmosphere. The reduced powder which was loosely sintered was broken up in an agate mortar, and again reduced for 1 hr at 800°C. A metal powder of minus-325 mesh particle size was obtained.

This powder could be sintered to 90% of theoretical density and the bars obtained in initial work could be rolled readily into sheet or drawn into wire. However, as the reprocessing of rhenium scrap and other rhenium residues continued, difficulties were encountered in fabrication and a gradual increase in potassium content was noted. The potassium impurity level finally reached 0.4% at which point the densities of the sintered bars decreased to 70% of the theoretical density and metal could not be fabricated. A typical analysis of rhenium powder prepared by the ammonium perrhenate method is given in Table I.

The cause of the increase in potassium in later batches of rhenium prepared from ammonium perrhenate is not known. However, it appears that hot spots developed in the charge during the oxidation reactions, and the temperature of these areas often exceeded the boiling point of potassium hydroxide. Potassium hydroxide was therefore probably carried over with the rhenium heptoxide during the oxidation reaction. The potassium transfer could undoubtedly have been avoided by careful control of the oxidation.

Halide Method

However, since the ammonium perrhenate method is complicated and tedious and a shorter method was desired, the chloride method was investigated. This appeared attractive in that (*a*) it eliminated, or at least minimized, the potassium problem by utilizing a vaporization step in which the potassium could be left in the residue, and (*b*) it gave a much simpler procedure.

In the chloride process, crude rhenium metal was treated in hydrogen for 1 hr at 1000°C to reduce any oxides present and then chlorinated at 750°C to give the pentachloride. Chloride was hydrolyzed by adding it cautiously to distilled water cooled to about 10°C in an ice bath. The main product of hydrolysis was hydrated rhenium dioxide. Perrhenic acid and chlororhenic acid were present in smaller amounts. If the hydrolysis is not carried out in cold water, the yield of rhenium dioxide is somewhat lower. Under the conditions specified, about 75% of the available rhenium was recovered as hydrated rhenium

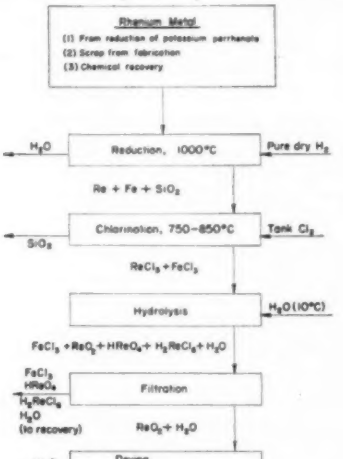

FIG. 2. Flow sheet for preparation of rhenium by the halide method.

dioxide. The hydrated oxide has the consistency of a gel and is difficult to filter. However, the filtration time can be reduced (2) substantially by bubbling carbon dioxide through the hydrolysis product for about 30 min before filtering.

The finely divided rhenium dioxide was filtered off or separated from the liquor by centrifuging, washed several times with distilled water, and dried in a vacuum desiccator.

To recover rhenium from the filtrate, a small amount of 30% H_2O_2 was added to convert all rhenium present to perrhenic acid. The perrhenic acid solution was then neutralized with concentrated NH_4OH and the resultant ammonium perrhenate crystals filtered off and set aside for recycling.

The major reaction product, rhenium dioxide, was hydrogen reduced in a ½-in. layer in molybdenum boat for 1 hr at 400°C and for a second hour at 600°C. The resultant rhenium powder, which was loosely sintered, was broken up in an agate mortar, and treated with hydrogen at 800°C for 2 hr, following which it was cooled to room temperature in an inert or reducing atmosphere.

A typical analysis of rhenium powder prepared by the halide method is given in Table I.

The powder produced by the halide process could be pressed to a density of almost 60% of the theoretical density (3), i.e., almost equal to the sintered density of metal made by the hydrogen reduction of potassium perrhenate. Despite the fact that the metal prepared from the halide had a higher as-pressed density than metal prepared by the other methods, its sintered density of 80% of theoretical was lower than the sintered density of metal produced from ammonium perrhenate. Nevertheless, metal produced from the chloride could be fabricated without difficulty.

The over-all rhenium recovery efficiency in the chloride process is about 95%, comparing favorably with the efficiency of recovery by the other methods.

Because the chloride process involves fewer steps than the ammonium perrhenate process and because it gives a purer product than either the ammonium perrhenate process or the potassium perrhenate process and, especially one free of potassium, the chloride process is now used in preparing rhenium for powder metallurgy studies at Battelle.

Acknowledgment

The powder metallurgy work was conducted by C. T. Sims of Battelle Memorial Institute, Division of Nonferrous Physical Metallurgy. The authors wish to express their appreciation of E. J. Hassell and the Air Research and Development Command, United States Air Force, Wright-Patterson Air Force Base, for permission to publish the results of work obtained at Battelle Memorial Institute under Contract No. AF 33(616)-232. They also are indebted to the Kennecott Copper Corporation for supplying the potassium perrhenate used in the preparation of rhenium powder.

Manuscript received November 4, 1955. This paper was prepared for delivery before the Pittsburgh Meeting, October 9 to 13, 1955.

Any discussion of this paper will appear in a Discussion Section to be published in the June 1957 JOURNAL.

REFERENCES

1. C. T. SIMS, C. M. CRAIGHEAD, AND R. I. JAFFEE, *J. Metals*, **7**, 168 (1955).
2. J. G. F. DRUCE, "Rhenium", p. 51, Cambridge University Press, Cambridge, England (1948).
3. C. T. SIMS, Unpublished data.

Uranium Purification by Electrorefining

LEONARD W. NIEDRACH AND ARTHUR C. GLAMM

Knolls Atomic Power Laboratory, General Electric Company, Schenectady, New York

ABSTRACT

The feasibility of a high temperature electrorefining process for decontamination of U from associated fission products was demonstrated. Low-melting alloys of U with Ni were used to obtain molten products at temperatures below the melting point of pure U. Effects of temperature, current, and salt-bath composition on cell efficiency and cell operation are discussed.

Periodically the fuel from nuclear reactors must be removed and reprocessed to repair radiation damage, to restore reactivity, and to remove fission products. In some applications a high degree of decontamination from the fission products is not essential, and the possibility of employing an electrorefining process to accomplish the required decontamination is feasible. A process employing a fused-salt electrolyte was chosen for investigation because the chemical activity of U precludes the use of aqueous electrolytes, and danger from radiation damage makes the use of organic solvents undesirable. A general description of the over-all process has been given elsewhere (1). Background investigations performed in connection with the demonstration of the electrolysis step of such a process for U are detailed in this paper.

In this work, U-rich alloys with Ni were used to obtain

molten products at temperatures considerably below the melting point of pure U. In this way, continuous cell operation was facilitated because a molten, salt-free product can be removed readily from an electrolysis cell. Probably the information gained from this work will result in a process that can be operated at temperatures at which the electrolysis product is molten U. Until then, if unalloyed U is desired as the ultimate product, it should be possible to choose an alloying agent that behaves like Ni during electrolysis, but which can later be removed from the product alloy. Details of this step have not yet been investigated intensively. However, in some exploratory experiments it was found that the Mn content could be reduced to a few ppm by distillation from a U-Mn eutectic alloy (6.0 wt% Mn) (2) by heating in a vacuum to about 1300°C. Because of the low Mn content in the eutectic alloy, use of reasonably pure metal should prevent serious recontamination of the U.

Only limited electrolysis work has been done on U. Driggs and Lilliendahl (3) used a salt bath containing NaCl, $CaCl_2$, and KUF_5 for electrowinning U. The electrolysis operation was performed at 775°C and produced powdered or dendritic deposits. Rosen (4) described a similar procedure in which powdered U was obtained by electrolysis of UF_4 in a mixture of alkali and alkaline earth halides at 800–850°C. A quantitative study of the effects of current density and temperature on the deposition characteristics of U obtained from mixed fluoride-chloride baths has been reported (5). The temperature range was 725–900°C, and finely divided metal was again obtained as the product.

An electrorefining process gave U of exceptional purity when fairly pure U was used as the starting material (6). Electrorefining has also been examined as a processing method for spent reactor fuels (7). In both cases, electrolyses were performed at temperatures below the melting point of U, and dendritic deposits were obtained.

In all of the work mentioned above, the metal produced at the cathode required thorough washing to remove adhering salts before the metal had been compacted. Because of the nature of the products a batch-type operation was dictated in order to remove bulky deposits from the electrolysis cells. This is an awkward procedure, but the literature contains no description of a process for U purification in which a readily handled, molten product is formed.

Experimental

Equipment and Operating Procedure

In most of the present work aimed at demonstrating the principles of an electrorefining process for U decontamination, alloys of U with Ni were formed as the electrolysis product by employing a Ni rod as the cathode in the electrolysis cell. The deposited U and the Ni interdiffuse and form a molten layer of alloy on the electrode surface. When molten material accumulates, it eventually drips from the cathode rod and collects as a pool in the bottom of the crucible. While this procedure has not been used before for the production of U alloys, electrolyses in which eutectic alloys are formed in other systems have been described. For example, Fischer and Dorsch (8) prepared Ti alloys by employing cathodes of Cu, Ni, Fe, Co, and Al. Andrieux (9) used a similar method to form boron alloys, and Steinberg and co-workers (10) reported the formation of Zr-Ni alloys by electrodepositing Zr on Ni cathodes.

Ni has been used as the alloying agent in most of the work because of its availability in the form of rods suitable for use as cathodes, and because phase data on the U-Ni system are available (11). Runs of a similar nature have also been made with Fe, steel, and a Mn-10 wt% Cu alloy as cathodes.

The diluent salt used in an electrorefining bath must be less readily reduced than that of the metal to be deposited. In the case of U, this requirement is satisfied by alkali or alkaline earth halides, and a brief consideration of vapor pressures narrows the choice to chlorides or fluorides or a mixture of the two. It is possible to start with a tetravalent U salt in the bath, but rapid reduction to the trivalent state occurs either electrolytically or by reaction with the anode material. Chlorides or mixtures of chlorides and fluorides were used for most of the work because they are easier to handle than pure fluorides. For example, it is easy to dissolve away any chlorides coating the deposited metal to obtain a clean piece of metal. In addition, samples of chloride baths are also readily dissolved to provide samples for analyses.

The literature contains very little information regarding the resistance of refractories to both U metal and alloys and to fused salts in the temperature range of interest. Therefore, tests were made on a number of materials. Included were magnesia, thoria-lined alumina, cerium sulfide, and various grades of graphite. National Carbon's AUC grade graphite was considered to be the most satisfactory material, and was used in all of the runs reported.

Several types of cell have been used. The simplest type employs a 3 in. high, 1½ in. OD graphite crucible to hold the salt melt and to retain the cathode alloy drippings. In this type of cell a U rod anode having a nominal diameter of ⅜ in. was used. Cathode rods ¼ in. in diameter were used. Salt depths of 1–2 in. were employed.

This type of crucible can be used only for relatively short batch-type runs because of the limited capacity for holding the cathode product. Therefore, electrolyses for extended periods of time were carried out in the graphite crucible shown in Fig. 1 which is referred to as the weir-type crucible. This type of crucible allows the product alloy to overflow to a collecting vessel as the electrolysis proceeds. Because the overflowing product drops to a collecting vessel, product alloy from short intervals of an extended run can be separated and analyzed. In this way, any variation in the alloy composition may be followed. Also, since anode and cathode weight losses can be taken without disturbing the crucible and its contents, the electrolysis can be resumed under a different set of electrolysis conditions while maintaining the same fused-salt and cell variables. In this manner, U alloys weighing up to 300 g have been produced.

A third type of cell is illustrated in Fig. 2. It employs a graphite anode basket and can be operated with a feed consisting of U pellets. For runs of short duration the product metal has been collected in a well of small diam-

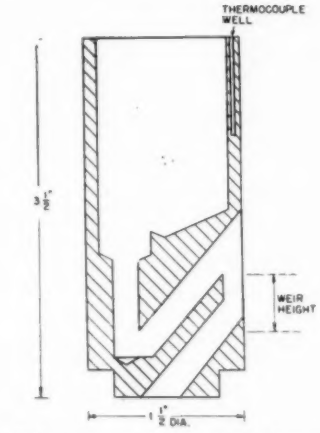

FIG. 1. Weir-type graphite crucible (cross section)

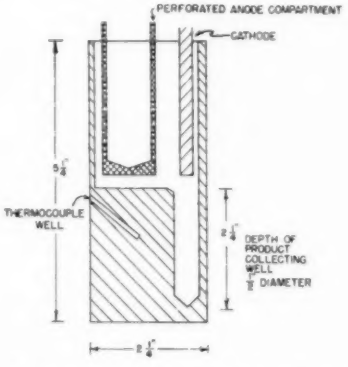

FIG. 2. Cross section of electrolysis cell with product collecting well.

eter as shown in the diagram; however, the weir arrangement for removing product alloy, as described above, can also be used with such a cell arrangement.

The general arrangement of the electrolysis cell when the weir-type crucible was used is shown in Fig. 3. A similar arrangement was used in the other cases. The crucible was supported by Mo rods inside a chamber which consisted of a lower quartz cylinder and an upper Pyrex cylinder. The latter was closed on the top by a brass plate. The seal between the brass plate and the Pyrex section was made with de Khotinsky cement, while the seal between the upper Pyrex glass section and the lower quartz section was made with Apiezon wax. The glass surfaces were ground for better seals. The entry of movable stainless steel electrode-supporting rods through vacuum seals attached to the brass plate permitted adjustment of the depth of immersion of the electrodes in the fused-salt bath and allowed continuous electrolysis to be maintained. The electrodes were insulated from each other by mounting the vacuum seals in Bakelite plugs, which in turn were attached to the brass plate.

A chromel-alumel thermocouple and the Mo supporting rods for the crucible entered the chamber through ball and socket joints on the Pyrex top section. The thermocouple was placed in the graphite crucible wall about 2 in. below

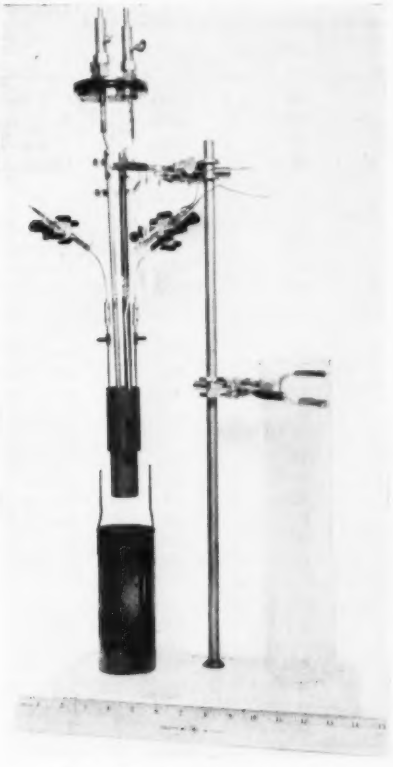

FIG. 3. Electrolysis cell assembly

the crucible top and definitely below the fused-salt bath surface. A Ta shield, which was lowered for the photograph, served as a heat reflector and allowed temperatures in excess of 1200°C to be obtained with a 6 kw Ajax-Northrup Spark-Gap Converter under usual electrolysis cell conditions.

In all cases the assembled electrolysis apparatus was connected to a vacuum system employing a mercury diffusion pump capable of producing and maintaining a vacuum of 1 μ. Provision was made to add purified gases to the system. Electrolyses were run under a pressure of about 1 atm He to prevent excessive volatilization of the salt during operation. Air cooling was provided for the Apiezon wax seal and for the quartz vessel at the induction coil region.

A continuous record was kept of temperature, cell voltage, and cathode-crucible voltage during an electrolysis run. The cathode-crucible voltage indicated which of the working electrodes required adjustment as its area decreased.

The source of electrolysis current was a 110-volt d-c line which had about 4% ripple. Desired cell current was obtained by the use of suitable resistances in series with the electrodes.

The general operating procedure used during an electrolysis was as follows. The graphite crucible was degassed by heating to 1200°C under vacuum, then cooled in a He atmosphere. This procedure was used to minimize surface contamination of the charged U as well as the alloy

TABLE I. *Summary of conditions and data for electrolysis runs with Ni cathodes*[1]

Run no.	Crucible type[2]	Temp,[3] °C	Salt phase wt %	*I*, amp	Length of run amp-hr	% Anode[4] efficiency	Wt % of U in product[5]
31	W	1050	66% $BaCl_2$—34% UF_4	5	15	53	(83)
34(A)	W	1025	As in Run 31	5	11.7	34	(84)
34(B)	W	1025	Reuse from A	1	9	82	(77)
34(C)	W	1035	Reuse from B	0.4	8.2	89	(73)
					28.9		
35	W	975	As in Run 31	2.5	7.9	59	(56)
36	W	975	Reuse from 35	2.5	5	55	(87)
37	W	1025	Reuse from 36	2.55	5.1	69	(85)
38	W	1075	Reuse from 37	2.55	5.1	60	(93)
					23.1		
41	W	1025	As in Run 31	2.6	25.6	59	(84)
46	S	850	62% $CaCl_2$—38% UCl_3	0.35	10.5	81	80 (83)
44	S	850	As in Run 46	2	16	56	86 (95)
47	S	850	As in Run 46	5	20	36	79 (81)
49A	W	950	As in Run 46	3	17.5	71	85.7
B	W	950	Reuse from A	3	19.5	46	87.6
C	W	950	Reuse from B	3	19.5	49	88.8
D	W	950	Reuse from C	3	19.5	71	87.5
E	W	950	Reuse from D	3	31.5	62	85
F	W	950	Reuse from E	3	36	55	84.5
G	W	950	Reuse from F	3	36	55	83.8
					180	Avg 58	
50	S	950	24% $CaCl_2$—76% UCl_3	3	18	66	86 (94)
51	S	950	75% $CaCl_2$—25% UCl_3	3	15	80	91
52	S	950	90% $CaCl_2$—10% UCl_3	3	13.5	70	95
65A	B-W	990	As in Run 46	3	18		84
B	B-W	1000	Reuse from A	3	15	79	77
C	B-W	1000	Reuse from B	3	15		70
D	B-W	1000	Reuse from C	3	18	79	68
66	B	900	As in Run 46	3	31	90	84
67	B	900	As in Run 46	10	50	70	(91)
69[6]	B	900	As in Run 46	10	49	58	(91)
70[7]	B	900	As in Run 46	10	55	78	(92)

[1] ¼ in.-diameter Ni rods used in all runs.
[2] S—simple; W—weired; B—basket anode.
[3] Temperature in °C ± 10°C.
[4] Based on theoretical reaction of $U^0 \rightarrow U^{+3}$ at anode.
[5] The weight per cent of U in the product was obtained by analysis. Values in parenthesis were calculated from electrode weight losses.
[6] Alloy anode run.
[7] Radioactive run.

product. When a weir-type crucible was used, sufficient Ni-U eutectic alloy (melting point 740°C) was added to the degassed crucible to fill the weir passages and to overflow a small quantity of alloy. The alloy was melted at low pressure, preferably less than 10 μ. The salt phase, which had been premelted under a He atmosphere, was then added to the cell. Heating of the electrolysis cell to about 500°C was carried out at 25 μ or less. Approximately 1 atm He was introduced into the system before the cell was heated to the operating temperature. The electrodes were then lowered into the salt, and when the temperature became stabilized, electrolysis was started. During a run the electrodes were lowered into the fused-salt bath as the voltage record indicated the need.

When the electrolysis run was completed and the circuit was opened, the electrodes were removed from the salt bath and heating was stopped. The system was not opened until the temperature of the cell had fallen to 50°C. Opening of the system at higher temperatures would have resulted in oxidation of the alloy product, preventing free flow of the product from the weir opening.

Results and Discussion

Detailed experimental conditions and data relating to electrolyses with a dripping alloy cathode are summarized in Table I. In all of the runs listed, a ¼ in. Ni rod cathode was used. A U rod was used for the anode in most of the runs. In the last few runs employing a basket-type anode, U was added in the form of pellets, chips, or short bars.

The total electrolysis current rather than current density is listed in the table because the continual change in electrode size during a run caused variations in the current density. However, it is estimated that the initial current densities when rod electrodes were employed varied from 0.1 to 1 amp/cm² as the electrolysis current was changed from 0.4 to 5 amp. Current densities for the material in the basket anode could not be readily estimated, but they were believed to be considerably lower than with the rod

anodes. Cell voltages during essentially all the runs were found to fall in the range 0.3–0.7 v.

Anode efficiencies shown in the table were calculated from the loss in weight of the anode and an assumed ideal reaction involving a three-electron oxidation to form trivalent U. This was done whether the initial charge to the salt bath consisted of trivalent or tetravalent U, because a consideration of existing thermal data for U halides indicated that the lower valence state is the stable one under the conditions employed (12). Preliminary experiments to determine the valence states in the bath at the end of an electrolysis indicated that the above assumption was correct.

Cathode efficiencies are not listed because complete recovery of the product was not attempted in most cases. Generally the product alloys wet the crucible, and complete recovery would have been difficult. The material that was recovered generally accounted for 70% or more of the metals that had been lost from the two electrodes proper. In the case of Run 49, a complete material balance was performed, and the product alloy was found to account for 98% of the charged materials.

Composition of the product alloy was often calculated from the weight losses of the two electrodes. This was generally necessary when a weired crucible was employed because of mixing of the product with the original metal. Because of the uncertainty of the calculated alloy compositions the alloys were analyzed directly whenever possible. A few comparative values are included in the table. Generally, calculated values indicated slightly low Ni contents. No attempt was made to determine the exact cause of the discrepancy. It was evident, however, that U held up on the cathode surface decreased the apparent weight loss of the cathode and could thereby be the cause. It is also possible that formation of some U^{+4} in the bath could contribute to the deviation.

In addition to the runs listed in the table a few were made using Fe, steel, and a Mn-10 wt % Cu alloy as the cathode. Actually, Mn would have been preferred over the alloy, but it was too brittle for fabrication into an electrode. The high C content of the steel resulted in formation of a solid on the cathode, presumably caused by carbide formation. Both the Fe and the Mn-Cu alloy produced molten U alloys that behaved like the Ni alloys. It was also found that Mn can be removed from such an alloy by heating at 1300°C.

Of primary concern in the investigation were the effects of temperature, current, and bath composition on cell efficiency and operation. The data for Runs 35–41 in particular indicated that the effect of temperature on anode efficiency was small relative to that of current. In addition, data for efficiency vs. cell current as plotted in Fig. 4 showed no marked trends attributable to temperature. However, the temperature range was limited by salt volatilization at high temperatures and by dendrite formation at low temperatures. An operating temperature as high as 1100°C was possible with baths containing chloride, and dendrites have been observed at 850°C.

The marked effect of cell current on efficiency is shown clearly in Fig. 4. This effect of current transcends the effects of temperature and of bath composition as illustrated by the mixed data. The scatter among the data was caused in large part by the ever changing current densities at the consumable electrodes. It is these variations which also prevent a correlation of the effects with current density.

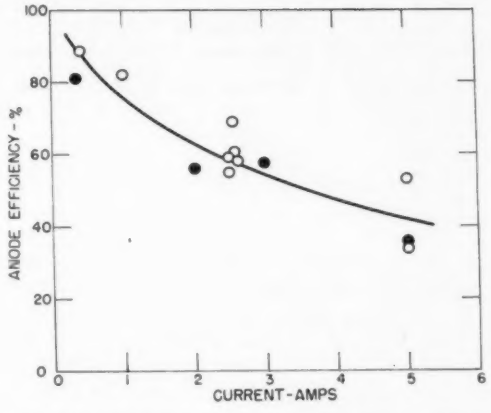

FIG. 4. Effect of current on anode efficiency. ○ = 66 wt % $BaCl_2$—34 wt % UF_4 at 975°–1075°. ● = 62 wt % $CaCl_2$—38 wt % UCl_3 at 850°–950°C.

While the effect of current density for the individual electrodes was not examined, it is still possible on the basis of the chemistry of U to arrive at a mechanism which explains the decrease in efficiency with increasing current. Thermal data indicate that trivalent U is the stable state in the bath at the operating temperatures (12). At low currents, then, U should enter the bath as U^{+3}, and diffusion away from the electrode should occur rapidly enough to prevent polarization to the extent that U^{+4} is formed. Since there are no stable oxidation states between U^{+3} and U^0, the only reaction possible at the cathode is reduction to the metal; and since the nickel alloying agent is present, difficulties from fog formation should be minimized. Therefore, high cell efficiencies are in order at low current densities. As the current is increased it seems probable that a point is eventually reached when diffusion of the oxidized species away from the electrode is not rapid enough to prevent formation of significant amounts of U^{+4}. When such a state is reached, current could be carried in part by a cyclic oxidation and reduction involving U^{+3} and U^{+4}, and the current efficiency would decrease.

In Runs 65–67 and 70, pellets or chips of U were used with the basket anode; therefore, a much larger than normal surface area of U was available, and the anode efficiencies were higher than previously observed. In Run 60 a $\frac{3}{8}$ in. diameter bar was charged to the basket. The surface area was, therefore, similar to the earlier runs and the efficiency was again lower.

The composition of the salt bath seemed to have a minor effect on the cell efficiency (Fig. 4). In addition, no effect on general operability of the cell was observed with the baths listed in Table I. However, U concentration in the salt bath was an important variable as far as product contamination by the bath diluent is concerned (Table II). These data show that the bath should contain a

TABLE II. *Effect of U concentration in bath on product alloy composition*

$CaCl_2$—UCl_3 bath; Ni cathode; T = 950°C; I = 3 amp

Wt % UCl_3 in salt bath	Wt % Ni in alloy	Wt % Ca in alloy
10	2.6	2.7
25	7.7	1.3
38	14.4	0.1–0.3
76	13.8	0.06

definite minimum amount of the U salt if the deposition of significant amounts of the diluent cation is to be avoided.

A few additional tests of the effect of salt composition were made with salt mixtures of BaF_2 containing 38–66 wt % UCl_3 and with an all-fluoride system of NaF with 50–91 wt % UF_4. All of the former mixtures performed satisfactorily but offered no advantages over the $BaCl_2$-UF_4 mixture which replaces the hygroscopic UCl_3 with the readily handled UF_4.

When the NaF-containing baths were used, distillation of Na metal was observed except when the highest concentration of UF_4 was employed. However, the metal produced in this run was encased in a black salt-like envelope about 1 mm thick which had apparently solidified from the bath while it was at operating temperature (1035°C). The envelope was found by x-ray diffraction analysis to be largely UF_3, which has a melting point higher than the operating temperature of the bath. Apparently the billet of product alloy reacted chemically with some unreduced UF_4 in the bottom of the bath and formed the solid-salt phase. Although this behavior was not observed with the $BaCl_2$-UF_4 baths, it was decided to use all chloride baths in later runs in order to preclude such a problem. In the $CaCl_2$-UCl_3 system no high melting salt phases are likely to form. These baths, however, do suffer from higher volatility if attempts are made to use them above 1000°C.

Both the current and the operating temperature have significant effects on the Ni content in the product alloy. This is shown roughly by the data in Fig. 5. The points correspond to actual alloy compositions obtained at the temperatures indicated. The alloys from Runs 51 and 52 are not plotted because they contained a large amount of Ca. Only one point is shown for Run 65 because of the gradual shift in composition during successive stages of this run. The alloy obtained in Run 65 contained that which was initially charged to the weir, and it was only after several throughputs that the composition of the overflowing product would be expected to correspond to that dripping from the cathode. Because of the variations in current density and probably other more subtle factors, the scatter in the data is too great to distinguish the effect of minor changes in current. For this reason the data were grouped; alloys obtained at 0.4 and 1 amp are in one group, those obtained at 2, 2.5, 3, and 5 amp are in a second group, and those obtained at 10 amp are in the third. In this way it becomes evident that at low currents the alloy composition tends toward that at equilibrium on the Ni-rich side of the eutectic. At higher current densities the composition moves toward the U-rich side of the eutectic This is expected since a greater rate of deposition of U at the cathode should result in less chance for the Ni to diffuse into the deposit before the drop grows heavy enough to fall. These results indicate that higher cathode current densities than have been employed would be desirable in order to increase the U content of the alloy. Care must be taken, however, to avoid excessive cathode current densities, or the rate of U deposition will so exceed the rate of diffusion of Ni into the deposit that a solid deposit will result and dendrites will grow.

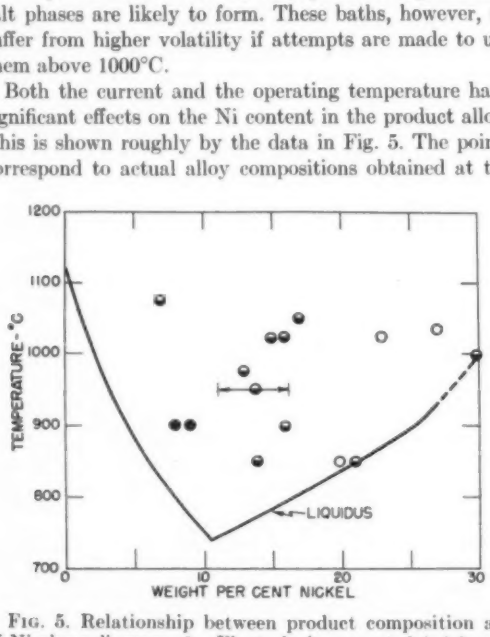

FIG. 5. Relationship between product composition and U-Ni phase diagram. ○—Electrolysis current, 0.4, 1.0 amp; ◒—electrolysis current 2, 2.5, 3, 5 amp; ●—Electrolysis current 10 amp. Liquidus from reference (11).

Continuous Operation and Decontamination Runs

The feasibility of continuous electrolysis for an extended period of time was demonstrated by Run 69 which was carried out for a duration of 60 hr or 180 amp-hr. During this time approximately 30 changes of uranium, or throughputs, occurred in the salt phase. Because of a larger holdup of uranium in the weir reservoir, this was equivalent to only ten throughputs in this reservoir. Electrodes and product from this run are shown in Fig. 6,

FIG. 6. Electrodes and products from extended electrolysis

TABLE III. *Summary of data for Run 49*
Temp: 950°C; *I*: 3 amp; Bath: 41.7 g of 62 wt % $CaCl_2$, 38 wt % UCl_3; anode: U; cathode: Ni; initial weir reservoir: 35 g of U-Ni (13 wt %) alloy

Increment	ΔT, hr	ΔA-hr, amp-hr	ΔW anode, g	ΔW, cathode, g	ΔW billet, g	Anode eff., %	Wt % Ni in product
A[1]	5.8	17.5	36.8	3.4	36.6	71	14.3
B	6.5	19.5	26.6	3.2	19.3	46	12.1
C	6.5	19.5	28.1	4.7	31.6	49	11.2
D	6.5	19.5	41.4	7.5	38.5	72	12.5
E	10.5	31.5	57.3	9.2	65.9	62	15.0
F	12	36	58.3	9.7	53.2	55	15.5
G	12	36	58.9	12.9	61.6	55	16.2
	60	180	307.4	50.6	306.7	58*	14.4*
					Alloy Residue in crucible	78.9	
					Total weight of alloy recovered	385.6	

* Weighted average.

and a summary of the data for the run is given in Table III. From Fig. 6 it is seen that a rather uniform consumption of each electrode occurred, and no signs of undercutting are evident. The condition of these electrodes is also typical of those from runs of shorter duration. The product is shown both as the button that forms in the collecting crucible suspended under the weir and in the form of recast billets.

An average anode efficiency of 58% based on a three electron valence change was obtained. Although some of the fluctuations are undesirably high, it is encouraging that the efficiency does not decrease with increasing time of electrolysis. Composition of the alloy produced is also satisfactory. Greater control to maintain uniform cathode current density should result in less variation in this composition.

Although the cathode efficiency for U production could not be determined accurately during the course of the run, it is evident from the good over-all material balance of 98% that the cathode efficiency must be essentially identical with that of the anode for the greater part of the run. However, this high material balance does not preclude the possibility of side reactions that would result in an initial or a gradual change in the bath composition during the run. In this connection no volatile products of side reactions were ever found. However, analyses for Ca in the product samples indicated that a very gradual reduction of Ca content in the bath occurred. A small change in U concentration resulted. In addition the possibility of an alteration due to changes in the U valence state in the bath must be considered. While analytical evidence was not obtained on this point, the lack of evidence in the literature for U halides with valence states below three would seem to eliminate such from serious consideration. An observation that the salt bath had not assumed the green color associated with U^{+4} coupled with the fact that the salt was reducing in nature at the end of the run and liberated H from water would indicate that extensive oxidation to a higher valence state also did not occur.

Fluctuations in material balances during the run were caused by inevitable variations in the amount of metal holdup in the weir reservoir. It was observed also that wetting of the crucible occurred; therefore, there was a greater hold-up of the alloy at the end of the run than was initially charged. These errors were eliminated from the final material balance by dissolving and analyzing the metal that was left in the crucible.

TABLE IV. *Analysis of products for minor constituents in Run 49*

Increment	C, ppm	O, ppm	Ca, ppm
A	—	—	600
B	—	—	500
C	—	—	700
D	—	—	600
E	450	8	900
F	240	12	1100
G	240	26	900

Typical analyses for minor constituents obtained on the recast billets are summarized in Table IV. Both C and O contents are satisfactory for the conditions employed. A considerable reduction in C content of the product should result on perfection of a satisfactory nongraphite container.

The Ca content too is satisfactorily low, indicating that the U content of the bath is high enough to be the principal current carrier at the electrodes.

While the feasibility of electrolysis over extended periods of time has been demonstrated for one set of conditions, it would appear from earlier data that a wide range of conditions should give equally satisfactory results.

Two runs were made to determine the magnitude of the decontamination from fission products that can be achieved with this method of processing. In one the anode charge consisted of a mixture of unirradiated U with about $\frac{1}{10}$ its weight of irradiated metal that had been cooled 2–3 yr. This gave enough activity so that decontamination through the cell could be followed through radioactivity. The second run used a U alloy containing 1 wt % each of Ru, Mo, and Zr. Data are summarized in Table V. An appreciable decontamination was achieved from both the active and noble metal fission products.

The two runs that are reported were made for a duration of only two bath throughputs, and the need for runs of greater throughput is evident. The data, however, do give an indication of the magnitude of decontamination that is possible with the method.

The information obtained to date on Pu decontamination are inconclusive; however, there is an indication that the Pu tends to concentrate in the salt phase when the chloride bath is used.

TABLE V. *Decontamination factors* obtained by electrorefining*

	Hot run	Alloy run
Cs	260	—
Sr-Y	80	—
Total Rare Earths	170	—
Zr-Nb	80	200
Mo	—	500
Ru	250	400

* Decontamination Factor = $\frac{\text{amount/g U at start}}{\text{amount/g U in product}}$

Summary and Conclusions

This study of U purification by electrorefining has shown that decontamination of U from fission products can be achieved by electrolysis through fused salts. The work has also demonstrated the feasibility of employing cathodes of transition metals in order to obtain U-rich alloy products that are molten at temperatures considerably below the melting point of pure U. The formation of such molten products should facilitate continuous cell operation without introducing the problems associated with operation at temperatures above the melting point of U.

The effects of temperature, current, and bath composition on cell efficiency and operation were investigated. Temperatures in the range 900°–1050°C are satisfactory, and changes in this range have little effect on cell efficiency. The lower temperatures are most satisfactory from the point of view of attack on container materials and salt volatilization. For high cell efficiency low current densities are indicated, especially at the anode. Bath composition has little effect on cell operation, but a minimum concentration of the U salt is required to prevent excessive contamination of the product with the cation of the salt diluent. In the case of $CaCl_2$-UCl_3 baths a minimum UCl_3 concentration of 38 wt % is desirable.

Acknowledgments

The authors express their appreciation to Burton E. Dearing for his work in fabricating most of the graphite crucibles and to the members of the Metallurgical and Chemical Analysis Activity at the Knolls Atomic Power Laboratory for the analytical work.

Manuscript received July 20, 1955.

Any discussion of this paper will appear in a Discussion Section to be published in the June 1957 Journal.

REFERENCES

1. L. W. Niedrach and A. C. Glamm, *Ind. Eng. Chem.*, **48,** 977 (1956).
2. H. A. Wilhelm and O. N. Carlson, *Trans. Am. Soc. Metals*, **42,** 1311 (1950).
3. F. H. Driggs and W. C. Lilliendahl, *Ind. Eng. Chem.*, **22,** 516 (1930); U S. Pat. 1,861,625, June 7, 1932.
4. R. Rosen, U. S. Pat. 2,519,792, Aug. 22, 1950.
5. S. K. Kantan, N. Shreenivasan, and G. S. Tendolkar, *Chem. Eng. Prog, Symposium Ser. No. 12*, **50,** 63 (1954).
6. C. Marzano and R. A. Noland, ANL-5102 (1953).
7. A. Glassner, N. R. Chellew, and R. C. Vogel, ANL-4872, 147 (1952); ANL-4922, 154 (1952).
8. H. Fischer and K. Dorsch, German Pat. 615,951, (1935).
9. J. L. Andrieux, French Pat. 753,394, (1933); U. S. Pat. 2,033,172, (1936). *Rev. met.*, **32,** 487 (1935).
10. M. A. Steinberg, M. E. Sibert, and E. Wainer, Chapter on "The Extractive Metallurgy of Zirconium by the Electrolysis of Fused Salts" in "Zirconium and Zirconium Alloys," pp. 58-60, American Society of Metals, Cleveland (1953).
11. J. D. Grogan and R. J. Pleasance, *J. Inst. Metals*, **82,** 141 (1953).
12. L. Brewer, L. Bromley, P. W. Gilles, and N. L. Lofgren, MDDC-1543, 9 (1945).

Technical Review

Report of the Chlor-Alkali Committee of the Industrial Electrolytic Division for the Year 1955

William C. Gardiner,[1] Morton S. Kircher,[2] and Warren D. Sherrow[3]

Production in 1955

There is little doubt that 1955 was the greatest year in the history of the chlor-alkali industry. Production of chlorine set a new record of 3,407,842 tons,[4] exceeding 1954 by 18%. The industry was running full for the last three months of 1955 and averaged 10,240 tons per day. The lowest month was April with an average of 7,600 tons per day of chlorine.

Caustic soda production was 3,907,149 tons,[4] an increase of 15% over 1954. Lime-soda caustic was 12% of the total and showed no decline during the year, indicating that the demand for caustic soda and chlorine were in balance. However, there were periods during the year when rayon grade liquid caustic and dry caustic were on the scarce side.

Caustic potash production was 90,000 tons. Solvay announced production of potash in mercury cells and several others have indicated their intention of entering the field with production by mercury cells.

Chlorine is estimated to have been produced in the following manner: 78% in 45 plants with diaphragm cells, 16% in 15 plants using mercury cells, 5% in 4 plants producing metallic sodium, and 1% by two chemical processes. Production at two electrolytic magnesium plants is not included because they consume more than they produce.

Canadian production capacity for chlorine is now 447 tons per day in ten plants, six of which use mercury cells.

Developments during 1955

Diamond Alkali brought their plant at Muscle Shoals, Ala., into production during the summer.

Dow Chemical started shipping soda ash made by carbonating caustic soda at Freeport, Texas.

Hercules Powder Co. ran into more trouble than they expected in their plant to oxidize by-product hydrogen chloride to chlorine at Brunswick, Ga. The plant is operating intermittently at 44 tons per day. They hope to be in regular production by the middle of 1956.

The price of mercury continued to be of considerable concern to mercury cell users. The average annual quotation in 1955 established a new peak at 10% above the previous high in 1954. Quotations ranged from $322 to $324 a flask through February, increased slightly in March and then declined gradually to $253–$255 a flask in August. The price then rose to $280–$284 a flask in November and remained there.

Expansion News in 1955

Columbia-Southern is adding 50 tons per day at each of their plants at Lake Charles, La., and Barberton, Ohio.

E. I. du Pont de Nemours and Co. is planning a sodium and chlorine plant at Antioch, Calif., for tetraethyl lead, ethyl chloride, trichlorethylene, and perchlorethylene.

Pennsylvania Salt Manufacturing Co. is adding more deNora mercury cells at Calvert City, Ky., to produce caustic potash early in 1956.

Solvay Process Division of Allied Chemical and Dye Corp. announced a new mercury cell plant at Brunswick, Ga., for late 1956.

Union Chemical and Materials (Frontier Chemical) is doubling capacity at Wichita, Kans. The chlorine is for production of chlorinated solvents.

Westvaco Chlor-Alkali Division of Food Machinery and Chemical Corp. will modernize its Charleston, W. Va., plant by replacing Vorce and Nelson cells with Hooker S3B cells. Production is 370 tons of chlorine per day.

The Weyerhauser Timber Co. is constructing a plant to make 75 tons of chlorine per day at Longview, Wash., using deNora mercury cells.

Announcements to Date in 1956

Canadian Industries, Ltd , will triple its capacity to produce chlorine, hydrochloric acid, and caustic soda at Cornwall, Ont., by mid 1956.

Dow Chemical Co. will build a $20 million plant to produce chlorine, caustic, and organics in the Baton Rouge, La., area.

General Aniline and Film Corp. started its 50 ton per day chlorine plant using Mathieson mercury cells at Linden, N. J.

Hooker Electrochemical Co. has merged with Niagara Alkali Co. at Niagara Falls. The Tacoma, Wash., plant is to be expanded 30%. A Canadian subsidiary, Hooker Chemicals, Ltd., is building a plant to cost $11 million at Vancouver, B. C. Hooker has joined Pennsylvania Salt to form the Chemical Salt Production Co. to produce solar salt from Great Salt Lake, Utah. This will assure a source of salt for the western operations of both companies.

Kaiser Aluminum Corp. will spend $8 million for a chlor-alkali plant at Gramercy, La. Hooker cells will probably be used. The caustic soda will be used for purifying bauxite.

Mathieson Alabama Chemical Corp., a subsidiary of Olin Mathieson Chemical Corp., is doubling capacity at McIntosh, Ala.

[1] Olin Mathieson Chemical Corp., Niagara Falls, N. Y.
[2] Hooker Electrochemical Co., Niagara Falls, N. Y.
[3] Great Lakes Carbon Corp., Niagara Falls, N. Y.
[4] U. S. Department of Commerce, "Facts for Industry."

Shawinigan Chemicals, Ltd., will probably install mercury cells at Shawinigan Falls, Que.

Wyandotte Chemical Corp. has purchased land for a 100 tons per day chlor-alkali plant in Louisiana.

Technical Developments

Ion permeable membranes are being investigated for use in chlor-alkali cells.

The search for a practical vertical mercury cell continues. Dr. deNora discussed his developments on a fluent amalgam cell at our Symposium last May in Cincinnati. French Patent 1,062,041 discloses a development of the Hooker Electrochemical Co. in which mercury flows down the outside of a multiplicity of steel cathode tubes surrounded by graphite anodes. At the San Francisco Meeting Dr. Shiro Yoshizawa discussed work with the rotating mercury cathode in Japan.

Germanium rectifiers for high currents are being used on hydrogen-oxygen cells but have not yet been applied to chlor-alkali cell circuits. Their development is being watched with interest.

The graphite industry is producing new grades of graphite for mercury cell anodes with particular emphasis on vanadium content. A standard grade contains 150 ppm vanadium maximum. Premium grades contain less than 50, 20, and 2 ppm vanadium, respectively. Several operators are willing to pay the extra cost to obtain better cell efficiencies, particularly at high current densities.

Diamond Alkali is offering to license their process for recovery of waste chlorine from "sniff gas" using a carbon tetrachloride absorption-desorption system.

Markets

The end use patterns of chlorine and caustic soda have shown no material change in 1955. The big uses of chlorine are in pulp and paper, organic chemicals, and insecticides. Caustic soda goes to rayon and film, petroleum, inorganic chemicals, and soap. Pulp bleaching with chlorine dioxide is increasing and replacing some chlorine. This has contributed to an expansion of sodium chlorate production.

It has been predicted by the Business and Defense Services Administration that chlor-alkali output and sales will hold at or may top 1955 for the first half of 1956. The new capacity coming in later in 1956 assures an easier supply for next year. The international caustic market will remain tight until 1957 when new foreign plants start up.

Feature Section

"In Favor of Thinking Creatively"

*Presidential Address**

HERBERT H. UHLIG

It is a privilege to address you on the occasion of our first national convention in this distinctive City. San Francisco, held in so high esteem by its inhabitants and by its many visitors, offers charm, culture, mild temperatures, and the ever-beckoning temptation to come often and stay as long as possible. It was not many years ago that the Russians made regular visits to these shores; but they were then in quest of furs which brought fancy prices in China. Uranium was not on their list; had they found some they probably would have scaled the mineral into the sea to observe how many times it bounced before sinking out of sight. Their intrusion on the Pacific coast was then feared, as was that of any foreign nation, first by the Spaniards, who were here long before Jamestown was settled in Virginia, and later in 1822 by the Spaniards turned Mexicans when California became part of Mexico. I was interested to learn that John Augustus Sutter, at whose mill gold was first discovered in California, bought in 1841 all the property owned by the Russians at Fort Ross, just north of San Francisco, whereupon the Russians left and presumably made no further attempt to establish a foothold in California.

The Spaniards were first of the Europeans to settle this part of the New World—on the one hand as dreaded conquistadores and, on the other, in marked contrast, as God-fearing courageous missionaries. It was the missionaries who left a mark on this part of the country worth remembering, as surviving names and several beautiful buildings testify. A little over one hundred years ago, in 1848 to be exact, San Francisco flew the American flag for the first time. This took place five years before Commodore Perry sailed to Japan to establish commercial relations with that country.

San Francisco perhaps more than most other American Cities typifies the material progress of this century. From an outpost of California territory with a population of 15,000 in 1848, it has grown to a city of over 775,000 today. All this occured within the span of a few generations. The city's history enters significantly into the theme of my brief discussion, in which you will sense that I am a proponent of what is called creative thinking. For it was in San Francisco in April 1945 that the Charter of the United Nations was adopted for the purpose of achieving international cooperation in "promoting and encouraging respect for human rights and fundamental freedoms for all without distinction as to race, sex, language or religion." This Charter incorporated the most important recent creative thinking with respect to world peace. It was also in the San Francisco area that the famous school of creative ideas in electrochemistry and physical chemistry was organized by the late Professor G. N. Lewis, at the University of California in Berkeley. This school of chemistry, in addition to its reputation for turning out research, has trained many of the world's outstanding scientists. There are several other examples which I could quote of social and scientific progress linked with San Francisco's claim to fame, but I mention these two as the areas of activity I should like to cover in my present discussion.

Scientific progress over the past fifty years, as all of us know, has been phenomenal. I doubt that anyone in the year 1900 had sufficient imagination to predict the extent of the advances that have since been made. I think it is fair to say that at mid-century we now have a tremendously better understanding of our physical universe than could have been foretold even twenty-five years ago, and the advances in each decade seem to bring progress orders of magnitude ahead of the previous decade. This understanding has been accompanied by numerous practical applications undreamed of when Michael Faraday announced the principles of electrolysis, when J. J. Thompson discovered the electron, and when Heinrich Hertz found evidence of electromagnetic radiation.

Electrochemical industries in this country alone now pour out each year over one million tons of aluminum and fifty thousand tons of magnesium. They produce annually over one million tons of refined copper, three million tons of chlorine, well over three million tons of caustic soda, and over two million tons of ferroalloys. Add to this over thirty million storage cells and well over a billion dry cells, and you begin to realize that we live in an expanding industrial era, in which electrochemistry plays a significant part. All of these electrochemical products together with the products of various other industries produce, for example, plastics in all shapes and forms, synthetic fibers, stainless steels, protective and decorative paints, and modern drugs. Many of these end-products in turn appear in one form or another in aircraft, automobiles, farm machinery, ships, houses, telephones, computing machines, home appliances, vitamin pills, and television sets.

Contrast the progress here with the continuing confusion in human relations, particularly on the international front. Our ally in one war is our enemy in the next; in times of supposed peace the stage shifts still further out of focus and the Iron Curtain slams down barring further access to people and ideas over a vast area of this planet. Suspicion, greed, dishonesty, and staggering war preparation budgets smear the entire scene, with the United Nations as one of the few bright stars on a dismal background of hopes and deeds.

Why has the world accomplished so much in science and technology and so little toward improving international relations, or what I shall call world diplomacy? Is it accidental? I think not. Are scientists more intelligent than diplomats? This I doubt. Are human relations hopelessly more complex than phenomena in science and technology? This certainly may be true. Even within specific fields of science, it is recognized that phenomena in biology and medicine are subject to many more variables than are those of the physical sciences like chemistry or physics, and when one reaches into the fields of psychology and the social sciences, the variables multiply still further. But the important reason, I think, is more basic than differences in number of variables or the complexity of one subject compared with another. The one important fundamental reason for the difference in progress, I believe, is the

* Delivered at the San Francisco Meeting, May 1, 1956.

mental attitude or intellectual honesty typical of the scientist in approaching his problems, and the relative lack of a similar approach by the professional diplomat in meeting his. Furthermore, whereas thinking creatively is accepted as desirable and even necessary in the various branches of science, it is almost completely discouraged in the fields of diplomacy.

What is creative thinking? To express it simply, it is the process of searching and observing, followed by synthesis of these observations into new-found truths which can be applied to the good of mankind. My colleague, Professor John E. Arnold, defines the creative process as one that combines various aspects of past experience with the present in order to solve some problem in the future, where the totality has a value greater than the sum of its parts and where a tangible new result is communicated to others. It is accepted that creative thinking is part of the job of the pure scientist and the applied scientist or engineer. A considerable portion of their training in science is devoted to use of the so-called scientific method for uncovering new truths and applying them to useful ends. The scientist seeks to what extent he can find order in an otherwise bewildering array of phenomena. He has, therefore, inherent faith in the laws of the universe, and is certain than an experiment conducted in one laboratory can be repeated elsewhere. He has deep respect for scientific truth. Furthermore, it makes no difference where such truth originates so long as it meets the definition implied by the word.

The diplomat when presented with a statement of fact first asks: "Who said it? Is he communist or anticommunist? A Frenchman, a Swede, or a Russian? Was the statement presented in accord with our requirements of protocol?" (Heaven forbid if the diplomatic pouch arrived by the wrong person or was addressed to other than the titular head of the proper Department.)

In contrast, the scientist asks, sometimes bluntly, but always forthrightly: "Is it true?"

In science, ideas are exchanged freely without the block interposed by the dead hand of protocol. An idea is respected for its worth regardless of the age, education, or social background of its proponent. An observation is reported as it occurred—it is published as representing the truth insofar as its author is able to distinguish truth, let the chips fall where they may. There may be difference of opinion as to what was seen, or as to interpretation, but, by and large, the sincerity of the author is not on trial. A strong grip of intellectual honesty motivates every true scientist. His single purpose in life is to uncover truth, and in this he links hands with his colleagues across international, racial, and religious boundaries. He synthesizes English, German, Italian, Russian, French, and any other pertinent observations into a new drug, a new electronic amplifier, a better fuel, or a stronger metal. The truth, simply and honestly reported by his colleagues a thousand miles or more away, and whom he may never have seen, becomes the foundation for his own contribution to the cathedral of science, and the flow of ideas is truly reversible.

I need not emphasize how differently diplomats and politicians go about their business. When they say no, they mean perhaps, and when they say perhaps, they may mean yes. Their protocol is set up to stifle free exchange of ideas, and to subjugate creative thinking as contradictory to what has been done before. Their reports are often painstaking legal masterpieces, confusing at best, and at worst aimed to distort, to deceive, and to prejudice. Now, I have nothing against diplomats as a group, and I most assuredly am in favor of diplomacy in our everyday contact with one another. Furthermore, it would be a mistake to assume that the attitudes I describe represent only the point of view of a few misguided individuals in high office. Instead, diplomats are often the spokesmen and representatives of a broad cross section of humanity. Their shortcomings express the deficiencies of this modern age in refusing to accept a forthright, honest outlook on human problems, in a lack of courage to do what is obviously required by looking at the facts, and in a depressing lack of faith in what science has proved to be an orderly universe.

Nor, of course, do all scientists have breadth of vision and the required noble attitudes. Nor do all of them act as scientists once outside their own specialty. Science has had its Blondlots claiming *n*-rays, its Ehrenhafts claiming the subelectron and magnetolysis, and a host of lesser shysters claiming various shades of falsehood. Notwithstanding, the list of charlatans and quacks known to have operated in the field of science is a short one, especially if one compares it with the list of obviously questionable characters in the fields of politics and international relations. The latter list would take much longer to read than you would be willing to listen. But, in the public mind, it is curiously the scientist who on T.V. programs must be distorted into being the villain of the plot. Actually, if one considers the matter, the villain appears at the beginning and end of the show. In this connection, have you ever stopped a moment to think of the effect on the character of your children exercised by the radio and T.V. advertisers who seem to have adopted one of Adolf Hitler's tenets to the effect that if a lie is big enough and repeated often enough, people will believe it? But the problem of borderline ethics and compromise principles permeates everyday life far deeper than this single instance illustrates.

The point I make is that disappointing lack of progress in international affairs is not an accident, any more than is the tremendous progress made in science and technology. To "Prove all things, hold fast that which is good" is sage advice first given to mankind a long time ago. The benefits of following such a policy are well established in applied science as is shown by the record. Today we say that research, meaning industrial research, pays, and so it does. Research, however, is nothing more than a systematic attempt to prove what is so, cast out what is not good, and apply what is true. Research on this basis would also pay in fields other than science and technology were it given a fair trial. A strong impulse to discover what is true and a deep respect for what is found to be fact accounts for the considerable information we have about our physical world today. There is no question in my mind that a similar scientific curiosity, and a similar respect for truth applied to the more complex inter-relations of human beings would provide the kind of insight that is needed to help solve some of our present difficult problems. May I remind you that such problems exist not only on the international front, but also between labor and management, between farmer and industrialist, between producer and consumer, and between town and gown. The spirit of scientific inquiry, for example, would suggest that we diligently extract whatever truth, however limited, there may be in socialistic points of view, or even in communistic philosophy. We would also under no circumstances allow our minds to be closed to the possibility of improving our democratic viewpoint, and we would welcome its improvement by others.

I have heard objections, and probably you have also, that the scientific approach is not adaptable to the more complex fields of social studies. For one thing one cannot do an experiment to verify his theories or conclusions. This notion, I believe, is essentially false. The problems of human interac-

tion are admittedly complex, but I have faith that they are also amenable to the regularities of the universe in the same sense, with some obvious variations, as are electrons and electromagnetic waves. However, I would not have you think that I believe human beings are machines whose actions and emotions are simply the fortuitous combination of the right chemicals. This mechanistic viewpoint of life, long since fallen out of favor, is not my thought. Instead, I am pointing out the benefits of adopting in other fields the same mental attitude, intellectual honesty, and respect for truth that are commonplace in science. There should be more incentive to accurate observations, and more implicit honesty in reporting such observations, followed by creative thinking at a higher level in order to improve on what we now know or do. It is especially creative thinking that has been so thoroughly neglected in the fields of human relations. Thinking differently than the mob, or seemingly flouting tradition is not an easy assignment, nor is it easy to convince others once the thinking has been done, but progress in all branches of human activity depends on courage to take a course different from any that has been taken before.

And of course the premise that the scientific method applies only to situations where experiments can be done, is an overstatement. The science of astronomy provides a good illustration of a subject not amenable to laboratory experiments but which, nevertheless, incorporates a respectable body of systematic knowledge and creative thought.

It is creative thinking that has made science the tremendous force that it presently occupies in our daily life. Thinking of this kind began centuries ago with the seemingly unimportant observations of the classical scientists, and it continues today in our universities, research laboratories, and industries.

Creative thought is an integral component of any worthwhile field of human activity. Coming closer to home, it is, for example, essential to the growth if not survival of a society like ours. I sometimes come away from a board of directors' meeting with the sinking feeling that all new ideas are suspect, and that any suggested improvement in the operations of our Society will be accomplished only over the dead bodies of several of our best members. But, of course, this is only in part an expression of my impatience, and in part my overconfidence in the merit of some of the ideas that are proposed. The democratic process inherently consists in shuffling of ideas, their vigorous scrutiny and crossexamination, and oftentimes their final delivery into this world only after what seems like unusually difficult labor pains. As Davenport states in his book "The Dignity of Man" it is a fact that "thinkers of the free (democratic) world disagree, not because they care nothing for the truth but because they seek it. It is sometimes supposed that agreement among observers means that truth has been ascertained. This may be so, but it is not necessarily so; total agreement, as in the case of the Communist 'party line' may mean that no one is really concerned with truth at all—The idea of a Free Man is not the idea of a man in agreement with every other man: it is man searching."

Looking at the record, much creative thinking has gone into our Society's activities, accounting for the marked progress we have made especially within the past ten or more years. I have only to remind you of the present prestige of the *Journal* which is extending the Society's influence to an ever-widening audience over all the world, the successful monograph series, the outstanding symposia by our nine Divisions, and the improved operations of our national conventions.

What has been the greatest contribution of science to our modern age? Is it perhaps the airplane, the automobile, the telephone, or television? Or perhaps the transistor, atomic fission, or antibiotics? Actually, not any one of these, nor all of them collectively. These products of our modern age, as Lecomte du Nõuy pointed out in "Human Destiny", "... are consequences, not prime movers; they are effects of intellectual activity, not causes of progress." This is not to belittle the value of modern inventions and machines. Properly used they make life more comfortable, permit us to place foods on our table from all lands of the world, improve our clothing and shelter, make possible our attendance at meetings such as this one, and help us to talk with, or even see, people hundreds of miles distant. But even the most remarkable gadgetry should not be confused with the essence of real scientific advance, or identified as a worthy objective of human effort and struggle in our present civilization. Over one hundred years ago Henry David Thoreau saw fit to make the indictment: "Our inventions are wont to be pretty toys, which distract our attention from serious things. They are but an improved means to an unimproved end." I shudder to think what he would say today about the traffic jams in his beloved Concord, and about the jet planes shattering the rural peace overhead. But he was right nevertheless in suggesting the necessity of spending some time thinking of where we are going, and not merely about the degree of speed, convenience, or comfort we have attained going nowhere in particular. A right sense of values continues to be essential for the individual as well as for the community.

The real contribution of science to this age, and my opinion is not original, is in changing the thinking of modern man. It is science that has freed us from superstition, from false concepts, and from the chaos of a seemingly disorderly environment. It has provided us instead with a profound faith in the laws of the universe, an optimism regarding the future, and a deep respect for the good that can come from knowing and applying truth. It has provided strong proof of the prosperity that can come from international sympathy, understanding, and creative thought among a group of scientists jointly devoted to a better understanding of the physical world. When similar cooperation is achieved by men of good will in other fields as well, I predict we shall experience prosperity far transcending what has so far been demonstrated to be possible in science and technology.

Photo shows a battery of Hooker type S-3A cells as used by licensees of Hooker Electrochemical Company.

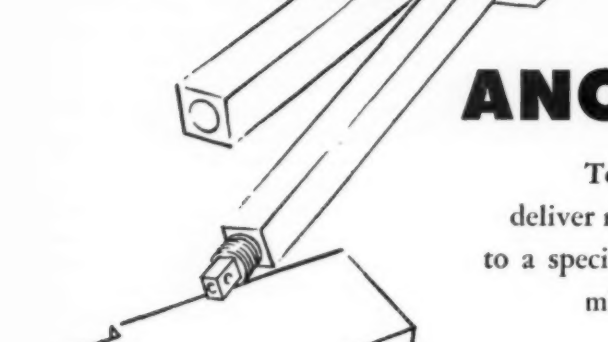

THIS *is* ANODE PROGRESS

Today's graphite anodes last longer — deliver more for the money . . . thanks to a special Stackpole treatment that minimizes deterioration, assures the economy of low-voltage operation.

Write for Catalog 40A . . . or send details of your carbon-graphite requirements for recommendation by Stackpole carbon-graphite specialists.

STACKPOLE CARBON COMPANY
St. Marys, Pa.

OTHER STACKPOLE PRODUCTS:

Brushes for all rotating electrical equipment (earth surface or high altitude) • Electrical Contacts • Graphite Nozzles • Carbon Bearings • Seal Rings • Friction Segments • Power Tube Anodes • Molds and Dies • Carbon Voltage Regulator Discs • Dash Pot Plungers • Ground Rods • Carbon Rods for Salt Bath Rectification . . . and many more.

Cleveland Program

THE ELECTROCHEMICAL SOCIETY

One Hundred and Tenth Meeting

—o—

Sunday through Thursday

September 30, October 1, 2, 3, and 4, 1956

CONDENSED TECHNICAL PROGRAM

Battery (Abstracts 1–20)

(All sessions in Pine Room)

Monday morning, Oct. 1—9:30 A.M.–12.00 M.

Monday afternoon, Oct. 1—3:00 P.M.–5:00 P.M.

Tuesday morning, Oct. 2—9:00 A.M.–12:00 M.

Tuesday afternoon, Oct. 2—2:00 P.M.–4:30 P.M.

Battery-Theoretical Electrochemistry (Abstracts 21–30)

(Both sessions in Pine Room)

Wednesday morning Oct. 3—9:00 A.M.–11:30 A.M.

Wednesday afternoon, Oct. 3—2:00 P.M.–4:30 P.M.

Corrosion (Abstracts 31–61)

(All sessions in Ohio Room)

Tuesday morning, Oct. 2—9:00 A.M.–11:45 A.M.

Tuesday afternoon, Oct. 2—2:00 P.M.–5:15 P.M.

Wednesday morning, Oct. 3—9:00 A.M.–11:45 A.M.

Wednesday afternoon, Oct. 3—2:00 P.M.–5:00 P.M.

Thursday morning, Oct. 4—9:00 A.M.–11:45 A.M.

Thursday afternoon, Oct. 4—2:00 P.M.–4:45 P.M.

Electrodeposition (Abstracts 62–66)

(Session in Ohio Room)

Monday morning, Oct. 1—9:30 A.M.–12:00 M.

Electrodeposition—Theoretical Electrochemistry (Abstracts 67–80)

(All sessions in Euclid Ball Room)

Monday afternoon, Oct. 1—2:00 P.M.–5:00 P.M.

Tuesday morning, Oct. 2—9:00 A.M.–12:15 P.M.

Tuesday afternoon, Oct. 2—2:00 P.M.—3:30 P.M.

Electronics—Semiconductors (No abstracts)

(All sessions in Euclid Ball Room)

Wednesday morning, Oct. 3—9:00 A.M.–12:00 M.

Wednesday afternoon, Oct. 3—2:00 P.M.–5:00 P.M.

Thursday morning, Oct. 4—9:00 A.M.–12:00 M.

Thursday afternoon, Oct. 4—2:00 P.M.–5:00 P.M.

Electrothermics and Metallurgy (Abstracts 81–103)

(All sessions in Parlors 1, 2, and 3)

Tuesday morning, Oct. 2—9:00 A.M.–11:00 A.M.

Tuesday afternoon, Oct. 2—2:00 P.M.–4:30 P.M.

Wednesday morning, Oct. 3—9:00 A.M.–11:30 A.M.

Wednesday afternoon, Oct. 3—2:00 P.M.–4:00 P.M.

Theoretical Electrochemistry (Abstracts 104–107)

(Session in Euclid Room)

Tuesday afternoon, Oct. 2—3:40 P.M.–5:20 P.M.

GENERAL INFORMATION

Convention Headquarters will be at the Hotel Statler, Euclid Ave. at East 12th St., Cleveland 1, Ohio.

Rates per day for rooms (with bath) will be: single-room $6.00, 6.50, 7.00, 7.50, 8.00, 8.50, 9.00, 10.50, 11.00, 13.00; double-bed room $9.50, 10.00, 10.50, 11.50, 12.00, 13.50, 14.00, 16.00; twin-bed room $11.00, 11.50, 12.00, 13.00, 13.50, 14.50, 15.00, 15.50, 16.50, 17.50, 20.00, 22.00, 24.00; suite $24.00, 30.00, 32.00.

Requests for room reservations at the Headquarters Hotel should be made to the Front Office Manager, Hotel Statler, Euclid Ave. at East 12th St., Cleveland 1, Ohio. Mention should be made of The Electrochemical Society.

The office of the Secretary will be in Parlor L on the Club Floor.

All technical sessions will be held on the Ball Room Floor.

Ladies' Headquarters will be in Parlor C, Club Floor. For details, see program under Ladies' Program.

REGISTRATION

The registration desk will be in the Grand Ball Room Mezzanine, Ball Room Floor. On Sunday, September 30, the registration desk will be open from 5:00 P.M. to 8:00 P.M. On Monday, Tuesday, and Wednesday, October 1, 2, and 3, it will be open from 8:00 A.M. to 5:00 P.M.; on Thursday, October 4, from 9:00 A.M. to 12:00 M.

Registration fees are:

Members	$7.00
Ladies	$5.00
Nonmembers	$13.00
Students	Complimentary by prior arrangement

INFORMATION ABOUT CLEVELAND

Members and visitors attending the Fall Meeting of The Electrochemical Society in Cleveland will have an opportunity to observe the burgeoning of one of America's great industrial centers. Already renowned for its key role in the fields of transportation, communication, research, industry, and manufacturing, the planned opening of the St. Lawrence Seaway is sparking another burst of industrial and civic expansion that makes Cleveland an exciting city for strangers to visit and for old friends to renew acquaintance with.

Those arriving by air will be welcomed by the sight of Cleveland's new air terminal, dedicated this year, which is one of the nation's most modern and convenient with every facility for the traveler. The new Ohio Turnpike, new express highways, and motels will facilitate the arrival of those driving to the convention. On all sides, visitors will see new factories, chemical plants, and research centers.

Electrochemists will have a chance to visit the brand new National Carbon Co. Research Labs. in Parma, Ohio, on the outskirts of Cleveland, and the famous Nela Park Lighting Institute of the General Electric Co. For those in a more academic frame of mind, visits to Western Reserve University and Case Institute of Technology are planned. These trips are scheduled so that there will be no conflict with the technical sessions or other Society functions.

Many attending the meeting will notice the activity for enlarging Cleveland's Port facilities, the arrangements for the Pan-American Games to be held here in 1959, the Urban Redevelopment program where blighted areas are being completely rebuilt, the new Cleveland Engineering Center being built, and many new and enlarged utility services to match the industrial and residential growth of the area.

Of particular interest will be the Acheson Memorial Exhibit which will be displayed at the Main Cleveland Public Library, just a few blocks from the Convention Headquarters. This display of historic material has been selected to illustrate the most significant inventions and works of Dr. Edward Goodrich Acheson on the occasion of the 100th Anniversary of Dr. Acheson's birth.

SPECIAL SYMPOSIA

The Battery Division has scheduled several general symposia, as well as one on the Life of Automotive Batteries, and another on Electrode Polarization.

The Corrosion Division has scheduled symposia on High Temperature Oxidation, Factors Related to Corrosion, Corrosion Kinetics, and the Electrochemistry of Corrosion.

The Electrodeposition and Theoretical Electrochemistry Divisions have both scheduled a general symposia, and jointly are sponsoring symposia on Structure of Metallic Deposits, Kinetics of Electrodeposition, and Diffusion and Convection in Electrodeposition.

The Electronics Division—Semiconductor Group has arranged short "late news" type papers for its four sessions.

The Electrothermics and Metallurgy Division has scheduled two sessions on Acheson Furnaces, Processes, Products, and Related Developments, as well as two on New Chemical Developments in the Extractive Metallurgy of Titanium.

BREAKFASTS, LUNCHEONS, AND DINNERS

Symposia Chairmen Breakfasts

On Monday, Tuesday, Wednesday, and Thursday, October 1, 2, 3, and 4, special breakfasts for all symposia chairmen are being arranged. Information on where breakfasts will be held will be available in the Secretary's office, Parlor L, Club Floor.

Monday, symposia chairmen for Battery and Electrodeposition are requested to attend; **Tuesday,** Battery, Corrosion, Joint Electrodeposition—Theoretical Electrochemistry, Electrothermics and Metallurgy, and Theoretical Electrochemistry; **Wednesday,** Battery, Corrosion, Electronics—Semiconductors, and Electrothermics and Metallurgy; **Thursday,** Corrosion and Electronics—Semiconductors.

Monday Dinner and Open House at National Carbon Research Lab.

On Monday evening, October 1, a buffet dinner will be served at National Carbon's new research laboratories, following which there will be an inspection trip of the laboratories. Ladies, ECS members, and guests are invited. Buses will leave the Hotel Statler at 6:30 P.M. for the laboratory. (Attendance will be limited.)

Tuesday Acheson Medal Banquet

On Tuesday, October 2, a reception and banquet will be held for the Acheson Medalist, Dr. Robert M. Burns. Cocktails will be served from 6:30 to 7:30 P.M. in Private Dining Rooms 1, 2, and 3; dinner at 7:30 in the Grand Ball Room. Dr. Burns will deliver the Acheson Medal Address.

Wednesday Open House

On Wednesday, October 3, at 5:45 P.M., buses will leave the Hotel Statler for Western Reserve University and Case Institute of Technology, both of which are holding open house and are located on adjoining campuses. Members, ladies, and guests may have dinner at Tomlinson Hall, Case Institute of Technology, and after dinner may visit either or both schools.

PLANT TRIPS

Four plant or inspection trips have been planned for the Cleveland Meeting. Participation in these trips must be arranged for at the time of registration at the meeting. Transportation by bus will be arranged.

Monday, October 1, 6:30 P.M.—Dinner and an inspection trip of National Carbon's new research laboratories, located about eight miles from downtown Cleveland, in Parma, Ohio, have been arranged. Transportation from the Hotel Statler to the laboratories will be available by chartered bus leaving at 6:30 P.M. Following dinner served at the laboratories, a tour of this very modern and unusual building is planned. Research facilities available for use in the field of physics, chemistry, and electrochemistry will be open for inspection. Members, guests, and ladies planning to attend are advised to purchase tickets for this trip at the time of registration. The cost per person is $4.00 for dinner and round-trip transportation. (Attendance will be limited.)

Wednesday, October 3, 5:45 P.M.—An open house will be sponsored jointly by the Departments of Chemistry at Western Reserve University and Case Institute of Technology which are located adjacent to each other in the cultural heart of Cleveland. Buses will leave the Hotel Statler for the campuses at 5:45 P.M. Dinner will be served for all attending the open house in the Ball Room of the new Case Student Union (Tomlinson Hall). Following the dinner will be a guided tour in small groups. The Case part of the tour will feature the new Chemistry Building just being completed. On the Western Reserve campus, the tour will include the Electrochemistry, Ultrasonics, Cryogenics, and Emission, Absorption, and Mass Spectroscopy Laboratories. Personnel of the Ultrasonics Research Laboratory at Western Reserve University will present a series of demonstrations of the more spectacular effects of ultrasonic waves. Return bus transportation to the Hotel Statler will also be provided. Registrants at the meeting are urged to obtain bus and dinner tickets for the Case-Western Reserve trip early in the week since the number of people who can be accommodated is limited.

Wednesday, October 3, 7:00 P.M.—Buses will leave the Hotel Statler for General Electric's Nela Park Lighting Institute. Members, ladies, and guests are invited to attend. (Nela Park attendance will be limited.) No dinner arrangements are included for this trip. The General Electric Lighting Institute, located at the Lamp Division headquarters in Nela Park, Cleveland, is a contemporary, dynamic, and commercial training facility, the primary purpose of which is education. Its displays and facilities are for training all segments of the lighting industry and its customers in the techniques and values of good lighting practice. The Institute is a part of the marketing organization of the Lamp Division and is staffed by 35 people.

LADIES' PROGRAM

Ladies' Headquarters will be in Parlor C, Club Floor, of the Hotel Statler. All ladies are invited to this Headquarters to obtain information on the program plans and general points of interest in and around Cleveland. A member of the Women's Committee will be in the Ladies' Headquarters on Sunday from 3:00 to 9:00 P.M. to welcome and assist the ladies in every way. The program has been planned to acquaint visitors with many of the interesting and better-known places in the Cleveland area.

Cleveland weather is very unpredictable at this time of the year, so it is rather difficult to advise on what type of clothing to bring. The Cleveland Weather Bureau, however, reports that the maximum afternoon temperature is about 70 degrees and the evening low about 50 degrees.

Monday morning—A get-acquainted period with coffee and rolls will be held in the Ladies' Headquarters, starting at 9:30 A.M.

Monday noon—A luncheon will be held at 12:30 P.M. at Monaco's, for many years a well-known restaurant in downtown Cleveland. Following the luncheon there will be an interesting talk by Florence LeGanke, Food Editor of the Cleveland Press. The remainder of the afternoon will be open for shopping or individual sight seeing.

Monday evening—The ladies are invited to accompany their husbands on the trip to the new National Carbon Research Labs. for a buffet dinner and tour of the bulding.

Tuesday morning and afternoon—Coffee will be served in the Ladies' Headquarters at 9:30 A.M. At 10:45 A.M., meet at the side entrance of the hotel to board a bus to drive along the eastern shore of Lake Erie past the cultural gardens and through some of the loveliest residential sections of the area. Luncheon will be served at Shaker Heights' exclusive Zephyr Room, followed by a drive through the heart of Cleveland's cultural center, and culminated by a visit to the Art Museum. Here, an expert will speak on the subject "Your Home, Traditional or Modern." Return to the hotel will be about 4:30 P.M.

Tuesday evening—The ladies are invited to attend the Acheson Reception and Dinner.

Wednesday morning and afternoon—Coffee will be served in the Ladies' Headquarters at 9:00 A.M. At 10 o'clock, meet at the side entrance of the hotel to journey along the western shore of Lake Erie, through the wooded valley of the Metropolitan Parks, to lunch at the Inn at Oberlin, Ohio. Oberlin is the home of Oberlin College, the first coeducational college in the United States. The return trip will be through the autumn-colored countryside to downtown Cleveland, arriving at the hotel about 3:30 P.M.

Wednesday evening—The ladies are invited to accompany their husbands on either the trip to Case Institute of Technology, Western Reserve University, or General Electric's Nela Park.

Thursday morning—Coffee will be served at 9:00 A.M. in the Ladies' Headquarters. Transportation will be furnished for a sight-seeing boat trip on Lake Erie and through the Cuyahoga River industrial area. The cost of this trip is $1.75 per person. The boat leaves from the dock at 10:00 A.M. and returns by noon.

LUNCHEONS AND BUSINESS MEETINGS OF DIVISIONS

Battery Division will hold a luncheon and business meeting on Tuesday, October 2, at 12:30 P.M. in the Grand Ball Room. C. E. Larson, Vice-President in Charge of Research, National Carbon Co., will speak on "Energy for the Future."

Corrosion Division will hold a luncheon and business meeting on Wednesday, October 3, at 12:30 P.M. in Room 345, 3rd floor.

Electrodeposition Division will hold a luncheon and business meeting on Tuesday, October 2, at 12:30 P.M. in Room 345, 3rd floor.

Electronics Division—Semiconductor Group will hold a luncheon on Thursday, October 4, at 12:30 P.M. in the Pine Room.

BOARD AND COMMITTEE MEETINGS

Sunday, September 30, 10:00 A.M.—Meeting of the Ways and Means Committee in the Tavern Room, Club Floor.

Sunday, September 30, 11:45 A.M.—Meeting of the Finance Committee. Be in Parlor L, the Secretary's office, at 11:45 A.M.

Sunday, September 30, 2:00 P.M.—Meeting of the Board of Directors in the Tavern Room, Club Floor.

Monday, October 1, 5:00 P.M.—Meeting of the Editorial Staff in Parlor B, Club Floor.

Tuesday, October 2, 5:00 P.M.—Meeting of the Membership Committee in Parlor B, Club Floor.

Wednesday, October 3, 5:00 P.M.—

Meeting of the Council of Local Sections in Parlor E, Club Floor.

COST OF VARIOUS FUNCTIONS

(other than registration)

Symposia Chairmen Breakfast	$2.00
Division Luncheons	$3.75
Acheson Medal Banquet (single)	$6.00
(couple)	$11.00
Trips to National Carbon Research Labs., Western Reserve University, Case Institute of Technology, transportation and dinner	$4.00
Trip to Nela Park Lighting Institute, transportation	$1.00

(Gratuities and taxes included in above prices)

JOURNALS

Copies of the June, July, August, and September issues of the Journal of The Electrochemical Society will be available at the registration desk. The price of a single copy of the JOURNAL is $1.25 to members and $1.75 to nonmembers.

EXTENDED ABSTRACTS

The Battery Division is making available an extended abstract booklet containing 1000-word abstracts of most of the papers presented at the Division's Cleveland symposia. Copies of the booklet will be on sale for $2.00 at the registration desk.

DISCUSSION

There will be no recordings made of oral discussions. Those contributing to the discussion of a paper and desiring their remarks published will be supplied by the symposium chairman with a printed form on which any discussion may be written. These forms should be given to the Secretary-Treasurer of the Division or to the Managing Editor of the JOURNAL after the session. The discussion will then be referred to the authors for reply. Written discussion should be submitted within two months following publication of any article in the JOURNAL.

A Discussion Section is published semiannually in the JOURNAL.

SLIDES AT TECHNICAL SESSIONS

The Board of Directors of the Society does not favor indiscriminate photographing of slides during technical sessions. It is requested that no such photographs be taken. Chairmen of technical sessions should administer this rule.

EMPLOYMENT POSTERS

Companies which desire to recruit employees at the Cleveland Meeting will have posters to this effect on a bulletin board near the registration desk.

Technical Program

Monday, October 1, 1956

9:00 A.M.—Formal Opening of the 110th Convention with Introduction by General Chairman W. H. Stoll and Response by President Hans Thurnauer (Pine Room).

NOTE

Address of author(s) is included with the abstract. In the Index to Authors, the abstract number is used instead of the page number.

BATTERY

Monday, October 1, 1956
with J. C. White presiding
(PINE ROOM)

9:30 A.M.—"The Silver Oxide-Cadmium Alkaline Secondary Battery" by P. L. Howard (Abstract No. 1)

10:00 A.M.—"A Reproducible and Stable Silver-Silver Oxide Electrode" by W. J. Hamer and D. N. Craig (Abstract No. 2)

10:30 A.M.—"Aqueous Potassium Hydroxide as Battery Electrolyte" by T. P. Dirkse (Abstract No. 3)

11:00 A.M.—"Solid Silver Halide Battery Systems" by W. J. van der Grinten (Abstract No. 4)

11:30 A.M.—"The Fused Salt Cell, $Mg/LiNO_3$, KCL/Ag" by C. W. Jennings (Abstract No. 5)

Battery (cont'd)

Monday, October 1, 1956
with E. J. Ritchie presiding
(PINE ROOM)

3:00 P.M.—"*N*-Halogen Organic Compounds as Cathode Materials for Primary Batteries" by C. K. Morehouse and R. Glicksman (Abstract No. 6)

3:30 P.M.—"An Investigation of the Discharge Characteristics of Groups Ib-Vb Oxides in an Alkaline Electrolyte" by R. Glicksman and C. K. Morehouse (Abstract No. 7)

4:00 P.M.—"Some Electrical Properties of Electrode Film Materials, I. Lead Sulfate" by I. H. S. Henderson (Abstract No. 8)

4:30 P.M.—"Supercooling, Preferred Orientation, and Inverse Segregration in Lead-Antimony Alloys" by A. C. Simon and E. L. Jones (Abstract No. 9)

Battery (cont'd)

Tuesday, October 2, 1956

Life of Automotive Batteries
with Eugene Willihnganz presiding
(PINE ROOM)

9:00 A.M.—"Appearance of Battery Components at the End of Life under Laboratory Test" by B. Agruss (Abstract No. 10)

9:25 A.M.—"Correlation of Laboratory Life Tests with Automotive Service Tests of Lead Acid Batteries" by J. F. Schaeffer (Abstract No. 11)

9:50 A.M.—"Effect of Arsenic and Silver in Grid Alloy on Storage Battery Life in Field Tests and Fleet Service" by Howard Stoertz (Abstract No. 12)

10:15 A.M.—"Effect of Normal Car Service on Intermediate and Final Periods of Lead Storage Battery Performance" by Dudley Haskell (Abstract No. 13)

10:40 A.M.—"Effect of Temperature on Cycling Life of Lead Acid Storage Batteries" by J. F. Macholl and A. G. Koch (Abstract No. 14)

11:05 A.M.—"Pulse Maintaining of Automotive Batteries" by J. B. Godshalk (Abstract No. 15)

11:30 A.M.—Open Discussion on Life of Automotive Batteries.

12:30 P.M.—Battery Division Luncheon and Business Meeting in the Grand Ball Room. C. E. Larson, Vice-President in Charge of Research, National Carbon Co., will speak on "Energy for the Future."

Battery (cont'd)

Tuesday, October 2, 1956
with N. C. Cahoon presiding
PINE ROOM

2:00 P.M.—"Positive Post Corrosion in Lead Acid Cells" by O. H. Bauer (Abstract No. 16)

2:30 P.M.—"Self-Discharge Reactions in Lead Acid Batteries" by P. Ruetschi and R. T. Angstadt (Abstract No. 17)

3:00 P.M.—"Self-Discharge of Positively Charged Nickel Oxide Electrodes of Alkaline Storage Batteries" by A. L. Pitman and G. W. Work (Abstract No. 18)

3:30 P.M.—"A Self-Discharge Reaction of Cells with Manganese Dioxide and Metal Electrodes" by W. C. Vosburgh, D. R. Allenson, and Stanley Hills (Abstract No. 19)

4:00 P.M.—"Instrumentation for Use

MEETING ROOM SCHEDULE

Meeting	Monday		Tuesday		Wednesday		Thursday	
	A.M.	P.M.	A.M.	P.M.	A.M.	P.M.	A.M.	P.M.
Battery	P	P	P	P	P	P		
Corrosion			O	O	O	O	O	O
Electrodeposition	E							
Electrodeposition—Theoretical		E	E	E				
Electrochemistry								
Electronics—Semiconductors					E	E	E	E
Electrothermics and Metallurgy			B	B	B	B		
Theoretical Electrochemistry				E				

P = Pine Room.
O = Ohio Room.
E = Euclid Room.
B = Private Dining Rooms 1, 2, and 3.

in Storage Battery Studies" G. W. Work and C. P. Wales (Abstract No. 20)

BATTERY—THEORETICAL ELECTROCHEMISTRY

Joint Symposium

Wednesday, October 3, 1956

Electrode Polarization with U. B. Thomas presiding

(PINE ROOM)

9:00 A.M.—"Corrosion and Polarization" by Norman Hackerman (Abstract No. 21)

9:30 A.M.—"Cathodic Polarization in the Leclanché Cell" by N. C. Cahoon (Abstract No. 22)

10:00 A.M.—"Metal Electrode Polarization" by L. O. Case (Abstract No. 23)

10:30 A.M.—"Polarization Studies of the Lead Electrode" by Eugene Willihnganz (Abstract No. 24)

11:00 A.M.—"Anodic Corrosion and Hydrogen and Oxygen Overvoltage on Lead and Lead-Antimony Alloys" by P. Ruetschi and B. D. Cahan (Abstract No. 25)

Battery—Theoretical Electrochemistry

Joint Symposium (cont'd)

Wednesday, October 3, 1956

Electrode Polarization (cont'd) **with C. W. Tobias presiding**

(PINE ROOM)

2:00 P.M.—"Activation Polarization in Battery Systems" by Ernest Yeager (Abstract No. 26)

2:30 P.M.—"Polarization Measurements on High Current Gas Electrodes and Their Conformity with Chemical Test Methods" by K. Kordesch (Abstract No. 27)

3:00 P.M.—"Polarization Characteristics of the Oxygen-Peroxide Couple on Active Carbon Electrodes" by Milton Clark, M. O. Davies, Ernest Yeager, and Frank Hovorka (Abstract No. 28)

3:30 P.M.—"The Overpotential of the Manganese Dioxide Electrode, II. Acid Electrolytes" by S. Yoshizawa and W. C. Vosburgh (Abstract No. 29)

4:00 P.M.—"Role of Ionic Diffusion and Mass Transfer in Kinetics of Electrode Reactions in Batteries" by Morris Eisenberg (Abstract No. 30)

CORROSION

Tuesday, October 2, 1956

High Temperature Oxidation with J. E. Draley presiding

(OHIO ROOM)

9:00 A.M.—"Oxidation of 50 Weight Per Cent Uranium-Zirconium Alloy" by Sidney Barnartt, R. G. Charles, and E. A. Gulbransen (Abstract No. 31)

9:30 A.M.—"Kinetics of the Oxidation of Chromium" by E. A. Gulbransen and K. F. Andrew (Abstract No. 32)

10:00 A.M.—"High Temperature Scaling of Cobalt-Chromium Alloys" by C. A. Phalnikar, E. B. Evans, and W. M. Baldwin, Jr. (Abstract No. 33)

10:45 A.M.—"High Temperature Scaling of Nickel-Manganese Alloys" by E. B. Evans, C. A. Phalnikar, and W. M. Baldwin, Jr. (Abstract No. 34)

11:15 A.M.—"Oxidation of Iron-Nickel Alloys, III. Kinetics and Mechanism" by R. T. Foley and C. J. Guare (Abstract No. 35)

Corrosion (cont'd)

Tuesday, October 2, 1956

Factors Related to Corrosion with M. A. Streicher presiding

(OHIO ROOM)

2:00 P.M.—"Hydrogen Diffusion through Steel" by T. J. Butler and R. T. Davis, Jr. (Abstract No. 36)

2:30 P.M.—"Low-Pressure Solubility and Diffusion of Hydrogen in Zirconium" by M. W. Mallett and W. M. Albrecht (Abstract No. 37)

3:00 P.M.—"Corrosion Characteristics of Uranium. An Electron Diffraction Study" by J. T. Waber and D. D. Whyte (Abstract No. 38)

3:45 P.M.—"Orientation Factors in Oxide Films on Uranium" by J. T. Waber (Abstract No. 39)

4:15 P.M.—"Variations of Alkaline Anodizing Baths for Magnesium" by W. McNeill and R. Wick (Abstract No. 40)

4:45 P.M.—"Potential-*p*H Diagram of the Antimony-Water System; Its Applications to Properties of the Metal, Its Corrosion, and Antimony Electrodes" by A. L. Pitman, Marcel Pourbaix, and N. de Zoubov (Abstract No. 40-A)

Corrosion (cont'd)

Wednesday, October 3, 1956

Corrosion Kinetics with A. H. Roebuck presiding

(OHIO ROOM)

9:00 A.M.—"Effect of Prior Corrosion History on the Corrosion of Zircaloy-2 in High Temperature Water by D. E. Thomas and S. Kass (Abstract No. 41)

9:30 A.M.—"A Reaction Rate Study of the Corrosion of Low-Hafnium Zirconium in Hydrofluoric Acid Solutions" by Tennyson Smith and G. R. Hill (Abstract No. 42)

10:00 A.M.—"Hydrogen Evolution from dissolving Titanium-Oxygen Alloys in Hydrofluoric Acid and the Constitution of the Ti-O Alloys" by M. E. Straumanis, C. H. Cheng, and A. W. Schlechten (Abstract No. 43)

10:45 A.M.—"Dissolution of Iron in Hydrochloric Acid-Chromic Chloride Solutions" by Robert Skomoroski and C. V. King (Abstract No. 44)

11:15 A.M.—"Kinetics of the Reaction of Steel with Hydrogen Sulfide-Hydrogen Mixtures" by A. Dravnieks and C. H. Samans (Abstract No. 45)

12:30 P.M.—Corrosion Division Luncheon and Business Meeting in Room 345, 3rd floor.

Corrosion

Wednesday, October 3, 1956

Corrosion Kinetics (cont'd) **with A. H. Roebuck presiding**

(OHIO ROOM)

2:00 P.M.—"Kinetic Studies on Alkaline Nitrite Formation of Black Oxide Coatings on Mild Steel" by R. M. Hurd and Norman Hackerman (Abstract No. 46)

2:30 P.M.—"Corrosion of Austenitic Stainless Steel in Circulating Uranyl Sulfate Solutions at High Temperatures, I. Experimental Results" by E. G. Bohlmann, J. C. Griess, Jr., and R. S. Greeley (Abstract No. 47)

3:00 P.M.—"Corrosion of Austenitic Stainless Steel in Circulating Uranyl Sulfate Solutions at High Temperatures, II. Mechanism of the Corrosion Process" by J. C. Griess, Jr., and E. G. Bohlmann (Abstract No. 48)

3:35 P.M.—"Corrosion of Austenitic Stainless Steel in Dilute Acid Solutions at High Temperature" by J. C. Griess, Jr., R. S. Greeley, E. G. Bohlmann, and S. R. Buxton (Abstract No. 49)

4:05 P.M.—"An Investigation of the Effect of Chemical Variables on the Corrosion of Copper" by W. D. Robertson, V. F. Nole, W. H. Davenport, and F. P. Talboom, Jr. (Abstract No. 50)

4:35 P.M.—"Corrosion of Single Crystals and Recrystallized Single Crystals of Iron and Steel in Citric Acid" by W. R. Buck, III, and Henry Leidheiser, Jr. (Abstract No. 51)

Corrosion (cont'd)

Thursday, October 4, 1956

Electrochemistry of Corrosion with Milton Stern presiding

(OHIO ROOM)

9:00 A.M.—"Anodic Behavior of Cu in HCl" by R. S. Cooper (Abstract No. 52)

9:30 A.M.—"Stress Potentials for Tension and Torsion Stresses" by W. F. Seyer, O. K. Miniato, and K. Nobe (Abstract No. 53)

10:00 A.M.—"Chemical and Electrochemical Properties of $FeSn_2$" by R. A. Covert and H. H. Uhlig (Abstract No. 54)

10:45 A.M.—"Electrochemical Polarization, I. A Theoretical Analysis of the Shape of Polarization Curves" by Milton Stern and A. L. Geary (Abstract No. 55)

11:15 A.M.—"Oxygen Concentration Cell as a Factor in the Localized Corrosion of Metals" by Wilson Lynes (Abstract No. 56)

Corrosion

Thursday, October 4, 1956

Electrochemistry of Corrosion (cont'd) **with Milton Stern presiding**

2:00 P.M.—"The Mechanisms of Aqueous Corrosion of Aluminum at 100°C" by K. M. Carlsen (Abstract No. 57)

2:30 P.M.—"Contribution to the Theory of Stress Corrosion in

Duralumin Alloys" by W. H. Colner and H. T. Francis (Abstract No. 58)

3:00 P.M.—"Galvanic Corrosion of the Aluminum-Lead Couple in Aqueous Pigment Extracts" by M. J. Pryor, R. J. Hogan, and F. B. Patten (Abstract No. 59)

3:45 P.M.—"Thermogalvanic Potentials and Currents at Aluminum Surfaces in Industrial Water" by E. C. Pitzer (Abstract No. 60)

4:15 P.M.—"Current Efficiency of Magnesium Anodes" by E. H. Phelps (Abstract No. 61)

ELECTRODEPOSITION

Monday, October 1, 1956

General Symposium on Electrodeposition with C. A. Snavely presiding

(OHIO ROOM)

9:30 A.M.—"Electroplating of Aluminum, I. Deposition from Strongly Acid Solutions" by J. T. N. Atkinson (Abstract No. 62)

10:00 A.M.—"Electroplating on Aluminum, II. Deposition of Copper from Oxalate-Pyrophosphate Solutions" by J. T. N. Atkinson (Abstract No. 63)

10:30 A.M.—"Electroplating Baths for Ultrahigh Strength Steel, I. Use of Aliphatic Amino Acids in Cadmium Baths to Reduce Hydrogen Embrittlement" by P. N. Vlannes, S. W. Strauss, and B. F. Brown (Abstract No. 64)

11:00 A.M.—"Electrodeposition of Uranium at the Microgram Level" by C. L. Rulfs, A. K. De, and P. J. Elving (Abstract No. 65)

11:30 A.M.—"Inclusion of Fuchsin in Bright Nickel Deposits" by J. L. Dye and O. J. Klingenmaier (Abstract No. 66)

(Electrodeposition and Theoretical Electrochemistry Division members may be interested in papers on hydrogen in metals and surface treatment of magnesium scheduled for the Corrosion Division session on Tuesday afternoon)

ELECTRODEPOSITION—THEORETICAL ELECTROCHEMISTRY

Joint Symposium

Monday, October 1, 1956

Structure of Metallic Electrodeposits with W. R. Meyer presiding

(EUCLID BALL ROOM)

2:00 P.M.—"Structure of Metallic Electrodeposits" (Keynote Address) by Hellmuth Fischer (Abstract No. 67)

3:00 P.M.—"On the Theory of Electrolytic Crystal Growth" by D. A. Vermilyea (Abstract No. 68)

3:30 P.M.—"Structure of Electrodeposits from Fused Alkalinous Chloride Electrolytes" by R. S. Dean, W. W. Gullett, and F. X. McCawley (Abstract No. 69)

4:00 P.M.—"Comments on Electrodeposition Research on Single-Crystal Substrates" by H. Bandes (Abstract No. 70)

4:30 P.M.—"Studies of the Natural Convection at Vertical Electrodes" by N. Ibl (Abstract No. 71)

Electrodeposition—Theoretical Electrochemistry

Joint Symposium (cont'd)

Tuesday, October 2, 1956

Kinetics of Electrodeposition with Ernest Yeager presiding

(EUCLID BALL ROOM)

9:00 A.M.—"Kinetics of the Deposition of Metals" (Keynote Address) by J. O'M. Bockris (Abstract No. 72)

9:45 A.M.—"High-Speed Polarization Measurements during Electrodeposition" by H. J. Read and C. O. McHugh (Abstract No. 73)

10:15 A.M.—"Electrochemical Calorimetry" by Abner Brenner and J. M. Sherfey (Abstract No. 74)

10:45 A.M.—"Electrodeposition of Nickel from Mixed Solvent Systems" by Robert Griffis, Ernest Yeager, and Frank Hovorka (Abstract No. 75)

11:15 A.M.—"A Study of Cathode Potentials in Aqueous Tungstate Solutions" by D. R. Markwell and M. L. Holt (Abstract No. 76)

11:45 A.M.—"Design of a New Electrolytic Cell for the Study of Electroplating Phenomena" by Roger Gilmont and R. F. Walton (Abstract No. 77)

12:30 P.M.—Electrodeposition Division Luncheon and Business Meeting in Room 345, 3rd floor.

Electrodeposition—Theoretical Electrochemistry

Joint Symposium (cont'd)

Tuesday, October 2, 1956

Diffusion and Convection in Electrodeposition with Sidney Barnartt presiding

(EUCLID BALL ROOM)

2:00 P.M.—"Diffusion and Convection Effects in Electrodeposition" (Keynote Address) by C. W. Tobias (Abstract No. 78)

2:40 P.M.—"Limiting Currents at Horizontal Electrodes in Free Convection" by E. J. Fenech and C. W. Tobias (Abstract No. 79)

3:05 P.M.—"Throwing Index; A New Graphical Method for Expressing the Results of Throwing-Power Measurements" by H. F. David and R. V. Jelinek (Abstract No. 80)

ELECTRONICS—SEMICONDUCTORS

Wednesday, October 3, 1956

(EUCLID BALL ROOM)

9:00 A.M.—Papers of the "late news" type. Program and abstracts will be available at the session.

Electronics—Semiconductors (cont'd)

Wednesday, October 3, 1956

(EUCLID BALL ROOM)

2:00 P.M.—Papers of the "late news" type. Program and abstracts will be available at the session.

Electronics—Semiconductors (cont'd)

Thursday, October 4, 1956

(EUCLID BALL ROOM)

9:00 A.M.—Papers of the "late news" type. Program and abstracts will be available at the session.

12:30 P.M.—Electronics Division—Semiconductor Group Luncheon in the Grand Ball Room.

Electronics—Semiconductors (cont'd)

Thursday, October 4, 1956

(EUCLID BALL ROOM)

2:00 P.M.—Papers of the "late news" type. Program and abstracts will be available at the session.

ELECTROTHERMICS AND METALLURGY

Tuesday, October 2, 1956

Acheson Furnaces, Processes, Products, and Related Developments with J. A. Shaw presiding

(PARLORS 1, 2, AND 3)

9:00 A.M.—"The Acheson Furnace, The Graphitization Process, and Certain Applications of Graphite" by R. C. Stroup, W. W. Palmquist, and M. Janes (Abstract No. 81)

9:30 A.M.—"A Survey of Processes in Which Synthetic Graphite Is Used" by B. L. Bailey and L. H. Juel (Abstract No. 82)

10:00 A.M.—"Graphite As A Mold Material" by R. S. Margeson and J. A. Shaw (Abstract No. 83)

10:30 A.M.—"A Resume of Products Dependent on Synthetic Graphite for Their Manufacture" by W. B. Arnold, W. D. Sherrow, and R. E. Lindenmeyr (Abstract No. 84)

Electrothermics and Metallurgy

Tuesday, October 2, 1956

Acheson Furnaces, Processes, Products, and Related Developments (cont'd) **with G. M. Butler presiding**

(PARLORS 1, 2, AND 3)

2:00 P.M.—"A Review of the Patents on Silicon Carbide Furnacing" by J. C. McMullen (Abstract No. 85)

2:30 P.M.—"Silicon Carbide Products: Present and Future" by G. M. Butler (Abstract No. 86)

3:00 P.M.—"Electrical Conduction in Silicon Carbide" by G. H. Fetterly (Abstract No. 87)

3:30 P.M.—"A Rutile Substitute for Ilmenite from the Production of Titanium Metal" by J. H. Brennan and J. G. Farmer (Abstract No. 88)

3:50 P.M.—"Design and Operation of a Laboratory Smelting Furnace" by R. R. Banks and J. J. Sima (Abstract No. 89)

4:10 P.M.—"Analysis of Power Requirements and Conditions for Similitude in Electrothermic Furnaces" by Edward Saibel, F. F. Ling, and W. J. Greene (Abstract No. 90)

Electrothermics and Metallurgy
(cont'd)

Wednesday, October 3, 1956

New Chemical Developments in the Extractive Metallurgy of Titanium with A. C. Loonam presiding

(PARLORS 1, 2, AND 3)

9:00 A.M.—"The ONR Basic Research Program on the Physico-Chemical Aspects of the Extractive Metallurgy of Titanium" by W. C. Arsem and J. J. Harwood
(Abstract No. 91)

9:20 A.M.—"The Equilibrium between Titanium and Titanium Chloride in a Sodium Chloride/Potassium Chloride Melt" by H. H. Kellogg and W. C. Kreye
(Abstract No. 92)

9:40 A.M.—"Equilibria between Titanium Metal and Solutions of Lower Titanium Chlorides in Fused Magnesium Chloride" by K. Komarek and P. Herasymenko
(Abstract No. 93)

10:00 A.M.—"Vapor-Phase Production of Titanium Metal" by Emil Perout (Abstract No. 94)

10:20 A.M.—"The Electrochemistry of Potassium Fluotitanate Melts" by A. J. Kolk, M. E. Sibert, and M. A. Steinberg
(Abstract No. 95)

10:40 A.M.—"Constitution of Alkali Metal Titanium Fluorides in the Molten KCl-LiCl Eutectic Mixture" by C. T. Brown, H. J. Gardner, and G. J. Janz
(Abstract No. 96)

11:00 A.M.—"Vapor Pressure and Thermal Properties of Titanium Tetrabromide" by J. M. Blocher, Jr., N. D. Veigel, and I. E. Campbell
(Abstract No. 97)

Electrothermics and Metallurgy

Wednesday, October 3, 1956

New Chemical Developments in the Extractive Metallurgy of Titanium
(cont'd)
with W. C. Arsem presiding

(PARLORS 1, 2, AND 3)

2:00 P.M.—"Density and Viscosity of Titanium Tetrabromide" by J. M. Blocher, Jr., R. F. Rolsten, and I. E. Campbell
(Abstract No. 98)

2:20 P.M.—"Heat of Formation of Titanium Tribromide by the Mercury Reduction of Titanium Tetrabromide" by E. H. Hall and J. M. Blocher, Jr.
(Abstract No. 99)

2:40 P.M.—"Vapor Pressure of Titanium Tetrafluoride" by E. H. Hall, J. M. Blocher, Jr., and I. E. Campbell (Abstract No. 100)

3:00 P.M.—"Deoxidation of Titanium with Selected Reducing Agents" by R. B. Liss, E. J. Chapin, and L. Secretan (Abstract No. 101)

3:20 P.M.—"Thermochemistry of the Titanium Tetrahalides" by W. H. Johnson, R. A. Nelson, A. Gilliland, and E. J. Prosen
(Abstract No. 102)

3:40 P.M.—"Purification of Titanium Halides and Criteria of Their Purity" by R. B. Johannesen, W. S. Clabaugh, and Raleigh Gilchrist
(Abstract No. 103)

THEORETICAL ELECTROCHEMISTRY AND BATTERY

Joint Symposium

Wednesday, October 3, 1956

Electrode Polarization with U. B. Thomas presiding

(PINE ROOM)

9:00 A.M.—*See* Battery—Theoretical Electrochemistry Joint Symposium, page 198C.

Theoretical Electrochemistry and Battery

Wednesday, October 3, 1956

Joint Symposium (cont'd)

Electrode Polarization (cont'd) **with C. W. Tobias presiding**

(PINE ROOM)

2:00 P.M.—*See* Battery—Theoretical Electrochemistry, Joint Symposium, page 198C.

THEORETICAL ELECTROCHEMISTRY AND ELECTRODEPOSITION

Joint Symposium

Monday, October 1, 1956

Structure of Metallic Electrodeposits with W. R. Meyer presiding

(EUCLID BALL ROOM)

2:00 P.M.—*See* Electrodeposition—Theoretical Electrochemistry Joint Symposium, page 199C.

Theoretical Electrochemistry and Electrodeposition

Joint Symposium (cont'd)

Tuesday, October 2, 1956

Kinetics of Electrodeposition with Ernest Yeager presiding

(EUCLID BALL ROOM)

9:00 A.M.—*See* Electrodeposition—Theoretical Electrochemistry Joint Symposium, page 199C.

Theoretical Electrochemistry and Electrodeposition

Joint Symposium (cont'd)

Tuesday, October 2, 1956

Diffusion and Convection in Electrodeposition with Sidney Barnartt presiding

(EUCLID BALL ROOM)

2:00 P.M.—*See* Electrodeposition—Theoretical Electrochemistry Joint Symposium, page 199C.

THEORETICAL ELECTROCHEMISTRY

Tuesday, October 2, 1956
with Frank Hovorka presiding

(EUCLID BALL ROOM)

3:40 P.M.—"The Hydrogen Evolution Reaction on Copper, Gold, Molybdenum, Palladium, Rhodium, and Iron: Mechanism and Measurement. Technique under High Purity Conditions" by N. Pentland, J. O'M. Bockris and E. Sheldon
(Abstract No. 104)

4:05 P.M.—"The A-C Response of Electrode Systems to Sinusoidal Pressure Variations, I. Theory" by Ernest Yeager and Frank Hovorka (Abstract No. 105)

4:30 P.M.—"Preparation and Reproducibility of the Thermal Electrolytic Type Silver-Silver Chloride Electrodes' by Harry Taniguchi and G. J. Janz
(Abstract No. 106)

4:55 P.M.—"A-C Streaming Potentials" by Irving Galperin, Ernest Yeager, and Frank Hovorka
(Abstract No. 107)

ABSTRACTS

BATTERY

Abstract No. 1

The Silver Oxide-Cadmium Alkaline Secondary Battery

P. L. Howard, Yardney Electric Corp., 40-46 Leonard St., New York 13, N. Y.

A battery has been developed which substitutes cadmium for the zinc as negative active material in the silver-zinc secondary battery. By this change in negative the ability to accept CP charge and withstand overcharging has been greatly improved. This couple is more suitable for medium and low rate applications than for high rate use. The discharge voltage is approximately 1.2 v per cell with 30 w hr/lb and 1.5 w hr/in.^{3}. The cycle performance of this battery is rather uniform for several hundred cycles. Two to three thousand shallow cycles (50% capacity) have been obtained from these batteries. General characteristics of this system will be discussed.

Abstract No. 2

A Reproducible and Stable Silver-Silver Oxide Electrode

W. J. Hamer and D. N. Craig, U. S. Dept. of Commerce, National Bureau of Standards, Washington 25, D. C.

A method is described for the preparation of stable and reproducible silver-silver oxide electrodes. In cells of the type: Ag(s), Ag_2O(s) | NaOH, aq. | HgO(s), Hg(l), the electrode potential is stable for 38 days. No evidence was found that Ag, Ag_2O electrodes evolve oxygen, that Ag_2O exists in different forms in aqueous solutions at normal temperatures, that it reverts to a lower oxide, or that it has crystal imperfections. Free energy and entropy changes for the cell reaction at 25°C are −11254 cal and −9.12 e.u. The standard electrode potential of the Ag, Ag_2O electrode is −0.342 v at 25°C.

Abstract No. 3

Aqueous Potassium Hydroxide as Battery Electrolyte

T. P. Dirkse, Calvin College, Grand Rapids 6, Mich.

A study has been made of KOH solutions for use as the electrolyte in alkaline batteries. Solubility relationships of ZnO in KOH were determined at temperatures ranging from −30° to +45°C.

A partial phase diagram of aqueous KOH was also obtained. There are indications that the slow precipitation of ZnO from such electrolytes may be hastened by seeding.

Abstract No. 4

Solid Silver Halide Battery Systems*

W. J. van der Grinten, Electronics Lab., General Electric Co., Syracuse, N. Y.

In spite of their low ionic conductivities at room temperature, anhydrous solid-electrolyte battery systems have been given considerable attention during the last few years. Early G. E. research in this area, performed on the systems

$$Ag/AgCl/CuCl_2 + C \quad \text{and}$$

$$Ag/AgBr/CuBr_2 + C$$

will be reviewed. While the discharge mechanism of these systems can be partially explained by assuming the presence of a low-pressure cathode gas, their functioning is not yet fully understood at the present time.

*Work done at the Research Lab., General Electric Co., Schenectady, N. Y.

Abstract No. 5

The Fused Salt Cell $Mg/LiNO_3$, KCl/Ag

C. W. Jennings, Dept. of Chemistry, N. C. State College, Raleigh, N. C.

The fused salt cell, $Mg/LiNO_3$, KCl/Ag, was studied at temperatures from 300° to 500°C. Cell characteristics varied with the KCl content. With greater than 20% KCl, open-circuit voltages of 1.4–1.6 were obtained. Both silver and magnesium reacted directly with the electrolyte. The extent of reaction of magnesium varied with the KCl content. Substitution of Pt, Ni, or graphite for silver increased the open-circuit voltage. A mechanism is proposed in which silver is involved in the cell reaction.

Abstract No. 6

***N*-Halogen Organic Compounds as Cathode Materials for Primary Batteries**

C. K. Morehouse and R. Glicksman, RCA Labs., Radio Corp. of America, Princeton, N. J.

Half-cell data showing discharge characteristics for various types of *N*-halogen compounds will be presented. Of the various compounds tested, *N*-halogen derivatives of cyclic ureides and amidine derivatives are attractive for use as cathode materials in primary cells. Experimental *N,N'* dichlorodimethylhydantoin-magnesium reserve-type cells have been made and shown to operate at potentials above 2.0 v and give watt-hour capacities per unit of weight and volume comparable to commercially available reserve batteries.

Abstract No. 7

An Investigation of the Discharge Characteristics of Groups Ib-Vb Oxides in an Alkaline Electrolyte

R. Glicksman and C. K. Morehouse, RCA Labs., Radio Corp. of America, Princeton, N. J.

Half-cell discharge data are presented for a number of Groups Ib-Vb oxides discharged in a strongly alkaline solution. Ag_2O, HgO, PbO, Bi_2O_3, and Sb_2O_3 cathodes exhibited flat discharge curves, while PbO_2 and Tl_2O_3 are reduced stepwise at potentials close to their theoretical value. Anomalous results were obtained for AgO and CuO, their discharge curves showing no break that would indicate a change in reaction mechanism. The relation between the solubility product and operating potential of various silver salts will be discussed.

Abstract No. 8

Some Electrical Properties of Electrode Film Materials, I. Lead Sulfate

I. H. S. Henderson, National Defense Research Council, Ottawa, Ont., Canada

(No abstract received)

Abstract No. 9

Supercooling, Preferred Orientation, and Inverse Segregation in Lead-Antimony Alloys

A. C. Simon and E. L. Jones, Naval Research Laboratory, Washington 25, D. C.

The previously reported high-Sb concentration in the surface layer of Pb-Sb alloy casting is confirmed and explained by a more exact mechanism. Preferred orientation of this Sb with the [111] direction normal to the surface and the preferred direction of growth parallel to the surface are caused by the strong covalent linkages within the closer pair of (111) planes, and these factors also influence the tensile strength and ductility of the hypereutectic Pb-Sb alloys.

Abstract No. 10

Appearance of Battery Components at the End of Life under Laboratory Test

B. Agruss, Research Labs., National Lead Co., 105 York St., Brooklyn 1, N. Y.

Photographs are shown of the components of batteries at the end of life under laboratory test conditions. The significance of these photographs is discussed in terms of previous battery history and published results of field surveys of batteries which failed in normal car service.

Abstract No. 11

Correlation of Laboratory Life Tests with Automotive Service Tests of Lead Acid Batteries

J. F. Schaeffer, Globe Union, Inc., 900 E. Keefe Ave., Milwaukee 1, Wis.

An experimental grid alloy has been found which is considerably better than standard antimonial lead when subjected to a laboratory test in which grid corrosion is measured. In field test, however, this alloy corrodes at the same rate as the standard alloy. A review is presented showing that the relative rate of grid corrosion of the two alloys depends on the precise conditions of test.

Abstract No. 12

Effect of Arsenic and Silver in Grid Alloy on Storage Battery Life in Field Tests and Fleet Service

Howard Stoertz, The Electric Storage Battery Co., P. O. Box 5723, Philadelphia 20, Pa.

Addition of As and Ag in small quantities to the grid alloy used in storage batteries produces a marked increase in the corrosion resistance of these grids and leads to greatly improved life in laboratory tests. The combination of As and Ag produces a degree of improvement well beyond the additive effects of the two elements. When used in fleet service, such as police cars and taxicabs, greatly increased life has been obtained.

Abstract No. 13

Effect of Normal Car Service on Intermediate and Final Periods of Lead Storage Battery Performance

Dudley Haskell, W. P. Fuller & Co., South San Francisco, Calif.

A report will be given on the intermediate and final performance records of 66 batteries tested in approximately 150 different cars. Tests were started in 1949 and, with additions since then, continue in progress. Typical causes of failure are discussed, diagnosed, and illustrated with appropriate photographic and photomicrographic examples. Battery performances in 20 hr rate and cold capacity are found to follow a characteristic pattern which might serve as a useful guide in contemplated revisions of the standard cycling life test.

Abstract No. 14

Effect of Temperature on Cycling Life of Lead Acid Storage Batteries

J. F. Macholl and A. G. Koch, Automotive Div., Electric Storage Battery Co., 246 East 131st St., Cleveland 1, Ohio

Results of cycling life tests on lead acid storage batteries are highly influenced by the temperature at which the test is conducted. Temperatures attained in a cell during testing are influenced not only by ambient temperature, but also by the location of that cell with respect to other cells and by the amount of cell area exposed to the surroundings. The behavior of the cells during the SAE life test has been found to correlate with the above, higher cell temperatures favoring longer life. Quantitative relationships are presented.

Abstract No. 15

Pulse Maintaining of Automotive Batteries

J. B. Godshalk, Fox Products Co., 4720 North 18th St., Philadelphia 41, Pa.

The maintenance of automotive batteries while on the shelf by cycles of

short time, high rate charges, followed by long dormant periods, is investigated along with the conventional method of continuous trickle charge. Results from various cycle combinations and continuous trickle rates show that "pulse" maintaining produces better charge maintenance and far less grid corrosion and water consumption than continuous charging. The efficiency of maintenance is shown to approach that of open-circuit storage at low temperatures.

Abstract No. 16
Positive Post Corrosion in Lead Acid Cells

O. H. Bauer, Bowers Battery & Spark Plug Co., Reading, Pa.

Post corrosion is confined to cells used in float service. It becomes manifest by a bulge of the cover around the post. This distortion is caused by a corrosion product underneath the cover. Corrosion is due to an electrolytic action which is produced by areas of different acid concentrations. For the initiation of intensive corrosion, a flaw in the casting is necessary. Fissures resulting from internal shrinkage cavities provide a suitable nucleus.

Abstract No. 17
Self-Discharge Reactions in Lead Acid Batteries

P. Ruetschi and R. T. Angstadt, Research Div., Electric Storage Battery Co., P. O. Box 5723, Philadelphia 20, Pa.

Self-discharge reactions in negative and positive plates of lead acid batteries have been studied under various conditions. The composition of the grid alloy and acid strength have a strong influence on these reactions. Three different reactions are shown to be responsible for the self-discharge of positive plates.

Abstract No. 18
Self-Discharge of Positively Charged Nickel Oxide Electrodes of Alkaline Storage Batteries

A. L. Pitman and G. W. Work, Naval Research Lab., Washington 25, D. C.

Alkaline nickel oxide-iron storage batteries have been charged and put on open circuit. On open circuit the rate of oxygen evolution is proportional to the square root of the water activity in the electrolyte. Therefore, oxygen deposited on the nickel sesquioxide requires interaction with water for its evolution. The potential on decay changes linearly with the quantity of oxygen on the electrode. Adsorption of oxygen on, and desorption from, the nickel sesquioxide is hypothesized.

Abstract No. 19
A Self-Discharge Reaction of Cells with Manganese Dioxide and Metal Electrodes

W. C. Vosburgh, D. R. Allenson, and Stanley Hills, Duke University, Durham, N. C.

Under certain conditions H_2O_2 can be formed by action of metal electrodes on oxygen, and the peroxide can reduce a MnO_2 electrode. Ag electrodes in NH_4Cl electrolyte, Zn in an electrolyte containing a phosphate buffer, and uncleaned Pb in $(NH_4)_2SO_4$ gave pronounced effects. Zn in NH_4Cl, and Ag and clean Pb in $(NH_4)_2SO_4$ gave no effect observable in a one-day period.

Abstract No. 20
Instrumentation for Use in Storage Battery Studies

G. W. Work and C. P. Wales, Electrochemistry Branch, Chemistry Div., Naval Research Lab., Washington 25, D. C.

A storage battery analyzer featuring simplicity and accuracy of control, a wide scope of variables measured, and a complete, continuous record is described and its use is briefly illustrated with actual data. A null-balance servo system controls either the output voltage or current of a rectified d-c power supply by continuously regulating the a-c input. Individual plate potentials, temperature, gas concentrations, and gas volumes are continuously measured and recorded. Optional equipment permits use in cycling and varied applications.

BATTERY — THEORETICAL ELECTROCHEMISTRY

Abstract No. 21
Corrosion and Polarization

Norman Hackerman, Dept. of Chemistry, University of Texas, Austin 12, Texas

A method for indirect determination of polarization characteristics of anodic reactions involving the electrode metal is described for severe corrosion conditions; possible extension to less corrosive environments is discussed.

Abstract No. 22
Cathodic Polarization in the Leclanché Cell

N. C. Cahoon, National Carbon Research Labs., P.O. Box 6116, Parma, Ohio

Cathodic polarization in the Leclanché cell is analyzed to show the relative importance of a series of factors responsible for its development. The changes in electrolyte *p*H, in the manganese content of the electrolyte, and in the pseudo-equilibrium at the cathode-electrolyte interface during cell discharge are shown to be the most important items responsible for cathode polarization. Use of potential and *p*H measurements on samples of cathode mix is described as a useful tool for studying these phenomena.

Abstract No. 23
Metal Electrode Polarization

L. O. Case, University of Michigan, Ann Arbor, Mich.

Between the terminal states represented by the metal ion in its lattice and as a hydrated, possibly complex, ion in the bulk of the solution, many stages intervene concerning which thermodynamics furnishes no information. In recent years important knowledge of the mechanism of the over-all process has gained by the systematic study of electrode kinetics. In this branch of kinetics, added complications arise in that electrode reactions are necessarily heterogeneous and that the interfacial potential difference may be a controlling rather than an incidental factor.

Abstract No. 24
Polarization Studies of the Lead Electrode

E. Willihnganz, Gould-National Batteries, Inc., Depew, N. Y.

The electrochemistry of a smooth clean sheet lead in H_2SO_4 was investigated. Short pulses of current 2–0.02 amp cm² were applied for a few thousandths of a second and the voltage changes measured on a cathode ray oscillograph. The meaning of the results in terms of cell resistance, double layer capacitance, and the Warburg equivalent circuit is discussed.

Abstract No. 25
Anodic Corrosion and Hydrogen and Oxygen Overvoltage on Lead and Lead-Antimony Alloys

P. Ruetschi and B. D. Cahan, Research Div., Electric Storage Battery Co., P.O. Box 5723, Philadelphia 20, Pa.

The anodic attack of Pb and Pb-Sb alloys has been studied in solutions of H_2SO_4 with constant current methods. Thin layers of PbO_2 were formed and discharged. The PbO_2 discharge step recorded under proper conditions provides a reasonable measure for the depth of attack. Results are discussed in the light of the theory of the metallic bond. Hydrogen and oxygen overvoltage on Pb-Sb alloys in the range from 0 to 11% Sb were measured with the interrupter technique. Corrosion and overvoltage on single-crystal faces of lead have been studied.

Abstract No. 26
Activation Polarization in Battery Systems

Ernest Yeager, Dept. of Chemistry, Western Reserve University, Cleveland, Ohio

Activation polarization represents departures from thermodynamics as the result of the irreversibility of some chemical or electrochemical step in the electrode reaction. Activation polarization is an important factor in the development of batteries because it often limits the performance of existing batteries and prevents the use of otherwise promising electrode systems. Theoretical factors associated with activation polarization are reviewed relative to battery application. Techniques for the determination of activation polarization are evaluated and procedures for minimizing activation polarization at both anodes and cathodes are described.

Abstract No. 27

Polarization Measurements on High Current Gas Electrodes and Their Conformity with Chemical Test Methods

K. Kordesch, National Carbon Research Labs., P. O. Box 6116, Cleveland 1, Ohio

An improved interrupter circuit using no mechanically moving parts is described and results of measurements on gas electrodes are presented. Processing active carbon material used for heavy duty oxygen electrodes is followed step-by-step and the polarization values at different gas pressures are compared with H_2O_2-decomposition rates and surface measurements. Polarization of Pt-catalyzed carbon electrodes for use with hydrogen has also been studied by the same technique; results are included.

Abstract No. 28

Polarization Characteristics of the Oxygen-Peroxide Couple on Active Carbon Electrodes*

Milton Clark (present address: National Carbon Co., Cleveland, Ohio), M. O. Davies, Ernest Yeager, and Frank Hovorka, Dept. of Chemistry, Western Reserve University, Cleveland, Ohio

Anodic and cathodic polarization associated with the oxygen-peroxide couple have been determined on air-cell carbon electrodes in alkaline solutions with an electronic interrupter. Various types of active carbons have been involved in the preparation of the electrodes. Polarization has been correlated with surface areas and pore size distributions as determined by gas adsorption and gas condensation-vapor pressure methods. Results support the conclusions that the oxygen-peroxide couple is substantially reversible even at apparent current densities through 1 amp/cm² and that peroxide and oxygen transport are the cause of polarization.

*Research partially supported by the Office of Naval Research.

Abstract No. 29

Overpotential of the Manganese Dioxide Electrode, II. Acid Electrolytes

S. Yoshizawa and W. C. Vosburgh, Dept. of Chemistry, Duke University, Durham, N. C.

The overpotential of electrodes prepared by electrodeposition on graphite was measured in solutions of H_2SO_4 and manganese (II) sulfate as a function of current density and also of temperature. The relation of overpotential to current density and the shapes of the growth and decay curves can be explained quantitatively on the assumption that the primary reduction product is MnOOH and the electrode potential is dependent on the ratio of MnOOH to MnO_2 on the MnO_2 surface.

Abstract No. 30

Role of Ionic Diffusion and Mass Transfer in Kinetics of Electrode Reactions in Batteries

Morris Eisenberg, Stanford Research Institute, Menlo Park, Calif.

The effect of diffusion and mass transfer on the over-all rate of reactions in batteries is discussed. Following the introduction of the basic concepts of concentration polarization, chemical polarization, and limiting currents, the method of mass transfer analysis is presented and related to electrode processes. A number of specific important cases are discussed. These include: pure diffusion, free convection at vertical plate electrodes, laminar and turbulent flow between parallel electrodes, and a rotating electrode. The importance of the mode of convection is illustrated by limiting current calculations for a given electrode under several different geometrical and hydrodynamic conditions, usually encountered in static and dynamic battery systems.

CORROSION

Abstract No. 31

Oxidation of 50 Weight Per Cent Uranium-Zirconium Alloy

Sidney Barnartt, R. G. Charles, and E. A. Gulbransen, Westinghouse Research Labs., Pittsburgh, Pa.

The reaction of 50% uranium-zirconium with oxygen at 1 atm pressure was studied over the temperature range 200°–500°C. Two forms of the alloy, the stable ϵ-phase and the quenched γ-phase, were reacted to an oxide-scale thickness of 0.1 mm at the higher temperatures. For thick scales on either phase of the alloy, the weight gain increased linearly with time, although in many cases the oxidation curve showed a bend and could be well represented by two straight lines. At 400°C and above, the stable ϵ-phase reacted considerably faster than the γ-phase. Thick oxide scales were porous and showed uranium enrichment.

Abstract No. 32

Kinetics of the Oxidation of Chromium

E. A. Gulbransen and K. F. Andrew, Westinghouse Research Labs., Pittsburgh, Pa.

The oxidation of high purity chromium is studied between 700° and 1100°C. Below 900°C, conventional oxidation curves are obtained which can be fitted to the parabolic rate law. Above 900°C, the rate of oxidation increases with temperature and time in an unusual manner. At 1050°C, the oxide film is no longer protective and rapid oxidation is observed. The breakdown in the oxidation of chromium is closely related to its high vapor pressure above 900°C.

Abstract No. 33

High Temperature Scaling of Cobalt-Chromium Alloys

C. A. Phalnikar, E. B. Evans, and W. M. Baldwin, Jr., Dept. of Metallurgical Engrg., Case Institute of Technology, Cleveland, Ohio

Scaling rates and scale composition of Co-Cr alloys were determined in the temperature range 900°–1200°C. At any given temperature the scaling rate increased with low Cr additions, then dropped precipitously with further additions reaching a minimum at about 25% Cr. Thereafter the scaling rate again increased approaching the scaling rate of Cr as the upper limit. Above about 25% Cr, the scale consisted exclusively of Cr_2O_3; complex scales were formed. The best scaling resistance was associated with a scale consisting predominantly of Cr_2O_3, not spinel. Schematic isothermal sections of the deduced Co-Cr-O phase diagram were applied as an aid in interpreting the scaling behavior.

Abstract No. 34

High Temperature Scaling of Nickel-Manganese Alloys

E. B. Evans, C. A. Phalnikar, and W. M. Baldwin, Jr., Dept. of Metallurgical Engrg., Case Institute of Technology, Cleveland, Ohio

Ni-Mn alloys scaled in air according to the parabolic rate law. The scaling rate increased with increasing manganese. Both an external scale and subscale were formed. Above a critical concentration of manganese (15% at 600°C to 60% at 1000°C), the external scale consisted exclusively of manganese oxides, and the subscale was MnO. The spinel ($NiO \cdot Mn_2O_3$) found at lower manganese contents was not associated with improved oxidation resistance. Isothermal sections of the Ni-Mn-O phase diagram were applied in interpreting the scaling behavior.

Abstract No. 35

Oxidation of Iron-Nickel Alloys, III. Kinetics and Mechanism

R. T. Foley and C. J. Guare, General Engrg. Lab., General Electric Co., Schenectady, N. Y.

A Chevenard automatic thermobalance and a high temperature electron diffraction unit were used to obtain kinetic and analytical data on the oxidation behavior of the relatively simple Fe-Ni system. The effect of varying oxidation atmosphere and surface preparation was investigated over the range 600°–1000°C for three alloys containing nominally 30, 41, and 78% Ni. Thermodynamic quantities, calculated from the kinetic data, are discussed along with the analytical information to indicate a mechanism for the oxidation.

Abstract No. 36

Hydrogen Diffusion through Steel

T. J. Butler and R. T. Davis, Jr., Applied Research Lab., U. S. Steel Lab., Monroeville, Pa.

A new method has been developed for detecting the hydrogen which diffuses through a steel plate, one side of which is exposed to acid. In this method one side of the plate is in contact with a passivating solution (0.05M sodium dichromate) and on the other side reaction with acid produces hydrogen which diffuses through the steel. With a steel plate 0.010-in. thick the potential of the

surface exposed to $Na_2Cr_2O_7$ starts to change in the anodic direction within about 15 sec after the addition of the attacking acid and continues to do so for several hours before becoming constant. The magnitude of the potential change (ca 500 mv) and the rate of change depend on the amount of hydrogen diffusing through the steel plate, the steel composition, and the nature of the attacking acid used in the experiment.

Abstract No. 37
Low-Pressure Solubility and Diffusion of Hydrogen in Zirconium*

M. W. Mallett and W. M. Albrecht, Battelle Memorial Institute, Columbus 1, Ohio

Hydrogen solubilities determined in alpha and beta zirconium and zirconium-oxygen alloys at 700°–1000°C at 0.1–4μ Hg followed Sieverts' law. Solubilities decreased with increasing temperature and increased with oxygen content. Diffusion coefficients and degassing coefficients were determined in the ranges 300°–600°C and 600°–800°C, respectively. Results show that degassing of zirconium is not a pure diffusion phenomenon.

*Work performed under AEC Contract W-7405-eng-92.

Abstract No. 38
Corrosion Characteristics of Uranium. An Electron Diffraction Study

J. T. Waber and D. D. Whyte (present address: Commercial Power Div., Westinghouse Electric Corp., Forest Hills, Pittsburgh, Pa.), Los Alamos Scientific Lab., University of California, Los Alamos, N. Mex.

The initial product formed on relatively oxide-free uranium has been shown by electron diffraction to be the alpha or low temperature form of uranium hydride. Such an oxide-free surface has been prepared by polishing the metal within the electron diffraction unit while maintaining a vacuum of 10^{-7} mm Hg. Uranium dioxide lines appear later and grow in intensity. Electron diffraction studies are reported on vacuum annealed metal.

Abstract No. 39
Orientation Factors in Oxide Films on Uranium

J. T. Waber, Los Alamos Scientific Lab., University of California, Los Alamos, N. Mex.

(No abstract received)

Abstract No. 40
Variations of Alkaline Anodizing Baths for Magnesium

W. McNeill and R. Wick, Pitman-Dunn Labs., Frankford Arsenal, Philadelphia, Pa.

The effects of some polyvalent metal anions in magnesium anodizing were compared. Corrosion resistance of coated panels was determined. Hardness and dielectric strength tests were also carried out. Coatings from chromate, stannate, vanadate, tungstate, and manganate baths were compared with those from a bath containing no polyvalent metal anion. Differences in corrosion resistance were noted; vanadate baths produced the best results. Differences in color were noted also.

Abstract No. 40-A
Potential-pH Diagram of the Antimony-Water System; Its Applications to Properties of the Metal, Its Corrosion, and Antimony Electrodes.

A. L. Pitman, Naval Research Lab., Washington 25, D. C.; Marcel Pourbaix, University of Brussels, Brussels, Belgium; and N. de Zoubov, Centre Belge D'Etude de la Corrosion, Brussels, Belgium

Using methods and conventions described previously, together with the available thermodynamics and electrochemical data, equations have been formulated and represented as a potential-pH diagram of the antimony-water system. Another diagram is presented showing zones of corrosion. Free energies of formation of the antimonate ion, $Sb(OH)_6^-$, and the SbO_2^+ ion have been calculated and are given.

Abstract No. 41
Effect of Prior Corrosion History on Corrosion of Zircaloy-2 in High Temperature Water

D. E. Thomas and S. Kass, Atomic Power Div., Westinghouse Electric Corp., P. O. Box 1468, Pittsburgh 30, Pa.

The corrosion of Zircaloy-2 is characterized by a transition from an initial quasi-cubic rate law to a linear rate law which occurs at very long exposure times at temperatures of about 600°F. The linear corrosion rate subsequent to the transition can be determined at low temperatures in a short time by transferring the specimen to the low temperature after having been exposed at higher temperatures for a time sufficient to reach the linear portion of the weight gain vs. time curve. Such experiments are described together with transient effects which persist for a time after a specimen has been transferred from one temperature to another.

Abstract No. 42
A Reaction Rate Study of the Corrosion of Low-Hafnium Zirconium in Hydrofluoric Acid Solutions

Tennyson Smith and G. R. Hill, Fuel Technology Dept., University of Utah, Salt Lake City, Utah

The rate of dissolution of zirconium in HF solutions has been studied using a radioactive tracer, Zr^{95}. By an appropriately designed system, continuous records of the rates could be made. The rate has been found to be dependent on the HF (free acid) activity alone, at constant temperature. A number of possible mechanisms for the slow step are suggested, the most likely one being the diffusion of HF to the zirconium surface. Reaction products are demonstrated to be mostly ZrF_3^+ ion in the solution, and H_2 in the gas phase. The activation energy for the slow step is 3.3 kcal/mole.

Abstract No. 43
Hydrogen Evolution from Dissolving Titanium-Oxygen Alloys in Hydrofluoric Acid and the Constitution of the Ti-O Alloys

M. E. Straumanis, C. H. Cheng (present address: 530 East Green St., Champaign, Ill.), and A. W. Schlechten, Dept. of Metallurgy, University of Missouri School of Mines and Metallurgy, Rolla, Mo.

Ti-O alloys dissolve in HF according to the reaction $TiO_x + 3HF \rightarrow TiF_3 + xH_2O + 0.5\,(3 - 2x)\,H_2$, with a maximum for $x = 1.5$, which means that Ti_2O_3 dissolves without hydrogen evolution. Higher titanium oxides do not dissolve in HF. The determination of the end point of the above reaction was affected by a secondary, but very slow, reaction $TiF_3 + HF \rightarrow TiF_4 + 0.5\,H_2$. Nevertheless, experimental results agreed within $\pm 2\%$ for the first reaction for Ti containing oxygen up to 33 at.%. Ti-O alloys do not represent titanium oxygen solid solutions but solid solutions of titanium oxides and titanium metal.

Abstract No. 44
Dissolution of Iron in Hydrochloric Acid-Chromic Chloride Solutions

Robert Skomoroski and C. V. King, Dept. of Chemistry, New York University, New York 3, N. Y.

The dissolution rate of rotating iron cylinders was studied in 4M HCl containing purple and green forms of $CrCl_3$ up to 0.2M. Only small changes in the rate in acid alone were found, with no reduction of chromic ion. Although the standard potentials predict that reduction is possible, the actual potential of iron in acid solutions is more noble. Cathodic polarization gave sufficiently negative potentials, but only resulted in cathodic protection to the iron, with no reduction of chromic ion. Further, it was shown that metallic iron catalyzes the oxidation of chromous ion by hydrogen ion.

Abstract No. 45
Kinetics of the Reaction of Steel with Hydrogen Sulfide-Hydrogen Mixtures

A. Dravnieks and C. H. Samans, Standard Oil Co. (Indiana), Whiting, Ind.

(No abstract received)

Abstract No. 46
Kinetic Studies on Alkaline Nitrite Formation of Black Oxide Coatings on Mild Steel

R. M. Hurd and Norman Hackerman, Defense Research Lab. and Dept. of Chemistry, University of Texas, Austin, Texas

Formation of black-oxide (magnetite) coatings on mild steel in hot concen-

trated solutions of NaOH and $NaNO_2$ was studied over the temperature range 130°–150°C. The following mechanism is proposed for the over-all reaction:

$$Fe \xrightarrow{OH^-} Fe^{++} \xrightarrow{NO_2^-} FeO_2^-$$

$$\xrightarrow{Fe^{++}} Fe(FeO_2)_2$$

Of the total iron dissolved, only about 30% was converted to black oxide on the surface. Rates for oxide-free surfaces, as $dC_{Fe^{++}}/dt$, were obtained from the initial slopes of rate curves of total iron dissolved vs. time. Plots of the initial rates vs. $1/T$ were linear, and the slopes gave an "activation energy" of 39,000 cal/mole. As the oxide coating built up, the rates dropped to a fraction of the initial rate, and were apparently controlled by diffusion of the reactants through the coat.

Abstract No. 47

Corrosion of Austenitic Stainless Steel in Circulating Uranyl Sulfate Solutions at High Temperatures, I. Experimental Results

E. G. Bohlmann, J. C. Griess, Jr., and R. S. Greeley, Oak Ridge National Lab., Oak Ridge, Tenn.

The successful development of aqueous homogeneous reactors has required a knowledge of the corrosion resistance of a number of metals and alloys to aqueous fuel solutions at high temperature. The present paper summarizes corrosion results that have been obtained in an extensive testing program in which several austenitic stainless steels have been exposed to circulating uranyl sulfate solutions in the absence of high-level radiation. Effects of uranyl sulfate concentration, temperature, flow rate, and additives, such as copper sulfate and oxygen, on the corrosion of stainless steel are discussed.

Abstract No. 48

Corrosion of Austenitic Stainless Steel in Circulating Uranyl Sulfate Solutions at High Temperature, II. Mechanism of the Corrosion Process

J. C. Griess, Jr., and E. G. Bohlmann, Oak Ridge National Lab., Oak Ridge, Tenn.

A reasonable mechanism for the corrosion of stainless steel in high temperature uranyl sulfate solutions has been formulated. It has been shown that, if the corrosion of stainless steel is to be minimized, a protective oxide coating must form on the surface of the steel. From a consideration of the chemistry of uranyl sulfate solutions and the hydrolytic behavior of the corrosion products, it is possible to explain the effect of flow rate, uranium concentration, and temperature on the formation of the oxide coating, and, consequently, on the corrosion of stainless steel. An examination of the chemical reactions involved in the corrosion process shows that it is necessary to maintain an oxidizing agent such as oxygen in the system and that, if oxygen is used, its consumption can be related to the quantity of steel corroded.

Abstract No. 49

Corrosion of Austenitic Stainless Steel in Dilute Acid Solutions at High Temperature

J. C. Griess, Jr., R. S. Greeley, E. G. Bohlmann, and S. R. Buxton, Oak Ridge National Lab., Oak Ridge, Tenn.

The corrosion of several austenitic stainless steels in dilute sulfuric, nitric, chromic, and phosphoric acid solutions has been studied under dynamic conditions at temperatures as high as 300°C. The severity of corrosion depended on the particular acid, its concentration, flow rate, temperature, and the presence of additives. The chemistry of the process is discussed and results are compared with those obtained in uranyl sulfate solutions.

Abstract No. 50

An Investigation of the Effect of Chemical Variables on the Corrosion of Copper

W. D. Robertson (Yale University, New Haven, Conn.; consultant), V. F. Nole, W. H. Davenport, and F. P. Talboom, Jr., Research and Development Dept., Chase Brass and Copper Co., Waterbury, Conn.

The corrosion rate of Cu has been measured as a function of *p*H in the range 1.6–6, anion type and concentration, oxygen and CO_2 concentration, and temperature in a system maintained at constant composition throughout a given test. Data show that the rate is proportional to hydrogen ion concentration and to oxygen concentration in the range of concentrations corresponding to air saturation; it is independent of the growth of films in time. Results indicate that the rate, *C.R.*, may be expressed in terms of the difference in a saturation concentration, C_E, and the concentration maintained in the system at any time, C: $C.R. = a + b(C_E - C)$. The temperature dependence of the rate, at constant oxygen concentration, for both chloride and sulfate solutions, is: rate $= Ae^{-9000/RT}$.

Abstract No. 51

Corrosion of Single Crystals and Recrystallized Single Crystals of Iron and Steel in Citric Acid

W. R. Buck, III, and Henry Leidheiser, Jr., Virginia Institute for Scientific Research, Richmond, Va.

Armco iron and L-steel (321) faces corroded approximately two times faster than (100) faces at 20° and 100°C. Fe(100) was cathodic to Fe(321) at 20°C. Recrystallization of single crystals to polycrystalline material resulted in an increased corrosion rate. In the presence of 40–45 ppm of Sn(II), corrosion rates of single crystals were reduced and no difference between the (100) and (321) faces was observed.

Abstract No. 52

Anodic Behavior of Cu in HCl

R. S. Cooper, Dept. of Physics, University of Illinois, Urbana, Ill.

(No abstract received)

Abstract No. 53

Stress Potentials for Tension and Torsion Stresses

W. F. Seyer, O. K. Miniato, and K. Nobe, Dept. of Engineering, University of California, Los Angeles 24, Calif.

Measurements of stress potentials annealed and cold worked copper wires were made with steady current flow in NaCl solutions. For the former, below the elastic limit, emf varied as $(\text{stress})^2$ for tension and torsion, that for cold worked varied directly. For annealed wire $T\Delta S \rightarrow 0$, not for the other. Here cold work is associated with entropy because of increased disorder of crystal lattice. For the same stress, emf for annealed was twice the cold worked.

Abstract No. 54

Chemical and Electrochemical Properties of $FeSn_2$

R. A. Covert and H. H. Uhlig, Corrosion Lab., Dept. of Metallurgy, Massachusetts Institute of Technology, Cambridge 39, Mass.

Corrosion properties of the $FeSn_2$ alloy layer existing between iron and tinplate are investigated. Corrosion potentials, cathodic polarization characteristics, and corrosion rates of Fe, Sn, and $FeSn_2$ in deaerated 4% NaCl + HCl (*p*H 2.0) and deaerated 0.1M citric acid solutions are reported. The possible effects of $FeSn_2$ on the corrosion behavior of tinplate are discussed on the basis of these measurements.

Abstract No. 55

Electrochemical Polarization, I. A Theoretical Analysis of the Shape of Polarization Curves

Milton Stern and A. L. Geary, Metals Research Labs., Electro Metallurgical Co., P. O. Box 580, Niagara Falls, N. Y.

The shape of polarization curves and the causes of deviation from "true" Tafel behavior are described. For a noncorroding electrode, deviations at low overvoltages are due to the reverse reaction of the oxidation-reduction system, at high overvoltages to concentration and/or resistance polarization. Representation of the local polarization diagram of a corroding electrode by considering the forward and reverse reactions of both oxidation-reduction systems forming the corrosion couple provides a clearer understanding of the factors affecting the corrosion rate and shape of polarization curves. A new approach to the study of corroding metals is provided by describing a region of linear dependence of potential on applied current. An equation relates the slope of this linear region to the corrosion rate and Tafel slopes.

Abstract No. 56

Oxygen Concentration Cell as a Factor in the Localized Corrosion of Metals

Wilson Lynes, Research Dept., Revere Copper and Brass Inc., Rome, N. Y.

The oxygen concentration cell has been reviewed in relation to metallic

corrosion, with emphasis on current determining factors. Its discovery and early history are outlined, and environmental conditions favorable to its development are classified and discussed. Theories of the mechanism of the cell are presented.

Abstract No. 57

The Mechanisms of Aqueous Corrosion of Aluminum at 100°C

K. M. Carlsen, % Joint Establishment for Nuclear Energy Research, Post Box 175, Lillestrom, Norway

Various alloys of aluminum, as well as super purity aluminum material, have been tested in aqueous solutions at 100°C. Samples have been polarized cathodically and anodically to study the effect of cathodic and anodic reactions, respectively, on the corrosion behavior. Results are interpreted as showing that the alkalinity produced at the cathodes facilitates film breakdown in these places. Consequently, alloys containing cathodic constituents are attached where these constituents are situated, while polycrystalline super purity material is attacked in the grain boundaries. Finally, the influence of cold work, bulk *p*H, and inhibitors is discussed in some detail.

Abstract No. 58

Contribution to the Theory of Stress Corrosion in Duralumin Alloys

W. H. Colner and H. T. Francis, Armour Research Foundation of Illinois Institute of Technology, Technology Center, Chicago 16, Ill.

Stress cracking of duralumin alloys was found to be greatly influenced by exposed area of the specimen (small areas showed long time-to-failure). Experiments with grain boundary-grain center couples showed that neither potentials nor couple current were influenced sufficiently by stress to account for the acceleration of failure by stress. At constant applied anodic current, however, stress was found to direct the attack perpendicular to applied stress. A theory is proposed in which final stages of failure result from plastic flow of grain boundary zones, preventing film maintenance, and resulting in direct and rapid metal attack.

Abstract No. 59

Galvanic Corrosion of the Aluminum-Lead Couple in Aqueous Pigment Extracts

M. J. Pryor, R. J. Hogan, and F. B. Patten, Kaiser Aluminum & Chemical Corp., Spokane 69, Wash.

Aqueous extracts from metallic lead and litharge accelerate the corrosion of high purity aluminum on account of the deposition of metallic lead from solution. Galvanic corrosion in these extracts is enhanced by high *p*H and high lead content of the extracts. Extracts from red lead and basic lead carbonate do not accelerate the corrosion of aluminum. Due to their low *p*H values and lower lead contents those extracts do not deposit metallic lead on aluminum. Lead linoleate is an excellent corrosion inhibitor for aluminum and, in addition, inhibits the galvanic corrosion of aluminum coupled to lead.

Abstract No. 60

Thermogalvanic Potentials and Currents at Aluminum Surfaces in Industrial Water

Edgar C. Pitzer, (present address: General Electric Co., Appliance Park, Louisville, Ky.), Hanford Atomic Products Operation, General Electric Co., Richland, Wash.

Potentials and galvanic currents at 28 aluminum surfaces in Columbia river water were studied between room temperature and 100°. The potential of the aluminum changed by approximately 0.6 v over this interval, becoming more anodic with increase in temperature. Similar but somewhat smaller changes in potential were noted in buffer solutions. By coupling identical aluminum samples, one at 100° and the other at room temperature, a maximum current density of 40 $\mu a/cm^2$ was maintained.

Abstract No. 61

Current Efficiency of Magnesium Anodes

E. H. Phelps, Applied Research Lab., U. S. Steel Corp., Monroeville, Pa.

Electrode potential measurements, hydrogen evolution measurements, weight loss determinations, and the rotogenerative method of detecting corrosion currents were used to study the corrosion of Mg in NaCl solutions. Results obtained were explained by the view that the major anode reaction of Mg consists of Mg entering the solution as monovalent Mg ions, a portion of which react with the solution to form divalent Mg ions and hydrogen gas. This view indicates why the current efficiency of Mg anodes is approximately 50% as a maximum when based on the Mg corroding directly to form divalent Mg ions.

ELECTRODEPOSITION

Abstract No. 62

Electroplating on Aluminum, I. Deposition from Strongly Acid Solutions

J. T. N. Atkinson, Naval Research Establishment, Dartmouth, N. S.

Development of a method for plating copper on aluminum from strongly acid solutions is recorded. The aluminum or aluminum alloy needs to be prepared for plating by a degreasing operation only, since the plating bath itself has sufficient reactivity toward the aluminum oxide film to allow plating on aluminum with substantial adhesion. Good results were obtainable with a surprisingly wide range of acid copper solutions.

Abstract No. 63

Electroplating on Aluminum, II. Deposition of Copper from Oxalate-Pyrophosphate Solutions

J. T. N. Atkinson, Naval Research Establishment, Dartmouth, N. S.

The best plating variants discussed in the previous paper are considered in more detail. A moderately acid copper solution containing oxalates, pyrophosphates, ammonia, and triethylamine has been found to be most effective for plating copper on aluminum. Rack and barrel plated work can be controlled to give adhesion in excess of the ultimate properties of tin-lead solder, and promising initial results have been obtained for copper plating aluminum wire in a continuous wire plating device.

Abstract No. 64

Electroplating Baths for Ultrahigh Strength Steels, I. Use of Aliphatic Amino Acids in Cadmium Baths to Reduce Hydrogen Embrittlement.

P. N. Vlannes, S. W. Strauss, and B. F. Brown, Physical Metallurgy Branch, Metallurgy Div., Naval Research Lab., Washington 25, D. C.

Noncyanide aqueous baths containing aliphatic amino acids were studied for their characteristics in plating cadmium on ultrahigh strength steel. Polarographic data, plating evaluation, and embrittlement characteristics (as determined by the delayed fracture, static fatigue test in tension using notched bars) are presented. Delayed fracture tests indicate that plating from such baths occasions markedly lower hydrogen embrittlement than plating from the accepted cyanide bath.

Abstract No. 65

Electrodeposition of Uranium at the Microgram Level

C. L. Rulfs, A. K. De and P. J. Elving, Dept. of Chemistry and Engineering Research Institute, University of Michigan, Ann Arbor, Mich.

The recovery of microgram and submicrogram quantities of uranium by electroplating has been studied, using as a tracer radioactive uranium-233 with and without the presence of microgram quantities of natural uranium as carrier. Optimum results were obtained in an ammonium oxalate medium with electrolysis at 80°–85° being first performed in acidic solution and then in alkaline solution. A small platinum disk, which fitted into a flow counter, was used as cathode and a platinum spiral served as anode. With 20 μg of uranium carrier present and a volume of 25 ml, an average recovery, based on alpha counting, of $94.3 \pm 3.0\%$ was obtained for amounts of uranium-233 ranging from 0.03 to 0.13 μg.

Abstract No. 66

Inclusion of Fuchsin in Bright Nickel Deposits

J. L. Dye and O. J. Klingenmaier, Dept. of Chemistry, Michigan State University, East Lansing, Mich.

Fuchsin, a brightener used in nickel plating, was recovered from nickel deposits by dissolving the deposits in HCl. The amount of fuchsin recovered per gram of nickel was roughly linear in fuchsin concentration and decreased with increasing current density. Some pertinent properties of fuchsin were

studied. The amount of fuchsin included and its brightening effect are correlated with a model which assumes preferential adsorption at grain corners and edges.

ELECTRODEPOSITION—THEORETICAL ELECTROCHEMISTRY

Abstract No. 67
Structure of Metallic Electrodeposits

Hellmuth Fischer, Siemens & Halske Aktiengesellschaft, Werkstoff-Hauptlaboratorium, Karlsruhe i.B.,Rheinbrückenstrasse 59, Germany

As-deposited structures are to be distinguished from poststructures. Characteristic of electrocrystallization is the wide scale of crystal imperfections, lattice dislocations caused by sorption or desorption of codeposited hydrogen, growth layers as most important base forms, spiral steps (with high Burgers vector), electrolyte components occluded at grain and subgrain boundaries, rhythmic lamellar bands, micropores, and outgrowths. Aggregates of layers and crystals classified according to typical growth forms are discussed.

Abstract No. 68
On the Theory of Electrolytic Crystal Growth

D. A. Vermilyea, Research Lab., General Electric Co., Schenectady, N. Y.

The electrodeposition of metals is considered in the light of the screw dislocation theory of crystal growth, which should be valid for electrodeposition on most metals. Equations are developed to give the current as a function of voltage for various conditions involving different combinations of the surface diffusion distance, the distance between kinks in the steps of the screw dislocations, and the current density relative to the exchange current density.

Abstract No. 69
Structure of Electrodeposits from Fused Alkalinous Chloride Electrolytes

R. S. Dean, W. W. Gullett, and F. X. McCawley, Chicago Development Corp., Riverdale, Md.

The structure and mechanism of formation of deposits formed by the electrolysis of fused systems of alkalinous metal, chlorine, and metals such as Ti, Zr, and Cr has been studied over wide ranges of electrolyte composition and conditions of electrolysis. The study has given particular attention to Ti. Conditions for making relatively thick, adherent, nonporous plates are given, and, more importantly from the standpoint of electrorefining conditions, for producing bundles of coarse filamentary particles having high bulk density yet freely draining the fused salt and adhering sufficiently to the cathode for practical operations.

Abstract No. 70
Comments on Electrodeposition Research on Single-Crystal Substrates

H. Bandes, Sylvania Electric Products Inc., Woburn, Mass.

A summary of some recent work in areas cognate to electrodeposition will be presented to support the contention that research on the structure of electrodeposits should be done on single-crystal substrates. Starting with Clark, Pish, and Weeg's x-ray structure investigations of about 1942, the argument will be advanced through a discussion of Gwathmey's etch and oxidation pattern work of the last several years and Müller's field emission microscopy studies. This discussion will then be tied into some comments on the energetics of electrode reactions and the basis of the contention will then be self-evident.

Abstract No. 71
Studies of the Natural Convection at Vertical Electrodes

N. Ibl, Laboratory for Physical Chemistry and Electrochemistry, Eidg. Technische Hochschule, Zurich, Switzerland

(No abstract received)

Abstract No. 72
Kinetics of the Deposition of Metals

J. O'M. Bockris, University of Pennsylvania, Philadelphia, Pa.

Methods of evaluating the mechanism of the deposition of metals from a knowledge of its kinetics are reviewed briefly. Potential energy surfaces for metal deposition reactions are examined and shown to allow the elimination of several hypothetical kinetic paths. Determination of the parameters of metal deposition and other fast reactions is examined; it is shown that previous attempts at such determinations may have been in error owing to the effects of dielectric loss in the solvent molecules in the double layer.

Abstract No. 73
High-Speed Polarization Measurements during Electrodeposition

H. J. Read and C. O. McHugh, Dept. of Metallurgy, Pennsylvania State University, University Park, Pa.

Through use of a suitable exploring electrode, a vacuum-tube voltmeter, a d-c amplifier, and a fast-writing recording oscillograph, it has been possible to measure polarization effects during short plating times at high current density and to observe phenomena which would not be detectable by the customary manual methods of polarization measurement. The usefulness of the technique is illustrated with data obtained from studies in tin plating solutions.

Abstract No. 74
Electrochemical Calorimetry

Abner Brenner and J. M. Sherfey, Div. of Chemistry, National Bureau of Standards, U. S. Department of Commerce, Washington 25, D. C.

The energetics of electrochemical reactions have been studied by means of calorimetry. Data obtained lead directly to the value of the enthalpy change which accompanies a reaction and indirectly to the thermodynamic constants of complex equilibria in solution. This method has been applied to a study of the cyanide complexes of monovalent copper. Theoretical considerations indicate the possibility of applying the technique to the study of polarization.

Abstract No. 75
Electrodeposition of Nickel from Mixed Solvent Systems

Robert Griffis, Ernest Yeager, and Frank Hovorka, Dept. of Chemistry, Western Reserve University, Cleveland 6, Ohio

Polarization and structural data were obtained for the deposition of nickel from pure and mixed solvent systems of methyl alcohol and water. Polarization measurements were made with an electronic interrupter. An all-glass cell was used in order to control such variables as concentration gradients, electrochemical purity, current distribution, temperature, and isolation from the atmosphere. Energies of activation in both systems as well as the Tafel slopes support the theory of slow discharge of the ion as being the rate-determining step. A face-centered cubic lattice structure was found for all deposits examined.

Abstract No. 76
A Study of Cathode Potentials in Aqueous Tungstate Solutions

D. R. Markwell and M. L. Holt, Chemistry Dept., University of Wisconsin, Madison, Wis.

Cathode potential measurements with a specially designed cell are used to obtain information about the cathode processes involved in the electrodeposition of tungsten alloys from aqueous solutions. Changes in observed cathode potential values resulting from varying the cathode current density and the electrolysis solution are noted. A hypothesis to explain some of the peculiarities of the cathodic reduction of aqueous tungstate solutions is proposed.

Abstract No. 77
Design of a New Electrolytic Cell for the Study of Electroplating Phenomena

Roger Gilmont, Manostat Corp., New York, N. Y., Polytechnic Institute of Brooklyn, Brooklyn, N. Y., and R. F. Walton, Tube Dept., RCA Labs., Radio Corp. of America, Harrison, N. J.

By means of the theory of the electropotential, the geometrical shape of a new electroplating cell was deduced in which the current density along the cathode is

linear and can be calculated directly from the total current and voltage of the cell. The new cell consists of a container with two straight sides intersecting at 45° and two curved sides consisting of rectangular hyperbolic cylinders orthogonal to each other, and each in turn orthogonal to one of the straight sides. One of the straight sides and its opposite curved surface are insulators, the other straight side is the cathode, while the remaining curved surface is the anode. The new cell may not only be used for current density studies, but also to determine the total polarization directly from simple measurements on the cell combined with the electrical conductivity of the solution.

Abstract No. 78

Diffusion and Convection Effects in Electrodeposition

C. W. Tobias, Dept. of Chemistry and Chemical Engineering, University of California, Berkeley 4, Calif.

Progress made in recent years in the quantitative interpretation of mass transport effects in electrodeposition is reviewed. At all practical current densities the interfacial composition of electrolyte at the cathode is substantially different from that in the bulk. Effect of stirring, flow of electrolyte, or movement of cathode on the interfacial composition can be estimated with an accuracy depending on the complexity of the system under investigation. The effect of local and average mass transport rates in the electrolyte on the character of deposits and on the macro- and micro- "throwing power" can often be predicted.

Abstract No. 79

Limiting Currents at Horizontal Electrodes in Free Convection

E. J. Fenech and C. W. Tobias, Dept. of Chemistry and Chemical Engrg., University of California, Berkeley 4, Calif.

Limiting currents for the deposition of copper from acid solutions of copper sulfate have been measured over a range of concentrations, viscosities, and with variations of cell geometry, in all cases in the absence of external stirring. For horizontal cathodes facing upward the data obtained could be correlated in a dimensionless form. On the basis of experimental data and theoretical considerations the mechanism of ionic mass transport at horizontal electrodes has been found to differ from that established for vertical electrodes.

Abstract No. 80

Throwing Index; A New Graphical Method for Expressing the Results of Throwing-Power Measurements

H. F. David and R. V. Jelinek, Dept. of Chemical and Metallurgical Engrg., Syracuse University, Syracuse 10, N. Y.

A new direct method is proposed for expressing results of throwing-power measurements made on plating solutions in a conventional rectangular throwing-power box with plane parallel electrodes. The metal distribution ratio (M) is plotted vs. the linear ratio (P) on arithmetic coordinates. The reciprocal of the slope of this plot is called "throwing index" and represents a direct measure of bath throwing power. Experimental data on several solutions are presented and advantages of this method are discussed.

ELECTROTHERMICS AND METALLURGY

Abstract No. 81

The Acheson Furnace, the Graphitization Process, and Certain Applications of Graphite

R. C. Stroup, W. W. Palmquist, and M. Janes, National Carbon Co., Niagara Falls, N. Y., and Cleveland, Ohio

The early history and continuing evolution of the Acheson furnace for the thermal conversion of carbon to artificial graphite are described. Data are presented on the changes in such properties as electrical and thermal conductivity, coefficient of thermal expansion, x-ray line shape, etc., with furnace temperature; the mechanism of the thermal recrystallization from carbon to graphite is discussed. Industrial utilization of the unique physical characteristics of graphite is illustrated through references to its use as a corrosion resistant material of construction and as a high temperature refractory material. Graphite, and especially impervious graphite, possesses particular advantages for chemical processing equipment items. Uses of graphite involving exposure to high temperatures are covered.

Abstract No. 82

A Survey of Processes in Which Synthetic Graphite Is Used

B. L. Bailey and L. H. Juel, Electrode Div., Great Lakes Carbon Corp., P.O. Box 637, Niagara Falls, N. Y.

A brief description will be given of commercial processes in which artificial graphite plays an important part. Processes covered include operations involving arc furnaces, resistance furnaces, induction furnaces, electrolytic and electromotive cells, metal casting, high temperature powder metallurgy, nuclear reactions, corrosive materials or atmospheres, sliding friction, commutation, and cathodic protection.

Abstract No. 83

Graphite as a Mold Material

R. S. Margeson and J. A. Shaw, International Graphite & Electrode Div., Speer Carbon Co., Niagara Falls, N. Y.

Graphite as produced in the Acheson type of furnace possesses properties which make it an ideal material with which to construct molds for casting a wide variety of metals, alloys, and other castable materials as well as hot pressing many powders requiring extremely high temperatures. Special applications involving coatings and impregnants of the graphite are also covered.

Abstract No. 84

A Resume of Products Dependent on Synthetic Graphite for Their Manufacture

W. B. Arnold, W. D. Sherrow, and R. E Lindenmeyr, Electrode Div., Great Lakes Carbon Corp., P.O. Box 637, Niagara Falls, N. Y.

A brief discussion will be given of the scope and importance of commercial products which depend on the unique properties of synthetic graphite for their manufacture. The commercial fields covered include ferrous and nonferrous arc furnace products, products of various electrolytic operations, and products where graphite is used as a component.

Abstract No. 85

A Review of Patents on Silicon Carbide Furnacing

J. C. McMullen, Engineering Research Branch, The Carborundum Co., Niagara Falls, N. Y.

A review of the progress in the manufacture of silicon carbide as reflected by the patent literature dating from Acheson's original patent issued in 1893 is given. A complete list of patents reviewed is presented while those considered most pertinent are discussed. Possible future trends are noted.

Abstract No. 86

Silicon Carbide Products: Present and Future

G. M. Butler, Engineering Research Branch, The Carborundum Co., Niagara Falls, N. Y.

The evolution of a whole family of products made with silicon carbide is outlined to show the importance of Acheson's discovery. Known properties of silicon carbide are used to forecast new areas for exploitation of this unique compound.

Abstract No. 87

Electrical Conduction in Silicon Carbide

G. H. Fetterley, Norton Co., Niagara Falls, Ont., Canada

Commercial silicon carbide is a semiconductor that can be prepared as predominantly n- or p-type at will. Body conductivity is linear, and determines the behavior of SiC heating elements, which are usually made from n-type. The interfacial conductivity is much lower, nonlinear, and is exploited in lightning arresters, which are made from p-type. While the electrical behavior of this material is still poorly understood in detail, the broad outlines are summarized in terms of semiconductor theory.

Abstract No. 88

A Rutile Substitute from Ilmenite for the Production of Titanium Metal

J. H. Brennan and J. G. Farmer, Electro Metallurgical Co., Niagara Falls, N. Y.

Ilmenite is processed by a partial reduction process in resistor furnaces to yield a titanium suboxide carbide prod-

uct and iron. Iron may be readily separated magnetically. The titanium suboxide carbide product is preferable to rutile for the production of titanium tetrachloride.

Abstract No. 89

Design and Operation of a Laboratory Smelting Furnace

R. R. Banks and J. J. Sima, Metallurgical Process Div., Air Reduction Co., Inc., Murray Hill, N. J.

A 120-kw open, in-line smelting furnace has been built to permit the evaluation of raw materials for the manufacture of calcium carbide and the study of electric smelting phenomena in general. Use of this furnace has permitted satisfactory testing of charge materials with appreciable savings in material and time over those required for plant-scale evaluation. Work is in progress on the refinement of predictions of the performance of large furnaces by analysis of laboratory furnace data.

Abstract No. 90

Analysis of Power Requirements and Conditions for Similitude in Electrothermic Furnaces

Edward Saibel, Dept. of Mathematics, Carnegie Institute of Technology, Pittsburgh, Pa.; and F. F. Ling and W. J. Greene, Air Reduction Co., Inc., Murray Hill, N. J.

Theoretical power requirements of electrothermic furnaces are discussed. Losses due to conduction, convection, and radiation are considered. Methods of scaling the model to prototype are considered in relation to the relative importance of the type of loss which, in turn, depends on furnace design and mode of operation. Application to the manufacture of calcium carbide is treated as an example.

Abstract No. 91

The ONR Basic Research Program on the Physico-Chemical Aspects of the Extractive Metallurgy of Titanium

W. C. Arsem and J. J. Harwood, Office of Naval Research, Washington, D. C.

(No abstract received)

Abstract No. 92

Equilibrium between Titanium and Titanium Chloride in a Sodium Chloride/Potassium Chloride Melt

H. H. Kellogg, Columbia University, New York, N. Y.; and W. C. Kreye, Brooklyn Polytechnic Institute, Brooklyn, N. Y.

(No abstract received)

Abstract No. 93

Equilibria between Titanium Metal and Solutions of Lower Titanium Chlorides in Fused Magnesium Chloride

K. Komarek and P. Herasymenko, Research Div., New York University, New York, N. Y.

Measurements of the total pressure of titanium chlorides over mixtures of $TiCl_2$ and fused $MgCl_2$ in the presence of metallic titanium indicate limited solubility of $TiCl_2$ in liquid $MgCl_2$ in the range from 720° to 800°C. Thermal analyses have shown that the system $TiCl_x$-$MgCl_2$ has a peritectic point at about 1 mole % $TiCl_x$. The peritectic temperature is 720°C. The system was investigated up to about 50 wt % $TiCl_x$ where complete solubility is attained at 930°C. The ratio of $TiCl_2$ to $TiCl_3$ in the salt is practically constant in the whole investigated range, and is equal to 7.7. No $TiCl_4$ was detected in the salt.

Abstract No. 94

Vapor Phase Production of Titanium Metal

Emil Perout, Clevite Research Center, Div. of Clevite Corp., Cleveland, Ohio

$TiCl_4$ and magnesium metal were reacted in the vapor stage to produce titanium metal. Two reactors were constructed during the period of the investigation. Both were similar in operation to a flow reactor. Investigations showed that a successful temperature, using molybdenum containers, was approximately 800°C. Pressure of about 100 μ Hg was needed. Titanium metal was recovered with efficiencies up to 55%.

Abstract No. 95

Electrochemistry of Potassium Fluotitanate Melts

A. J. Kolk, M. E. Sibert, and M. A. Steinberg, Horizons, Inc., Cleveland, Ohio

(No abstract received)

Abstract No. 96

Constitution of Alkali Metal Titanium Fluorides in the Molten KCl-LiCl Eutectic Mixture

C. T. Brown, H. J. Gardner, and G. J. Janz, Dept. of Chemistry, Rensselaer Polytechnic Institute, Troy, N. Y.

The conductance and cryoscopic behavior of the alkali metal titanium fluorides in the molten KCl-LiCl eutectic mixture have been investigated to gain information on the ionic nature of the melts. A large decrease in conductance is observed on the addition of alkali metal titanium fluorides, indicating a decrease in electrovalency of the melt as a whole. Data are reported for the conductance and cryoscopic behavior for these compounds and more simple alkali halide salts in the KCl-LiCl eutectic melt. The structure and constitution of these melts are considered in the light of these results.

Abstract No. 97

Vapor Pressure and Thermal Properties of Titanium Tetrabromide

J. M. Blocher, Jr., N. D. Veigel, and I. E. Campbell, Battelle Memorial Institute, Columbus, Ohio; and R. F. Rolsten, E. I. du Pont de Nemours & Co., Wilmington, Del.

The vapor pressure of liquid titanium tetrabromide was measured over the temperature range from the melting point (38.2°C) to the boiling point (231.6°C) with the following results:

$$TiBr_4(l) = TiBr_4(g)$$

$$\log p_{atm} = 16.6190 - 3.8117 \log T - 3188.18/T$$

$$\Delta H_{504.8} = 10.16 \text{ kcal}$$
$$\Delta H_{298.2} = 13.02 \text{ kcal}$$
$$\Delta S_{298.2} = 27.48 \text{ e.u.}$$

In order to treat the data thermodynamically, the following properties were measured or calculated: heat capacity, heat of fusion, and melting point of the solid, heat capacity of the liquid, and the heat capacity and standard entropy of the vapor.

Abstract No. 98

Density and Viscosity of Titanium Tetrabromide

J. M. Blocher, Jr., and I. E. Campbell, Battelle Memorial Institute, Columbus, Ohio; and R. F. Rolsten, E. I. du Pont de Nemours & Co., Wilmington, Del.

Measurements were made of the density and viscosity of liquid titanium tetrabromide between 40° and 130°C leading to the equations

$$d = 2.953 - 0.00225(t - 40)$$

and

$$\eta = \frac{3.746}{1 + 0.0246t - 0.0000243t^2}$$

where d is in g/cc, η is in centipoises, and t is in °C. Measurements of the vapor density at the boiling point indicate that titanium tetrabromide is monomolecular.

Abstract No. 99

Heat of Formation of Titanium Tribromide by the Mercury Reduction of Titanium Tetrabromide

E. H. Hall and J. M. Blocher, Jr., Battelle Memorial Institute, Columbus, Ohio

Equilibrium data on the mercury reduction of titanium tetrabromide were combined with the heat of formation of titanium tetrabromide and mercurous bromide to obtain, for the heat of formation of titanium tribromide,

$$\tfrac{3}{2}Br_2(l) + Ti(\alpha) = TiBr_3(s)$$
$$\Delta H_{298.2} = -130.8 \pm 1.1 \text{ kcal}$$

Complications in the system:

$$TiBr(g) + Hg(l) = \tfrac{1}{2}Hg_2Br_2(s) + TiBr_3(s)$$

are discussed.

Abstract No. 100

Vapor Pressure of Titanium Tetrafluoride

E. H. Hall, J. M. Blocher, Jr., and I. E. Campbell, Battelle Memorial Institute, Columbus 1, Ohio

Measurements of the vapor pressure of titanium tetrafluoride were made by three independent methods over the tem-

perature range 435°-555°K with the result for

$$TiF_4(s) = TiF_4(g)$$

$$\log p_{atm} = 33.787 - 6507.9/T - 8.05 \log T$$

With an estimated value of $\Delta C/_p = -16$, the data lead to: $\Delta H_{298.2} = 25.00$ kcal; $\Delta S_{298.2} = 47.43$ e.u.

Abstract No. 101
Deoxidation of Titanium with Selected Reducing Agents

R. B. Liss, E. J. Chapin, and L. Secretan, Nonferrous Alloys Branch, Metallurgy Div., Naval Research Lab., Washington 25, D. C.

Since relatively small amounts of oxygen contamination produce a marked reduction in the ductility of titanium, a means for deoxidation of contaminated metal is of major industrial importance. Pure thorium and gadolinium each have been found to deoxidize molten titanium containing 1 wt % oxygen. An 8.4 wt % addition of thorium removes about 82 wt % of the oxygen from solution by forming ThO_2 while an addition of 7.5 wt % gadolinium removes about 90 wt % of the oxygen from solution by forming gadolinium oxide. Recovery of ductility as a result of deoxidation is evidenced by hardness measurements and mechanical properties.

Abstract No. 102
Thermochemistry of the Titanium Tetrahalides

W. H. Johnson, R. A. Nelson (present address: Alcohol Tax Unit, Treasury Dept., Washington, D. C.), A. Gilliland, and E. J. Prosen, Thermochemistry Section, Div. of Chemistry, National Bureau of Standards, Washington 25, D. C.

Direct calorimetric measurements have been made on the heat of formation of $TiCl_4(g)$ and $TiBr_4(c)$ from Ti(c) and gaseous halogen. Reduction of the data to standard conditions gives the following results: $Ti(c) + 2Cl_2(g) = TiCl_4(liq)$; $\Delta H°_{(298.16°K)} = -192.1 \pm 0.7$ kcal/mole; $Ti(c) + 2Br_2(liq) = TiBr_4(c)$; $\Delta H°_{(298.16°K)} = -147.40 \pm 1.10$ kcal/mole. Heats of hydrolysis of $TiCl_4(liq)$, $TiBr_4(c)$, and $TiI_4(c)$ in acid solutions have also been measured. Details of the apparatus and experimental techniques will be given.

Abstract No. 103
Purification of Titanium Halides and Criteria of Their Purity

R. B. Johannesen, W. S. Clabaugh, and Raleigh Gilchrist, Chemical Div., National Bureau of Standards, Washington 25, D. C.

Procedures are described for preparing titanium halides in a state of high purity, as well as for determining their purity by cryoscopic, spectrochemical, and infrared absorption measurements. Detailed account is given of the preparation of titanium tetrachloride, the starting material for preparing the other halides, with a purity of 99.9990 mole %, and of titanium tetrabromide with a purity of 99.998 mole %. Description is also given of the preparation of titanium trichloride and of titanium tetraiodide.

THEORETICAL ELECTROCHEMISTRY

Abstract No. 104
Hydrogen Evolution Reaction on Copper, Gold, Molybdenum, Palladium, Rhodium and Iron: Mechanism and Measurement Technique Under High Purity Conditions.

N. Pentland, J. O'M. Bockris, and E. Sheldon, University of Pennsylvania, Philadelphia 4, Pa.

During the past five years, a number of experimental and theoretical techniques have been devised whereby the attack on the mechanism of electrode reactions need no longer be prosecuted by qualitative inference but by the evaluation of diagnostic criteria which allow unambiguous decisions between mechanisms to be made. The determination of the most important relevant parameters used for the evaluation of diagnostic criteria for the hydrogen evolution reaction have been applied to Cu, Au, Mo, Pd, Rh, and Fe cathodes. The necessary details of the technique of measuring currents of electrodes under ultrahigh purity conditions for electrode reactions which are easily vitiated by the presence of trace impurities are also given here for the first time.

Abstract No. 105
A-C Response of Electrode Systems to Sinusoidal Pressure Variations, I. Theory*

Ernest Yeager and Frank Hovorka, Dept. of Chemistry, Western Reserve University, Cleveland 6, Ohio

Sinusoidal pressure variations at sufficiently low frequencies produce alternating components in the potential of a reversible electrode in accord with thermodynamics. With increasing frequency, instantaneous equilibrium is no longer maintained at the electrode and the effect decreases. Equations have been derived which relate the a-c response of the electrode to frequency in terms of the reaction constants of the rate-determining steps and the double-layer capacity. The dependence of the a-c response on frequency should provide information concerning the kinetics of the electrode processes. With the proper electrode system, it should be possible also to calculate the partial molal volume of a single type of ion with a minimum of controversial assumptions.

*Research partially supported by the Office of Naval Research.

Abstract No. 106
Preparation and Reproducibility of the Thermal Electrolytic Type Silver-Silver Chloride Electrodes

Harry Taniguchi and G. J. Janz, Dept. of Chemistry, Rensselaer Polytechnic Institute, Troy, N. Y.

A procedure in detail is described for the preparation of the thermal-electrolytic silver-silver chloride for precision use. A reproducibility of the electrodes by this procedure of only ±0.1 mv can be expected unless the freshly prepared electrodes are evaluated relative to equilibrated silver-silver chloride electrodes selected as reference standards. With care, reference standards corresponding to an electrode in the ground energy state, and of constant potential (±0.005 mv) for periods of several months can be attained. It is suggested that the difference in the values of the standard potential of this electrode may be attributed in part to the limited reproducibility of these electrodes. The importance of the factors of porosity, amount of silver chloride, and color, relative to the attainment of stable electrodes that equilibrate rapidly are considered in this communication.

Abstract No. 107
A-C Streaming Potentials*

Irving Galperin, Ernest Yeager, and Frank Hovorka, Ultrasonics Research Lab., Western Reserve University, Cleveland, Ohio

Apparatus has been developed for the measurement of the streaming potentials associated with bi-directional sinusoidal flow of electrolytic solutions through porous media. Results of a-c measurements are compared with those obtained with unidirectional flow in terms of the following porous materials: surgical cotton, nylon, Pyrex, and ion-exchange resins of both the cation and anion type. The primary advantage of the a-c method is the relatively small amount of solution required for the measurements.

*Research partially supported by the Office of Naval Research.

SPRING MEETING

at the

STATLER HOTEL

Washington, D. C.

May 12, 13, 14, 15, and 16, 1957

Sessions probably will be scheduled on

Electric Insulation

Electronics (including Luminescence, Semiconductors, Oxide Cathodes, Instrumentation, and possibly Screen Applications)

Electrothermics and Metallurgy

Industrial Electrolytics

Theoretical Electrochemistry (including a special symposium on electrolytes)

Abstracts for the Spring Meeting (*not exceeding 75 words in length*) must reach the Secretary's Office, 216 West 102nd Street, New York 25, N. Y. *not later than January 2, 1957* in order to be included in the program.

Indicate on abstract for which Division's symposium the paper is to be scheduled.

INDEX TO AUTHORS

(The number in the right hand column is the abstract number used in the Technical Program and in the Abstracts.)

	Abstract No.
Agruss, B.	10
Albrecht, W. M.	37
Allenson, D. R.	19
Andrew, K. F.	32
Angstadt, R. T.	17
Arnold, W. B.	84
Arsem, W. C.	91
Atkinson, J. T. N.	62, 63
Bailey, B. L.	82
Baldwin, W. M., Jr.	33, 34
Bandes, H.	70
Banks, R. R.	89
Barnartt, Sydney	31
Bauer, O. H.	16
Blocher, J. M., Jr.	97, 98, 99, 100
Bockris, J. O'M.	72, 104
Bohlmann, E. G.	47, 48, 49
Brennan, J. H.	88
Brenner, Abner	74
Brown, B. F.	64
Brown, C. T.	96
Buck, W. R., III	51
Butler, G. M.	86
Butler, T. J.	36
Buxton, S. R.	49
Cahan, B. D.	25
Cahoon, N. C.	22
Campbell, I. E.	97, 98, 100
Carlsen, K. M.	57
Case, L. O.	23
Chapin, E. J.	101
Charles, R. G.	31
Cheng, C. H.	43
Clabaugh, W. S.	103
Clark, Milton	28
Colner, W. H.	58
Cooper, R. S.	52
Covert, R. A.	54
Craig, D. N.	2
Davenport, W. H.	50
David, H. F.	80
Davies, M. O.	28
Davis, R. T., Jr.	36
De, A. K.	65
Dean, R. S.	69
de Zoubov, N.	40A
Dirkse, T. P.	3
Dravnieks, A.	45
Dye, J. L.	66
Eisenberg, Morris	30
Elving, P. J.	65
Evans, E. B.	33, 34
Farmer, J. G.	88
Feneeh, E. J.	79
Fetterly, G. H.	87
Fischer, Hellmuth	67
Foley, R. T.	35
Francis, H. T.	58
Galperin, Irving	107
Gardner, H. J.	96
Geary, A. L.	55
Gilchrist, Raleigh	103
Gilliland, A.	102
Gilmont, Roger	77
Glicksman, R.	6, 7
Godshalk, J. B.	15
Greeley, R. S.	47, 49
Greene, W. J.	90
Griess, J. C., Jr.	47, 48, 49
Griffis, Robert	75
Guare, C. J.	35
Gulbransen, E. A.	31, 32
Gullett, W. W.	69
Hackerman, Norman	21, 46
Hall, E. H.	99, 100
Hamer, W. J.	2
Harwood, J. J.	91
Haskell, Dudley	13
Henderson, I. H. S.	8
Herasymenko, P.	93
Hill, G. R.	42
Hills, Stanley	19
Hogan, R. J.	59
Holt, M. L.	76
Hovorka, Frank	28, 75, 105, 107
Howard, P. L.	1
Hurd, R. M.	46
Ibl, N.	71
Janes, M.	81
Janz, G. J.	96, 106
Jelinek, R. V.	80
Jennings, C. W.	5
Johannesen, R. B.	103
Johnson, W. H.	102
Jones, E. L.	9
Juel, L. H.	82
Kass, S.	41
Kellogg, H. H.	92
King, C. V.	44
Klingenmaier, O. J.	66
Koch, A. G.	14
Kolk, A. J.	95
Komarek, K.	93
Kordesch, K.	27
Kreye, W. C.	92
Leidheiser, Henry, Jr.	51
Lindenmeyr, R. E.	84
Ling, F. F.	90
Liss, R. B.	101
Lynes, Wilson	56
Macholl, J. F.	14
Mallett, M. W.	37
Margeson, R. S.	83
Markwell, D. R.	76
McCawley, F. X.	69
McHugh, C. O.	73
McMullen, J. C.	85
McNeill, W.	40
Miniato, O. K.	53
Morehouse, C. K.	6, 7
Nelson, R. A.	102
Nobe, K.	53
Nole, V. F.	50
Palmquist, W. W.	81
Patten, F. B.	59
Pentland, N.	104
Perout, Emil	94
Phalnikar, C. A.	33, 34
Phelps, E. H.	61
Pitman, A. L.	18, 40A
Pitzer, E. C.	60
Pourbaix, Marcel	40A
Prosen, E. J.	102
Pryor, M. J.	59
Read, H. J.	73
Robertson, W. D.	50
Rolsten, R. F.	97, 98
Ruetschi, P.	17, 25
Rulfs, C. L.	65
Saibel, Edward	90
Samans, C. H.	45
Schaeffer, J. F.	11
Schlechten, A. W.	43
Secretan, L.	101
Seyer, W. F.	53
Shaw, J. A.	83
Sheldon, E.	104
Sherfey, J. M.	74
Sherrow, W. D.	84
Sibert, M. E.	95
Sima, J. J.	89
Simon, A. C.	9
Skomoroski, Robert	44
Smith, Tennyson	42
Steinberg, M. A.	95
Stern, Milton	55
Stoertz, Howard	12
Straumanis, M. E.	43
Strauss, S. W.	64
Stroup, R. C.	81
Talboom, F. P., Jr.	50
Taniguchi, Harry	106
Thomas, D. E.	41
Tobias, C. W.	78, 79
Uhlig, H. H.	54
van der Grinten, W. J.	4
Veigel, N. D.	97
Vermilyea, D. A.	68
Vlannes, P. N.	64
Vosburgh, W. C.	19, 29
Waber, J. T.	38, 39
Wales, C. P.	20
Walton, R. F.	77
Whyte, D. D.	38
Wick, R.	40
Willihnganz, Eugene	24
Work, G. W.	18, 20
Yeager, Ernest	26, 28, 75, 105, 107
Yoshizawa, S.	29

FUTURE MEETINGS OF
The Electrochemical Society

Cleveland, September 30, October 1, 2, 3, and 4, 1956

Headquarters at the Statler Hotel

Sessions will be scheduled on

**Batteries, Corrosion, Electrodeposition,
Electronics—Semiconductors,
Electrothermics and Metallurgy, Theoretical
Electrochemistry (joint with Electrodeposition),
and Theoretical Electrochemistry**

★ ★ ★

Washington, D. C., May 12, 13, 14, 15, and 16, 1957

Headquarters at the Statler Hotel

**Sessions probably will be scheduled on
Electric Insulation, Electronics (including Luminescence,
Semiconductors, Oxide Cathodes, Instrumentation,
and possibly Screen Applications),
Electrothermics and Metallurgy, Industrial
Electrolytics, and Theoretical
Electrochemistry (including a special symposium on electrolytes)**

★ ★ ★

Buffalo, October 6, 7, 8, 9, and 10, 1957

Headquarters at the Statler Hotel

★ ★ ★

New York, April 27, 28, 29, 30, and May 1, 1958

Headquarters at the Statler Hotel

★ ★ ★

Ottawa, September 28, 29, 30, October 1, and 2, 1958

Headquarters at the Chateau Laurier

★ ★ ★

Papers are now being solicited for the meeting to be held in Washington, D. C. Triplicate copies of each abstract (*not exceeding 75 words in length*) are due at the Secretary's Office, 216 West 102nd St., New York 25, N. Y., *not later than January 2, 1957* in order to be included in the program. *Please indicate on abstract for which Division's symposium the paper is to be scheduled.* Complete manuscripts should be sent in triplicate to the Managing Editor of the JOURNAL at the same address.

News Notes in the Electrochemical Field

New Patron Member

Union Carbide & Carbon Corp., Divisions: Electro Metallurgical Co. and National Carbon Co., New York, N. Y., recently became a Patron Member of the Society.

New Sustaining Member

Jones & Laughlin Steel Corp., Pittsburgh, Pa., recently became a Sustaining Member of the Society.

National Colloid Symposium

At the 30th National Colloid Symposium at Madison, Wis., on June 18, Dr. H. J. Dawe, Director of Research and Development, Acheson Colloids Co., Port Huron, Mich., presented a memorial lecture dedicated to Dr. Edward Goodrich Acheson, whose centennial is currently being celebrated. An abstract of Dr. Dawe's lecture, entitled "Edward Goodrich Acheson: Pioneer in Colloid Chemistry," follows.

Dr. Edward Goodrich Acheson's attempts to use electric-furnace graphite in the manufacture of crucibles led to his observation that the well-known widely different characteristics of clays seemed to be related to the nature of the clay bed as opposed to its chemical composition. He postulated that certain sedimentary clays acquired plasticity while suspended in the water from which the bed was deposited. His investigation of the effect of organic extracts on clays revealed that tannin-related materials affected the plasticity and strength of clay bodies. At the same time, the clay became, as he termed it, "deflocculated" in water.

He was able to show that clays could be up-graded by the use of deflocculants. Acheson termed his treatment "Egyptianizing" and the treated clay he called "Egyptianized Clay," in tribute to the early Egyptian Israelites who made clay bricks with the aid of straw. Straw extract was an effective deflocculant. Furthermore, the fact that stable clays are precipitated from suspension by the presence of electrolytes explained satisfactorily, for the first time, the method of formation of river deltas like those of the Nile and the Mississippi.

After Acheson prepared pure electric furnace graphite suitable for lubrication purposes in 1906, it was characteristic of him that he should see how his earlier studies on clay could make the graphite still more useful. He found that graphite could be deflocculated by a large number of natural extracts. The research necessary to produce a commerical product was pursued with vigor, and in 1908 the Acheson Oildag Co. was founded to manufacture and sell 'Aquadag' and 'Oildag,' the suffix 'dag' being a contraction of "Deflocculated Acheson Graphite."

Acheson was a keen observer, quick to realize industrial potential in his discoveries. He pursued an idea relentlessly and made the most of it. Without the advantages of broad academic training, he could undertake the study of as complex a field as clay technology and soon see relationships not apparent to others. It was his unbounded curiosity spurred on by burning ambition, and tempered by a practical appreciation of the potential value of his discoveries, that marked Edward Goodrich Acheson as a practicing scientist of continuing significance.

New York Recommended as Engineering Center Site

The Special Task Committee appointed to make recommendations with regard to the site of the Engineering Societies Center has proposed that the Center be located in New York City; that the present Engineering Societies Bldg., at 29–33 W. 39th St., New York, be remodeled and continued in use as the site of the Center; that, if rebuilding in that area does not prove practicable, a comparable location be sought in midtown New York.

NACE Meetings

The Northeast Region, National Association of Corrosion Engineers, will hold sessions devoted to protective coatings, experimental design, analysis, and application; plastics, new alloys, and cermets, at the meeting in Philadelphia, October 15–17.

* * *

The South Central Region, NACE, will hold sessions in San Antonio, Texas, October 23–26. Numerous significant corrosion problems in the oil and gas producing and refining industries are scheduled for consideration. Symposia on corrosion of oil and gas well equipment, elevated and high temperature corrosion, and six committee meetings on problems in the chemical and petrochemical industries are planned.

The four papers related to the oil production industry cover inhibitors, hydrogen sulfide absorption plants, and cathodic protection. High temperature corrosion problems to be covered in four papers pertain to oxidation of iron-nickel alloys, hydrogen sulfide's effect on various metals, catalytic refining equipment corrosion, and zirconium corrosion in water over 200°C. Another symposium devoted to the transportation industry will include papers on internal protection of ships, external ship hull protection, and chemically deposited nickel alloy coatings for tanks.

Among other things arranged for the meeting are an exhibition of corrosion control materials and equipment, the first held at a regional meeting, and technical committee meetings on hydrogen sulfide corrosion, cooling water, plastic materials of construction, stress corrosion cracking of stainless steels, and industrial maintenance painting.

ASTM Second Pacific Area National Meeting

The Second Pacific Area National Meeting and Apparatus Exhibit of the American Society for Testing Materials will be held at the Hotel Statler in Los Angeles, Calif., September 17–21.

The technical program, consisting of 43 separate sessions and 225 papers, includes symposia dealing with radio-

(*Continued on page 215C*)

San Francisco Close-Ups

I, Part of the Local Committee which produced one of the Society's most successful meetings—Mrs. Zimmerly, R. L. Zimmerly, Mrs. Dreisbach, S. L. Dreisbach, Mrs. Bechtold, R. F. Bechtold, and Morris Feinleib. II, The line-up for Monday's buffet supper. III, 1955-56 President H. H. Uhlig and Mrs. Uhlig. IV, More of the Local Committee—Mr. and Mrs. C. D. Hunt, Mrs. Tobias, C. W. Tobias, Mrs. Baldwin, R. L. Baldwin, Mrs. Doub, D. V. Doub, and Bernard Porter. V, Lunch time for C. A. Hampel, R. M. Hunter, W. C. Gardiner, Milton Janes, H. B. Linford, and F. W. Koerker. VI, Near the registration desk almost any time. VII, Dr. and Mrs. R. M. Burns, and Mr. and Mrs. J. C. Schumacher. VIII, K. F. Bonhoeffer.

News Notes

(*Continued from page 213C*)

active isotopes, effects of radiation on materials, titanium, railroad materials, fuels and lubricants, wood, and numerous other materials of concern to industry. The program was developed under the guidance of the Pacific Area Program Committee and the society's Administrative Committee on Papers and Publications.

In addition, there will be a national President's Luncheon, seven industry luncheons, special West Coast Apparatus and Photographic Exhibits, meetings of ASTM technical committees, and plant and laboratory inspection trips.

National Electronics Conference

The 12th annual National Electronics Conference will be held October 1–3 at the Hotel Sherman in Chicago, Ill. More than 100 technical papers and 240 exhibits will be featured.

For further information write to: J. S. Powers, Executive Secretary, National Electronics Conference, 84 E. Randolph St., Chicago 1, Ill.

EJC Report on Professional Standards and Employment Conditions

Engineers Joint Council, New York City, has been mailing out questionnaires to representative segments of industrial and governmental organizations employing engineering graduates, for its second triennial survey of the earnings of engineering graduates throughout the country. This month questionnaires will be sent to faculty members of engineering colleges through their respective Deans of Engineering. The replies to the basic questionnaires to industry and government, which will be prepared by key personnel or administrative managers of the organizations together with the replies from engineering educators, will serve as the basis for the publication "Professional Income of Engineers—1956." The survey will analyze the current structure of salaries of engineering graduates employed in the United States which will be of unquestionable value to those interested in engineering employment conditions. Engineers Joint Council seeks the cooperation of the organizations receiving these questionnaires, requesting that the forms be completed and returned promptly.

Copies of the Report on "Professional Standards and Employment Conditions" can be obtained without charge from Engineers Joint Council, 29 W. 39th St., New York 18, N. Y.

Dow Aid-to-Education Program

Gifts to educational institutions by The Dow Chemical Co. will total $320,000 in the school year beginning this fall. Dow's 1956–57 program will include 62 fellowships and 27 scholarships at 46 institutions. The cash amount represents a 9% increase over the company's previous program.

The program has two major phases. One authorizes $154,600 in grants to 46 institutions for the the establishment of graduate fellowships and undergraduate scholarships and to two educational foundations for assistance to deserving students. The other phase covers the allocation of $153,000 to 20 institutions, most of it earmarked for use in expansion and operating programs. The school authorities themselves will specify how the money should be used.

Over and beyond this grant-in-aid program, the company expects to make $160,000 available to colleges and universities for specific research projects expected to be beneficial to Dow in the chemical field. This includes consultative research for the company by college faculty members.

Crane Co. and Republic Steel Joint Owners of Cramet, Inc.

Crane Co. and Republic Steel Corp. have become equal partners in Cramet, Inc., producer of titanium sponge. Cramet, formerly a wholly owned subsidiary of Crane, will remain a separate corporation. A new board of directors, consisting of four representatives of each of the parent companies, has been organized.

Cramet, formed by Crane Co. in 1953, has constructed a plant at Chattanooga, Tenn., which will have a capacity of 6000 tons of titanium sponge annually. In addition to the government's requirements, Cramet's titanium sponge will be available both to Crane and Republic as well as for sale to other users.

Both parent companies have sources of the minerals from which titanium is extracted. While construction of the Cramet plant has been under way, Crane uncovered sources of rutile at Aiken, S. C., and near Panama City, Fla. Republic is developing important deposits of rutile in Southwest Mexico.

Dutch Subsidiary Holds Annual Meeting

Substantial progress in the preparation of the site for a proposed plant in Rotterdam, The Netherlands, was reported at the annual meeting of shareholders of Nederlandsche Dow Maatschappij N.V., wholly owned subsidiary of The Dow Chemical Co., marking the close of the subsidiary's first fiscal year.

It was announced that half of the company's 50-acre site in the Third Petroleum Harbor in Rotterdam has been raised above sea level. Several test piles have been driven, soil tests completed, and further site development for the projected processing plant has been authorized by the board of directors. It was also announced that Dow and its subsidiary are carrying on an appraisal of Dow products and their economic applicability in Europe to develop the production program planned in Holland.

The Dutch subsidiary was formed to import, manufacture, and distribute domestically and abroad a variety of chemicals, plastics, and magnesium.

Industrial Expansions

The new Parma, Ohio, Research Labs. of National Carbon Co., A Div. of Union Carbide & Carbon Corp., will be dedicated September 18. Designed primarily for basic research in chemical and solid state physics, the multimillion dollar laboratory brings to seven the number of major research centers operated by divisions of Union Carbide. The laboratory facilities are already in operation, with research scientists studying ways to improve existing materials and, more importantly, methods to create new materials for the metal, electronic, power, chemical, and electrochemical industries.

Heading the new laboratory is National Carbon physicist, Dr. Robert G. Breckenridge.

The Dow Chemical Co. has announced formation of its Eastern Research Lab. at Framingham, Mass., and appointment of Dr. Fred W. McLafferty as its director. The laboratory will be responsible for fundamental research on a long-range basis in various fields of interest to the company, including the areas of organic and inorganic chemicals and plastics, and will also

carry on analysis and testing work. Activities will be closely coordinated with company-wide research operations.

Two new divisions, with headquarters at Exide's Philadelphia plant, have been announced by the Exide Industrial Division, The Electric Storage Battery Co.

An Alkaline Division has been formed in the Engineering Dept. Appointed manager is Electrochemical Society member William W. Smith, former head of pilot plant activities which have been integrated into the new division. The purpose of the reorganization is to consolidate alkaline battery programs, a field in which product research and development have been under way at Exide for many years. The division conducts experimental work with batteries containing both silver-zinc and nickel-cadmium active materials in alkaline electrolyte.

A Silver Battery Division has been set up under the management of J. J. Sullivan. The new unit will manufacture, process, and inspect batteries with silver-zinc active materials in alkaline electrolyte. While Exide has produced these units for many years, the new division has been created because of increasing demand for Exide silver batteries.

Foote Mineral Co. plans a substantial expansion of production facilities at its Electromanganese Division, Knoxville, Tenn. Construction, to have started in July, is expected to be completed in early 1958. The expansion program affects the company's Lorraine St. plant, newest of the division's two operating units. Increasing demands for electrolytic manganese, particularly for use in the new low-nickel stainless steels, necessitated the move.

American Potash & Chemical Corp. has established offices at Washington, D. C., for the purpose of improved liaison between governmental agencies and the company's Dept. of Defense Programs. Herbert W. Yeagley, previously with Monsanto Chemical Co., has joined American Potash to head the Washington office, located in the Investment Bldg. at 15th and K Sts.

The Electrode Div. of Great Lakes Carbon Corp. has announced plans to add more than 45% to its annual production capacity of carbon and graphite electrodes, anodes, mold stock, and graphite specialties.

The new facilities will be at the Division's plants in Morganton, N. C., and Niagara Falls, N. Y., and are scheduled for completion in May of 1957. With the new facilities and others constructed since 1952, production capacity of the Division will have more than doubled in a five-year period.

The plans also call for greatly increased research and development facilities, and substantial additions to the plant offices.

SECTION NEWS

Chicago Section

At the June meeting of the Section, the following officers were elected for the 1956–57 season:

Chairman—Robert Misch
Vice-Chairman—D. V. Louzos
Treasurer—Ralph Hovey
Secretary—William Colner, Armour Research Foundation, 10 West 35th St., Chicago 16, Ill.
Program Chairman—Jerry Kuderna
Representatives on Council of Local Sections—C. A. Hampel (1 yr) and H. T. Francis (2 yr)

WILLIAM COLNER, *Secretary*

Niagara Falls Section

The 1955–56 season was concluded on May 24 with Ladies' Night. A buffet lunch was served at the Lasalle Yacht Club, following which Mr. Walter Wooldridge of Electro Metallurgical Co. spoke on "The Cutting of Gems." The talk was illustrated by a technicolor film and samples of synthetic gems manufactured by Linde Air Products Co. The history of the development of techniques for making synthetic gem stones was reviewed; the first practical method was developed by Linde during World War II for making instrument bearings.

The April 11th meeting, National Officers' night, was held at the Red Coach Inn. The following slate of officers was unanimously elected to serve for the 1956–57 season:

Chairman—R. B. MacMullin
Vice-Chairman—L. A. Stoyell
Secretary-Treasurer—W. E. Kuhn
Members-at-large—Karl Kunkel, Leslie Juel, E. R. Hogan, H. B. Morley

Our National President, Dr. H. H. Uhlig, gave an excellent talk on "Corrosion Inhibitors." Dr. Uhlig illustrated the different classes of inhibitors and pointed out their economic value to industry. The mechanism of inhibition was mentioned in terms of physical and chemical adsorption on metal surface. Potential measurements with systems like CrO_4^- on iron and Fe^{+++} and Cu^{++} on titanium indicate that these ions adsorb in accordance with the Langmuir adsorption isotherm. A new inhibitor, the pertechnetate ion, is reportedly the most efficient material yet discovered. It is effective in extremely small amounts and maintains inhibition at temperatures considerably higher than any other known passivator. An electrochemical method for the measurement of corrosion rates of passive metals was described, and supporting data presented. If further experiments indicate this technique has wide applicability, the method will prove extremely useful, both in research and in practice. The National Association of Corrosion Engineers was invited and many of their members were present. High interest in the talk was evidenced by the number of queries in the discussion period.

A joint meeting with The American Chemical Society was held at the Prospect House on March 20. The scheduled speaker, Dr. H. H. Uhlig, was snowbound in the New England States. His place was nicely filled by Dr. Charles Clark of the local Olin-Mathieson Corp., who talked on "Hydrazine." He gave the history, methods of manufacture, and problems faced in producing members of the hydrazine family. The most publicized use of hydrazine is as a rocket fuel. Considerable research is being underwritten to develop and extend the field of hydrazine chemistry. We were guests of the American Chemical Society for coffee and doughnuts after the meeting.

The Sorel titanium operation was outlined by Mr. C. J. Lenz, Assistant Superintendent of the Sorel operation in the province of Quebec, at the February 18 meeting held at the Red Coach Inn. Technicolor slides were shown of the titanium slag smelter as well as the general plant layout. The metallurgy involved in the beneficiation of ilmenite to produce a 70% TiO_2 slag was discussed. Methods used in overcoming problems were explained. An extended "Question and Answer" period following the talk highlighted the interest in this process along the Niagara Frontier.

On January 18, an excellent talk was given by Mr. Arthur Guay, Supervisor of Physical Metallurgy at the Ferrald

Division of the National Lead Co. He gave a thorough resumé of the metallurgy involved in the production of uranium metal from ores and concentrates. Flow sheets of each stage of the process were shown.

L. A. STOYELL, *Secretary*

Washington-Baltimore Section

The annual dinner meeting and election of officers was held May 17 at the University of Maryland. The following officers were elected for next year:

Chairman—D. T. Ferrell, Jr.
Vice-Chairman—Jeanne Burbank
Secretary—Gwendolyn B. Wood, National Bureau of Standards, Chemistry Bldg., Rm. 115, Washington 25, D. C.
Treasurer—David Schlain

Following the installation of officers, T. D. Callinan, Naval Research Lab., presented a thought-provoking and entertaining speech entitled "The Second Stone Age." The history of man's use of raw materials was humorously sketched from the days of Adam through the "Cellulose Age" to the present time. We find ourselves on the threshold of a Second Stone Age using inorganic materials in ever increasing quantity.

Mr. Callinan dramatically described the rocks and stones of idle mountain terrain as the future industrial lifelines of our country, far removed from the present coal and oil sources. This talk at first appeared to be scientific whimsy but, when, two days later, the New York Times devoted a front page column to similar views expressed by the California Institute of Technology through its Industrial Associates Program, Mr. Callinan took on the stature of a major prophet.

JEANNE BURBANK, *Secretary*

PERSONALS

C. H. AALL, formerly of St. Louis, Mo., has joined The American Metal Co., Ltd., Carteret, N. J., as Director of Research and Development.

SAMUEL HEIMAN, Chief Chemist and Technical Director of the Philadelphia Rust Proof Co., and HERBERTH E. HEAD, Supervisor of Electro Plating and Related Operations of the Automotive Body Division of the Chrysler Corp., were elected President and Second Vice-President, respectively, of the American Electroplaters' Society at its Annual Convention held recently in Washington, D. C.

HUGH S. TAYLOR of Princeton, N. J., Dean of the Princeton University Graduate School and professor of chemistry there, has been awarded an Honorary Doctor of Science degree from Western Reserve University.

JOSEPH C. SCHUMACHER recently was appointed vice-president in charge of research for the American Potash & Chemical Corp. Research functions at the company's Trona, Whittier, and Los Angeles, Calif., and Henderson, Nev., installations will be centered in a new department under Mr. Schumacher.

WALTON S. SMITH has retired as Vice-President in charge of Manufacturing, Metal & Thermit Corp., after 37 years of service with the company. Joining Metal & Thermit in 1919 as a mechanical engineer, he became assistant superintendent of the Carteret, N. J., plant in 1925 and superintendent in 1937. He was elected Vice-President in 1942 and became a director in 1943. He will continue as a director and consultant for the company.

HERBERT BANDES has been appointed to the newly created post of Chief Engineer—Semiconductors of the Electronics Division of Sylvania Electric Products Inc. Dr. Bandes is responsible for the development and engineering of transistors, diodes, and other semiconductor devices manufactured at the division's plants in Woburn, Mass., and Hillsboro, N. H. His office is at division headquarters in Woburn. Previously Dr. Bandes was Engineering Manager—Semiconductors.

HENRY MAHLSTEDT has been named Product Manager for plating products for Metal & Thermit Corp., New York City. He has been connected with associated companies of Metal & Thermit since 1927.

HENRY F. IVEY has been appointed section manager in charge of phosphor development at the Westinghouse Lamp Division in Bloomfield, N. J.

MYRON B. DIGGIN, Vice-President and Technical Director of Hanson-Van Winkle-Munning Co., Matawan, N. J., recently received the Award of Merit of the American Electroplaters' Society at its 43rd Annual Convention. The award was made for "outstanding contributions to the American Electroplaters' Society."

A. L. JENNY, supervisor of electrolytic development at the General Electric Co., Hudson Falls, N. Y., recently was granted a patent for a method of etching tantalum, which he developed in the Capacitor Dept. laboratory. This is the fourth patent to be taken out by G. E. in his name.

JULES BEBIE

Jules Bebie, consulting chemist and retired officer of the Monsanto Chemical Co., died on June 9 at the age of 79.

Dr. Bebie was born in Zurich, Switzerland. He attended the Federal Polytechnic Institute and the University of Zurich, from which he received a Ph.D. degree in 1901. After five years' work in organic chemistry in Europe,

1956 Extended Abstracts

The Electronics Division has available copies of the "Enlarged Abstracts" booklet, "printed but not published," containing 1000-word abstracts of papers presented at the Division's symposia on Luminescence and Semiconductors at the San Francisco Meeting of the Society, April 29–May 3.

The booklets are available at $2.00 each from:
Martin F. Quaely
Research Dept., Lamp. Div.
Westinghouse Electric Corp.
Bloomfield, N. J.

* * *

The Theoretical Electrochemistry Division also has available copies of the extended abstracts booklet of papers presented at the sessions of the Theoretical Division at the San Francisco Meeting of the Society. The booklet also contains abstracts of papers presented at the Symposium on "Adsorption Phenomena at Electrode Surfaces" sponsored jointly by the Theoretical Electrochemistry and Corrosion Divisions.

Copies can be obtained at $2.00 each from:
Ernest Yeager
Dept. of Chemistry
Western Reserve University
Cleveland 6, Ohio

he came to the United States to assist in developing Monsanto Chemical Co.'s manufacturing processes. He was named a vice-president and research director of the company in 1925. After his retirement in 1931, he became a consulting chemist and was a member of the chemical engineering faculty of Washington University in St. Louis, Mo. Dr. Bebie was a specialist in plastics, nitrocellulose, and organic synthesis, and conducted an engineering training course in explosives at the university during the Second World War.

He is survived by his wife, two daughters, and a son.

ANNOUNCEMENTS FROM PUBLISHERS

TEN YEAR INDEX TO CORROSION, 1945–54. Pub. No. 56-10, 32 pages, 8½ x 11¼ in. paper. Compiled by Norman E. Hamner and J. F. Van der Henst, Jr., May 1956. Published by the National Association of Corrosion Engineers, 1061 M & M Bldg., Houston 2, Texas. Per copy, postpaid, NACE members, $5; all others, $7.50. Add 65¢ for Book Post Registry to addresses outside the United States, Canada, and Mexico.

The alphabetical subject index consists of approximately 4000 reference phrases and alphabetical author index of 1056 names. Titles are included of 629 articles published in the first decade (1945–54) of publication of *Corrosion*, the monthly journal of the National Association of Corrosion Engineers. The subject index, organized around the system developed for the NACE Abstract Filing Index, is intended to be of maximum service to the general corrosion worker. No effort was made to limit the number of cross references, with the result that there is more than one reference per page of indexed material. The index is characterized by a wide variety of subject matter with data on pipeline and petroleum corrosion problems in greater volume than other topics. Of special interest to corrosion engineers are the numerous tables of data.

INVESTIGATION OF THE METALLURGICAL CHARACTERISTICS OF THE 36% ALUMINUM TITANIUM-BASE ALLOY by J. B. McAndrew and D. J. McPherson, Armour Research Foundation, for Wright Air Development Center, U. S. Air Force, January 1955. Available as report PB 121005.* 66 pages, $1.00.

STUDY OF EFFECTS OF ALLOYING ELEMENTS ON THE WELDABILITY OF TITANIUM SHEET by H. M. Myer, Armour Research Foundation, for Wright Air Development Center, U. S. Air Force, June 1955. Available as report PB 121006.* 316 pages, $4.00.

PRECIPITATION HARDENING AND EMBRITTLEMENT OF HIGH-STRENGTH TITANIUM ALLOYS by W. M. Parris, C. M. Schwartz, and P. D. Frost, Battelle Memorial Institute, for Wright Air Development Center, U. S. Air Force, June 1955. Available as report PB 111990.* 74 pages, $2.00.

BATTERY ANALYZER FOR USE IN STORAGE BATTERY STUDIES by G. W. Work and C. P. Wales, Naval Research Lab., February 1956. Available as report PB 111932.* 20 pages, 50 cents.

CORROSION IN ENGINE COOLING SYSTEMS CONTAINING ALUMINUM: A LITERATURE SURVEY by Mildred Benton, Naval Research Lab., July 1955. Available as report PB 111817.* 31 pages, $1.00.

ELECTROFORMING OF COPPER FOR HIGH-VACUUM APPLICATIONS by L. H LaForge, Jr., W. W. Hansen Labs., Stanford University, sponsored by the Army Signal Corps, Air Force, and Office of Naval Research, February 1955. Available as report PB 111960.* 23 pages, 75 cents.

ANALYSIS AND CONTROL OF BLACK CHROMIUM PLATING SOLUTIONS by Oren Littig, Rock Island Arsenal, U. S. Army, July 1955. Available as report PB 111830.* 19 pages, 50 cents.

STUDY OF EFFECTS OF ALLOYING ELEMENTS ON THE WELDABILITY OF TITANIUM SHEET, H. M. Meyer and W. Rostoker, Armour Research Foundation for Wright Air Development Center, U. S. Air Force, May 1954. Available as Report PB 111885.* 107 pages, $2.75

Reactions of three basic categories of titanium alloys to heliare welding were studied, including the influence of preheat and postheat treatments on bend ductility, tensile strength and elongation, hardness, and other mechanical properties.

ELECTRICAL RESISTANCE STUDY OF THE EFFECTS OF OXYGEN ON THE ALLOTROPIC TRANSFORMATION OF TITANIUM, L. A. DePue and E. J. Chapin, Naval Research Lab., Feb. 1956. Available as Report PB 111741.* 26 pages, 75 cents.

The allotropic transformation of eight titanium-oxygen alloys ranging from 0.028 to 2.7% was studied by determining their change of electrical resistance with temperature. The resistance of the specimens was measured in vacuum by obtaining the voltage drop across a gauge length of 1.75 in., using a low current ranging from 51 to 91 ma. This method of measuring the electrical resistance as a function of temperature was found to be a highly sensitive and reproducible means for continually following the progress of the allotropic transformation of titanium oxygen alloys.

MATERIALS FOR HANDLING FUMING NITRIC ACID AND PROPERTIES OF FUMING NITRIC ACID WITH REFERENCE TO ITS THERMAL STABILITY, Part IV, Mars G. Fontana, Ohio State University Research Foundation for Wright Air Development Center, May 1955. Available as Report PB 111950.* 140 pages, $3.50.

Fourth annual report of the Air Force's experimental investigation of materials for handling fuming nitric acid, a rocket fuel.

BASIC STUDIES ON THE CHEMISTRY OF FLUORINE COMPOUNDS, W. T. Miller, Cornell University, Sept. 1954. Available as Report PB 111959.* 148 pages, $3.75.

Research on new methods of synthesis of potentially polymerizable fluorine-containing monomers and related work aimed at obtaining a better understanding of the basic chemistry of organic fluorine compounds.

* Order from Office of Technical Services, U. S. Dept. of Commerce, Washington 25, D. C.

BOOK REVIEWS

ULTRASONIC ENGINEERING by Alan E Crawford. Published by Academic Press Inc., New York, 1955. 344 + X pages, $8.00.

At the present time, industrial applications for ultrasonic waves in the United States are limited for the most part to material testing, drilling, cutting, and cleaning operations. A number of additional industrial applications, however, are on the horizon and should prove quite significant to the chemist. Before these applications can materialize, much development work and basic research are necessary. Ultrasonic techniques are generally foreign to both chemical engineers and research chemists. A. E. Crawford's new text on ultrasonic engineering is an attempt to meet the need for education in this field.

Although Crawford has chosen to title his book "Ultrasonic Engineering," the subject matter is not restricted to the ultrasonic frequencies, but includes the entire acoustical spectrum insofar as significant applications are involved.

In this text, emphasis is placed on techniques for generating high intensity sound waves for industrial applications. Considerable attention is given to the phenomena associated with cavitation in liquids. This is particularly appropriate inasmuch as most processing applications for ultrasonic waves involve liquids and are dependent on cavitation. Specific applications described by the author in considerable detail include: precipitation and agglomeration, formation of colloidal suspension, and sonochemical reactions. Specific reference is made to the effects of ultrasonic waves on electrodeposition and corrosion as well as the cleaning of metal surfaces. The final chapter relates to applications of ultrasonic waves in testing and control. The book contains a number of tables with useful data with respect to the propagation of sound waves through solids, liquids, and gases. At the end of each chapter is an adequate bibliography.

With but minor exceptions, the material can be easily understood by chemists and metallurgists who do not have any special knowledge of acoustics or, for that matter, physics. This book is not intended primarily for physical chemists or theoretical chemists interested in fundamental studies, but rather for individuals interested in application.

ERNEST YEAGER

ADVANCED ANALYTICAL CHEMISTRY by Walter Wagner, Clarence J. Hull, and Gerald E. Markle. Published by Reinhold Publishing Corp., New York, 1956. v + 282 pages, $5.50.

This book is designed for a two-term graduate course in analytical chemistry aiming to provide information on certain instrumental methods and to summarize existing methods of various types for the actual analyses of the chemical elements; accordingly, the book is divided into Part I, Analytical Techniques, and Part II, The Analytical Chemistry of the Elements.

In Part I, the following subjects are discussed in about 100 pages: organic reagents, gas analysis, colorimetry and spectrophotometry, polarography and amperometric titrations, chromatography and ion-exchange techniques, thermogravimetric analysis, radiochemistry, and statistics.

The space allotted does not permit adequate coverage of all the topics; for example, radiochemistry is discussed in about four pages of text, chromatography and ion-exchange in six pages. On the other hand, the chapter on organic reagents is quite satisfactory and contains a good bibliography, and the chapter on gas analysis is useful. The remainder of the chapters on techniques are less satisfactory and in some cases no mention is made of the standard references the student would need. Apart from the creditable chapters on organic reagents and gas analysis, there is almost no theory or basic information in Part I. There are exterior views of colorimeters, spectrophotometers, and polarographs, but no circuit diagrams or sketches showing how the black boxes work. The chapter on statistics would be improved if less space were devoted to procedures for determining the mean of a large number of observations (a problem unlikely to arise in analysis); rather curiously, although the t-test and Chi-square test are used, no tables are provided. There appear to be one or two mistakes in this chapter, probably due to printing errors.

Part II contains descriptive information on the analyses of 69 elements, treated according to the groups of the periodic table. Each element is discussed separately and there is a separate list of references of methods for each element. In many cases, particularly of less frequently encountered elements, there is a discussion of qualitative methods and in every case there is a summary of quantitative methods which have been reported for the element. In addition, a gravimetric procedure is described for each element; this is usually the standard method and, while it is not sure that the procedure as given could be used for laboratory directions, it provides a good understanding of what the method entails. The elements with which this reviewer has had personal experience are covered intelligently and fully, and it is believed that Part II of this text will be most useful to many analysts as well as graduate students. The references in Part II have been brought up to July 1, 1954, and include more than 850 titles.

One's judgment of the value of a text is so much a matter of opinion that an evaluation must be offered with caution. If one feels that descriptive material is the best basis for teaching analytical

1956 Directory

The 1956 Directory of Members of the Electrochemical Society should be available early in September, rather than the latter part of July as stated in the July JOURNAL. The Directory contains an alphabetical and geographical list of members of the Society as of March 1, 1956, and a list of Patron and Sustaining Members, Past Presidents, and winners of Society prizes and awards.

Members who wish to receive the Directory are requested to fill in and return the order form below, accompanied by check, to Society Headquarters, 216 West 102 St., New York 25, N. Y.

Please send_____copy(ies) of the 1956 Membership Directory to:

Name_____

Company_____

Street_____

City_____ Zone____ State_____

Attached is check for $_____ for Directory. (Single copies cost $2.00.)

chemistry to graduate students, then Part II is ideal, while Part I is of questionable value. If one believes that only principles should be taught, then the book is not useful as a text although Part II is a valuable reference source to any practicing analytical chemist. The problem of teaching analytical chemistry to graduate students is difficult, and what appears to this reviewer to be inadequacy of Part I is a result of the difficulties. Many physical methods have been applied to chemical analysis within the past decade; for example, spectrophotometry, x-ray techniques, chromatography, polarography, radiochemistry, etc., have been introduced. Each of these subjects is a specialty in itself and excellent texts are available on each. The problem is to describe the necessary principles without reproducing the specialized texts in large part, assuming that a textbook is desirable in a course of this type. Several texts have appeared recently which attempt to solve the problem, of which the present book is one. It seems to be demonstrated that the new techniques cannot be discussed adequately in anything like 100 pages; none the less, many analytical chemists will be indebted to the authors for their work in compiling the material of Part II.

JOHN E. VANCE

ATOMIC ENERGY RESEARCH AT HARWELL by K. E. B. Jay. Published by Philosophical Library, Inc., New York, 1955. 144 pages, $4.75.

This book is a general guide to the work at Harwell and is divided into two parts. The first deals with the major programs and covers reactor development, separations processes, isotope production, contract work, and administrative details. This section is well written and aimed primarily at nontechnical readers. The commentary is enlivened by such comparisons as the cost ratio between heavy water and whiskey (35:1). The second part deals in more detail with selected researches and is for a more scientific audience. The style here is discursive with less continuity than in Part I. The book covers the period 1952–54 and supplements a previous volume. A broad range of information is covered, and the book is well organized but necessarily terse.

Similar considerations have guided reactor development in both the U. S. and England. Atomic energy is not a luxury for the English, and they do not have the variety of reactors found in America. Otherwise, the A. E. R. E. is an A. E. C. in miniature, and this book provides an insight on work in the U. S. as well. The size of Harwell may be judged by the fact that 2500 people arrive at work in buses every day. It compares with one of the largest of the A. E. C. installations such as Oak Ridge.

A Glossary is provided at the beginning of the book and the author is careful in Part I to define new terms as they occur. The material in Part II does not lend itself to such treatment, but bibliographies are appended to each section. The objectivity of the author is evidenced by credits given for work done in the U. S. Interesting side lights are given on various projects, but the general level of security is similar to that in this country.

This book does not contain an index and the price is somewhat high. However, it forms an easy introduction to a rapidly growing field and is a handy reference. Anyone in the field of atomic energy should find this volume interesting and profitable.

R. D. MISCH

LITERATURE FROM INDUSTRY

CORROSION-RESISTANT PIPE AND FITTINGS. Catalogue illustrates and describes line of corrosion-resistant polyethylene and polyvinyl chloride pipe, tubing, ducting, valves, and fittings for industrial applications. *American Agile Corp.*, P. O. Box 168, Bedford, Ohio.

EXIDE-MANCHEX BATTERIES. New line of Exide-Manchex batteries, featuring increased life and higher instantaneous discharge rates, is illustrated and described in a recently published catalogue. *Exide Industrial Div., Electric Storage Battery Co.*, Philadelphia, Pa.

PYROMETERS AND RESISTANCE THERMOMETERS. Data sheet GEC-1324A describes features, accessories, application, specifications, and special calibration of instruments for temperature indication and control of industrial processes. *General Electric Co.*, Schenectady 5, N. Y.

PERMANENT MAGNET THICKNESS GAUGE. Bulletin GEA-6458 describes features, application, specifications, calibration, and operation of the hand-held, self-powered instrument. *General Electric Co.*, Schenectady 5, N. Y.

"APPARATUS AND ACCESSORIES FOR CHROMATOGRAPHY AND ELECTROPHORESIS." Catalogue includes such items as chromatocabs, drying ovens, fraction collectors, electrophoresis apparatus, filter paper, plus an entire section on special glassware. *Scientific Glass Apparatus Co. Inc.*, Bloomfield, N. J.

"THE ACHESON 'DAG' DISPERSER," Vol. I, No. 1. Literature recently published by Acheson Colloids Co. shows what industry and research are doing with 'dag' colloidal dispersions. *John Mather Lupton Co., Inc.*, 420 Lexington Ave., New York 17, N. Y.

ALUMINUM FLOW CHART. Illustrated flow chart outlining the production of aluminum, from mining of the ore through reduction to the metal, has been prepared and is available without charge. The 15-by-21-in. chart, printed in color, will be mailed folded. It is also

JUNE 1957 DISCUSSION SECTION

A Discussion Section, covering papers published in the July–December 1956 JOURNALS, is scheduled for publication in the June 1957 issue. Any discussion which did not reach the Editor in time for inclusion in the December 1956 Discussion Section will be included in the June 1957 issue. Those who plan to contribute remarks for this Discussion Section should submit their comments or questions in triplicate to the Managing Editor of the JOURNAL, 216 W. 102nd St., New York 25, N. Y., *not later than March 1, 1957*. All discussions will be forwarded to the author, or authors, for reply before being printed in the JOURNAL.

available on heavy paperboard for teachers and others who want the chart for wall mounting. *Desk FC, Reynolds Metals Co.*, 2500 S. Third St., Louisville 1, Ky.

EPOXY COMPOUNDS. Becco's new long-chain epoxidized olefins, Octylene oxide, Dodecene oxide, and C_{16}—C_{18} Olefin oxide are described in Bulletins 72, 73, and 74, respectively. Structure, typical properties, and chemical reactivity of each of these highly reactive epoxy compounds are presented. A number of suggested uses as intermediates, solvents, and specialty chemicals are listed. *Becco Chemical Div., Food Machinery & Chemical Corp.*, Buffalo 7, N. Y.

TITANIUM CORROSION RESISTANCE. New bulletin contains currently available data on the corrosion resistance of titanium, and suggests to the product designer where this new metal can be applied to overcome corrosion problems. Various uses of titanium, based on its corrosion resistance, are described, and the booklet contains corrosion ratings for titanium when exposed to many common types of corrosive agents. *Mallory-Sharon Titanium Corp.*, Niles, Ohio.

DIFFERENTIAL REFRACTOMETER. Brochure completely describes the new Barnes Differential Refractometer. It discusses the theory and principles of refractometry: measurement of refractive index, and its significance, when done continuously, for the process industries. Several applications of continuous refractive index measurements

To receive further information on any New Product or Literature from Industry listed write directly to the company at the address given in each item.

are given as well as features and complete specifications of the three available models. *Barnes Engineering Co.*, Stamford, Conn.

INFRARED SPECTROSCOPY. A handy package of Beckman reprints on infrared spectroscopy is available without charge. Included in the package is Beckman Bulletin 472 on the new Beckman IR-4 Infrared Spectrophotometer, a copy of Infrared Notes, and a complete index of all infrared reprints now available. *Scientific Instruments Div., Beckman Instruments, Inc.*, 2500 Fullerton Rd., Fullerton, Calif.

MOLYBDENUM CARBIDES AND NITRIDES; REFRACTORY MOLYBDENUM BORIDES. Two bulletins, Cdb-7 and Cdb-8, summarizing applications; physical, chemical, and mechanical properties; and preparation of molybdenum carbides and nitrides and molybdenum boride compounds, are available on request. *Climax Molybdenum Co.*, Dept. L, 500 Fifth Ave., New York 36, N. Y.

TRI-CLAD 55® EXPLOSION PROOF MOTORS. Bulletin GEA-6341 discusses design features and maintenance of new induction motors, one through 30 hp, for use in hazardous locations. *General Electric Co.*, Schenectady 5, N. Y.

"WHAT'S AVAILABLE ON MICROPRINT CARDS," an 8-page summary of information available to scholars and librarians in the comparatively new microprint cards, has been compiled and is ready for distribution. The findings have been classified by subject field and indicate sources from which purchases may be made. *Graphic Reproduction Div., Eastman Kodak Co.*, Rochester 4, N. Y.

NEW PRODUCTS

DETECT-O-PORE TEST PAPER, a new means for making rapid tests on tin, nickel, and chromium plating for pores, is available. For use, the paper is moistened with buffer solution, made with a buffer powder furnished, and then pressed down on the surface to be tested. Pores are shown by dark spots that develop on the paper. *R. P. Cargille Labs., Inc.*, 117 Liberty St., New York 6, N. Y.

MOLECULAR STILL. A simplified 2-in. version of the Arthur F. Smith Co.'s Rota-Film Molecular Still has been announced, which offers a relatively inexpensive method of molecular distillation for users who do not require the capacity of full-size models. It is capable of handling batches from 10 ml to 20 l. The vacuum range is from atmospheric to 1 μ Hg, and the temperature range is to 450°C. *Arthur F. Smith Co.*, Rochester 3, N. Y.

POLYETHYLENE PILLOWS, designed to retard the evaporation of liquids

MANUSCRIPTS AND ABSTRACTS FOR SPRING MEETING

Papers are now being solicited for the Spring Meeting of the Society, to be held at the Statler Hotel in Washington, D. C., May 12, 13, 14, 15, and 16, 1957. Technical Sessions probably will be scheduled on Electric Insulation, Electronics (including Luminescence, Semiconductors, Oxide Cathodes, Instrumentation, and possibly Screen Applications), Electrothermics and Metallurgy, Industrial Electrolytics, and Theoretical Electrochemistry (including a special symposium on electrolytes).

To be considered for this meeting, triplicate copies of abstracts (*not to exceed 75 words in length*) must be received at Society Headquarters, 216 West 102nd St., New York 25, N. Y., *not later than January 2, 1957. Please indicate on abstract for which Division's symposium the paper is to be scheduled.* Complete manuscripts should be sent in triplicate to the Managing Editor of the JOURNAL at the same address.

* * *

The Fall 1957 Meeting will be held in Buffalo, N. Y., October 6, 7, 8, 9, and 10, 1957, at the Statler Hotel. Sessions will be announced in a later issue.

such as chromium plating baths in open tanks, are available. With an average density less than 9 lb/ft³, these pillows have virtually unlimited life anb are chemically resistant to almost all reagents. *American Agile Corp.*, P. O. Box 168, Bedford, Ohio.

EXIDE-TYTEX BATTERY. New grid alloys and other product improvements have been introduced in a line of batteries for stationary power applications. They are expected to extend service life up to 10% and reduce maintenance requirements. Retaining basic features, the Exide-Tytex line for the first time includes positive grids of Silvium, an Exide patented alloy of lead, silver, and other metals. *Dept. T, Exide Industrial Div., Electric Storage Battery Co.*, Box 8109, Philadelphia 1, Pa.

LIQUID-COOLED GERMANIUM RECTIFIER. A 100-kw liquid-cooled germanium power rectifier, capable of delivering 80 volts d.c. at 1350 amp with a maximum input of 66 volts d.c. and approximately 1150 amp a.c. and with rectifier efficiencies to 98.4%, has been designed. It is recommended for a-c to d-c power conversion where high current at moderate voltage output and small unit size is required. *International Rectifier Corp.*, Product Information Dept., El Segundo, Calif.

AMINCO-WINSLOW-POROSIMETER. A complete pore-structure analysis of any porous material can be performed in a 10-min operating cycle by means of the new Aminco-Winslow Porosimeter, which measures sizes of pores ranging from 0.1 mm to 0.06μ, and pore volumes as small as 0.0005 ml at each pore diameter. This versatile tool affords a portable and accurate means for analyzing pore structure of critical materials for numerous applications. *American Instrument Co., Inc.*, Silver Spring, Md.

ION-EXCHANGE RESINS, in 100-to-200 mesh and in finer-than-200 mesh, especially designed for use in chromatography and research, are available in laboratory quantities. Among the new resins available are: (*a*) a weakly basic anion-exchange resin in free base form; (*b*) a weakly acidic cation-exchange resin in hydrogen form; (*c*) a strongly acidic cation-exchange resin in sodium form; (*d*) a strongly basic anion-exchange resin in chloride form. Offered in a specially-purified *analytical* grade, ready for use. *Fisher Scientific Co.*, 310 Forbes St., Pittsburgh 19, Pa.

CHEMICAL ENGINEER

Opening for a man with some electrochemical background and a basic grounding in chemical engineering. Opening is now available in our Engineering Development Laboratory. This presents an excellent opportunity for advancement. Contact will be had with present plant processes and the engineering and development of all new ones. For a man with real imagination this chance to work on his own in the engineering development of the leading producer of peroxygen chemicals presents a real challenge.

Address inquiries to:

BECCO CHEMICAL DIVISION
Food Machinery and Chemical Corporation
Station B
BUFFALO 7, NEW YORK

ADVERTISERS' INDEX

Allis-Chalmers Manufacturing Company 187C
Becco Chemical Division, Food Machinery & Chemical Corporation 222C
Bell Telephone Laboratories, Inc. 190C
Dow Chemical Company ...188C–189C
Enthone, Incorporated ... Cover 4
Great Lakes Carbon Corporation ..... Cover 2
Mallinckrodt Chemical Works 184C–185C
Stackpole Carbon Company . 194C

EMPLOYMENT SITUATIONS

Please address replies to box shown, % The Electrochemical Society, Inc., 216 W. 102nd St., New York 25, N. Y.

Positions Available

ELECTROCHEMIST. Major Midwest chemical manufacturer has immediate opening for B.S. or M.S. electrochemist. Industrial experience desirable but not required. Should be able to apply fundamental knowledge of corrosion to solution of plant problems and to develop improved test procedures. The work will include cathodic protection investigation and polarization studies. *Reply to Box A-267.*

RESEARCH METALLURGIST

A B.S. or M.S. in Metallurgy is required for studies of the corrosion and stress corrosion characteristics of light alloys. Good background in physical metallurgy is essential. Some experience of corrosion and welding is desirable. Location Pacific Northwest. The position offers outstanding opportunities for advancement. Salary according to age, experience, and capabilities. Please reply to:

M. J. Pryor
Kaiser Aluminum & Chemical Corporation
Department of Metallurgical Research
Spokane 69, Washington